UNIVERSITY OF CALIFORNIA

Los Angeles

Cancer Risk Reduction Through Active Management of Genotoxicity

A dissertation submitted in partial satisfaction of the requirements for the degree

Doctor of Philosophy in Molecular Toxicology

by

Michael Joshua Davoren

2018

ABSTRACT OF THE DISSERTATION

Cancer Risk Reduction Through Active Management of Genotoxicity

by

Michael Joshua Davoren

Doctor of Philosophy in Molecular Toxicology

University of California, Los Angeles 2018

Professor Robert H. Schiestl, Chair

Cancer is the second leading cause of death in developed countries. Despite advances in both therapies and our understanding of the carcinogenesis process itself, consistently effective treatments remain elusive for a large number of cancer subtypes. For this reason, the minimization of cancer risk is a high priority subject. At the moment, cancer risk management is generally characterized by abstention rather than active engagement. The importance of avoiding activities associated with carcinogenesis-inducing genotoxicity, such as smoking, is well ingrained in the public consciousness as an anticancer strategy. The development of treatments that positively reduce genotoxicity poses a novel method of protection against general cancer risk, as well as the mitigation of risk from scenarios such as inflammation-inducing infections or genotoxic radiation exposure.

The first part of this thesis describes the development of a genotoxicity mitigating compound, Yel002. In yeast and mouse models, Yel002 reduced both genotoxicity and lethality resulting from radiation exposure. Administration of this compound up to 24 hours after an otherwise lethal dose of ionizing radiation reduced radiation-induced hematopoietic depletion

and systemic DNA damage markers. Although issues with compound stability made it difficult to use consistently, its development establishes a pipeline for the testing and use of similar compounds.

The second part of this thesis work describes the characterization of a *Lactobacillus* strain, *L. johnsonii* 456, associated with anti-inflammatory and anti-genotoxic outcomes in mice. Although originally derived from a murine host, the strain survives in both *in vivo* and *in vitro* models of the human gut, suggesting that these protective effects could be applicable to humans as well. Importantly, the strain's ability to inhibit pathogen growth and binding to human gut monolayer cells was demonstrated experimentally. As pathogenic bacteria are a major source of inflammation in the gastrointestinal tract, future probiotic intervention with this strain could result in active intervention strategies to manage local and systemic genotoxicity.

The third part of this work is a reprint of the previously published review article, *Mouse models for radiation-induced cancers*, included with the gracious approval of *Mutagenesis*. The mouse models described represent important animal models for the testing of active genotoxicity management interventions.

Finally, two appendices are included to describe subtle factors that influence the carcinogenesis pathway. Appendix I is a version of the article in submission *Glyphosate Based Herbicides and Cancer Risk: A Post IARC Decision Review of Potential Mechanisms, Policy, and Avenues of Research*, describing the heavily debated carcinogenic potential of the pesticide glyphosate and how it might exert effects through the microbiome. Appendix II is a reprint of the article *BALR-6 regulates cell growth and cell survival in B-lymphoblastic leukemia*, and elucidates a novel lncRNA-based mechanism of gene dysregulation in leukemic progression, to which I contributed bone marrow data analysis. As Yel002 suppresses leukemic progression in DBA/2 mice by an unknown mechanism, lncRNAs should be considered as a potential mechanism by which radiation mitigators affect hematopoietic stem cells.

The active management of systemic genotoxicity by both probiotic and pharmaceutical methods is a relatively untapped area in cancer risk reduction. This work describes the characterization process of two potential mitigators of genotoxicity-induced cancer risk, and establishes baseline criteria by which future interventions of these types can be identified and tested.

The dissertation of Michael Joshua Davoren is approved.

Patrick Allard

Rita Effros

Oliver Hankinson

Robert H. Schiestl, Chair

University of California, Los Angeles

2018

DEDICATION

To my parents Ben and Lisa, who made my education their priority throughout my childhood,

And to my wife Norma Iris, without whom my happiness would not be possible

TABLE OF CONTENTS

ACKNOWLEDGEMENTS

I must first thank my advisor and committee chair, Dr. Robert H. Schiestl for all he has done for me over the course of my graduate research. This work would not be possible without the guidance, mentorship, and academic freedom he afforded me. In particular, Dr. Schiestl set the strong example of optimism and persistence in the face of adversity. My committee also deserves special thanks. Dr. Rita Effros was a strong advisor and colleague over four years of reaching that helped me to find my confidence and an educator. Dr. Patrick Allard's input has driven me to constantly aim to refine and improve my speaking and presentation style. Dr. Oliver Hankinson has provided the best leadership and personal academic guidance of any department I have been a part of.

My time in the Schiestl Lab has been spent in the company of many other dedicated and generous researchers. Irene Maier, Aaron Chapman, Daniel Malkin, Liuba Parfenova, Zorica Scuric, Aya Westbrook, Lynn Yamamoto, Bill Mahon all provided invaluable advice, support, and camaraderie. My student volunteers Nora Alsakran, Debby Paiz, Vanessa Jung, Laura Gomez, and Chris Lu were all critical to making this work possible. Three other students, in particular, merit special mention and gratitude. Yelena Rivina, my student mentor, deserves more credit than any other for shaping my development as a researcher. Much of the work within this thesis, especially with regards to radiation damage mitigators and Yel002, is a result of our partnership. I was glad to be able to pass on that mentorship to my colleague Jocelyn Castellanos, with whom my work with probiotics would not have been possible. Lastly, my colleague and co-author Jared Liu provided invaluable collaboration over the entire course of our time in the Schiestl Lab.

The work presented in this thesis was supported in part by the NIEHS training grant in Molecular Toxicology for 2011-2013.

The work presented in Chapter 2 concerns our group's unpublished studies of the development and testing of the radiation mitigator Yel002. This work was performed under the direction of PI Robert H. Schiestl. Most of the original conceptualization and experimental planning was performed by Yelena Rivina. I contributed to later experimental design and planning as well as experimental performance, analysis, and interpretation of results. The synthesis and testing of Yel002 involved a great amount of collaboration and work from many gifted researchers, especially from our collaborating chemists in the lab of Michael E. Jung. I would like to thank Aaron Chapman for collaboration with regards to cigarette smoke extract experiments, the lab of William McBride for TIL-1 irradiation experiments, and the lab of Dr. Alexandra Miller for induced leukemia experiments with Yel002.

The work presented in Chapter 3 is a version of Davoren et al. "A Novel Probiotic, Lactobacillus Johnsonii 456, Resists Acid and Can Persist in the Human Gut for Over 30 Days" which is currently in final revision for journal submission. This work was performed under the direction of PI Robert Schiestl. I designed research, performed research, analyzed the data, and prepared the manuscript. Jared Liu, Jocelyn Castellanos, Norma I. Rodríguez Malavé, and Robert H. Schiestl also contributed to research, analysis, and manuscript preparation.

The work presented in Chapter 4 is a reprint of Davoren et al. "Mouse models for radiation-induced cancers" published in May 2016 with permission from Mutagenesis and Oxford University Press. The version of record is available online at https://doi.org/10.1093/mutage/gew019. Myself, Yelena Rivina, and Robert Schiestl all contributed to the review of literature and construction of this manuscript.

The work presented in Appendix 1 is a version of Davoren and Schiestl "Glyphosate Based Herbicides and Cancer Risk: A Post IARC Decision review of Potential Mechanisms, Policy, and Avenues of Research" which has been submitted to Environmental Health

Perspectives. The research was under the direction and conceptualization of PI Robert Schiestl. I reviewed literature, compiled, and constructed the manuscript.

The work presented in Appendix 2 is a reprint of Rodriguez-Malave et al. “BALR-6 regulates cell growth and cell survival in B-acute lymphoblastic leukemia”” published in December 2015 with permission from Molecular Cancer, as per the Creative Commons Attribution (CC-BY) license. I contributed to the interpretation of experimental results and construction of the manuscript for this article.

Finally, I would like to thank all my friends and family for their unconditional love and support. I could not have made it so far without all of you.

VITA

MICHAEL JOSHUA DAVOREN

Molecular Toxicology Interdisciplinary Program,

University of California, Los Angeles

Email: mdavoren@g.ucla.edu

EDUCATION

2010 – Present:	Ph.D. program Molecular Toxicology – University of California, Los Angeles
2006 -2010:	B.S. in Microbiology – University of California, Santa Barbara

---

ARTICLE PUBLICATIONS

Rivina, L., **Davoren, M.J.** and Schiestl, R.H., 2016. Mouse models for radiation-induced cancers. *Mutagenesis*, *31*, p. 491-509.

Rodríguez-Malavé, N.I., Fernando, T.R., Patel, P.C., Contreras, J.R., Palanichamy, J.K., Tran, T.M., Anguiano, J., **Davoren, M.J.**, Alberti, M.O., Pioli, K.T. and Sandoval, S., 2015. BALR-6 regulates cell growth and cell survival in B-lymphoblastic leukemia. *Molecular cancer*, *14*(1), p.214.

Rivina, L., **Davoren, M.** and Schiestl, R.H., 2014. Radiation-induced myeloid leukemia in murine models. *Human genomics*, *8*(1), p.13.

Rivina, L., **Davoren, M.** and Schiestl, R.H., 2014. Radiation-induced lung cancers in murine models. *Advances in Lung Cancer*, *3*(02), p. 38

Rivina, L., **Davoren, M.** and Schiestl, R.H., 2014. Mouse Models for Radiation-Induced Breast Cancer. *Cancer and Oncology Research*, *2*(6), p. 80-86.

RESEARCH EXPERIENCE

2010-present: **Graduate student researcher** with Dr. Robert Schiestl UCLA

Novel mitigators of radiation induced genotoxicity – yeast and mouse models

Probiotic interventions against inflammation

2009-2010 **Undergraduate Researcher** with Dr. Stephen Poole, UC Santa Barbara

Protein upregulation screens in *Drosophila*

TEACHING EXPERIENCE

2012: Teaching Assistant, Microbiology 101 at UC, Los Angeles

2013-2017: Lead Teaching Fellow, GE80 Cluster Course: Human Longevity at UC, Los Angeles

MANAGEMENT EXPERIENCE

2015-present: Acting Laboratory Manager, Schiestl Lab, UCLA

AWARDS AND GRANTS

2011-2013 NIEHS Training Grant in Molecular Toxicology

PENDING PUBLICATIONS

Davoren, M.J., Liu, J., Castellanos, J., Rodríguez-Malavé, N.I., and Schiestl, R.H., 2018. A Novel Probiotic, Lactobacillus Johnsonii 456, Resists Acid and Can Persist in the Human Gut for Over 30 Days.

Davoren, M.J. and Schiestl, R.H., 2018. Glyphosate Based Herbicides and Cancer Risk: A Post IARC Decision Review of Potential Mechanisms, Policy, and Avenues of Research.

Chapter 1: Introduction

Carcinogenesis: A Case for Early Intervention

Cancers take a heavy toll on both life and economy in developed nations. By 2020, the cost of cancer care in the United States is projected to reach 173 billion dollars per year [1]. However, many of the difficulties posed by cancers come with how late treatment is often implemented. In many cases, screening and detection only occur at high staging, when cancers are more likely to be metastatic and resistant to treatment, cutting 5-year survival rates and ballooning costs. If cancers are treated earlier in development, outcomes improve [2, 3]. Most effective of all would be interventions that reduce risk before a putative tumor cell acquires the set of mutations necessary to initiate oncogenesis in the first place. The accumulation of mutations and DNA damage is strongly associated with genotoxic and inflammatory events over a lifetime. Management of this damage by actively inducing anti-inflammatory processes and repair poses a new method to lower cancer risk using our growing understanding of these complex processes.

Ionizing Radiation and DNA Damage

At high levels, the damage caused by ionizing radiation (IR) exposure can be lethal. Acute radiation exposure syndrome (ARS) from doses above about 5 Gy will kill a human, with victims irradiated above even about 2 Gy suffering from hematopoietic ARS [4]. Although pharmaceutical interventions are currently under development, at the moment only swift bone marrow transplantations are capable of saving individuals, but even those have a low success rate at higher levels of irradiation [5, 6]. In survivors, exposure to such radiation levels is strongly associated with cancer development [7-10].

Ionizing radiation is a “complete carcinogen,” capable of both cancer induction and promotion [11-13]. Carcinogenic induction occurs through the relatively straightforward mechanism of DNA damage, leading to mutations and genome rearrangements that can disable

tumor suppressing genes and activate oncogenes. Ionizing radiation can induce DNA damage in two different ways. Direct damage occurs when the particle or photon directly impacts the DNA strand, transferring enough energy to ionize the molecule and break bonds. IR can also ionize water into reactive oxygen species (ROS) by a process called radiolysis. These free radicals are responsible for 50-80% of total damage induction. Both types of IR induced damage are completed on the order of seconds [4, 14-16]. Of all damage events, double strand breaks (DSBs) are some of the most consequential and carcinogenic. If not repaired accurately, these breaks can lead to necrosis, apoptosis, chromosomal aberrations, and loss of genome stability [4]. Loss of genome stability, in particular, can strongly accelerate oncogenic progression [17-19]. Chapter 4 of this dissertation describes how mouse models can be used to study the mechanisms by which ionizing radiation induces cancers, and how interventions might reduce risk or delay progression [20].

Double-Strand DNA Break (DSB) Repair

Any incidence of DNA damage can potentially introduce mutations that increase risk of carcinogenesis, but the induction of a double strand break is a catastrophic event for a cell's genome. The cell must quickly decide how to repair the break, as the induction of multiple unrepaired breaks in the same area make repair exponentially more difficult [21]. A common first event in DSB repair is the engagement of the MRX complex (MRN in humans). RAD50 proteins, with their long tails, physically hook together and sterically constrain both sides of the break [22]. Mre11 and Xrs2 (Nbs1 in humans) are capable of signaling to multiple downstream effectors, including general proteins that signal to the rest of the cell that repair is necessary, such as ATM, or specific enzymes that will push the repair process into one of two overarching courses [23]. The major DSB repair pathways of homologous recombination (HR) and nonhomologous end joining (NHEJ) deviate at an end processing decision point: If the core NHEJ proteins Ku70 and 80 cap the broken ends, they prevent further resection of the

overhanging strand, a step necessary for progression down the HR pathway [22, 24]. In humans (but not yeast) Ku proteins recruit the catalytic subunit of DNA-dependent protein kinase (DNA-PKcs), which is capable of phosphorylating the histone H2AX, relaxing chromatin and allowing further repair proteins more access to the break site [25]. The DNA ligase IV complex (with Lif1 and Nej1 in yeast, XRCC4 and XLF in humans) is recruited to the site to do the actual ligation [26]. Active presence of this complex inhibits HR of the break site, and recruits Pol4 and Rad 27 to further process gaps and flaps [27]. Evidence suggests that if NHEJ does not proceed in a timely manner, capping proteins may dissociate, allowing for strand resection and progression down another repair pathway – either HR or the particularly mutagenic microhomology-mediated end joining (MMEJ) pathway, a repair method of last resort [22, 28]. MMEJ can be induced by irradiation in human cells, and its propensity for errors and deletions may contribute to the development of radiotherapy resistance in cancers [29]. HR functions most accurately when the sister chromatid of the damaged site, present only after S-phase, is used as the template, although other sources of homologous DNA can serve as potential templates for less precise repair [30]. Both HR and MMEJ are less accurate than NHEJ during G_0/G_1 [31].

Key events in the alternative decision to go down the homologous repair pathway stem from the resection of broken strands. Without Ku caps, Mre11 endonuclease activity slowly chews back the strand, exposing ssDNA [32]. In humans, this process is assisted by the BRCA1 gene [33]. Single strand DNA is a magnet for the RPA protein but this is soon displaced by Rad51 (with the help of other proteins), which promotes strand invasion to homologous dsDNA, leading to HR [34]. Alternatively, RAD52 can directly overcome RPA and promote direct annealing to complementary single strand sequences, leading to single strand annealing (SSA), an intrachromosomal subpathway of HR [35]. While true HR requires a sister chromatid or second chromosome to serve as the template (leading to better accuracy) this limits its implementation. SSA, while generally inducing deletions, only requires long (>100bp) regions of homology within a single chromosome [34].

Both of these pathways are important in the recovery of a cell following irradiation. NHEJ, however, is a more versatile rejoining method, capable of rescuing double-strand breaks without backup templates. As repair progresses, HR often comes to predominate; NHEJ enzymes like Ku are displaced and DNA resected. HR, though, has a weakness: the presence of a donor sequence cannot be determined until a strand has already committed to HR via resection [22]. If HR fails at this point, DSBs are left unrepaired, a prospect that will surely be fatal [36]. NHEJ, which may not repair with as high fidelity under ideal conditions, are capable of impressive accuracy under conditions that HR fails. Chapter 2 of this dissertation describes the development of a radiation mitigator compound which might modulate the choice between repair processes in irradiated cells.

Inflammation and DNA Damage

Inflammation is a double-edged sword. Transient inflammatory cascades are designed to quickly and effectively mobilize the body's defenses to meet the source of damage, destroying invaders and stimulating repair. However, chronic inflammation is extremely damaging to the body, perpetuating cascades of cytokine and oxidative stress that can cause great harm instead [37]. This process is strongly associated with genotoxicity and carcinogenesis epidemiologically [38]. For example, chronic inflammation of the colon is associated with the risk of colon cancer [39].

Although localized inflammation can often lead to higher levels of damage and therefore cancer risk at the specific site [40], any source of chronic inflammation in the body contributes to total inflammatory load and ultimately systemic genotoxicity [41]. Reactive oxygen and nitrogen species (ROS and RNS), such as hydrogen peroxide and NO, are produced by immune cells as part of the inflammatory cascade. Chronic inflammation is associated with increased lipid peroxidation and genotoxic ROS, RNS, and aldehyde production [42]. These compounds and their byproducts can cause direct damage to DNA, and are designed to make quick work of

pathogens [43]. Chronic production, though, causes collateral damage to human cells, which can often still emigrate to other sites in the body. At the same time, inflammatory cytokine production can reach levels high enough to induce autonomous, cytokine-receptor mediated feedback cascades of free radicals and genotoxic damage systemically [41]. The induction of these inflammatory, defense oriented signaling pathways themselves is also associated more directly with cancer. For example, overactivation of the inflammation-driving complex NF-κB is strongly associated with carcinogenesis [44]. Pro-growth signaling processes, intended to induce regrowth and repair following tissue damage, could act as a pseudo "first hit" for oncogenic initiation if induced for an anomalously long period of time [45, 46].

The microbiome and Inflammation

The human gastrointestinal (GI) tract is home to over 500 species of bacteria in a given individual [47]. Revised estimates suggest that there are roughly as many bacterial cells as human cells in a human body [48]. The microbiome has been demonstrated to have an impact on many aspects of human health, including inflammatory state. Certain microbiome compositions are a risk factor for inflammatory bowel diseases (IBDs) such as Crohn's Disease and ulcerative colitis [49]. Gut dysbiosis is well associated with increased cancer risk via the inflammation that it induces. Some studies have estimated that up to 20% of cancers are linked with a microbial infection [50]. Mucosal associated tissue lymphomas, for instance, are associated with bacterial inflammation and colitis [51]. The stomach pathogen *H. pylori* is especially strongly linked to stomach inflammation and gastric cancers [52, 53].

Other resident bacteria play more beneficial roles. The presence of bacteria in the gut is critical for the development of healthy immune system function [54]. Some strains have been suggested to exert influence on host inflammatory signaling during close association with the gut mucosa, such as by decreasing the function of the pro-inflammatory transcription factor NF-κB [55]. Other studies have shown an immunoregulatory effect through regulatory T cell (Treg)

induction [56]. Probiotic strains are strains that have some sort of beneficial effect on human health. Many claims have been made about the wondrous capabilities of probiotics in recent years, and some of them lean towards pseudoscience. However, it is clear that many species of probiotic bacteria have the capability to mitigate inflammation in the gut through multiple mechanisms.

One of the most clearly demonstrable means by which probiotic strains can reduce inflammation is by reducing the adherence and subsequent activity of pathogenic strains. This useful service can be performed via a number of mechanisms, including competition for nutrients and binding sites in the host [57], and by the production of bacteriocins, acids, and other compounds [58-60]**.** Lactic acid bacteria (LAB), like the *Lactobacillus* and Bifidobacterium genera, are some of the best known probiotic bacteria. Multiple probiotic formulations, including many using these bacteria, have been shown to reduce the duration of diarrhea and enterocolitis in children [61]. In Chapter 3, we describe a *Lactobacillus johnsonii* strain previously associated with anti-inflammatory outcomes in a mouse model [62], and show its capacity for inhibiting pathogen adhesion in a model of the human gut epithelial mucosa.

1. Mariotto, A.B., et al., *Projections of the cost of cancer care in the United States: 2010–2020.* Journal of the National Cancer Institute, 2011. **103**(2): p. 117-128.
2. Sant, M., et al., *Stage at diagnosis is a key explanation of differences in breast cancer survival across Europe.* International journal of cancer, 2003. **106**(3): p. 416-422.
3. Balch, C.M., et al., *Final version of the American Joint Committee on Cancer staging system for cutaneous melanoma.* Journal of Clinical Oncology, 2001. **19**(16): p. 3635-3648.
4. Hall, E.J. and A.J. Giaccia, *Radiobiology for the Radiologist*. 2006: Lippincott Williams & Wilkins.
5. Classen, J., et al., *Radiation-induced gastrointestinal toxicity. Pathophysiology, approaches to treatment and prophylaxis.* Strahlentherapie und Onkologie: Organ der Deutschen Rontgengesellschaft...[et al], 1998. **174**: p. 82-84.
6. Saha, S., et al., *Bone marrow stromal cell transplantation mitigates radiation-induced gastrointestinal syndrome in mice.* PLoS One, 2011. **6**(9): p. e24072.
7. McGregor, D.H., et al., *Breast cancer incidence among atomic bomb survivors, Hiroshima and Nagasaki, 1950–69.* Journal of the National Cancer Institute, 1977. **59**(3): p. 799-811.
8. Preston, D., et al., *Solid cancer incidence in atomic bomb survivors: 1958–1998.* Radiation research, 2007. **168**(1): p. 1-64.
9. Preston, D.L., et al., *Cancer incidence in atomic bomb survivors. Part III: Leukemia, lymphoma and multiple myeloma, 1950-1987.* Radiation research, 1994. **137**(2s): p. S68-S97.
10. Thompson, D.E., et al., *Cancer incidence in atomic bomb survivors. Part II: Solid tumors, 1958-1987.* Radiation research, 1994. **137**(2s): p. S17-S67.
11. Barcellos-Hoff, M.H. and S.A. Ravani, *Irradiated mammary gland stroma promotes the expression of tumorigenic potential by unirradiated epithelial cells.* Cancer Res, 2000. **60**(5): p. 1254-60.
12. Little, J.B., *Radiation carcinogenesis.* Carcinogenesis, 2000. **21**(3): p. 397-404.
13. Fry, R., et al., *Studies on the Multistage Nature of Radiation Carcinogenesis.* 1982.
14. Brenner, D. and J. Ward, *Constraints on energy deposition and target size of multiply damaged sites associated with DNA double-strand breaks.* International journal of radiation biology, 1992. **61**(6): p. 737-748.
15. Hill, M., *Radiation damage to DNA: the importance of track structure.* Radiation measurements, 1999. **31**(1): p. 15-23.
16. Korystov, Y.N., *Contributions of the direct and indirect effects of ionizing radiation to reproductive cell death.* Radiation research, 1992. **129**(2): p. 228-234.
17. Huang, L., A.R. Snyder, and W.F. Morgan, *Radiation-induced genomic instability and its implications for radiation carcinogenesis.* Oncogene, 2003. **22**(37): p. 5848.
18. Morgan, W.F., *Non-targeted and delayed effects of exposure to ionizing radiation: II. Radiation-induced genomic instability and bystander effects in vivo, clastogenic factors and transgenerational effects.* Radiation research, 2003. **159**(5): p. 581-596.

19. Morgan, W.F., *Non-targeted and delayed effects of exposure to ionizing radiation: I. Radiation-induced genomic instability and bystander effects in vitro.* Radiation research, 2003. **159**(5): p. 567-580.
20. Rivina, L., M.J. Davoren, and R.H. Schiestl, *Mouse models for radiation-induced cancers.* Mutagenesis, 2016. **31**(5): p. 491-509.
21. Lisby, M., U.H. Mortensen, and R. Rothstein, *Colocalization of multiple DNA double-strand breaks at a single Rad52 repair centre.* Nature cell biology, 2003. **5**(6): p. 572-577.
22. Daley, J.M., et al., *Nonhomologous end joining in yeast.* Annu. Rev. Genet., 2005. **39**: p. 431-451.
23. Nakada, D., K. Matsumoto, and K. Sugimoto, *ATM-related Tel1 associates with double-strand breaks through an Xrs2-dependent mechanism.* Genes & development, 2003. **17**(16): p. 1957-1962.
24. Mimitou, E.P. and L.S. Symington, *Ku prevents Exo1 and Sgs1-dependent resection of DNA ends in the absence of a functional MRX complex or Sae2.* The EMBO journal, 2010. **29**(19): p. 3358-3369.
25. Park, E.J., et al., *DNA-PK is activated by nucleosomes and phosphorylates H2AX within the nucleosomes in an acetylation-dependent manner.* Nucleic acids research, 2003. **31**(23): p. 6819-6827.
26. Yang, H., et al., *Role of the yeast DNA repair protein Nej1 in end processing during the repair of DNA double strand breaks by non-homologous end joining.* DNA repair, 2015. **31**: p. 1-10.
27. Zhang, Y., et al., *Role of Dnl4–Lif1 in nonhomologous end-joining repair complex assembly and suppression of homologous recombination.* Nature structural & molecular biology, 2007. **14**(7): p. 639-646.
28. Pace, P., et al., *Ku70 corrupts DNA repair in the absence of the Fanconi anemia pathway.* Science, 2010. **329**(5988): p. 219-223.
29. Dutta, A., et al., *Microhomology-mediated end joining is activated in irradiated human cells due to phosphorylation-dependent formation of the XRCC1 repair complex.* Nucleic acids research, 2016. **45**(5): p. 2585-2599.
30. Sonoda, E., et al., *Sister chromatid exchanges are mediated by homologous recombination in vertebrate cells.* Molecular and cellular biology, 1999. **19**(7): p. 5166-5169.
31. Ottaviani, D., M. LeCain, and D. Sheer, *The role of microhomology in genomic structural variation.* Trends in Genetics, 2014. **30**(3): p. 85-94.
32. Sartori, A.A., et al., *Human CtIP promotes DNA end resection.* Nature, 2007. **450**(7169): p. 509-514.
33. Powell, S.N. and L.A. Kachnic, *Roles of BRCA1 and BRCA2 in homologous recombination, DNA replication fidelity and the cellular response to ionizing radiation.* Oncogene, 2003. **22**(37): p. 5784-5791.
34. Jasin, M. and R. Rothstein, *Repair of strand breaks by homologous recombination.* Cold Spring Harbor perspectives in biology, 2013. **5**(11): p. a012740.
35. Davis, A.P. and L.S. Symington, *The yeast recombinational repair protein Rad59 interacts with Rad52 and stimulates single-strand annealing.* Genetics, 2001. **159**(2): p. 515-525.
36. Lord, C.J. and A. Ashworth, *BRCAness revisited.* Nature Reviews Cancer, 2016.

37. Reuter, S., et al., *Oxidative stress, inflammation, and cancer: how are they linked?* Free Radical Biology and Medicine, 2010. **49**(11): p. 1603-1616.
38. Grivennikov, S.I. and M. Karin, *Inflammation and oncogenesis: a vicious connection.* Current opinion in genetics & development, 2010. **20**(1): p. 65-71.
39. Meira, L.B., et al., *DNA damage induced by chronic inflammation contributes to colon carcinogenesis in mice.* The Journal of clinical investigation, 2008. **118**(7): p. 2516-2525.
40. Schetter, A.J., N.H. Heegaard, and C.C. Harris, *Inflammation and cancer: interweaving microRNA, free radical, cytokine and p53 pathways.* Carcinogenesis, 2009. **31**(1): p. 37-49.
41. Westbrook, A.M., et al., *Intestinal mucosal inflammation leads to systemic genotoxicity in mice.* Cancer research, 2009. **69**(11): p. 4827-4834.
42. Bartsch, H. and J. Nair, *Chronic inflammation and oxidative stress in the genesis and perpetuation of cancer: role of lipid peroxidation, DNA damage, and repair.* Langenbeck's Archives of Surgery, 2006. **391**(5): p. 499-510.
43. Krieglstein, C.F., et al., *Regulation of murine intestinal inflammation by reactive metabolites of oxygen and nitrogen: divergent roles of superoxide and nitric oxide.* Journal of Experimental Medicine, 2001. **194**(9): p. 1207-1218.
44. Gudkov, A.V. and E.A. Komarova, *p53 and the carcinogenicity of chronic inflammation.* Cold Spring Harbor perspectives in medicine, 2016. **6**(11): p. a026161.
45. Grivennikov, S.I., F.R. Greten, and M. Karin, *Immunity, inflammation, and cancer.* Cell, 2010. **140**(6): p. 883-899.
46. Vogelstein, B. and K.W. Kinzler, *The multistep nature of cancer.* Trends in genetics, 1993. **9**(4): p. 138-141.
47. Ciorba, M.A., *A gastroenterologist's guide to probiotics.* Clinical gastroenterology and hepatology, 2012. **10**(9): p. 960-968.
48. Sender, R., S. Fuchs, and R. Milo, *Revised estimates for the number of human and bacteria cells in the body.* PLoS biology, 2016. **14**(8): p. e1002533.
49. Sheehan, D., C. Moran, and F. Shanahan, *The microbiota in inflammatory bowel disease.* Journal of gastroenterology, 2015. **50**(5): p. 495-507.
50. Elinav, E., et al., *Inflammation-induced cancer: crosstalk between tumours, immune cells and microorganisms.* Nature reviews. Cancer, 2013. **13**(11): p. 759.
51. Yamamoto, M.L. and R.H. Schiestl, *Intestinal microbiome and lymphoma development.* Cancer journal (Sudbury, Mass.), 2014. **20**(3): p. 190.
52. Smoot, D.T., et al., *Influence of Helicobacter pylori on reactive oxygen-induced gastric epithelial cell injury.* Carcinogenesis, 2000. **21**(11): p. 2091-2095.
53. Group, E.S., *An international association between Helicobacter pylori infection and gastric cancer.* The Lancet, 1993. **341**(8857): p. 1359-1363.
54. Hooper, L.V., D.R. Littman, and A.J. Macpherson, *Interactions between the microbiota and the immune system.* Science, 2012. **336**(6086): p. 1268-1273.
55. van Baarlen, P., et al., *Human mucosal in vivo transcriptome responses to three lactobacilli indicate how probiotics may modulate human cellular pathways.* Proceedings of the National Academy of Sciences, 2011. **108**(Supplement 1): p. 4562-4569.
56. Smits, H.H., et al., *Selective probiotic bacteria induce IL-10–producing regulatory T cells in vitro by modulating dendritic cell function through dendritic cell–specific intercellular*

adhesion molecule 3–grabbing nonintegrin. Journal of Allergy and Clinical Immunology, 2005. **115**(6): p. 1260-1267.
57. Servin, A.L. and M.-H. Coconnier, *Adhesion of probiotic strains to the intestinal mucosa and interaction with pathogens.* Best Practice & Research Clinical Gastroenterology, 2003. **17**(5): p. 741-754.
58. Barefoot, S.F. and T.R. Klaenhammer, *Detection and activity of lactacin B, a bacteriocin produced by Lactobacillus acidophilus.* Applied and Environmental microbiology, 1983. **45**(6): p. 1808-1815.
59. Ocaña, V.S. and M.E. Nader-Macías, *Production of antimicrobial substances by lactic acid bacteria II: screening bacteriocin-producing strains with probiotic purposes and characterization of a Lactobacillus bacteriocin.* Public Health Microbiology: Methods and Protocols, 2004: p. 347-353.
60. Midolo, P., et al., *In vitro inhibition of Helicobacter pylori NCTC 11637 by organic acids and lactic acid bacteria.* Journal of Applied Bacteriology, 1995. **79**(4): p. 475-479.
61. Reid, G., et al., *Potential uses of probiotics in clinical practice.* Clinical microbiology reviews, 2003. **16**(4): p. 658-672.
62. Yamamoto, M.L., et al., *Intestinal bacteria modify lymphoma incidence and latency by affecting systemic inflammatory state, oxidative stress, and leukocyte genotoxicity.* Cancer research, 2013. **73**(14): p. 4222-4232.

Chapter 2: Mitigation of Genotoxicity and Hematopoietic Depletion by Yel002

ABSTRACT

Ionizing radiation (IR), capable of inducing widespread damage to both cellular structures and genetic information, is a potent threat to the survival of cells and organisms. Significant levels of exposure can kill a cell or individual outright, but even survivors are left with damage to their genetic material such as DNA strand breaks. Multiple competitive DNA repair pathways, each with their own set of requirements and disadvantages, work to repair these breaks after insult. As each pathway is closely linked with other critical cell systems such as cycling, survival, and apoptosis, modulation of these repair pathways could serve as a potential point of pharmaceutical intervention against genotoxicity and lethality induced by IR and other sources of damage.

A druglike small molecule, Yel002, was previously uncovered via a high-throughput cytotoxicity and genotoxicity yeast screen using the DEL assay. Yel002 and its derivative molecules appear capable of mitigating IR-induced damage via modulation of cell survival and DNA repair pathways. The compounds activity as an “ideal mitigator” – one that decreases both lethality and long term genotoxic effects - spans from yeast to vertebrates. Treatment up to 24 hours after otherwise lethal levels of irradiation is capable of protecting the hematopoietic stem cell niche in mice, allowing for full recovery in some animals. Weekly treatment also increases median life expectancy in cancer-prone, DNA repair deficient mouse models. Protein and mRNA analysis showed upregulation of double-strand break repair and survival pathways in exposed murine lymphocytes. Although quality control and stability issues led to some inconsistency in vertebrate models, Yel002’s development serves as a proof-of-concept for the use of small molecules to modulate DNA repair pathways in response to genotoxic threats, and establishes a framework by which future interventions can be judged.

INTRODUCTION

Potential sources of ionizing radiation (IR) are widespread in the modern world. Key technologies involved in energy production, medicine, war, and even space travel all lead to scenarios is which exposure is common [1]. While careful engineering and policy implementation will doubtless play a critical role in limiting exposure, the development of interventions capable of mitigating biological damage after exposure is equally important.

The risk of a terrorist attack utilizing a “dirty bomb” method of radioactive material release is considered to be a very real threat by the United States government [2]. At the same time, a growing number of nations maintain or are in the process of developing a nuclear arsenal [3]. The 2011 Fukushima reactor leak demonstrated that unintentional releases of large amounts of radioactive material pose a public health risk, as well [4]. With all of these potential sources of large-scale ionizing radiation, a massive public exposure scenario is well within the realm of possibility. The National Cancer Institute (NCI) and other organizations have recognized the gap in our medical capability to respond to radiation emergencies and have identified research priorities, including the development of chemical countermeasures [5].

In such an emergency, treating acute radiation exposure syndrome (ARS) is the top priority. ARS at doses relevant to humans can be divided into three categories. At the highest doses (> 12 Gy) cerebrovascular syndrome leads to unavoidable death within 24-48 hours, depending on the dose [6]. At intermediate doses (~5-12 Gy) the compromise of the gastrointestinal mucosal barrier (GI-ARS) leads to probable death within ten days. Only “heroic” treatments, such as immediate access to isolated intensive care units and bone marrow transplants, are capable of saving these patients, but at higher levels of exposure even this treatment may fail [7, 8]. Victims irradiated between 2 and 5 Gy will suffer from hematopoietic ARS [9]. The untreated human IR LD50 falls at roughly 4 Gy because of this syndrome [10]. Swift action such as bone marrow transplantation is a relatively reliable treatment in this range, but experts have estimated that in a catastrophic situation delays of up to 24 hours may occur

before a first response can reach affected populations [11, 12]. In addition, bone marrow transplantations can be quite risky on their own, with roughly 40% of recipients dying to graft vs. host disease or other complications within the first year [13]. Xiao et al estimate that, with the detonation of a 1 kiloton nuclear device in a city of two million, roughly 100,000 individuals would be exposed to doses between 1.5 and 5 Gy [14]. This population should be prioritized for any distributable intervention capable of mitigating the effects of irradiation at the 24 hour mark.

Although preventing immediate death is the obvious priority, long term effects, such as highly elevated risk of cancers, are well documented in populations exposed to radiological disasters [15-18]. This fact must be kept in mind during the development of lethality mitigating compounds. One could quite easily propose the use of a hypothetical compound that might strongly suppress apoptotic cell programs and greatly upregulate cell proliferation after IR-induced depletion of the bone marrow, but heavily add to the sum total cancer incidence in survivors. An ideal mitigator should promote cell survival and repair after irradiation, but not at a significant expense of tumor suppressing mechanisms.

The compound Yel002 was previously identified using a high throughput screen of over 5000 compounds from a synthesized chemical library (ASINEX) as a candidate molecule for the mitigation of radiation induced damage in yeast [19]. The selection process used, the DEL assay, comprises a sensitive method for the detection of both carcinogenic and cytotoxic compounds, significantly outperforming commonly used assays such as the Ames assay [20-22]. This sensitivity also allows the DEL assay to be used in the identification of compounds that mitigate cytotoxic and genotoxic effects, particularly those that interfere with the generation of double-strand breaks and subsequent induction of deletion events by homologous recombination (HR) and single-strand annealing (SSA) based repair processes.

The experimental evidence presented in this article suggests that Yel002 has a significant impact on pro-survival and DNA repair pathways, although it is not yet clear whether these profound effects are the result of multiple binding targets or the intrinsically

linked nature of these pathways in the cell. The compound's range of efficacy is impressive so far – mitigation of IR-induced damage is observed in yeasts, human cells, and both murine cell culture and full animal models. Although most tests described use IR as a prototypical inducer of double-strand breaks and cell death, the scope of mitigation applies to other sources of genotoxicity as well. Application of the compound helps to rescue the carcinogenic effects of some genetic DNA repair deficiencies, such as ataxia telangiectasia mutated (ATM) and base excision repair (BER) defects. The compound has also previously been shown to work synergistically with perchlorate to prophylactically prevent the induction of DSBs induced by radioactive I-131 [23].

RESULTS

Yel002 reduces IR-induced DNA deletions and lethality in RS112 yeast. Compound efficacy was tested with the more accurate plated viability DEL assay (**Fig. 1**). The addition of Yel002 after exposure to irradiation increased viable CFU from 3.46% to 5.50% ($p<0.05$) and decreased the number of DEL events from 12.38 to 4.47 per 10,000 surviving cells ($p<.0001$).

Yel002 reduces IR-induced cell death in Til-1 murine lymphocytes. To assess viability in mammalian cells, post irradiation Yel002 treatment was tested in a murine lymphocyte model (**Fig. 2)** After otherwise lethal IR, compounds were loaded onto cells and after 24hrs viability was assessed with luminescence-based measurement of ATP production. Yel002 concentrations of .001 and .01 μM had no significant effect on ATP production, but 10 and 50 μM increased luminescence by roughly 50% vs. untreated irradiated cells ($p<0.05$)

Yel002 incubation induces transcriptional changes in Til-1 cells. RNA sequencing analysis (RNA-seq) was used to analyze changes in expression level for a broad array of mRNAs following a 7 hour incubation with Yel002 after radiation. Genes differentially affected by Yel002 exposure after radiation are detailed in **Table 1.** 35 genes modulated by radiation (either reduced or increased in expression) had their IR-induced change mitigated or reversed by

subsequent Yel002 exposure. Of these 35 genes, 3 involved in regulation of cell survival and apoptosis were chosen for secondary analysis by RT-qPCR: *Tgfβ3* (Transforming growth factor beta 3), *Pik3ip1* (Phosphoinositide-3-kinase-interacting protein 1) and *Chac1* (Botch, Cation transport regulator-like protein 1). **Figure 3** shows small but significant decreases in *Pik3ip1* ($p=0.018$) and *Chac1* ($p<0.001$) mRNA in unirradiated Yel002 treated cells – a reversal of the small inductions seen in those two genes with Yel002 exposure alone. Interestingly, there was no significant difference in Tgfβ3 levels as measured by qPCR.

Yel002 incubation induces changes in detectable protein in Til-1 cells. A Kinexus microarray was used to examine differentially activated signaling pathways in Til-1 cells after a one hour incubation with Yel002. Of the 800 different antibodies this array, 270 have affinity for specific phosphorylation states of target proteins. Our screen revealed 110 significantly altered (Z-score > 1.5) protein expression or phosphorylation states in response to Yel002 exposure alone, which are fully detailed in **Supplemental Table 1.** Protein levels with significant changes between irradiated control cells and irradiated Yel002 treated cells represented perturbations in pathways related to growth, apoptosis, and cell cycling. These changes are detailed in **Table 2**.

Yel002 mitigates radiation-induced senescence and affects proteins involved in cell cycling. Yel002 in DMSO solvent was added to primary human oral keratinocyte culture (NHOKs) after a dose of 5 Gy of radiation, normally sufficient to induce senescence. Two weeks after irradiation, cells treated with 10μM Yel002 had roughly 5 times the cell density of DMSO treated controls (**Figure 4*a***). The levels of 5 proteins directly involved in cell cycling and senescence were analyzed via western blot (**Figure 4*b*)**. Regardless of irradiation, the phosphorylation state of retinoblastoma-associated protein (pRb) tended to increase gradually over the course of the experiment with Yel002 treatment. Yel002 treatment conversely decreased levels of the cyclin-dependent kinase inhibitors p16 and p21. No significant effect was observed on levels of Bmi1 or PCNA.

Yel002 increases RAD50 levels in the presence of the translation inhibitor cycloheximide. EBV-immortalized human lymphoblastoid cells were incubated with Yel002 to determine its effects on components of the MRN complex. 24 hours of Yel002 incubation significantly increased MRE11 levels ($p < 0.05$) (**Figure 5**). No increase, however, was observed when translation of new proteins was blocked by co-incubation with cycloheximide (CHX), suggesting that this increase is due to *de novo* protein synthesis. Levels of RAD50 showed the opposite effect, with a significant increase only observed with Yel002 and CHX co-incubation vs. a decreased amount of detectable RAD50 when translation was inhibited, suggesting that Yel002 leads to stabilization of that protein rather than synthesis.

γH2AX foci are decreased in base excision repair deficient mouse peripheral blood lymphocytes treated with Yel002 after cigarette smoke extract exposure. To ascertain whether Yel002 could mitigate damage to lymphocytes exposed to other sources of genotoxic damage, mouse peripheral blood lymphocytes from wild type and $Ogg^{-/-}$ / $Myh^{-/-}$ double knockout (OMM) mice were exposed to cigarette smoke extract (CSE). γH2AX foci, indicative of double strand breaks, were greatly elevated in WT exposed mice, and even further in exposed OMM mice (**Figure 6**). Interestingly, Yel002 treatment did not significantly affect average foci per cell after CSE exposure in wild type mice. However, treatment significantly reduced foci in base excision repair deficient OMM mice at both 6 ($p < 0.05$) and 24 ($p < 0.01$) hours post exposure, bringing γH2AX levels down to that of wild type CSE exposed mice.

Yel002 mitigates lethality in lethally irradiated mice. To determine the extent of Yel002's mitigative capacity in irradiated vertebrates, C3H mice were exposed to 8 Gy of ionizing radiation (LD100/30). Yel002 subcutaneous treatment beginning one day after IR rescued 75% of irradiated animals that would have otherwise expired within the 30 day period critical for hematopoietic failure ($p = 0.0019$). Additionally, a full 50% of irradiated animals were otherwise healthy out to a year beyond initial irradiation (**Figure 7*a***). To establish Yel002's dose modifying factor (DMF) within the hematopoietic critical dose range, we exposed groups of C3H mice to

various doses ranging from 7 Gy to 9.1 Gy and subcutaneously treated with Yel002 on the same 5 x 24 protocol (**Figure 7*b***). Although Yel002 did not reduce lethality in the most heavily irradiated group, it significantly reduced death in all others, yielding a dose-modifying factor (DMF) of 1.15 by changing the LD50 from 7.185 in irradiated controls to 8.247 in treated mice.

Yel002 is relatively hydrophobic, and is difficult to dissolve in pure saline to the concentration necessary for efficacy in the mouse. Kolliphor EL, a surfactant excipient, was used for better suspension and systemic distribution of the drug. With 2% Kolliphor, the same dose of Yel002 led to 100% of mice surviving the LD100/30 dose through the month (**Fig. 7*c***).

Yel002 increases rate of hematopoietic recovery following sublethal irradiation. Blood samples were taken from mice irradiated at 6 Gy with or without Yel002 treatment in order to track the reconstitution of the hematopoietic system after IR-induced depletion. Differential blood count analysis was monitored during the well-established recovery period of 7 to 16 days post-exposure (**Fig. 8**). Levels of total white blood cells (WBC), neutrophils (NE), lymphocytes (LY), Eosinophils (EO), Monocytes (MO), Basophils (BA) and platelets (PLT) reached their respective nadirs at day 10 after irradiation. Importantly, Yel002 treated mice exhibited no significant difference in circulating cells of these categories at day 10, suggesting that Yel002 has no protective effect on circulating cells. However, recovery of all these parameters was hastened significantly in treated animals ($p < 0.05$). Hematocrit (HTC), hemoglobin (HB), and red blood cell (RBC) counts were not significantly changed by irradiation, nor did Yel002 treatment have any effect on them. Precise counts and p-values can be found in **Table 3**.

Yel002 treatment prolongs lifespan in DNA-repair deficient mice. Mice deficient in the ATM gene are deficient in double-strand break repair and develop lymphomas at a much higher rate than wild type mice. To determine whether Yel002 might be able to mitigate this cancer rate, *Atm*$^{-/-}$ mice were injected subcutaneously once weekly for their entire lives after genotyping. **Figure 9** is Kaplan-Meier plot of tumor-free survival. Untreated *Atm*$^{-/-}$ mice in the same room had a median lifespan of 48 weeks, but the 13 treated mice survived for a median of 64 weeks,

a significant increase ($p > 0.05$, chi square test). One treated mouse in particular survived for over two and a half years.

Yel002 reduces the rate of irradiation-induced leukemic induction in DBA/2 mice. Leukemia is also one of the common secondary cancers in radiotherapy patients, and can be induced by radiation exposure after a relatively short latency period [24]. The FDC-P1 post-IR injection model leads to leukemia in most irradiated mice due to IR-induced systemic effects such as granulocyte-macrophage colony stimulating factor (GM-CSF) release [25, 26]. In addition, a low number of animals develop leukemia from the injection of immortalized cells even in the absence of irradiation. Treatment with Yel002 significantly reduced the incidence of radiation induced leukemia from 90% in control animals to 40% ($p < 0.05$) Interestingly, the administration of Yel002 also decreased the rate of leukemia in unirradiated animals from 10% to 0% (**Figure 10**).

DISCUSSION

The development of pharmaceutical interventions against the biological effects of ionizing radiation is a high priority for a number of different fields. Beyond the treatment of ARS, radioprotectors and mitigators have been identified as an important potential solution to the biological damage accumulated by exposure to radiation during space travel [27] and as a co-treatment with radiation therapy of cancers, differentially protecting healthy tissue and allowing tumors to be treated with more effective, higher doses [28-31]. Currently, only a single agent is approved by the FDA (Food and Drug Administration) for the purpose of reducing radiation damage to healthy tissue. This agent, amifostine, is only functional in a radioprotective role, with intravenous administration given a few minutes prior to radiotherapy in clinical practice [32]. The use of other antioxidant compounds, such as glutathione, is known to give effective radioprotection, but these too only function in a protective manner [33-35]. Viable radiation mitigators, capable of rescue after IR, will need to act on mechanisms beyond that of simple

ROS scavenging. Bone marrow transplantation models have proven effective against both hematopoietic and GI-ARS, but this is a difficult procedure to implement in a disaster situation, or on a spacecraft or colony and has a middling success rate [8, 13, 36, 37]. Treatments are under development against tissue specific radiation injury, such as lung fibrosis or heart arrhythmias [38-40]. These protocols are an important addition to the radiation toolkit, but for total body irradiation rescue from hematopoietic depletion is the first priority, with maintenance of gastrointestinal integrity a close second. For strong candidate radiation mitigators, clear experimental benchmarks should be set based on the realities of emergency logistics: the rescue of a significant number of vertebrate animals, irradiated at a total body LD50/30 dose or above, with treatment initiated 24 hours after the event [11, 12].

Over the past few years, several different compounds have entered the development pipeline based on experimental results meeting those benchmarks. The most effective act on a number of disparate systems to stimulate cell survival and division in the wake of IR-induced depletion, but due to the complex nature of cell cycling and repair few have completely understood mechanisms. Hemamax, a recombinant IL-12, stimulates HPSC recovery and can rescue 70% of animals irradiated at LD70/30 doses. Vitamin E analogs, such as GTDMG and γ-tocotrienol have been shown to cause higher levels of post-IR rescue (~35%) than one would expect from an antioxidant mechanism alone, likely through stimulation of granulocyte-colony stimulating factor [41, 42]. The antithrombotic, activated protein C (aPC), increases survival by 40% in LD70/30 irradiated mice when administered 24 hours later [43]. Interestingly, several compounds that aim to directly mitigate GI-ARS have an effect against hematopoietic ARS as well. The somatostatin analog SOM230 inhibits pancreatic enzyme activity to improve GI survival after IR, but also improves survival in TBI mice [44]. Administration of the nitroxide JP4-039 within 24 hours of LD75/30 radiation doses mitigated damage to the intestinal epithelium but also prevented hematopoietic ARS death [45]. These results suggest connections between bone marrow and gastrointestinal ARS that are not yet fully understood. The stimulation of the

lysophosphatidic acid receptor (LPA2) pathway with direct receptor agonists appears to be a very promising point of intervention, especially for the mitigation of GI-ARS. Multiple agonist mitigators targeting this receptor have been identified and are under investigation, including octodenyl thiophosphate (IR-DMF: 1.2 for 6-8 Gy) and DBIBB, capable of increasing survival after IR by 50% even when treatment begins 24 hours later [46, 47]. Yel002's own hematopoietic mitigative capability seems to be comparable, with a DMF of 1.14 and 75%-100% rescue at the C3H mouse's LD100/30. Clearly, multiple biological pathways represent relevant targets for intervention against all forms of ARS.

These impressive results should be considered cautiously, though. Many of the mechanisms of recovery described above rely on strong inducers of growth and cell survival. While the immediate survival of the irradiated subject is obviously of primary importance, overriding apoptosis programs and normal growth limits could have carcinogenic consequences in survivors. For example, the LPA2 pathway is linked to the growth of some cancers [48]. TLR-5 activation, like that induced by Hemamax, is associated with proliferation and survival for some cancers [49-51], but growth inhibition in others [52, 53]. Such contrasting effects could potentially be exploited when well understood, allowing for the compound's use with radiotherapy as a differential protector of healthy cells. It is clear, though, that these compounds' mechanisms of action, and their long-term risk profiles, must be studied more thoroughly before use in humans. Experimentation with vertebrate models for different radiation induced cancers will be an important step in preclinical testing [54].

Having a large number of candidate radiation mitigators that operate via different mechanisms is beneficial. Different radiation exposure profiles lead to different types of DNA damage and even cancers. For example, high-LET ionizing radiation particles cause more clustered DNA damage in the cell than more distributed low-LET radiation exposure [55]. The dose-rate of exposure, rather than just the total dose, can affect the level of damage and even the type of repair preferentially used [56]. Ideally, an arsenal of well understood radiation

mitigators, functioning through different mechanisms, would allow for a carefully considered ARS intervention tailored to each individual case's exposure profile and genetics.

The compound Yel002 is a strong candidate addition to that arsenal, as its mechanism of action is likely different from that of other candidate mitigators so far. While most mitigators were designed to target a pathway, Yel002 was uncovered by a high-throughput screen for compounds capable of mitigating IR-genotoxicity and cytotoxicity, with no pretensions as to how [19, 20]. Although no direct binding partner was identified (despite failed attempts with biotin-tagged Yel002 pulldowns), a number of perturbations to components involved in the cell cycling, survival, and repair processes were detected.

Among the most important proteins found to be affected by Yel002 incubation was pRb, an important regulator of cell cycle progression through the G_1 phase. Incubation of NHOKs with Yel002 both with and without irradiation led to persistent, dose-dependent increases in pRb. Yel002 incubation alone also led to increases in the phosphorylation state of serine residue 807/811 in particular, a site suggested to "prime" for the phosphorylation of other residues on the protein [57]. Older models of pRb phosphorylation and cell cycle control suggested that pRb was gradually phosphorylated at more and more sites until it finally relinquished its grip on transcription factor E2F and allowed for cell cycle progression. More recent models suggest distinct roles for unphosphorylated, monophosphorylated, and hyperphosphorylated pRb [58]. Monophosphorylation of pRb by Cyclin D can occur at multiple locations, including s807/811, while unphosphorylated pRb promotes cell cycle exit and differentiation or senescence [59]. Importantly, the CyclinD:CDK4/6 complex is observed to become active in G_0 during a DNA damage response, essentially driving these cells to actively enter the early cell cycle via pRb monophosphorylation to undergo repair. Yel002's apparent induction of monophosphorylated Rb may be promoting mechanisms that drive irradiated cells out of quiescence and into active repair. Yel002 incubation also decreased the level of CDK inhibitors, p21 and $p16^{ink4a}$, both of which play a role in the induction of senescence and G_0 entry [60].

Cycloheximide experiments also revealed important effects on two proteins from the MRN complex, a critical protein involved in DSB repair. Mre11, the primary component of MRN, signals through ATM kinase, but also has independent nuclease activity of its own [61]. Yel002 lead to the increase in translation of new MRE11, but stabilized RAD50 rather than stimulated new production. This data fits with observations of MRE11 deficient cells in culture. These cells were unable to form functional MRN complexes to properly undergo S-phase arrest to repair DNA before replication, but transfection with MRE11 both rescued the S-phase arrest machinery and led to increased levels of MRN components RAD50 and NBS1 through stabilization, rather than *de novo* synthesis [62]. Knockdown of MRE11 has also been linked to higher levels of $p16^{ink4a}$, directly tying the increased levels of MRE11 to the increased phosphorylation state of Rb [63].

As a central axis of cell cycle progression, the pRb pathway is the downstream target of many mitogenic signals. The PI3K/AKT pathway is one of these, increasing pRb activation via increased cyclin D1 [64]. Multiple components of this pathway, including the PI3K negative regulators PTEN and PIKIP1 as well as AKT itself, were observed to be perturbed by Yel002 exposure in our various protein and mRNA screens. However, these perturbations were not consistent between irradiated and unirradiated cells. Without IR, Yel002 exposure decreased *Pi3kip* and *Chac1* mRNA vs. control exposures, but with IR Yel002 increased them beyond levels in control irradiated cells. A similar situation occurs with the negative regulator PTEN. Total protein levels rise with Yel002 incubation alone, but in irradiated cells incubated with Yel002 lower levels of triple-phosphorylated PTEN are detected. The phosphorylation of these three sites, 380, 382, and 385, is associated with decreased activity against PTEN substrates [65]. The inconsistent effects of Yel002 vs. Yel002 and irradiation on these high-level signaling effectors suggests that they are likely not the direct targets. Instead, the vacillating transcript, protein, and phosphorylation levels could be systemic attempts to normalize signaling via

perturbation induced by Yel002 elsewhere in the cell, as this pathway is connected to many cell functions related to growth and survival [66].

Yel002's effects do not solely relate to cell division and survival. The screen from which it was chosen specifically selected for molecules that also reduce the incidence of reversion events. A DEL event is the induction of a deletion at the site of a DSB within the gene cassette as part of a specific successful repair process. Only the single strand annealing (SSA) subpathway of homologous recombination (HR) will lead to deletion of the *Leu* gene around the site of the break, switching trophic condition from leucine to histidine autotrophy [20, 67]. Decreased observation of DEL events in these experiments does not signify a reduction in double strand breaks, as most direct damage from ionizing radiation and secondary radiolysis-induced ROS damage (responsible for 50-80% of total DSB induction) is complete on the order of seconds [9, 68-70]. Rather, the observed effect might result from the preferential shunting of DNA repair from deletion-inducing HR to another competitive pathway, such as nonhomologous end-joining (NHEJ) [71, 72].

With regard to cigarette smoke induced oxidative damage, Yel002 had no direct mitigative effect in mice with a fully functional base excision repair (BER) pathway, but rescued elevated sensitivity in BER deficient animals. The promotion of an alternative DNA repair mechanism in those cases – for example, complete removal of the damaged bases by end processing prior to NHEJ - could remove the same 8-oxo-G lesions that BER normally would, albeit in a more complicated way [73].

Functional ATM is clearly dispensable for Yel002 activity based on ATM-deficient mouse experiments. The ATM protein is a critical repair/cell cycle signaling protein, and repair defective mice exhibit a cancer prone phenotype much like human ataxia telangiectasia sufferers [74]. The promotion of an alternative pathway for DSB repair, rather than HR, could explain the increased lifespan and decreased cancer rate in these animals as well. ATM is critical for DSB repair via HR, especially in the G_2 phase of the cell cycle [75], but is less important for NHEJ.

For example, cells deficient in MRE11 or NBS1, but not ATM, exhibit a major repair defect in NHEJ repair of DSBs during G_1 [76].

Yel002's inhibition of leukemic transformation also gives evidence that its mechanism is not the simple promotion of growth. FDC-P1 cells have a very low (~$1/10^9$ cells) rate of spontaneous leukemic transformation after injection, and are generally dependent on the post-irradiation microenvironment to proceed with carcinogenesis [77, 78]. Yel002 decreased the spontaneous rate of leukemia as well as the IR-induced rate, suggesting that the mechanism by which this occurred did not necessarily rely on countering the effects of radiation itself on the microenvironment. Increased repair fidelity in the pre-leukemic cells, though, might prevent the accumulation of further genetic hits leading to full blown cancer.

Yel002 clearly promotes survival and hematopoietic recovery from the stem cell niche, as evidenced by the recovery kinetics. In a healthy mammal, roughly 90% of HSCs are in a quiescent G_0 at any given time [79]. NHEJ is the preferred mechanism of DSB repair for both G_0 and G_1 phase cells, particularly in progenitors first emerging into the cell cycle [80, 81]. Yel002's promotion of HSC recovery may be based on induction of entry into G_1 and promotion of NHEJ repair through a mechanism related to pRb or another cell cycle modulator.

Although NHEJ is often referred to as more error-prone than HR, it is a more versatile repair mechanism due to its lack of a template requirement. Strong activation of NHEJ is preferable when the lack of sister chromatid makes HR less conducible, as in cells irradiated during early G_0/G_1 [82]. Importantly, the upregulation of NHEJ machinery could competitively inhibit the use of even more error prone repair methods, like microhomology mediated recombination (MMEJ). MMEJ is induced by irradiation in human cells, and its propensity for errors and deletions may contribute to the development of radiotherapy resistance in cancers [83]. Both HR and MMEJ are less accurate than NHEJ during G_0/G_1 [84]. Because HPSCs in this phase are the target of mitigation, it follows that competitive inhibition of these two pathways, and promotion of NHEJ, are likely part of the DNA damage mitigation mechanism of

Yel002. Further studies to conclusively demonstrate the mechanism should involve the use of dedicated assays to measure the relative rates of these repair pathways [85].

As a nonbiological molecule, Yel002 cannot be generated by culture like some recombinant ARS treatments. Its chemical synthesis is relatively complex, and imperfect synthesis, degradation, or delivery can lead to the complete loss of any protective effect in experiments. Many of the experimental results carried out in this study were unable to be replicated with stocks of the compound dating to over two years in age, and not all chemistry collaborators were capable of synthesizing fully functional Yel002. Before further studies, stringent quality control methods will need to be established to ensure that test compounds are capable of accurately recapitulating the experimental results described here.

The capacity to mitigate radiation damage and improve repair via multiple pathways is an important enough goal that research into Yel002's exact mechanism should continue. This compound has the potential to mitigate ARS from catastrophic radiation exposure as well as a differential radiation mitigator in conjunction with therapeutic radiotherapy.

METHODS

Plated validation of high throughput screen with the DEL assay. The plated DEL assay was performed as described previously [19, 20]. *Saccharomyces cerevisiae* RS112 cells were grown in –Leu media, synchronized, and grown to a density of 2 x 10^6 cells/mL. Cells were then irradiated with 2000 Gy using a Cs-137 Mark 1 irradiator at a dose rate of roughly 14Gy/min. 30 minutes after irradiation, Yel002 was added to a final concentration of 15 μM. Samples were then incubated with agitation for 17 hours at 30°C. After incubation, cells were counted using a hemacytometer, diluted, and plated at appropriate densities onto +13 and –His agar plates. Colonies were scored after 72 hours incubation at 30°C. Survival was calculated from +13 plate CFU vs cells plated. DEL events/ 10,000 were calculated from *His3* revertant CFU capable of growth on –His media.

Til-1 irradiation and viability testing. $CD4^+CD8^+$ murine T-lymphocyte cells (Til-1) were cultured to approximately 75% confluence at 37° C in a 5% CO_2 atmosphere using Dulbecco's modified Eagle Media (DMEM) supplemented with 10% fetal bovine serum and 1% antibiotic-antimycotic solution (Corning, Tewksbury, MA). Cells were suspended in PBS to an approximate density of 1 x 10^6 and irradiated for 0 or 2 Gy using a Cs-137 Mark 1 irradiator. 1 hour after irradiation, Yel002 was added to solution to a final concentration of 100, 50, 10, 1, 0.1, 0.01, or 0.001 μM. 24 hours after irradiation cell viability was determined by luminescence-based measurement of ATP production according to manufacturer instructions (ATPlite reagent; Perkin-Elmer) with a SpectraMax M5 microplate reader (Molecular Devices).

Til- 1 RNA sequencing (RNA-seq) and Quantitative real-time PCR (qRT-PCR). Til- 1 cells were grown up and subjected to 2 or 0 Gy irradiation with 15uM Yel002 post-treatment as above. RNA was isolated from Til-1 cells with an RNeasy Mini Kit with RNAse free DNAse (Qiagen, Valencia, CA) according to manufacturer instructions. This RNA was used to make cDNA libraries using a TruSeq RNA kit (Illumina, San Diego, CA) which were sequenced on an Illumina HiSeq 2000 (Illumina) using a single-end-sequencing length of 50 nt. Data was analyzed with Ingenuity Pathway Analysis software (Redwood City, CA). For RNA-seq experiments, a threshold value of 1.5-fold change was set as a floor of significant change. Full heatmap of all Z-scores is shown in **Supplemental Figure 1.** Real-Time quantitative Polymerase Chain Reaction (RT-qPCR) was used to determine levels of three candidate mRNAs. RNA was harvested as from irradiated and/or treated cells as above. RT-qPCR was performed under universal cycling conditions on a Roche LightCycler (Roche, Indianapolis, IN) using LC480 SYBR Green I master dye (Roche). Samples were analyzed in technical triplicates. GAPDH expression was used for normalization. DNA was diluted to a working solution of 10 ng/uL and 1 μl was used per replicate of each sample. Primers used are detailed in **Supplemental Table 2**.

Til-1 Proteomics. Til- 1 cells were grown up and subjected to 2 or 0 Gy irradiation with 15uM Yel002 post-treatment as above. 2 hours after irradiation, protein lysates of cells were prepared according to manufacturer instructions using a Kinex protein expression and phosphorylation profiling antibody microarray (Kinexus Bioinformatics, Vancouver, BC, Canada). The Z-score threshold for significant change in protein level was set to 1.5.

NHOK culture and western blot analysis. Normal human oral keratinocytes (NHOKs) were isolated from primary human specimens as previously described [86], under approval from UCLA IRB. Detached oral keratinocytes were cultured at 37° C in a 5% CO_2 atmosphere in keratinocyte growth medium (KGM) (Cambrex, East Rutherford, NJ) in collagen-treated flasks. Population doublings (PDs) and replication kinetics were monitored as previously described [87]. Cells were seeded at 1 x 10^5 cells/well, and plates were irradiated at 5 Gy using a Cs-137 Mark 1 Irradiator. 1 hour after irradiation, each well was treated with 0, 5, or 10 μM Yel002 in DMSO and then returned to incubator conditions. On days 3, 9, and 14, cell concentration was recorded and cells were lysed for protein extraction and detection via Western Blot. NHOKs were lysed with lysis buffer (1% Triton X−100, 20mM Tris-HCl (pH7.5), 150mM NaCl, 1mM EDTA, 1mM EGTA, 2.5mM sodium pyrophosphate, 1mM β- glycerolphosphate, 1mM sodium orthovandate and PMSF) and sonicated. Whole cell lysates (40-50 μg) were run on SDS-PAGE and transferred onto an Immobilon protein membrane (Millipore, Billerica, MA). Immobilized proteins were incubated with primary antibodies against $p21^{WAF1}$, $p16^{INK4A}$ (EMD Biosciences, San Diego, CA); pRb, $p\text{-}pRb^{807/811}$, PCNA and GAPDH (Santa Cruz Biotechnology, Santa Cruz, CA); and Bmi-1(F-6) from (Upstate, Charlottesville, VA). Following incubation with primary antibodies, the membrane was probed with appropriate secondary antibodies. Results were normalized to GAPDH levels and quantitated with Scion Image software (Frederick, MD).

Immortalized human lymphoblastic cell translation inhibition and western blot. Immortalized human lymphoblastic cells were generated using Epstein-Barr virus and cultured as previously described [88]. Cells were incubated with Yel002 (15 μM) for 24 hrs with and

without the protein synthesis inhibitor cycloheximide (CHX, 25 μM). Cells were lysed, run on SDS-PAGE, and immobilized as described above. Immobilized proteins were incubated with primary antibodies against RAD50 (#3427) and MRE11 (#4847) (Cell Signaling Technology, Inc., Danvers, MA). Protein amounts were normalized to GAPDH in each treatment group and quantitated with Scion Image software (Frederick, MD).

H2AX Focus Reduction in Peripheral Lymphocytes Exposed to CSE. Mice deficient in two base excision repair genes were previously generated [89]. Myh and Ogg1 deficient mice were bred from mice heterozygous for each mutation and backcrossed to their C57/BL6 background as previously described [90]. Mice were bred in an institutional specific pathogen free animal facility under standard conditions with a 12 hr light/dark cycle according to Animal Research Committee regulations. Mice were provided standard diet food and water ad libitum. To obtain peripheral blood lymphocytes, blood was collected via terminal right ventricle cardiac puncture using a heparin-coated syringe (American Pharmaceutical Partners, Inc. Schaumburg, IL). At least 1 mL of blood was collected from each animal and aliquoted into EDTA-coated tubes (Sarstedt Aktiengesellschaft, Numbrecht, Germany). Whole peripheral blood samples were administered with cigarette smoke extract (CSE) diluted to a final concentration of 3 puff/mL alone or in co-incubation with 10μM Yel002 for 6 or 24 hrs in a shaking 37°C incubator. After erythrocyte lysis, cells were laid over poly-D-lysine-coated coverslips and fixed with 4% paraformaldehyde (Electron Microscopy Sciences), then permeabilized with 0.5% Triton X-100 (Sigma) and rinsed 5 times in PBS. Cells were blocked under aluminum-covered plates overnight at 4°C in 10% FBS. Primary antibody incubation occurred for 1 hour at room temperature with mouse anti-phospho-Histone H2AX (Upstate, Temecula, CA), and secondary staining was carried out with FITC-conjugated anti-mouse IgG (Jackson ImmunoResearch, West Grove, PA) for 1 hour at room temperature. Coverslips were mounted onto slides using VECTASHIELD with DAPI (Vector Laboratories, Burlingame, CA) and foci were analyzed on a Zeiss automated microscope. Scoring was performed as previously described by Muslimovic et

al [91]. Cells with more than four distinct foci in the nucleus were considered positive for γH2AX, but highly fluorescent apoptotic cells were excluded. Statistical analyses were performed using two-way ANOVA with Tukey's post hoc test.

Mouse survival after irradiation. C3Hf/Kam mice were bred and maintained in a strict defined-flora, pathogen-free environment in the American Association of Laboratory Animal Care–accredited animal facilities of the Department of Radiation Oncology, University of California at Los Angeles. The University of California at Los Angeles Animal Care and Use Committee approved all experiments, which were done in accordance with all local and national guidelines for the care and use of animals. Mice were provided food and water ad libitum from before and during the entire duration of the experiment. Male mice aged 8 to 12 weeks received total body irradiation (TBI) from 7 to 9 Gy (LD100/30) from a Gamma Cell 40 irradiator (Cs-137 source; Atomic Energy of Canada) at a dose rate of roughly 67 cGy/min. Mice were subcutaneously injected with 75 mg/kg Yel002 in warmed saline or 2% Kolliphor EL (Sigma) in saline for 5 days beginning 24 hours after irradiation. Supportive care beyond additional sources of water was not provided to avoid confounding data. Mice were monitored a minimum of twice a day for the critical period of 30 days using standard criteria for humane euthanasia as an endpoint.

Enumeration of hematopoietic recovery by differential blood count. C3H mice were irradiated at 6 Gy and treated with Yel002 for 5 days as described above. On days 7, 10, 13, and 16 post-irradiation, 60 µL of blood was drawn supraorbitally and analyzed using a HemaVet 950 hematology system (Drew Scientific, Waterbury, CT).

Long term survival of ATM-deficient mice. *Atm*$^{+/-}$ mice were previously generated and crossed onto the parental C57BL/6J p^{un}/ p^{un} background in the defined flora facility of UCLA Radiation Oncology, as mentioned above [92, 93] . All mice were provided with standard food and water ad libitum over the entire course of their lives, and subject to a 12/12 light/dark cycle. Within one month of birth, a tissue sample was taken to determine *ATM* genotype. Once identified, experimental *Atm*$^{-/-}$ mice received subcutaneous injections of 75mg/kg Yel002 in

saline once weekly for the rest of their lives. Mice were monitored at least once per day for changes in health. Experimental endpoints were a moribund state or the development of a visible tumor. All research was carried out in accordance with the UCLA Animal Research Committee guidelines.

Suppression of Leukemic Development in a DBA/2 + FDC-P1 mouse model. 2-3 month old DBA/2 males were bred and housed at the Armed Forces Radiobiology Research Institute (AFRRI) AALAC approved animal care facility under the direction of Dr. Alexandra Miller. 15 DBA/2 mice per group were bilaterally irradiated in well-ventilated Lucite boxes with 3.5Gy using a Co-60 source, at a dose rate of roughly 0.6 Gy/min. 24 hours later, mice were transplanted intravenously with 5 x 10^6 FDC-P1 cells according to established leukemic induction protocols [77, 78]. Immediately after transplantation, mice were injected subcutaneously with Yel002 in saline (25 mg/kg) with followup injections every 24 hours 4 additional days. Leukemogenesis was monitored with blood draws every 21 days. Mice were monitored daily and at specific times after FDC-P1 cell injection, and euthanized upon onset of leukemia or after 270 days.

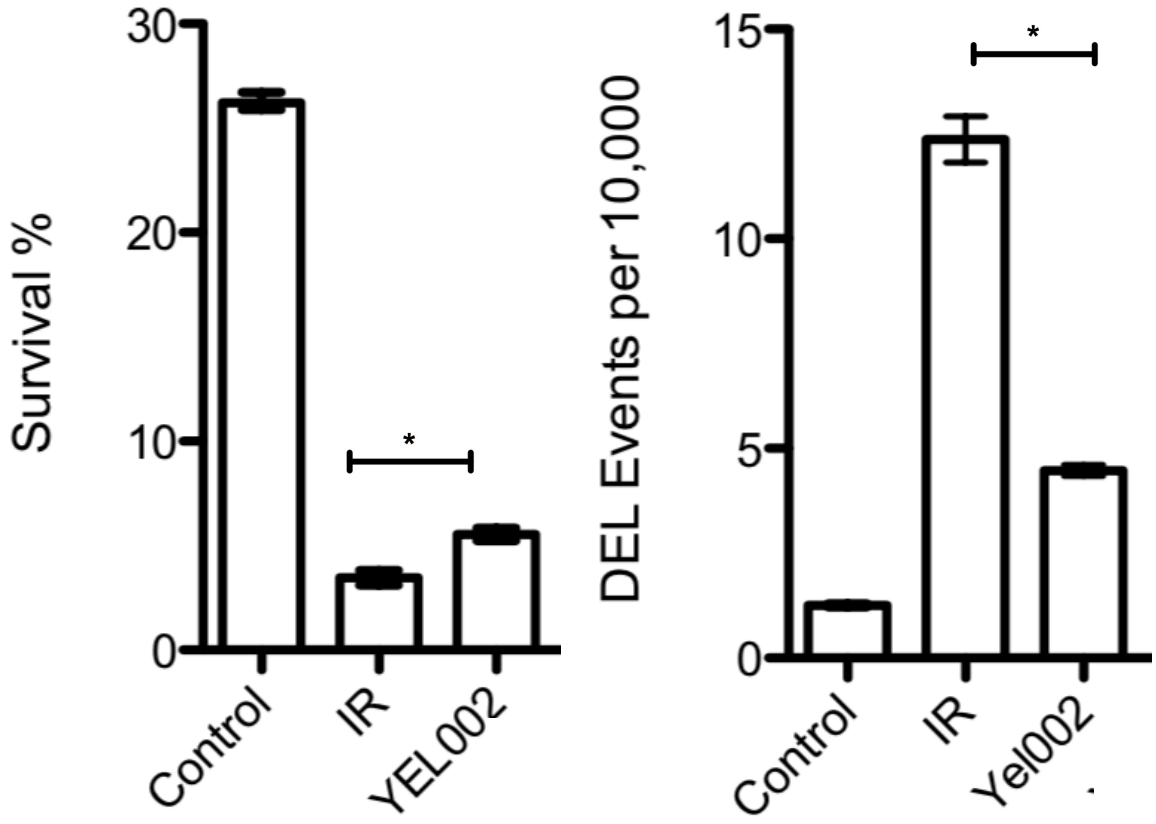

Figure 1. Yel002 incubation decreases radiation-induced lethality and *his3* deletion-recombination-reversion events in RS112 *Saccharomyces cerevisiae*. 2000 Gy irradiation of RS112 cells significantly reduced survival of cells as well as induced a large increase in DEL events. Yel002 treatment from 30 minutes after irradiation increased survival, measured as CFU formed on +13 aa plates, and reduced DEL events/10,000 surviving cells, measured by CFU on –His plates. $p < 0.05$ for both metrics by student's t-test. Treatments plated in triplicate.

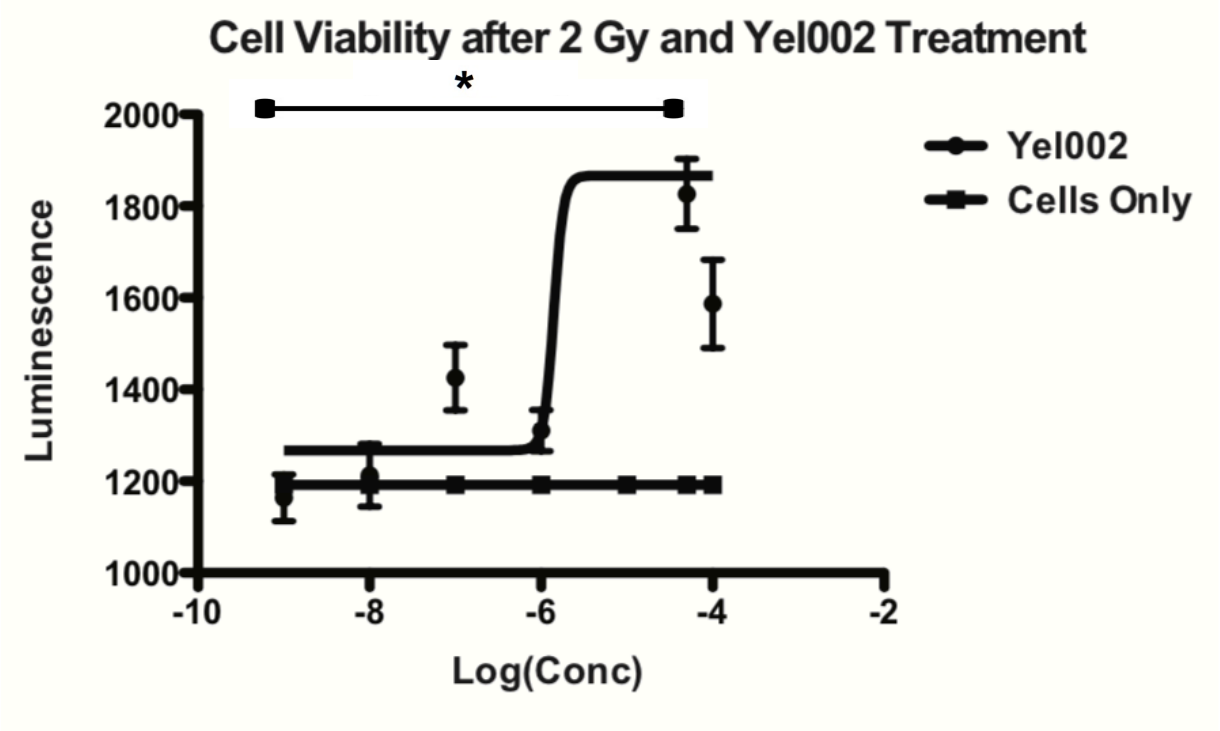

Figure 2. Yel002 incubation decreases radiation induced lethality in TIL-1 cells. Til-1 cells were irradiated with 2 Gy and treated with 0.001, 0.01, 0.1, 1, 10, 50, or 100 μM Yel002. 24 hours later, cell viability was measured with a luminescence based ATP production assay. Optimal mitigation is reached between 10 and 50 μM ($p < 0.05$ vs untreated, student's t-test). N = 4

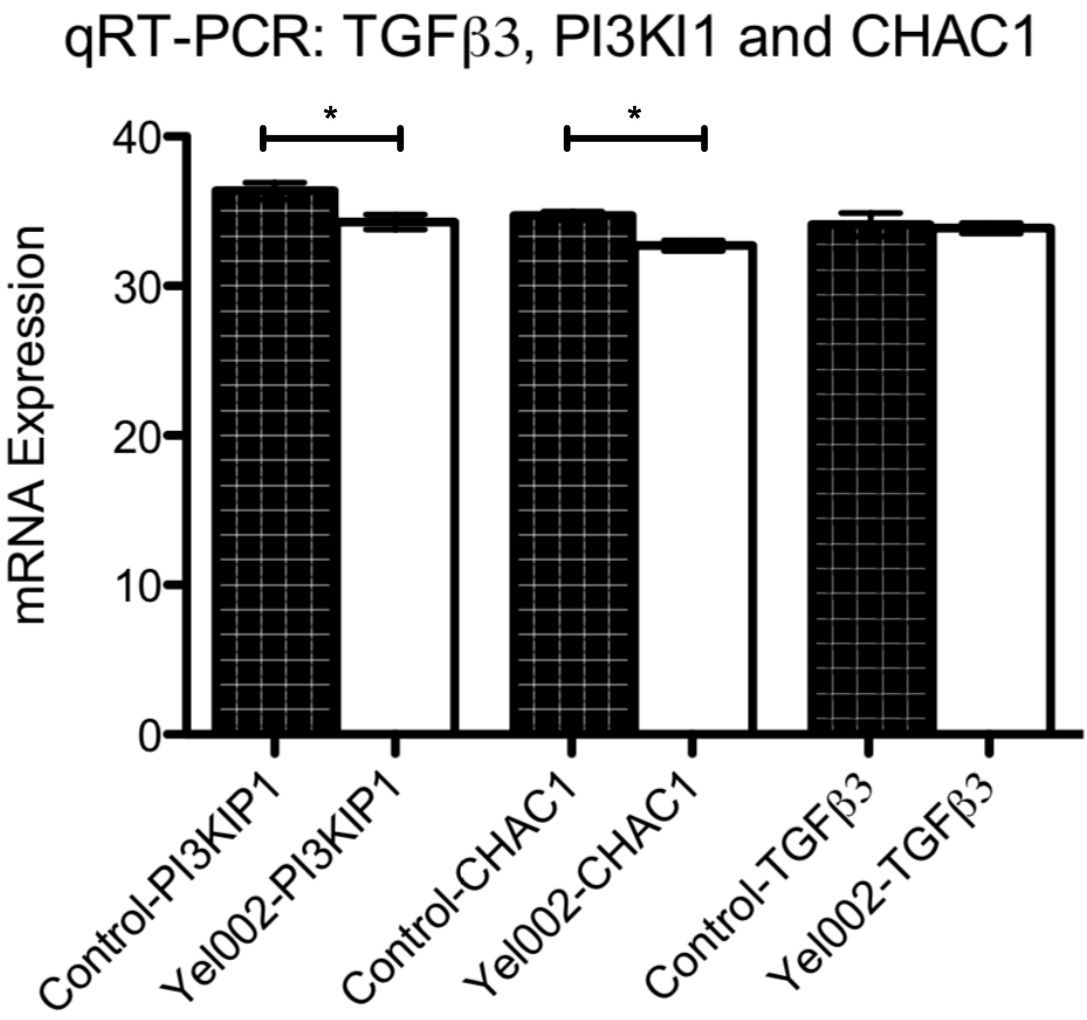

Figure 3. Incubation with Yel002 decreases expression of PI3KIP1 and CHAC1 mRNA in Til-1 cells. Til-1 cells were incubated with 15 μM Yel002 for 7 hours before RNA harvest and subsequent RT-qPCR. Exposure significantly reduced levels of PI3KIP1 ($p = 0.02$) and CHAC1 ($p = 0.001$), but not TGF β3 mRNA. Samples run in triplicate.

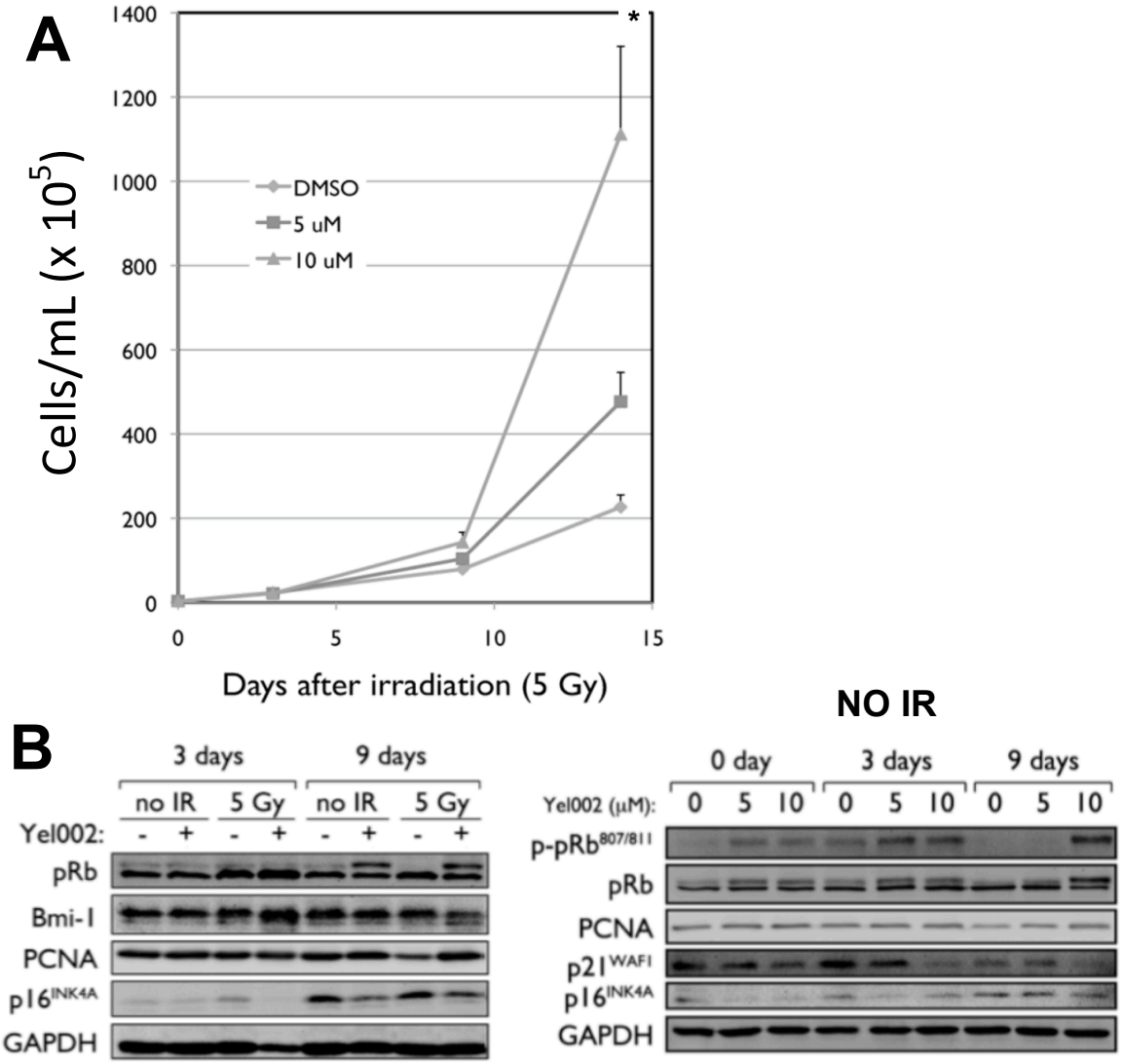

Figure 4. Incubation with Yel002 increases pro-cycling protein signaling and mitigates induced senescence in irradiated primary human keratinocyte culture. Keratinocytes harvested from donors undergoing oral surgery were irradiated then incubated with Yel002 after 1 hour. **A.** 10 μM Yel002 was more effective than 5 μM Yel002, and lead to a significant increase in cell proliferation by day 14 over those treated with DMSO carrier ($p < 0.05$, $n = 6$). **B.** Yel002 incubation leads to a steady increase in the phosphorylation state of pRb over time in both irradiated and unirradiated NHOKs. Yel002 appears to induce a transient suppression of IR-induced p16 expression, and a more long-lived suppression of p21 expression.

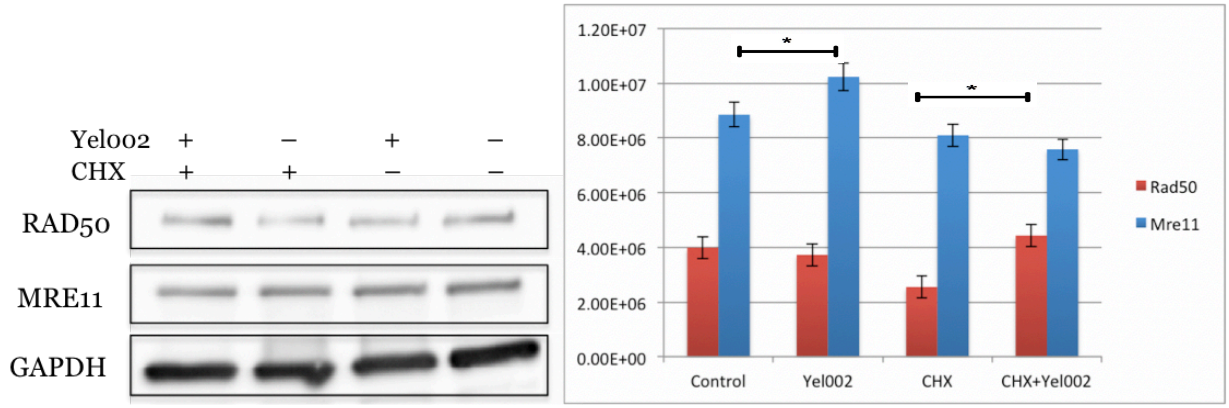

Figure 5. Yel002 incubation increases Mre11 protein synthesis and stabilizes RAD50 levels in the presence of cycloheximide. EBV-immortalized human lymphoblastoid cells were incubated with 15 μM Yel002 for 24 hrs, differentially affecting the total amount of two components of the MRN complex. Left: Western Blot image. Right: Relative western blot saturation normalized to GAPDH. Yel002 appears to stimulate de novo synthesis of MRE11 but not RAD50. Increase in RAD50 protein concentration following a co-incubation of Yel002 with 25 μM cycloheximide (CHX) might be partially explained by the protein stabilization in response to Yel002. * = $p < 0.05$

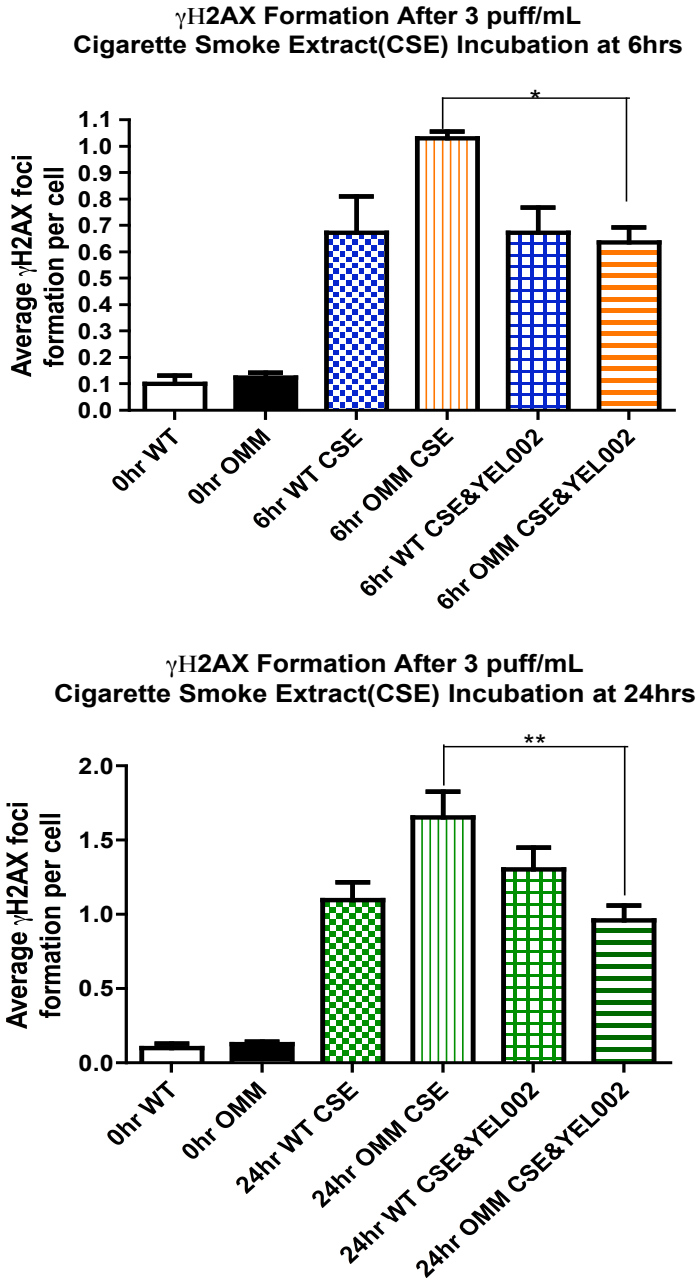

Figure 6. Yel002 incubation after exposure of Ogg$^{-/-}$ / Myh$^{-/-}$ double knockout (OMM) mice to cigarette smoke extract (CSE) reduces γH2AX foci. γH2AX foci were strongly induced in both WT and OMM mice, but were induced most heavily in OMM. Treatment with 15 μM Yel002 did not significantly affect number of foci in wild type mice. However, treatment significantly reduced foci in base excision repair deficient OMM mice at both 6 and 24 hours post exposure, bringing their levels down to that of wild type CSE exposed mice. * = $p < 0.05$, ** = $p < 0.01$

A

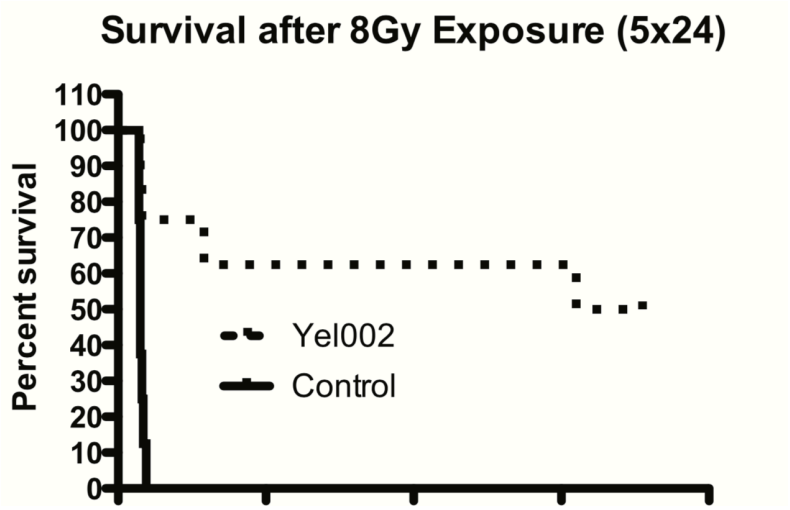
Survival after 8Gy Exposure (5x24)
Percent survival
110
100
90
80
70
60
50
40
30
20
10
0
Yel002
Control

B

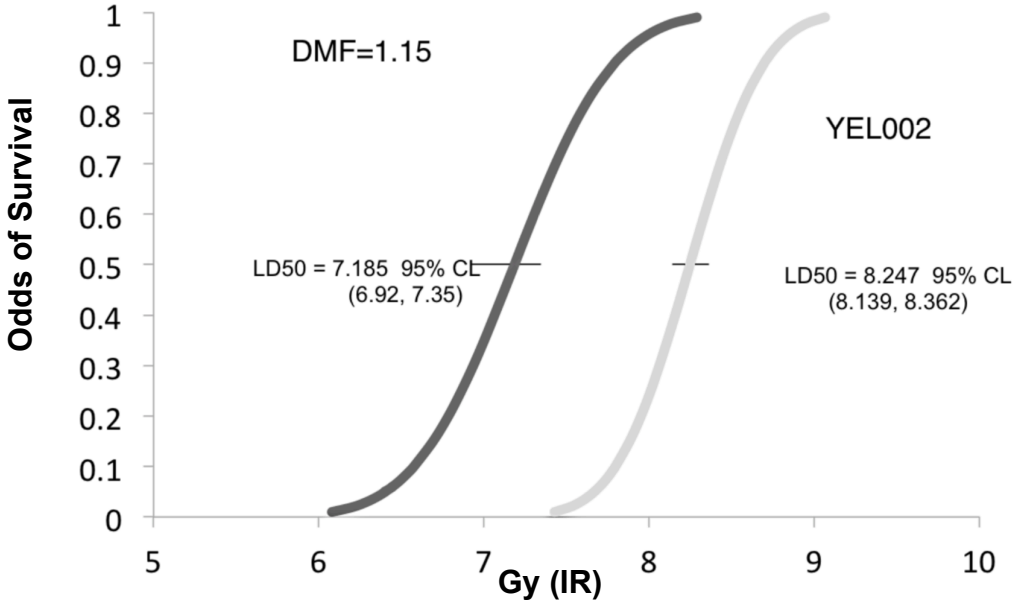
Odds of Survival
1
0.9
0.8
0.7
0.6
0.5
0.4
0.3
0.2
0.1
0
DMF=1.15
YEL002
LD50 = 7.185 95% CL
(6.92, 7.35)
LD50 = 8.247 95% CL
(8.139, 8.362)
5
6
7
8
9
10
Gy (IR)

C

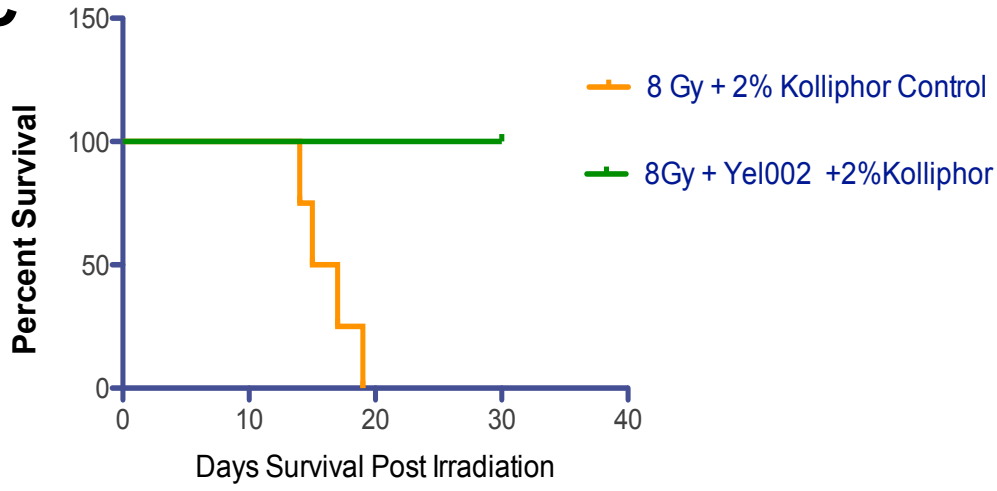
Percent Survival
150
100
50
0
0
10
20
30
40
Days Survival Post Irradiation
8 Gy + 2% Kolliphor Control
8Gy + Yel002 +2%Kolliphor

Figure 7. Yel002 mitigates IR-induced lethality in mice. A. 8 week old male C3H mice were irradiated at the LD100/30 dose of 8 Gy. 24 hours later, mice were subcutaneously injected with Yel002 (75mg/kg in saline) and again every 24 hours afterwards for 4 additional days (5 x 24 protocol). At 30 days post IR, 75% of treated mice survived while irradiated control mice did not survive. ($p < 0.05$, chi square test, $n = 8$). **B.** Groups of 8 male C3H mice were irradiated with doses from 7.0 to 9.0 Gy and treated with 5 x 24 Yel002. The LD50 of Yel002 treated mice occurs at 8.247 Gy, while the LD50 for unirradiated mice occurs at 7.185 Gy. **C.** In an attempt to improve consistency with the relatively hydrophobic Yel002, 2% Kolliphor EL in saline was used as a carrier emulsifier. 100% of irradiated mice treated with 2% Kolliphor/Yel002 survived an LD100/30 dose of IR vs 0% of 2% Kolliphor only controls. ($p < 0.05$, chi square test)

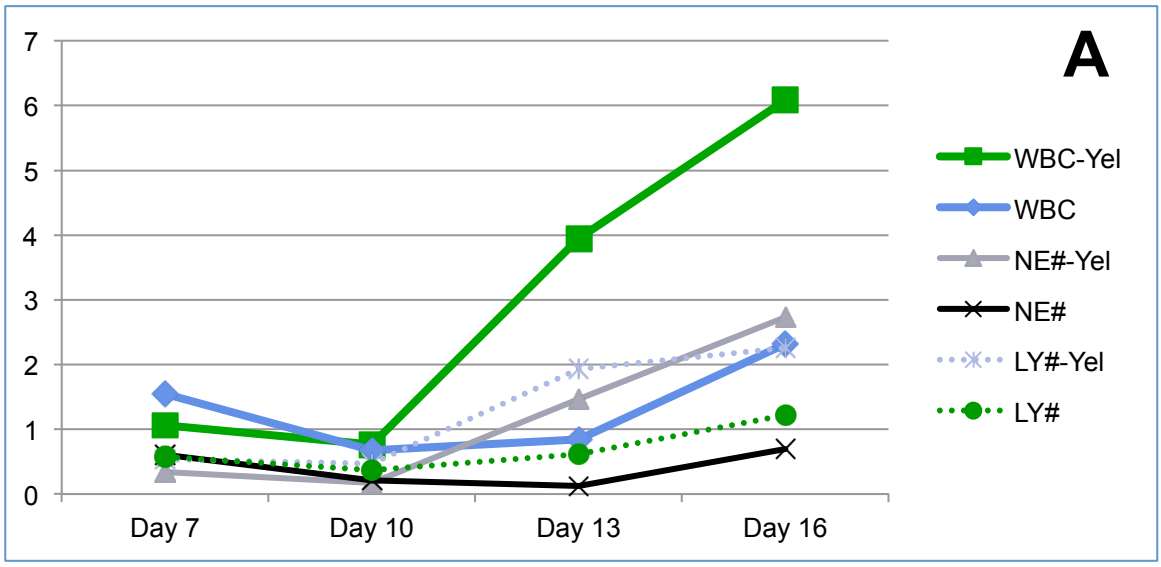
A
7
6
5
4
3
2
1
0
Day 7
Day 10
Day 13
Day 16
WBC-Yel
WBC
NE#-Yel
NE#
LY#-Yel
LY#

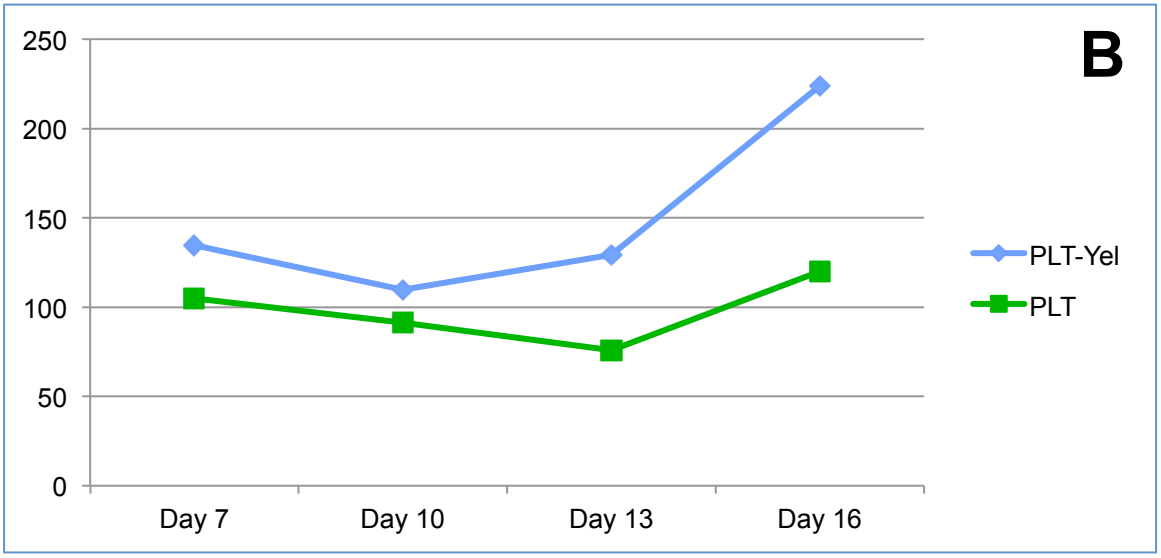
B
250
200
150
100
50
0
Day 7
Day 10
Day 13
Day 16
PLT-Yel
PLT

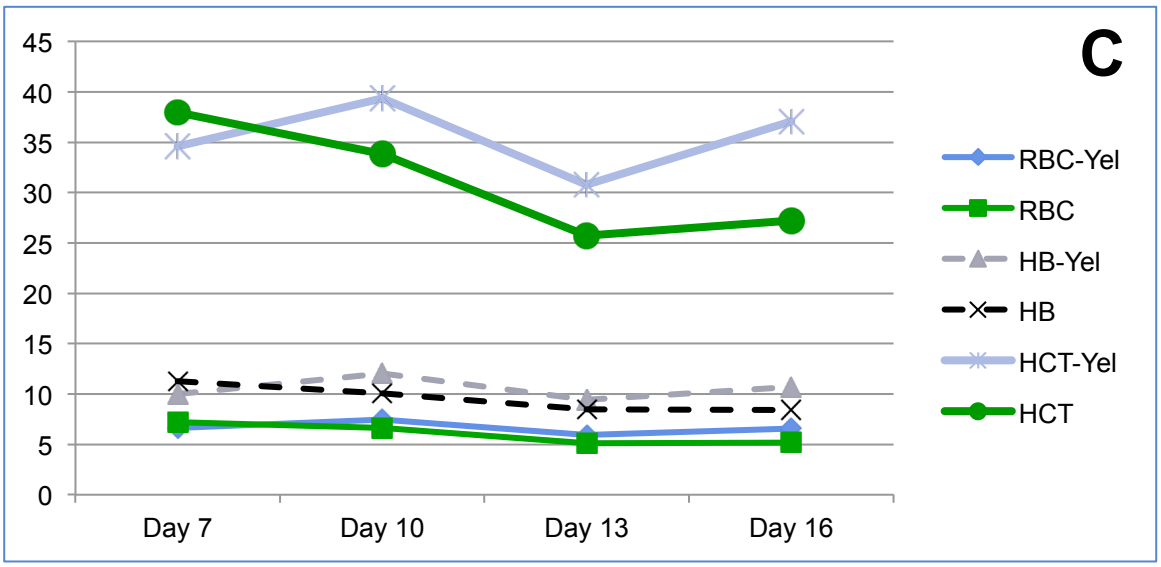
C
45
40
35
30
25
20
15
10
5
0
Day 7
Day 10
Day 13
Day 16
RBC-Yel
RBC
HB-Yel
HB
HCT-Yel
HCT

Figure 8. Yel002 leads to increased hematopoietic reconstitution in irradiated mice. C3H mice (n = 4) were irradiated with 6 Gy and subcutaneously injected with Yel002 (75mg/kg) on the 5x24 treatment protocol. From day 7 after irradiation animals were bled supraorbitally and differential blood counts were obtained with HemaVet analytical instrument. **A.** On days 13 and 16, overall white blood cell (WBC) counts in the Yel002 treated group were higher than in non-treated controls suggesting increased recovery speed. **B.** Irradiated animals treated with Yel002 had significantly increased platelet levels by day 16. **C.** Treatment with Yel002 did not significantly affect red blood cell (RBC) or related counts in animals irradiated with 6 Gy. For p-values calculated by student's t-test, see **Table 3**.

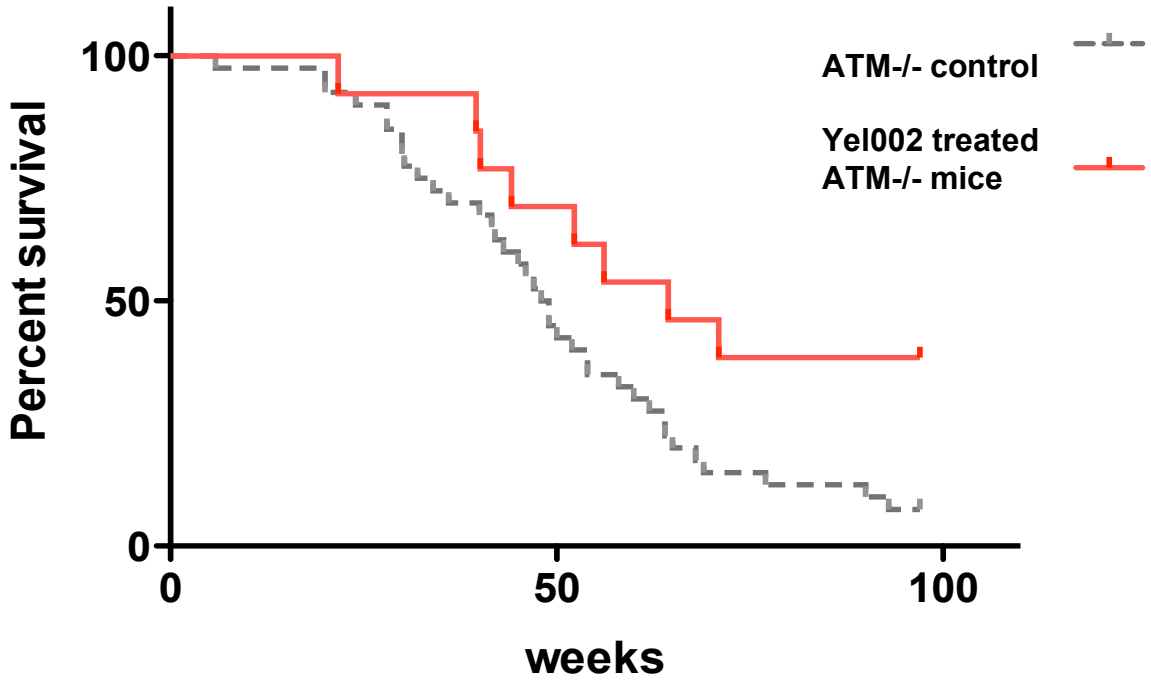

Figure 9. Weekly Yel002 Exposure increases median life expectancy in ATM-KO mice. *Atm*$^{-/-}$ C57BL/6J p^{un}/ p^{un} mice were kept in a barrier facility and monitored for lymphoma or other moribund condition. 13 ATM deficient mice were injected with 75 mg/kg Yel002 once weekly. Median survival time = 64 weeks vs. 48 for controls. Yel002 was injected subcutaneously at 75 mg/kg weekly for 97 weeks in the experimental cohort ($p < .05$, chi square test). *Atm*$^{-/-}$ control n = 40, experimental *Atm*$^{-/-}$ + Yel002 n = 13.

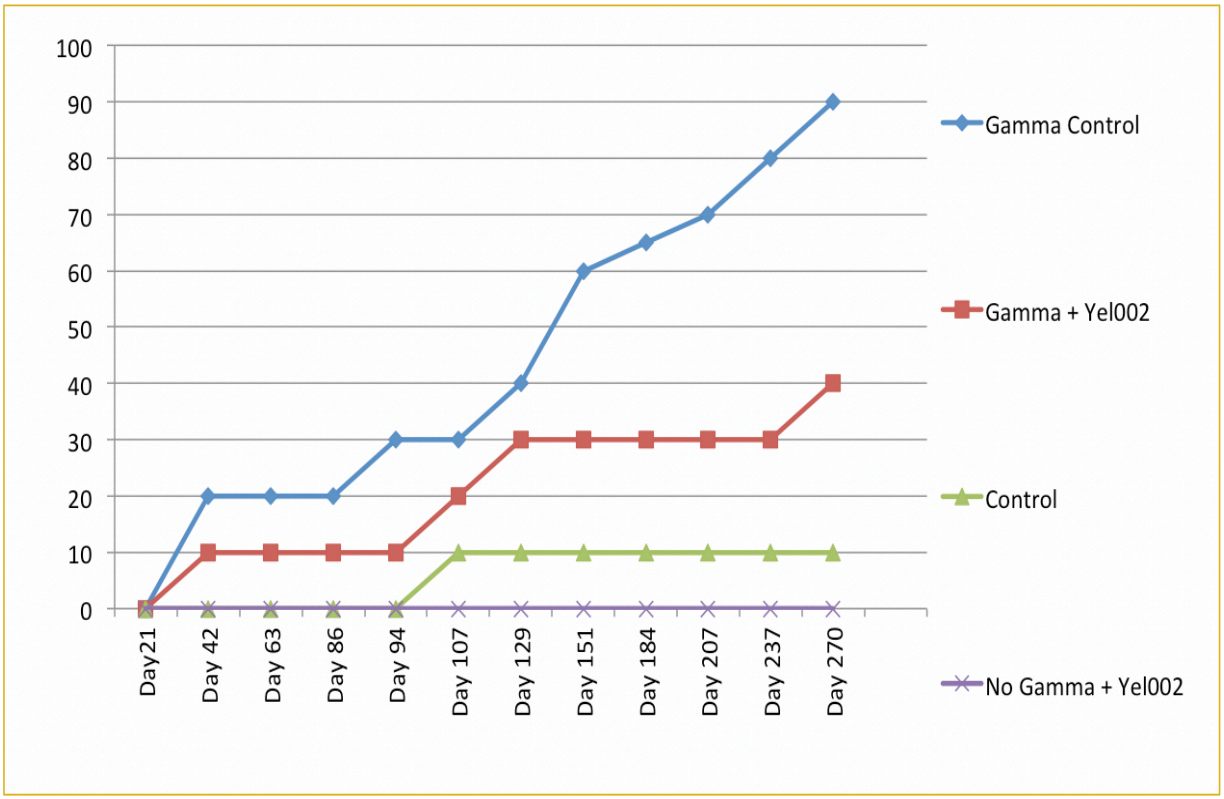

Figure 10. Yel002 reduces IR-induced leukemia induction in DBA/2 mouse model.

Administration of Yel002 to irradiated mice decreases induction penetrance and prolongs latency period before leukemia development. DBA/2 mice irradiated and transplanted with pre-leukemic FDC-P1 cells developed leukemia in 90% of the animals versus 40% in Yel002V treated mice by Day 270 ($p < .05$, $n = 15$).

Genes	Fold Change (IR+Y_8h vs. IR_8h)	Genes	Fold Change (IR+Y_8h vs. IR_8h)	Genes	Fold Change (IR+Y_8h vs. IR_8h)
Trav14-2	-2.31	Rabl5	-1.53	Gm5161	1.59
Pde6a	-1.77	Ccdc22	-1.64	Zfp455	2.07
Pacsin3	-1.52	Tgfb3	-1.53	Zfp114	2.96
Spata9	-1.86	Sgip1	-1.64	Asns	1.66
Mcart6	-2.50	Ptpre	-1.58	Stc2	1.72
Ccdc15	-1.59	Pgap2	-1.60	Slc7a5	1.70
Gpr39	-1.52	Nipal3	1.50	Aldh18a1	1.64
Vkorc1	-2.05	Herpud1	1.59	Tmem170b	1.79
Itgb3bp	-1.84	Ccdc115	1.57	Chac1	2.11
Pax7	-1.53	Pik3ip1	1.62	G630016D24Rik	2.53
Lrrc16a	-1.98	Rab23	1.53	Abcg3	2.32
Tbc1d12	-1.76	Gm13342	1.58		

Table 1. Yel002 administration differentially affects mRNA levels of 35 genes in murine lymphocytes after a 2 Gy irradiation. Til-1 cells were irradiated and 1 h later treated with 15 μM Yel002. After 7 hours incubation, mRNA was harvested and converted into cDNA libraries. Genes presented in this table were significantly and differentially affected by Yel002 incubation in irradiated cells (1.5 fold difference threshold, $p < .05$). Full heatmap is shown in **Supplementary Figure 1.**

Table 2. Yel002 administration after IR affects protein levels in Til-1 cells.

Target Protein	Phospho site (human)	Z-ratio (IR+Yelo02 vs. IR)	Target Protein	Phospho site (human)	Z-ratio (IR+Yelo02 vs. IR)
4E-BP1	T70	-5.67	GRK2 (BARK1)	S670	-1.77
B23 (NPM)	T234/T237	-1.89	GRK3 (BARK2)	Pan-specific	-1.58
Bcl2	Pan-specific	-2.19	GroEL	Pan-specific	-1.53
Bcl-xL	Pan-specific	-2.28	Grp94	Pan-specific	-1.84
BLNK	Y84	-1.91	GSK3a + GSK3b	Pan-specific	-2.58
BMX (Etk)	Pan-specific	-2.40	Haspin	Pan-specific	-1.58
BRD2	Pan-specific	-1.51	Histone H2B	S15	-2.46
Btk	Pan-specific	-1.61	IkBa	Pan-specific	3.13
Btk	Y223	-2.26	IKKb	Pan-specific	1.54
Calnexin	Pan-specific	-2.54	IR	Pan-specific	-1.55
CDK1/2	Y15	-1.52	JNK1	Pan-specific	-1.69
DAPK2	Pan-specific	2.13	JNK2/3	Pan-specific	1.61
DNAPK	Pan-specific	1.57	JNK3	Pan-specific	2.19
eEF2K	Pan-specific	4.38	Jun	Pan-specific	2.29
EGFR	Y1197	2.49	Jun	S63	-1.70
EGFR	Y1197	2.70	Jun	S73	3.37
eIF4E	Pan-specific	3.14	Kit	Y730	1.58
ErbB2 (HER2)	Pan-specific	2.75	Kit	Y936	2.13
ErbB2 (HER2)	Y1248	2.72	LATS1	Pan-specific	2.61
Erk1 + Erk2	Pan-specific	1.57	Lck	Pan-specific	3.17
Erk1 + Erk2	Pan-specific	2.11	Lck	Y505	2.44
Erk1 + Erk2	[T202+Y204] + [T185+Y187]	1.63	LIMK1	Pan-specific	4.58
Erk2	Pan-specific	1.81	Lyn	Y508	2.11
Erk5	Pan-specific	-2.29	LATS1	Pan-specific	2.61
Erk5	T218+Y220	-2.19	Lck	Pan-specific	3.17
ERP57	Pan-specific	-1.96	Lck	Y505	2.44
FAK	Y576	-1.72	LIMK1	Pan-specific	4.58
FAK	S722	-2.00	Lyn	Y508	2.11
FAK	S910	-1.75	MAK	Pan-specific	1.60
FasL	Pan-specific	-1.51	MAPKAPK2a + MAPKAPK2b	T334	2.09
FKBP52	Pan-specific	-1.87	MARCKS	S159+S163	2.66
FKHRL1	T32	-1.84	MEK1 (MAP2K1)	Pan-specific	2.03
GAP-43	S41	-1.62	MEK1 (MAP2K1)	T386	1.51

Table 2 cont. Yel002 administration after IR affects protein levels in Til-1 cells.

Target Protein	Phospho site (human)	Z-ratio (IR+Yel002 vs. IR)	Target Protein	Phospho site (human)	Z-ratio (IR+Yel002 vs. IR)
MAK	Pan-specific	1.60	PKM2	Pan-specific	1.71
MAPKAPK2a + MAPKAPK2b	T334	2.09	Plk2	Pan-specific	1.54
MARCKS	S159+S163	2.66	PP5C	Pan-specific	-1.86
MEK1 (MAP2K1)	Pan-specific	2.03	PP6C	Pan-specific	-1.64
MEK1 (MAP2K1)	T386	1.51	PRK1 (PKN1) + PRK2 (PKN2)	T774 + T816	-2.23
MEK2 (MAP2K2)	T394	-1.60	PSD-95	Pan-specific	-1.91
MEK3 (MAP2K3)	S218	-1.93	PTEN	S380+T382+S385	-2.58
MEK3/6 (MAP2K3/6)	S218/S207	-1.90	PTP1B	Pan-specific	-2.70
MEK5 (MAP2K5)	Pan-specific	-1.77	PTP1D	S580	-1.82
MKP2	Pan-specific	-1.95	PTPD1	Pan-specific	-1.55
MLK3	T277+S281	-1.73	Rab5	Pan-specific	-1.59
PDGFRa/b	Y572+Y574/Y579+Y581	-1.80	Rac1	Pan-specific	-2.08
PKA Ca/b	Pan-specific	-2.41	RIP2/RICK	Pan-specific	-1.80
PKBa (Akt1)	T308	-1.76	RIPK1	Pan-specific	1.76
PKCd	T507	1.55	ROKa (ROCK2)	Pan-specific	-1.56
PKCg	Pan-specific	1.53	ROKb (ROCK1)	Pan-specific	-2.12
PKCh	S674	1.60	RSK1/2	S380/S386	-2.45
PKCm (PKD)	S910	1.55	S6Kb1	T412	2.75
PKCq	T538	1.52	Smad2/3	Pan-specific	-2.51
PKCz	Pan-specific	1.71	VHR	Pan-specific	-1.76
PKCz/l	T410/T412	1.93			

Til-1 Cells were irradiated at 2 Gy then treated for 1 hour with 15 μM Yel002 prior to protein harvest. Z-scores shown passed the significance threshold of 1.5 fold Z-score ($p < 0.05$)

Table 3. Hemavet Counts

	No IR	Day 7	Day 10	Day 13	Day 13 p	Day 16	Day 16 p
WBC (K/µL)	16.8	1.55	0.66	0.84		2.32	
WBC + Yel002 (K/µL)		1.07	0.77	3.95	0.03	6.09	0.03
NE (K/µL)	9.6	0.61	0.18	0.13		0.69	
NE + Yel002 (K/µL)		0.34	0.20	1.47	0.03	2.73	0.03
LY (K/µL)	5.8	0.58	0.37	0.62		1.22	
LY + Yel002 (K/µL)		0.54	0.44	1.93	0.03	2.26	0.06
MO (K/µL)	0.4	0.11	0.05	0.04		0.14	
MO + Yel002 (K/µL)		0.06	0.08	0.20	0.01	0.32	0.04
EO (K/µL)	0.5	0.17	0.05	0.04		0.19	
EO + Yel002 (K/µL)		0.09	0.04	0.26	0.06	0.56	0.04
BA (K/µL)	0.5	0.08	0.01	0.02		0.08	
BA + Yel002 (K/µL)		0.04	0.01	0.09	0.11	0.22	0.05
RBC (M/µL)	8.65	7.21	5.37	5.11		5.18	
RBC + Yel002 (M/µL)		6.62	7.31	5.94	0.07	6.59	0.17
HB (g/dL)	15.6	11.30	8.20	8.45		8.40	
HB+ Yel002 (g/dL)		9.98	11.68	9.40	0.16	10.70	0.17
PLT (K/µL)	710	104.75	84.75	75.75		120.75	
PLT + Yel002 (K/µL)		134.5	96.25	129.29	0.05	223.75	0.04
HCT (%)	42.4	37.95	27.43	25.73		27.23	
HCT + Yel002 (%)		34.60	38.05	30.78	0.12	37.08	0.12

Supplemental Figure 1. Genes differentially affected by Yel002 after 2 Gy.

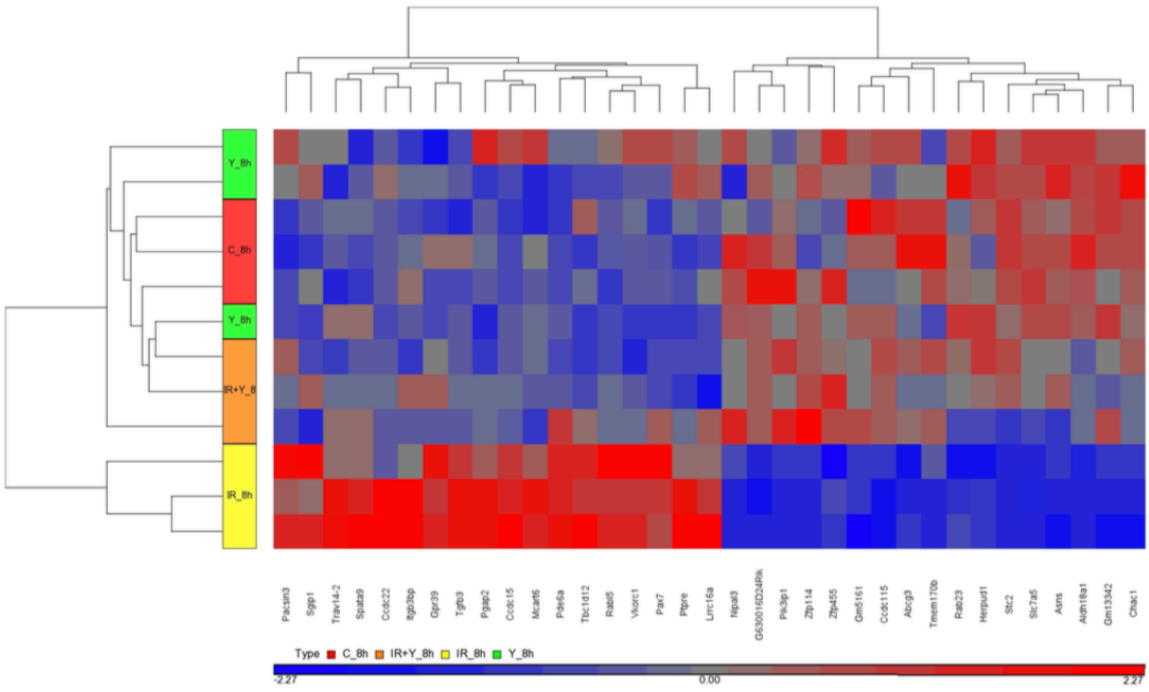

Supplemental Figure 1. Incubation with Yel002 for 7 hrs following irradiation differentially affected 35 genes shown in **Table 1**. Yel002 treatment reversed IR induced increases or decreases in these genes. Analysis used Ingenuity software. Significance thresholds were set at 1.5 fold change ($p < 0.05$).

Supplementary Table 1. Yel002 Affects Protein Expression and Phosphorylation in Non-Irradiated Cells

Target Protein	Phospho site (human)	Z-score ratio (Yel002 vs. Control)	Target Protein	Phospho site (human)	Z-score ratio (Yel002 vs. Control)
Arrestin b1	Pan-specific	-1.97	ErbB2 (HER2)	Pan-specific	1.54
B23 (NPM)	T234/T237	-1.86	Erk5	Pan-specific	-1.5
BMX (Etk)	Pan-specific	-1.94	Erk5	T218+Y220	-1.73
Btk	Y223	-1.54	FAK	S722	-1.81
Caldesmon	S789	1.62	FAK	S732	-1.59
CaMK4	Pan-specific	-1.72	FasL	Pan-specific	-1.78
CAS	Pan-specific	-3.17	Fos	T232	-1.92
CASK/Lin2	Pan-specific	-1.66	GFAP	S8	-1.68
CASP1	Pan-specific	-1.68	Histone H3	T12	1.7
CASP3	Pan-specific	-1.73	Hsp90a/b	Pan-specific	-2.16
CASP6	Pan-specific	-1.71	Hsp90b	Pan-specific	-1.66
Caveolin 2	Pan-specific	-3.18	HspBP1	Pan-specific	-1.8
Cdc25C	S216	-2.73	IkBa	Pan-specific	1.57
CDK1/2	Y15	-2.06	IKKg (NEMO)	Pan-specific	-2.15
CDK2	Pan-specific	-2.09	IR	Pan-specific	-1.9
CDK6	Pan-specific	-1.51	IRS1	Y612	-1.56
Cofilin 1	Pan-specific	-2.25	JNK1/2/3	T183 + Y185	-1.64
Cofilin 1	S3	-1.72	KHS	Pan-specific	1.71
COX2	Pan-specific	-2.21	Ksr1	Pan-specific	2.75
CPG16/CaMKinase VI	Pan-specific	-2.47	LATS1	Pan-specific	2.42
CREB1	S129+S133	-1.79	Lck	Pan-specific	1.78
CREB1	S133	-1.52	Lck	Y505	1.72
Crystallin aB	Pan-specific	-1.78	MAPKAPK2	Pan-specific	1.74
Crystallin aB	Pan-specific	-1.58	MAPKAPK2	T222	1.64
Csk	Pan-specific	-2.21	MAPKAPK2a + MAPKAPK2b	T334	2.04
eEF2K	Pan-specific	2.75	MARK	Pan-specific	1.51
EGFR	Y1197	2.23	Mcl1	Pan-specific	1.52
eIF4E	S209	-1.94	MEK1 (MAP2K1)	Pan-specific	1.57

(Supplementary Table 1 continued)

Target Protein	Phospho site (human)	Z-score ratio (Yel002 vs. Control)	Target Protein	Phospho site (human)	Z-score ratio (Yel002 vs. Control)
MEK2 (MAP2K2)	T394	-1.61	RSK1/2	S380/S386	3.32
MKP2	Pan-specific	-2.07	S6Kb1	Pan-specific	2.92
MST3	Pan-specific	-1.8	S6Kb1	T252	2.12
p38g MAPK (Erk6)	Pan-specific	1.57	S6Kb1	T444+S447	1.82
PACSIN1	Pan-specific	1.83	S6Kb1	T412	-1.78
PAK3	Pan-specific	1.68	Smad1/5/8	S463+S465/S463+S465/S465+S467	1.55
PI4KCB	Pan-specific	1.68	SMC1	S957	1.86
PKA Ca/b	Pan-specific	-2.25	SODD	Pan-specific	2.03
PKBa (Akt1)	Pan-specific	2.32	STAT1a + STAT1b	Pan-specific	2.75
PKBa (Akt1)	T308	-2.59	STAT2	Y690	3.28
PKBb (Akt2)	Pan-specific	1.59	Synapsin 1	S9	1.68
PKCq	Pan-specific	-1.87	TAK1	Pan-specific	2.15
PKCz/l	T410/T412	-2	TAK1	Pan-specific	1.89
PKG1	Pan-specific	1.67	Tau	S516	2.87
PKR1	Pan-specific	-2.42	Tau	S516+S519	3.67
PKR1	T451	-2.28	Tau	S713	2.31
PP2A/Ca + PP2A/Cb	Pan-specific	-2.17	Tau	S721	3.37
PTEN	Pan-specific	1.71	Tau	S519	2.4
PTP1B	Pan-specific	-2.11	Tau	S739	2.1
PTP1C	Pan-specific	-1.71	TBK1	Pan-specific	2.12
Pyk2	Y579	-1.72	TRADD	Pan-specific	2.58
Rb	Pan-specific	-1.99	Tyk2	Pan-specific	1.8
Rb	S807+S811	-2.54	Tyrosine Hydroxylase	S18	1.75
RIP2/RICK	Pan-specific	-2.56	Vrk1	Pan-specific	2.22
ROKa (ROCK2)	Pan-specific	1.62	YSK1	Pan-specific	1.6
ROKb (ROCK1)	Pan-specific	-1.69	ZIPK	Pan-specific	2.14
RONa	Pan-specific	-1.66			

Supplementary Table 1. One-hour incubation with Yel002 affected the total concentration and phosphorylation states of 110 proteins in non-irradiated murine lymphocytes. Til-1 cells were incubated for 1 hr with Yel002 (15 μM) prior to total protein harvest. The samples were then shipped to Kinexus™ where the proteins were stained, applied onto antibody microarray chips and readouts were analyzed. Here were compared Z-score ratios of Yel002-treated and untreated samples with a threshold of 1.5 (*P <.05)*.

Supplemental Table 2. Primer sequences used

Primer Name	Description	
TGFßF	TGF Beta forward primer	GGG GTG GAG CCA CAC ATT TA
TGFßR	TGF Beta reverse primer	CTC CTT CGG GTG CTT CAG TT
PIK3IP1F	PI3K interacting protein 1 forward primer	TTG GAC ACT GGC TGT TGA GT
PIK3IP1R	PI3K interacting protein 1 reverse primer	CAG CCA AAACCT TCC TTC CC
Chac1F	Chac1 forward primer	GCC CTG TGG ATT TTC GGG TA
Chac1R	Chac1 reverse primer	CAC TCC AGG ATA CGA GTG CC

1. Cucinotta, F.A., et al., *Space radiation cancer risks and uncertainties for Mars missions.* Radiation research, 2001. **156**(5): p. 682-688.
2. Hogan, D.E. and T. Kellison, *Nuclear terrorism.* The American journal of the medical sciences, 2002. **323**(6): p. 341-349.
3. Wit, J.S. and S.Y. Ahn, *North Korea's Nuclear Futures: Technology and Strategy*. 2015: US-Korea Institute at SAIS.
4. Boice Jr, J.D., *Radiation epidemiology: a perspective on Fukushima.* Journal of Radiological Protection, 2012. **32**(1): p. N33.
5. Stone, H.B., et al., *Models for evaluating agents intended for the prophylaxis, mitigation and treatment of radiation injuries report of an NCI workshop, December 3-4, 2003.* Radiation research, 2004. **162**(6): p. 711-728.
6. López, M. and M. Martín, *Medical management of the acute radiation syndrome.* Reports of Practical Oncology & Radiotherapy, 2011. **16**(4): p. 138-146.
7. Classen, J., et al., *Radiation-induced gastrointestinal toxicity. Pathophysiology, approaches to treatment and prophylaxis.* Strahlentherapie und Onkologie: Organ der Deutschen Rontgengesellschaft...[et al], 1998. **174**: p. 82-84.
8. Saha, S., et al., *Bone marrow stromal cell transplantation mitigates radiation-induced gastrointestinal syndrome in mice.* PLoS One, 2011. **6**(9): p. e24072.
9. Hall, E.J. and A.J. Giaccia, *Radiobiology for the Radiologist*. 2006: Lippincott Williams & Wilkins.
10. Donnelly, E.H., et al., *Acute radiation syndrome: assessment and management.* Southern medical journal, 2010. **103**(6): p. 541-546.
11. Williams, J.P., et al., *Animal models for medical countermeasures to radiation exposure.* Radiation research, 2010. **173**(4): p. 557-578.
12. Pellmar, T.C. and S. Rockwell, *Priority list of research areas for radiological nuclear threat countermeasures.* Radiation research, 2005. **163**(1): p. 115-123.
13. Wingard, J.R., et al., *Long-term survival and late deaths after allogeneic hematopoietic cell transplantation.* Journal of Clinical Oncology, 2011. **29**(16): p. 2230.
14. Xiao, M. and M.H. Whitnall, *Pharmacological countermeasures for the acute radiation syndrome.* Current molecular pharmacology, 2009. **2**(1): p. 122-133.
15. McGregor, D.H., et al., *Breast cancer incidence among atomic bomb survivors, Hiroshima and Nagasaki, 1950–69.* Journal of the National Cancer Institute, 1977. **59**(3): p. 799-811.
16. Preston, D., et al., *Solid cancer incidence in atomic bomb survivors: 1958–1998.* Radiation research, 2007. **168**(1): p. 1-64.
17. Preston, D.L., et al., *Cancer incidence in atomic bomb survivors. Part III: Leukemia, lymphoma and multiple myeloma, 1950-1987.* Radiation research, 1994. **137**(2s): p. S68-S97.
18. Thompson, D.E., et al., *Cancer incidence in atomic bomb survivors. Part II: Solid tumors, 1958-1987.* Radiation research, 1994. **137**(2s): p. S17-S67.

19. Hafer, K., Y. Rivina, and R.H. Schiestl, *Yeast DEL assay detects protection against radiation-induced cytotoxicity and genotoxicity: adaptation of a microtiter plate version.* Radiation research, 2010. **174**(6a): p. 719-726.
20. Brennan, R.J. and R.H. Schiestl, *Detecting carcinogens with the yeast DEL assay.* Genetic Recombination: Reviews and Protocols, 2004: p. 111-124.
21. Brennan, R.J. and R.H. Schiestl, *Free radicals generated in yeast by the Salmonella test-negative carcinogens benzene, urethane, thiourea and auramine O.* Mutation Research/Fundamental and Molecular Mechanisms of Mutagenesis, 1998. **403**(1): p. 65-73.
22. Kirpnick, Z., et al., *Yeast DEL assay detects clastogens.* Mutation Research/Genetic Toxicology and Environmental Mutagenesis, 2005. **582**(1): p. 116-134.
23. Hershman, J.M., et al., *Prevention of DNA double-strand breaks induced by radioiodide-131I in FRTL-5 thyroid cells.* Endocrinology, 2011. **152**(3): p. 1130-1135.
24. Hall, E. and J. Giaccia, *Radiobiology for the radiologist.* 7th ed. Radiobiology for the radiologist. . 2012, Philadelphia: Lippincott Williams & Wilkins.
25. Metcalf, D. and J. Rasko, *Leukemic transformation of immortalized FDC-P1 cells engrafted in GM-CSF transgenic mice.* Leukemia, 1993. **7**(6): p. 878-886.
26. Dührsen, U. and D. Metcalf, *A model system for leukemic transformation of immortalized hemopoietic cells in irradiated recipient mice.* Leukemia, 1988. **2**(6): p. 329-333.
27. Franco Cortese, D.K., Andreyan Osipov, Jakub Stefaniak, Alexey Moskalev, Jane Schastnaya, *Vive la radiorésistance!: converging research in radiobiology and biogerontology to enhance human radioresistance for deep space exploration and colonization.* Oncotarget, 2018(9): p. 14692-14722.
28. Zelefsky, M.J., Z. Fuks, and S.A. Leibel, *Intensity-modulated radiation therapy for prostate cancer.* Semin Radiat Oncol, 2002. **12**(3): p. 229-37.
29. de Arruda, F.F., et al., *Intensity-modulated radiation therapy for the treatment of oropharyngeal carcinoma: the Memorial Sloan-Kettering Cancer Center experience.* Int J Radiat Oncol Biol Phys, 2006. **64**(2): p. 363-73.
30. Chen, J., et al., *Dose-guided radiation therapy with megavoltage cone-beam CT.* The British journal of radiology, 2014. **79**(special issue 1): p. 87-98.
31. Timmerman, R., et al., *Stereotactic body radiation therapy for inoperable early stage lung cancer.* Jama, 2010. **303**(11): p. 1070-1076.
32. Rubin, P., *Late effects of cancer treatment on normal tissues : CURED I, LENT*. Medical radiology. 2008, Berlin ; New York: Springer. xxii, 140 p.
33. Robbins, M. and W. Zhao, *Chronic oxidative stress and radiation-induced late normal tissue injury: a review.* International journal of radiation biology, 2004. **80**(4): p. 251-259.
34. Kuefner, M.A., et al., *Effect of antioxidants on x-ray–induced γ-H2AX foci in human blood lymphocytes: preliminary observations.* Radiology, 2012. **264**(1): p. 59-67.
35. Weiss, J.F. and M.R. Landauer, *Protection against ionizing radiation by antioxidant nutrients and phytochemicals.* Toxicology, 2003. **189**(1-2): p. 1-20.
36. Baranov, A., et al., *Bone marrow transplantation after the Chernobyl nuclear accident.* New England Journal of Medicine, 1989. **321**(4): p. 205-212.

37. Baranov, A., et al., *Hematopoietic recovery after 10-Gy acute total body radiation.* Blood, 1994. **83**(2): p. 596-599.
38. Kalash, R., et al., *Amelioration of radiation-induced pulmonary fibrosis by a water-soluble bifunctional sulfoxide radiation mitigator (MMS350).* Radiation research, 2013. **180**(5): p. 474-490.
39. Medhora, M., et al., *Radiation damage to the lung: Mitigation by angiotensin-converting enzyme (ACE) inhibitors.* Respirology, 2012. **17**(1): p. 66-71.
40. Morgan, G.M., et al., *The Radiation Mitigator MMS350 Prevents Bradyarrhythmias in Irradiated Mice*. 2017, Am Heart Assoc.
41. Anzai, K., et al., *Gamma-tocopherol-N, N-dimethylglycine ester as a potent post-irradiation mitigator against whole body X-irradiation-induced bone marrow death in mice.* Journal of radiation research, 2013. **55**(1): p. 67-74.
42. Kulkarni, S., et al., *Granulocyte colony-stimulating factor antibody abrogates radioprotective efficacy of gamma-tocotrienol, a promising radiation countermeasure.* Cytokine, 2013. **62**(2): p. 278-285.
43. Geiger, H., et al., *Pharmacological targeting of the thrombomodulin–activated protein C pathway mitigates radiation toxicity.* Nature medicine, 2012. **18**(7): p. 1123.
44. Fu, Q., et al., *Preclinical evaluation of Som230 as a radiation mitigator in a mouse model: postexposure time window and mechanisms of action.* Radiation research, 2011. **175**(6): p. 728-735.
45. Wei, L., et al., *The GS-nitroxide JP4-039 improves intestinal barrier and stem cell recovery in irradiated mice.* Scientific reports, 2018. **8**(1): p. 2072.
46. Deng, W., et al., *Mitigation of the hematopoietic and gastrointestinal acute radiation syndrome by octadecenyl thiophosphate, a small molecule mimic of lysophosphatidic acid.* Radiation research, 2015. **183**(4): p. 465-475.
47. Patil, R., et al., *Combined mitigation of the gastrointestinal and hematopoietic acute radiation syndromes by an LPA2 receptor-specific nonlipid agonist.* Chemistry & biology, 2015. **22**(2): p. 206-216.
48. Benesch, M.G., et al., *Tumor-induced inflammation in mammary adipose tissue stimulates a vicious cycle of autotaxin expression and breast cancer progression.* The FASEB Journal, 2015. **29**(9): p. 3990-4000.
49. Kauppila, J., et al., *Toll-like receptor 5 (TLR5) expression is a novel predictive marker for recurrence and survival in squamous cell carcinoma of the tongue.* British journal of cancer, 2013. **108**(3): p. 638.
50. Rutkowski, M.R., et al., *Microbially driven TLR5-dependent signaling governs distal malignant progression through tumor-promoting inflammation.* Cancer cell, 2015. **27**(1): p. 27-40.
51. Song, E.-J., et al., *Flagellin promotes the proliferation of gastric cancer cells via the Toll-like receptor 5.* International journal of molecular medicine, 2011. **28**(1): p. 115-119.
52. Sfondrini, L., et al., *Antitumor activity of the TLR-5 ligand flagellin in mouse models of cancer.* The Journal of Immunology, 2006. **176**(11): p. 6624-6630.
53. Cai, Z., et al., *Activation of Toll-like receptor 5 on breast cancer cells by flagellin suppresses cell proliferation and tumor growth.* Cancer research, 2011. **71**(7): p. 2466-2475.

54. Rivina, L., M.J. Davoren, and R.H. Schiestl, *Mouse models for radiation-induced cancers.* Mutagenesis, 2016. **31**(5): p. 491-509.
55. Ito, A., et al., *Contribution of indirect action to radiation-induced mammalian cell inactivation: dependence on photon energy and heavy-ion LET.* Radiation research, 2006. **165**(6): p. 703-712.
56. Nakamura, H., et al., *DNA repair defect in AT cells and their hypersensitivity to low-dose-rate radiation.* Radiation research, 2006. **165**(3): p. 277-282.
57. Rubin, S.M., *Deciphering the retinoblastoma protein phosphorylation code.* Trends in biochemical sciences, 2013. **38**(1): p. 12-19.
58. Bertoli, C. and R.A.M. de Bruin, *Cell Division: Turning cell cycle entry on its head.* Elife, 2014. **3**: p. e03475.
59. Narasimha, A.M., et al., *Cyclin D activates the Rb tumor suppressor by mono-phosphorylation.* Elife, 2014. **3**.
60. Robles, S.J. and G.R. Adami, *Agents that cause DNA double strand breaks lead to p16 INK4a enrichment and the premature senescence of normal fibroblasts.* Oncogene, 1998. **16**(9): p. 1113.
61. Buis, J., et al., *Mre11 nuclease activity has essential roles in DNA repair and genomic stability distinct from ATM activation.* Cell, 2008. **135**(1): p. 85-96.
62. Garner, K.M. and A. Eastman, *Variations in Mre11/Rad50/Nbs1 status and DNA damage-induced S-phase arrest in the cell lines of the NCI60 panel.* BMC cancer, 2011. **11**(1): p. 206.
63. Gao, R., et al., *Targeting of DNA damage signaling pathway induced senescence and reduced migration of cancer cells.* Journals of Gerontology Series A: Biomedical Sciences and Medical Sciences, 2014. **70**(6): p. 701-713.
64. Liang, J. and J.M. Slingerland, *Multiple roles of the PI3K/PKB (Akt) pathway in cell cycle progression.* Cell cycle, 2003. **2**(4): p. 336-342.
65. Masson, G.R., et al., *The intrinsically disordered tails of PTEN and PTEN-L have distinct roles in regulating substrate specificity and membrane activity.* Biochemical Journal, 2016. **473**(2): p. 135-144.
66. Hemmings, B.A. and D.F. Restuccia, *Pi3k-pkb/akt pathway.* Cold Spring Harbor perspectives in biology, 2012. **4**(9): p. a011189.
67. Jasin, M. and R. Rothstein, *Repair of strand breaks by homologous recombination.* Cold Spring Harbor perspectives in biology, 2013. **5**(11): p. a012740.
68. Brenner, D. and J. Ward, *Constraints on energy deposition and target size of multiply damaged sites associated with DNA double-strand breaks.* International journal of radiation biology, 1992. **61**(6): p. 737-748.
69. Hill, M., *Radiation damage to DNA: the importance of track structure.* Radiation measurements, 1999. **31**(1): p. 15-23.
70. Korystov, Y.N., *Contributions of the direct and indirect effects of ionizing radiation to reproductive cell death.* Radiation research, 1992. **129**(2): p. 228-234.
71. Schiestl, R.H., et al., *Carcinogens induce intrachromosomal recombination in yeast.* Carcinogenesis, 1989. **10**(8): p. 1445-1455.
72. Schiestl, R.H., S. Igarashi, and P. Hastings, *Analysis of the mechanism for reversion of a disrupted gene.* Genetics, 1988. **119**(2): p. 237-247.

73. Slupphaug, G., B. Kavli, and H.E. Krokan, *The interacting pathways for prevention and repair of oxidative DNA damage.* Mutation Research/Fundamental and Molecular Mechanisms of Mutagenesis, 2003. **531**(1): p. 231-251.
74. Xu, Y., et al., *Targeted disruption of ATM leads to growth retardation, chromosomal fragmentation during meiosis, immune defects, and thymic lymphoma.* Genes & development, 1996. **10**(19): p. 2411-2422.
75. Beucher, A., et al., *ATM and Artemis promote homologous recombination of radiation-induced DNA double-strand breaks in G2.* The EMBO journal, 2009. **28**(21): p. 3413-3427.
76. Quennet, V., et al., *CtIP and MRN promote non-homologous end-joining of etoposide-induced DNA double-strand breaks in G1.* Nucleic acids research, 2010. **39**(6): p. 2144-2152.
77. Miller, A.C., et al., *Leukemic transformation of hematopoietic cells in mice internally exposed to depleted uranium.* Molecular and cellular biochemistry, 2005. **279**(1-2): p. 97-104.
78. Miller, A.C., M. Stewart, and R. Rivas, *DNA methylation during depleted uranium-induced leukemia.* Biochimie, 2009. **91**(10): p. 1328-1330.
79. Rossi, D.J., et al., *Deficiencies in DNA damage repair limit the function of haematopoietic stem cells with age.* Nature, 2007. **447**(7145): p. 725.
80. Tilgner, K., et al., *A human iPSC model of Ligase IV deficiency reveals an important role for NHEJ-mediated-DSB repair in the survival and genomic stability of induced pluripotent stem cells and emerging haematopoietic progenitors.* Cell death and differentiation, 2013. **20**(8): p. 1089.
81. Tilgner, K., et al., *Brief report: a human induced pluripotent stem cell model of cernunnos deficiency reveals an important role for XLF in the survival of the primitive hematopoietic progenitors.* Stem Cells, 2013. **31**(9): p. 2015-2023.
82. Kadyk, L.C. and L.H. Hartwell, *Sister chromatids are preferred over homologs as substrates for recombinational repair in Saccharomyces cerevisiae.* Genetics, 1992. **132**(2): p. 387-402.
83. Dutta, A., et al., *Microhomology-mediated end joining is activated in irradiated human cells due to phosphorylation-dependent formation of the XRCC1 repair complex.* Nucleic acids research, 2016. **45**(5): p. 2585-2599.
84. Ottaviani, D., M. LeCain, and D. Sheer, *The role of microhomology in genomic structural variation.* Trends in Genetics, 2014. **30**(3): p. 85-94.
85. Sharma, S., et al., *Homology and enzymatic requirements of microhomology-dependent alternative end joining.* Cell death & disease, 2016. **6**(3): p. e1697.
86. Kang, M., W. Guo, and N. Park, *Replicative senescence of normal human oral keratinocytes is associated with the loss of telomerase activity without shortening of telomeres.* Cell growth & differentiation: the molecular biology journal of the American Association for Cancer Research, 1998. **9**(1): p. 85-95.
87. Kim, R.H., et al., *Bmi-1 extends the life span of normal human oral keratinocytes by inhibiting the TGF-β signaling.* Experimental cell research, 2010. **316**(16): p. 2600-2608.
88. Hussain, T. and R. Mulherkar, *Lymphoblastoid cell lines: a continuous in vitro source of cells to study carcinogen sensitivity and DNA repair.* International journal of molecular and cellular medicine, 2012. **1**(2): p. 75.

89. Yamamoto, M.L., A.M. Chapman, and R.H. Schiestl, *Effects of side-stream tobacco smoke and smoke extract on glutathione-and oxidative DNA damage repair-deficient mice and blood cells.* Mutation Research/Fundamental and Molecular Mechanisms of Mutagenesis, 2013. **749**(1): p. 58-65.
90. Xie, Y., et al., *Deficiencies in mouse Myh and Ogg1 result in tumor predisposition and G to T mutations in codon 12 of the K-ras oncogene in lung tumors.* Cancer research, 2004. **64**(9): p. 3096-3102.
91. Muslimovic, A., et al., *An optimized method for measurement of gamma-H2AX in blood mononuclear and cultured cells.* Nature protocols, 2008. **3**(7): p. 1187.
92. Reliene, R. and R.H. Schiestl, *Antioxidant N-acetyl cysteine reduces incidence and multiplicity of lymphoma in Atm deficient mice.* DNA repair, 2006. **5**(7): p. 852-859.
93. Westbrook, A.M. and R.H. Schiestl, *Atm-deficient mice exhibit increased sensitivity to dextran sulfate sodium–induced colitis characterized by elevated DNA damage and persistent immune activation.* Cancer research, 2010. **70**(5): p. 1875-1884.

Chapter 3: A Novel Probiotic, Lactobacillus Johnsonii 456, Resists Acid and Can Persist in the Human Gut for Over 30 Days

A Novel Probiotic, Lactobacillus Johnsonii 456, Resists Acid and Can Persist in the Human Gut for Over 30 Days

Michael J. Davoren[a,1,*], Jared Liu[b,*], Jocelyn Castellanos[a], Norma I. Rodríguez-Malavé[c], and Robert H. Schiestl[a]

[a]Molecular Toxicology Interdepartmental Program, Environmental Health Sciences, Fielding School of Public Health, University of California Los Angeles, 650 Charles E. Young Dr. S., Los Angeles, CA 90095
[b]School of Medicine, University of California, San Francisco, 513 Parnassus Ave, San Francisco, CA 94143
[c]Department of Biomedical Sciences, Cedars-Sinai Medical Center, 8700 Beverly Boulevard, Los Angeles CA 90048
[*]These authors contributed equally to this work.

Probiotics are considered to have multiple beneficial effects on the human gastrointestinal tract, including immunomodulation, pathogen inhibition, and improved host nutrient metabolism. However, extensive characterization of these properties is needed to define suitable clinical applications for probiotic candidates. *Lactobacillus johnsonii* 456 (LBJ 456) was previously demonstrated to have anti-inflammatory and anti-genotoxic effects in a mouse model. Here, we characterize its resistance to gastric and bile acids as well as its ability to inhibit gut pathogens and adhere to host mucosa. While bile resistance and in vitro host attachment properties of LBJ 456 were comparable to other tested probiotics, LBJ 456 maintained higher viability at lower pH conditions compared to other tested strains. LBJ 456 also altered pathogen adhesion to LS 174T monolayers and demonstrated contact-dependent and independent inhibition of pathogen growth. Importantly, we show that ingestion of *Lactobacillus johnsonii* 456 over a one week yogurt course leads to persistent viable bacteria detectable beyond one month, far longer than other related species have been demonstrated to persist.

gut microbiota | probiotics | microbiology | bacteria | lactobacillus

The human gastrointestinal (GI) tract is home to over 500 species of bacteria in a given individual [1]. These microbes and their byproducts play as important a function in our bodies as any other organ, and have been subject to co-adaptation with their hosts for at least 500 million years [2]. The microbiome has been demonstrated to have an impact on nearly every aspect of human health. Gut microbiota composition is a risk factor for inflammatory bowel diseases (IBDs) such as Crohn's Disease and ulcerative colitis [3]. Resident bacteria play a critical role in the

Significance

Bacterially derived diarrheal disease is a major contributor to worldwide deaths for children under the age of five. On the other end of the spectrum, chronic inflammation contributes to cancer, which claims more lives in developed countries than any other illness beside cardiovascular disease. Probiotic bacteria offer a method of intervention that could reduce fatalities from both of these seemingly disparate diseases. It is imperative that new strains of probiotic bacteria be characterized while we simultaneously develop our understanding of their mechanisms of action. Lactobacillus johnsonii 456 is associated with reduced inflammation and genotoxicity in vertebrate models, pathogen inhibition in vitro, and unprecedented persistence in human trials, making it a powerful option for populations without consistent access to resources.

Author contributions: R.H.S. designed research and prepared manuscript, M.J.D. and J.L. designed research, performed research, analyzed data, and prepared manuscript; J.C. and N.I.R.M. performed research, analyzed data, and prepared manuscript. All authors read and approved the final manuscript.
Conflict of Interest Statement: R.H.S. has a financial interest in MicroBio Pharma, Inc, which might benefit from the commercialization of the results of this research.
[1]The author to whom correspondence should be addressed. Email: mdavoren@g.ucla.edu

development of healthy immune system function [4]. Microbial metabolic processes generate short-chain fatty acids (SCFAs) that provide a primary energy source for the cells of the gut [5], as well as vitamins and amino acids necessary for systemic health [6]. Microbiome composition affects efficiency of nutrient metabolism, playing a role in obesity risk and even cholesterol levels [7-9]. There is even evidence to suggest that the microbiome plays a role in normal CNS function and depression incidence [10]. The manipulation of the microbiome by purposefully seeding certain probiotic, or beneficial, strains for their properties may allow us to better control every one of these endpoints – with the right level of understanding. However, these multifactorial effects are often difficult to study in a well-controlled environment.

The most clearly demonstrable attribute of most probiotic strains is their capability to reduce the adherence and subsequent activity of pathogenic strains. Probiotic bacteria can perform this useful service via a number of mechanisms, including indirect competition for nutrients and binding sites in the host [11], and directly through the production of bacteriocins, acids, and other compounds [12-14]**.** Multiple probiotic formulations, including *Lactobacillus* and *Bifidobacterium* strains, have been shown to reduce the duration of diarrhea and enterocolitis in children [15]. However, the results are not as consistent for the treatment of inflammatory syndromes [16]. Despite a global market value in the tens of billions of US dollars, growing by over 10% per year [17], there is, as of the end of 2017, no probiotic that is clinically approved by the FDA. The popular probiotic *Lactobacillus rhamnosus GG* did not yield significant results in a clinical trial against vancomycin-resistant enterococcus (VRE) [18], and *L. johnsonii* NCC 533 failed in a clinical trial against Crohn's disease [19].

Considering the strong evidence for anti-inflammatory and antipathogenic effects, it is clear that both the search for new probiotic strains and the continued testing of existing ones should eventually yield clinically effective treatment methods. For dedicated clinical application, strains will need to be characterized based on their effects on individual disease states. For example, a strain that induces a beneficial cytokine response under certain circumstances might exacerbate pathogen-induced disease in others by interfering with the immune response [20]. For this reason, it is imperative that every isolated strain of probiotic bacteria be individually tested and characterized in multiple models. A rationally designed set of experiments demonstrating survival, adhesion, and pathogen inhibition should be carried out with strains that show promising attributes [21].

Lactobacillus johnsonii strain 456 (LBJ 456) was discovered by examining bacterial strains overrepresented in the microbiota of a cancer-resistant colony of DNA-repair deficient mice [22]. Considering that oral gavage with this strain over the course of 4 weeks was capable of significantly reducing systemic inflammation and genotoxicity in this mammalian model, LBJ 456 represents a strong candidate probiotic strain. In this article, we further demonstrate this strain's potential for use in humans by characterizing its acid and bile resistance as well as its host adhesion, pathogen inhibition, and colonization properties. We also analyze the LBJ 456 genome to investigate the genetic basis underlying some of these properties.

Results

***Lactobacillus johnsonii* 456 shows exceptional resistance to gastric acid and moderate bile acid tolerance.** To assess LBJ 456's viability in the GI tract, we compared its relative tolerance to gastric acid and bile against a panel of type strains representing commonly used probiotic species, including the two commercially available strains *B. lactis* HN019 and *L. plantarum* 299V (**Table 1**). We also included *S. salivarius subsp. thermophilus,* which is not a *Lactobacillus* or *Bifidobacterium* species but is still considered a "probiotic" by the European Food Safety Administration for its potential assistance in lactose digestion, and

traditional role in yogurt preparation [23]. We measured the viable bacteria recovered for each strain after incubation for 2 hours in gastric conditions that ranged from pH 3 to pH 1.2 (**Fig. 1*A*, Fig. S1**). While recoverable CFU from each strain generally decreased with lower pH conditions, the viability of the two *L. johnsonii* strains LBJ 456 and VPI 7960 was observed to increase beyond the input CFU at pH 3. Moreover, the viability of LBJ 456 in particular was consistently the highest at all pH conditions tested. Importantly, LBJ 456 was also the only strain to show viability at pH 1.2, albeit at a 1000-fold reduction compared to its viability in a control pH 6 incubation.

Next, we compared the growth of the probiotic strain panel in media under different physiologically relevant bile acid conditions (**Fig. 1*B*, Fig. S2**). A relatively bile acid rich environment (0.3% / ~6mM) impairs the growth of LBJ 456 to a certain extent, but it still reached concentrations of around 4-5 x 10^6 cells/mL after 24 hours (as opposed to nearly 1 x 10^9 cells in bile-free media control). Interestingly, bile acid resistance among strains allowed for clear delineation between genera, especially at 0.2 and 0.3%. *B. lactis* growth was only decreased to about 10% of control at 0.3% bile acid. *Lactobacillus* species as a whole had moderate resistance, but *L. plantarum* 299V's growth was impaired the least of all *Lactobacillus* strains. *S. salivarius* was highly sensitive to acid and bile acid exposure and was unable to grow at all in 0.3% bile acid, suggesting that this strain likely does not survive in the human GI tract.

***L. johnsonii* 456 adheres most strongly to goblet cell-like monolayer forming line LS 174T.** Bacterial adhesion to the intestinal epithelium, as well as the associated mucus secretions, has long been considered an important probiotic criterion [24, 25]. The interaction with the outer layer of human cells in the gut was modeled by the culture of two monolayer-forming human cancer cell lines, Caco-2 and LS 174T (**Fig. 2**). LBJ 456 adhered best to the extracellular mucin-rich LS 174T cells. For both *L. johnsonii* strains, a little over 10% of plated cells maintained adherence through multiple washes. *L. casei* adhered even better to LS 174T, but LBJ 456 maintained better adhesion than the two commercial probiotic strains. Both LBJ 456 and *L. casei*, however, had much lower relative adherence to the enterocyte-like Caco-2 monolayers, with only about 0.1% of plated cells adhering, even though other strains had about 1% adhesion rates. These data suggest potential specialization of different *Lactobacillus* strains to better adhere to different gut mucin phenotypes. Interestingly, *S. salivarius* adhered relatively well to both cell lines, despite the fact that its survival until that point in the digestive tract would seem unlikely based on acid sensitivity.

L. johnsonii* 456 significantly alters pathogen adhesion to LS 174T, but not to Caco-2 monolayers.** We examined the capacity of adherent LBJ 456 to inhibit the adhesion of three pathogenic strains of gut bacteria (**Table 1**) to both LS 174T and Caco-2 cell monolayers. Pretreatment of Caco-2 monolayers with LBJ 456 did not lead to any significant difference in the level of pathogen adhesion, likely because of the LBJ 456's limited ability to adhere to this cell type (**Fig. 3*A). However, LBJ 456 pretreatment of LS 174T monolayers led to significant changes in pathogen adherence (**Fig. 3*B***). Enterotoxigenic (ETEC) *E. coli* and *S. enterica* adhesion were reduced by about 30% ($p = 0.0423$) and 40% ($p = 0.0658$), respectively. Interestingly, *E. faecalis* adhesion increased slightly after pretreatment with LBJ 456, indicating that the inhibitory capability of this strain is not universal.

***L. johnsonii* 456 significantly inhibits pathogen growth in co-culture.** We determined whether LBJ 456 can directly inhibit the growth of pathogens by co-culturing it with equal CFU ratios of each pathogenic strain. The growth of all three pathogens was significantly reduced when they were co-cultured with LBJ 456 (**Fig. 4**). *E. coli* growth was suppressed roughly 60%, from a final concentration of 5 to 2 x 10^8 cells/mL. Final *E. faecalis* concentrations

were cut by a little more than 50% as well. The greatest effect was seen against *Salmonella*, with an over 90% decrease in viable CFU detected from coincubation. ($p < .0001$ for all comparisons) Lactobacillus was readily capable of growth in media other than its own (**Fig. S3**)

Filter sterilized supernatant of *L. johnsonii* 456 significantly inhibits the survival of *Salmonella* and *E. faecalis*, but not of *E. coli*. As shown in **Table 2**, *E. coli* was unaffected by filtered supernatant (FS) from any *Lactobacillus* strain except *L. plantarum*, which completely prevented its survival. LBJ 456 FS significantly inhibited *E. faecalis* survival by about 50% ($p = 0.0427$), while *L. plantarum* FS killed off over 99% of that species ($p = 0.0051$). All tested *Lactobacillus* strains significantly decreased *Salmonella* survival, with all tested strains beside *L. casei* leading to a complete absence of viable CFU after 18-20 hours. Surprisingly, all tested FS led to significantly decreased *Bifidobacterium* viability as well, around 60% with *L. johnsonii* 456, *L. johnsonii* VPI 7960, and *L. casei. L. plantarum* led to a decrease of roughly 40%. As pH was controlled for, another acellular factor must be responsible for these differences.

L. johnsonii* 456 can persist in the human gut for over one month after ingestion.** We determined whether LBJ 456 was capable of survival through the human gut. 11 individuals completed a 7 day LBJ yogurt trial and supplied fecal samples before yogurt consumption (day 0), immediately after (day 7) and at 30 and 60 days after initiation. Over the course of the study, no adverse side effects or diarrhea symptoms were reported for any of the volunteers. After sample collection, the subset of volunteers that tested negative for background *Lactobacillus* before study initiation were grouped for secondary analysis. First, stool samples were analyzed for the presence of live lactic acid bacteria (LAB) (**Fig. 5*A). There was a statistically significant difference between all time points in the full group of participants that consumed LBJ 456 yogurt over the course of the 60 day period ($p < 0.001$, Friedman test). Post hoc analysis with Wilcoxon signed rank tests were conducted and a Bonferroni correction applied, resulting in a significance level set at $p < 0.0083$. After correction statistical significance was observed only between baseline and day 7 samples ($p = 0.008$). Individuals with *Lactobacillus*-negative baseline fecal readings also showed statistical significance over the 60 day course ($p < 0.001$, Friedman test). Post hoc analysis with Wilcoxon signed rank tests were conducted and a Bonferroni correction applied, resulting in a significance level again set at $p < 0.0083$. After Bonferroni correction, no differences were significant in this group due to the low number of participants. Despite this, there was a clear upward trend in detectable live *Lactobacillus* counts in both the whole group and the LB-negative background subset that lingered through at least one month after the weeklong course. Viable LAB increased by about an order of magnitude (~$10^{4.5}$ to $10^{5.5}$ CFU/gram feces) at days 7 and 30 in the full group, and was still about a half order of magnitude higher at day 60. Quantitative polymerase chain reaction (qPCR) was performed on the same fecal samples to confirm results with a higher specificity for LBJ 456 (**Fig. 5*B*, Fig. S4**). Overall, a similar pattern was observed with regards to the ratio of LBJ 456-specific DNA to total bacterial DNA over time. Background counts increased from LBJ 456-negative at day 0 (<1 copy/million bacterial genomes) to an average of roughly one copy per 50,000 bacterial genomes from days 7-30. These increases trended towards but did not quite reach significance due to the high variance and low number of participants ($p = 0.0547$ for Day 0 vs. Day 30, Wilcoxon signed rank test, $n = 11$).

According to recent estimates, about 3.8×10^{13} bacteria make their home in the average human, with most of those in the gut [26]. Of these, approximately 10^{11} cells are shed with every gram of feces. Based on our qPCR estimates, at least two million LBJ 456 genomes would be represented in the feces of individuals recently inoculated with the strain, assuming the average cell has one

detectable copy of the 16sRNA gene (a conservative estimate, considering that many species encode multiple copies) [27]. This number is relatively consistent with the viable CFU numbers on the order of $10^{5.5}$ CFU/gram, especially considering cells rendered nonviable by the freezing process.

Potential genetic basis of LBJ 456 persistence and inhibition properties revealed by comparative genomics. To better understand the genomic basis underlying the probiotic properties of LBJ 456, we sequenced its genome and compared it to 23 publically available *L. johnsonii* genomes. The 24 *L. johnsonii* genomes share 1.2 Mb of conserved genomic sequence. Alignment of 101,088 SNPs in this core genome revealed two groups of highly similar *L. johnsonii* genomes, one consisting of 117a, 117c, 117d, 117k, 117q, and 117x, and the other consisting of UMNLJ21 and UMNLJ22 (**Fig. 6*A***). The isolates within these groups differ by less than 300 SNPs and may represent isolates of the same strain. Considering 117a and UMNLJ22 as representative isolates for these groups, we found that the *L. johnsonii* strains differ by an average of 29,943 core genome SNPs. In particular, LBJ 456 differs more from VPI 7960 (33,051 core SNPs), an isolate from human blood, than W1 (20,369 core SNPs), another isolate from mouse gut [28], consistent with previous observations that genetic similarity among *L. johnsonii* strains is highest among strains from the same host organism [29].

We then identified 550 genomic regions that are not shared among all 24 *L. johnsonii* strains. These non-core regions total 1,067,226 bp and include regions unique to each of LBJ 456, NCC 533, 117c, 117d, 117q, and 16 (**Fig. 6*B*)**. Within the LBJ 456 genome, we identified 11 non-core regions totaling 41,781 bp. As shown in **Table 3**, these regions encode proteins mostly involved in replication (e.g. FtsK/SpoIIIE family protein, plasmid replication protein), and antiviral defense (restriction-modification enzymes), suggesting that cell proliferation strategies and phage exposure may be important processes that determine the compatibility and viability of LBJ 456, and *L. johnsonii* strains in general, within particular hosts.

Moreover, we observed two mucus binding proteins (MBPs) encoded in the non-core regions unique to LBJ 456. A more comprehensive comparison of MBPs across the 24 *L. johnsonii* strains revealed between 3 and 18 MBPs (average 7) in each genome, with LBJ 456 containing the most. These MBPs represent a repertoire of 34 unique homologs based on clustering by 70% identity. 13 of these homologs are encoded only by single strains, including two that are uniquely encoded by LBJ 456 (PROKKA_00690 and PROKKA_00875).

We also identified two bacteriocin-encoding loci in the LBJ 456 genome (**Figure S6, Table S2**). The first locus contains three putative type II bacteriocins (PROKKA_00793, PROKKA_00800, and PROKKA_00806) and two other genes (PROKKA_00798 and PROKKA_00799) predicted to encode proteins involved in bacteriocin processing and secretion. The second locus contains a single predicted bacteriocin gene, PROKKA_00732, surrounded by genes with no clear bacteriocin processing or secretion function. However, as two transposase-related proteins, PROKKA_00728 and PROKKA_00729, were also detected in this locus, it is possible that this putative bacteriocin may be part of a mobile genetic element.

Discussion

The stomach poses several challenges to ingested bacteria, both through low pH itself as well as strong proteases active in the acidic environment. Resistance to gastric acid is one of most important selection criteria for any potential probiotic. Strong acid tolerance is not universal amongst LAB, even at the species level, and must be tested on a strain-by-strain basis [30]. Survival at pH 3 is generally considered to be the absolute minimum necessary for a probiotic strain to remain viable *in vivo*, although pH 2 is a

much more commonly encountered level of acidity [31]. In a fasting stomach, pH can drop as far as 1.2-1.5 [32]. *Lactobacillus johnsonii* 456 has particularly high resistance to SGA compared to other strains at these levels, both experimentally and in the literature [33]. Literature values for well researched strains conform well with our results, including high tolerance to pH 2 for *B. lactis HN019* but strongly decreased viability for *L. acidophilus* 4356 [33, 34]. Most strains of *Lactobacillus*, including those isolated from probiotic foods and human samples, have large decreases in viability when exposed to pH values between 1.5 and 2 [35-37]. Strains with high resistance to gastric acid appear rarely in the literature, but none appear to be as fully resistant as LBJ 456. For example, Aiba et al report > 10% viability in *L. johnsonii* 1088 and *L. gasseri* OLL 2716 at pH 1, and 1% survival of *L. johnsonii* NCC533 [38]. However, this experiment used a simplified gastric assay without pepsin by diluting media 1:9 with solution of the reported pH, increasing the available nutrients and distorting the actual pH value. Increased availability of metabolizable sugar is a known driver of higher acid tolerance [39], while pepsin decreases survival in synergy with low pH. Maragkoudakis et al found 6 of 29 tested *Lactobacillus* strains remained viable after 1 hour at pH 1 without pepsin, but inhibition with pepsin at pH 2 was nearly as heavy for most strains [40]. For this reason, the inclusion of pepsin is an important part of a full simulation of gastric acid. In our own experiments, both LBJ 456 and its type strain *L. johnsonii* VPI 7960 showed no significant decrease in viability after incubation in pH 2 SGA. However, only LBJ 456 endured extremely low pH under conditions with pepsin with over 10% survival at pH 1.6 and 3 log decreased viability at pH 1.2. Although these levels of acidity would only be encountered in a nearly empty stomach, a fraction of LBJ 456 can survive whether or not food or drink is co-ingested. The mechanism of this strong acid tolerance is not yet understood.

Bile acids in the small intestine inhibit growth via their detergent effects on bacterial cell membranes. Some probiotic species can hydrolyze these bile acids directly [40, 41]. They are very rarely lethal for LAB at the lower end of physiological concentrations, which can vary from up to 10mM in the upper ileum to 2mM in the lower ileum after a meal [42, 43]. We observed moderately retarded growth rates in all LAB strains exposed to physiologically relevant bile acid concentrations. Literature values generally agree with our observations, including our assessment of *L. acidophilus* 4356 being particularly sensitive, and *B. lactis* being relatively bile acid tolerant [33, 34]. Although *L. johnsonii* 456 is not in the upper tiers of bile tolerant strains, it remains viable and capable of slower growth at bile acid concentrations between 0.1 and 0.3% (~2 – 6 mM).

Even in light of the strain's *in vitro* survival through simulated GI tract barriers, *L. johnsonii* 456's persistence in the human gut seems exceptional. A weeklong course of a small, daily amount of live culture led to elevated fecal counts by both plate and qPCR analysis through at least a month. Current understanding suggests that, while each individual has a unique and relatively stable set of "core" species [44], specific composition can vary enormously over short periods of time in response to diet [45]. Most probiotic strains, like *Lactobacillus* and *Bifidobacterium,* are transient. They interact with the host on their journey through the gut, but in general do not actively reproduce or colonize for long periods [46]. Most tested strains, including *L. plantarum* 299V, *L. rhamnosus* GG, and *L. casei* shirota are not recoverable in host feces after more than a week or so post ingestion [47-49]. Beyond survival, unique binding properties to host factors must be involved in LBJ 456's long duration of detectability.

Host mucins provide a common binding site for both beneficial and pathogenic bacterial strains [50]. We observed a broad array of MBPs encoded by *L. johnsonii* strains, some of which appeared to be unique to LBJ 456. Different combinations of these MBPs may confer unique binding properties and contribute to

host specificities previously observed among *L. johnsonii* subtypes [29]. The secreted mucin Muc2 constitutes the main mucus glycoprotein in the mouse small intestine, from which LBJ 456 was derived [51]. Its ortholog, MUC2, is the main secreted mucin in the human gut as well, comprising most of the upper, gel-like layer of mucus [52]. The enterocyte-like cell line Caco-2's mucin profile is almost purely limited to the expression of membrane-bound mucins like MUC1. The goblet cell-like line LS 174T, however, has much higher expression of secretory mucins, including MUC2 [53]. As the secreted mucus layer is the major site of microbe-host interaction, increased adhesion of LBJ 456 to LS 174T could explain this strain's persistence *in vivo,* especially if MUC2 or another secreted mucin is assumed to be a putative binding target [54].

Although adhesion to mucins and other mucosal proteins is difficult to study in the human intestine proper, cell monolayer assays correlate reasonably well with *in vivo* persistence data and provide a method for the investigation of both relative adhesion and adhesion inhibition between microbes [55, 56]. The adherence of LAB to monolayer models such as Caco-2 and LS 174T is highly variable between strains. Many probiotic *Lactobacillus* species barely adhere to enterocyte-like Caco-2 cells at all, while others adhere reasonably well [57]. Interestingly, while none of the strains tested here were especially adherent to Caco-2 monolayers, LBJ 456's adhesion was particularly low, roughly 1/20th that of its type strain LBJ VPI 7960. This may be a result of the species and environment from which it was derived. Todoriki et al report that the likewise murine-derived *L. johnsonii* strain JCM 8792 exhibits very low adhesion to Caco-2 cells relative to such strains as the chicken derived *L. reuteri* JCM 1081 [58], strengthening our suggestion that *Lactobacillus* of murine origin may be less specialized to adhere to secreted mucin-poor culture. LBJ 456 adhered to LS 174T monolayers particularly well. Adhesion was observed to a greater extent than the commercially available probiotic strains *L. plantarum* 299V and *B. lactis* HN019. LBJ 456 also adhered to LS 174T an order of magnitude better than *L. acidophilus* ATCC 4356, which demonstrated strong adhesion in the 5 hour exposure model used by Jung et al [59].

The pathogenic activity of many diarrheagenic bacteria, such as ETEC and *Salmonella,* is dependent upon adhesion to the gut mucosa and can therefore also be modeled with monolayers *in vitro* [60, 61]. *Salmonella enterica* typhimurium and ETEC strain H10407 are both prototypical diarrhea inducers, and require close adhesion to the host cell in order to cause disease [62-64]. *E. faecalis*, although normally considered a commensal, can also become an opportunistic pathogen and diarrhea inducer in immunocompromised individuals, with multidrug resistant strains causing particularly stubborn nosocomial infections [65]. A number of studies have demonstrated that adherent *Lactobacillus* species can inhibit subsequent pathogen adhesion. Todoriki showed that *L. crispatus* JCM 8779 itself reduced *E. faecalis* adhesion by 99% in a Caco-2 model, as well as *Salmonella* and ETEC adhesion by 28 and 47% respectively. Filtered supernatant from *L. crispatus* inhibited *E. faecalis* growth, but not *Salmonella* or ETEC [58]. Maragkoudakis et al showed that Caco-2 adherent strains could reduce *E. coli* and *Salmonella* adhesion by 10-50%, although they noted no inhibition from supernatant-localized factors [40]. *L. johnsonii* 456's capacity to inhibit pathogen adhesion appears to depend on its own ability to adhere to the monolayer in question. Pre-treatment with one hour of LBJ 456 led to no significant change in pathogen adhesion on Caco-2 cells. On LS 174T monolayers, both ETEC and *Salmonella* adhesion were cut by about 33 and 40%, respectively. Unexpectedly, *E. faecalis* adhesion increased slightly with LBJ 456 incubation, suggesting that LBJ 456 would not necessarily displace other commensals from its milieu. Moreover, this observation raises the possibility that LBJ 456 may promote the attachment of certain gut flora, perhaps through direct binding to

the cell surface or via substrates secreted, induced, or modified by it.

In co-culture conditions, LBJ 456 drastically reduced the growth of all three pathogenic strains, particularly *Salmonella*, although the mechanisms appear to be different. FS from an LBJ 456 culture grown to the beginning of stationary phase was capable of completely inhibiting *Salmonella* growth and reducing *E. faecalis* growth by half, while ETEC viability was unaffected by the addition of sterilized media. *B. lactis* HN019 growth was also inhibited by a nonacid, acellular factor. As *L. johnsonii* VP 7960 FS induced nearly the same effects, a common *L. johnsonii* factor may be responsible for this inhibition. Interestingly, *L. plantarum* 299V FS inhibited all three pathogenic strains. This strain is not known to produce any bacteriocins itself, but other *plantarum* strains produce a class of two-peptide, class IIB bacteriocins called plantaricins [66, 67]. Most plantaricins are effective against other gram-positive bacteria, like *Listeria* and *Enteroccoccus*, so this particular class of peptide antimicrobial likely does not explain the strong inhibition of ETEC. However, supernatant inhibition of *E. faecalis* growth could be due to a bacteriocin. *L. johnsonii* strains have been shown to produce a bacteriocin, lactacin F, that inhibits the growth of both *E. faecalis* and other LAB through membrane disrupting pore formation [68]. Based on our genomic analysis, it is likely that LBJ 456 does in fact produce functional bacteriocins, some of which may be responsible for this cell-independent inhibitory effect.

At least two proposed mechanisms exist regarding probiotic-mucin interaction and pathogen binding inhibition. Through competitive adherence, *Lactobacillus* or other beneficial species could compete directly for mucin binding sites with pathogens, preventing them from having a chance to interact with host cells [69]. Alternatively, it has been suggested that *Lactobacillus* binding to host mucins can lead to the secretion of even more mucins, essentially flushing pathogens from the lumen [70, 71]. This increased mucin production could potentially counteract the mucin degradation induced by pathogens like enterotoxigenic *E. coli* (ETEC) [72]. Regardless of the precise mechanism, secreted mucins are critical for gut homeostasis. Lower levels of Muc2 expression are associated with increased inflammation, colitis, and even rates of colon cancer in mice [73, 74]. These conditions have all been associated with gut pathogen infection [75, 76].

Our laboratory previously demonstrated *L. johnsonii* 456's anti-inflammatory properties in a mouse model [22]. However, the specific mechanisms by which this effect was exerted remained unclear. *Lactobacillus* species have been suggested to exert effects such as regulatory T cell induction and modulation of host inflammatory factors [77, 78]. These mechanisms are often complex to study, however, and might not be universally beneficial. The inhibition of pathogens, and subsequent reduction of pathogen-induced inflammation, is a more straightforward potential pathway for probiotic benefit. Adhesion inhibition is associated with reduced pathogen associated inflammatory response [79]. Other strains of *L. johnsonii*, including NCC 533 and FI9785 have reduced intestine and stomach inflammation by inhibiting the colonization of pathogens as varied as *H. pylori, C. perfringens,* ETEC, and even the diplomonad *G. intestinalis* in a large variety of vertebrate models [80-86].

Probiotic bacteria represent a potential method for both prevention and treatment of diarrheal diseases [87, 88]. Diarrheal infections are a major complication in hospital patients. Gao et al showed that prophylactic administration of a blend of two *Lactobacillus* species cut antibiotic and *C. dificile* associated diarrhea by over half in a clinical environment [89]. Intervention is even more important in children. Diarrheal diseases, including those induced by ETEC and salmonella infection, are responsible for an eighth of childhood deaths below the age of 5 worldwide [90]. Probiotics are effective here, too; vigilant and repeated *L. rhamnosus* GG and *B. lactis* BB-12 supplementation have been demonstrated to reduce the

duration of acute diarrhea in a number of studies [91-94]. Unfortunately, the majority of this burden occurs in developing nations with lower rates of regular access to healthcare. Large outbreaks of diarrheal disease are also common after disasters, like floods, that disrupt stable access to clean water and services [95]. An inexpensive probiotic supplement with a relatively wide "useful prophylactic duration" could be of great use in situations where repeated supplementation is difficult.

L. johnsonii 456 represents a promising probiotic *Lactobacillus* strain. Unique attributes include exceptional acid resistance and well-documented, inoculation-inducible anti-inflammatory effect in mice. The strain is capable of inhibiting the growth and adhesion of multiple types of pathogens *in vitro*. Importantly, the human pilot study described here suggests that *L. johnsonii* 456 is more persistent in the human gut than many other documented strains of probiotic bacteria. Although larger scale clinical studies are needed, the combination of attributes demonstrated here suggest future use as part of an antidiarrheal regimen, or even in the treatment of gut inflammation.

Methods

Bacterial strains and growth culture conditions used. Bacterial strains used are detailed in **Table 1.** *Lactobacillus johnsonii* 456 was isolated from wildtype mice with restricted gut microflora, housed under specific pathogen free (SPF) conditions at UCLA, by Yamamoto et al [22]. The samples used in this study were derived from frozen stock stored by the Schiestl laboratory. *Lactobacillus plantarum 299V* was isolated from Goodbelly Probiotic Juice Drink (NextFoods; Boulder, CO). *Bifidobacterium lactis* HN019 was isolated from Tropicana Essentials Probiotic Juice (Tropicana Products; Chicago, IL). *Lactobacillus johnsonii* VPI 7960, *Lactobacillus casei* 03, *Lactobacillus acidophilus* ATCC 4356, *Streptococcus salivarius subsp. thermophilus* NCDO 573, *Escherichia coli* H10407, *Enterococcus faecalis* NCTC775, and *Salmonella enterica subsp. enterica serovar typhimurium* were obtained from the American Type Culture Collection (ATCC; Manassas, VA).

All *Lactobacillus* species were cultured in MRS (De Man, Rogosa, and Sharpe) broth (Sigma-Aldrich; St. Louis, MO) for 18-20 hours at 37° C under microaerophilic conditions with sealed test tubes. Colony-forming units (CFU) of *Lactobacillus* were enumerated after 48 hours of growth at 37° C on MRS agar (Sigma) incubated in chambers with anaerobic sachets (Sigma). *L. johnsonii* 456 colonies are distinguishable as smooth bordered, white colonies (**Supp. Fig S5**) *B. lactis* was cultured and enumerated similarly, except that MRS broth and agar were supplemented with 0.5g/L Cysteine-HCl. *S. salivarius* was cultured in tryptic soy (TS) broth (Sigma) for 18-20 hours at 37° C with no special anaerobic considerations (aerobically), and enumerated on TS agar plates after 48 hours aerobically at 37° C. *E. coli* and *S. enterica* were cultured in TS broth for 18-20 hours at 37° C aerobically, and enumerated on TS agar plates after 24 hours at 37° C aerobically. *E. faecalis* was cultured in Brain-Heart (BH) broth (Sigma) for 18-20 hours at 37° C aerobically, and enumerated on BH agar plates after 24 hours at 37° C aerobically.

Acid resistance during simulated gastric transit. Simulated gastric acid (SGA) was prepared by dissolving 3.3ppm pepsin (Sigma) and 0.2% NaCl w/v in 0.1% peptone water (Becton Dickinson; Franklin Lakes, NJ). The pH of this solution was then brought to 1.2 with the addition of 11.65M hydrochloric acid to recapitulate concentrated gastric fluid in an otherwise empty human stomach. This solution was diluted using additional 0.1% peptone water to pHs of 1.6, 2.0, and 3.0. The probiotic strains (*L. johnsonii* 456, *L. johnsonii* VPI 7960, *L. casei*, *L. acidophilus*, *L. plantarum*, *B. lactis*, and *S. salivarius*) were grown to a concentration of roughly 1 x 10^8 CFU/mL by the methods described above. 10^6 mid-log phase cells were inoculated into 10mL SGA or 0.1% peptone water control

(pH 6) and incubated for 2 hours at 37° C to simulate gastric transit. After incubation, samples were diluted in 0.1% peptone water and plated on agar for enumeration.

Bile acid tolerance. Bile acid tolerance was evaluated using a modified version of the method of Gilliland and Walker [96]. Each probiotic strain was evaluated based on addition of bile salts to their standard growth conditions. Freshly inoculated culture media was vortexed heavily and then split evenly into either a fresh vial or one containing ox gall extract (Sigma) to 0.1, 0.2, or 0.3% of final solution by weight (2.12, 4.24, and 6.36 mM based on rough Sigma ox gall extract bile acid salt composition: 10% glycocholic acid, 15% glycodeoxycholic acid, 30% taurocholic acid, 55% cholic acid) Culture media was then incubated anaerobically for 18-20 hours at 37° C, and samples were plated and enumerated.

Human gut monolayer culture conditions. Caco-2 and LS 174T cell lines were initially obtained from ATCC. Cells were cultured in Eagle's Minimal Essential Media with 4mM glutamine (Caisson Labs; Smithfield, UT) supplemented with the following: 20% fetal Bovine Serum by volume (Corning Cellgro; Manassas, VA), non-essential amino acids (from 100x, Corning), sodium pyruvate (from 100x, Lonza; Walkersville, MD), and 100u/mL PEN-STREP (penicillin-streptomycin mixture, from 100x, Corning). Cells were grown at up to 50% confluence, trypsinized, and subcultured at a 1:4 ratio roughly every 3 days. Conditions were maintained at 37° C in a 5% CO_2 atmosphere.

Caco-2 monolayers were prepared with small modifications to the method described by Natoli et al [97]. Approximately 3 x 10^5 Caco-2 cells/cm^2 were seeded into a 12 or 24 well plate (BD). Cells were maintained in these plates while growing to confluence under the same controlled conditions as previous. The nascent monolayers were rinsed with warmed PBS and given fresh EMEM media containing all previous additives except antibiotics three times a week. After 15 days of culture, the Caco-2 monolayer was considered to be "mature" for adhesion experimental purposes. LS174 T monolayers were prepared similarly to Caco-2 cells, with a few modifications to the conditions used by by Jung et al [59]. After approaching 50% confluence in growth culture, cells were trypsinized and resuspended in fresh EMEM without antibiotics, then seeded into a 12 or 24 well plate at approximately 3 x 10^5 cells/cm^2. After 3 days, the LS174T monolayer was inspected and rinsed in warmed PBS. Small areas of the growing monolayer that became detached from the substrate were carefully removed during this rinse step, then the media was replaced. Fresh media without antibiotics was then added after PBS rinsing 3 times a week. After roughly 10 days, the LS 174T monolayer was fully confluent and considered "mature" for adhesion experimental purposes.

Monolayer adhesion assay. Bacterial adhesion to monolayers was assayed with small modifications to previously described methods [57, 58]. Overnight cultures of probiotic associated test strains (*L. johnsonii* 456, *L. johnsonii* VPI 7960, *L. casei*, *L. acidophilus*, *L. plantarum*, *B. lactis*, and *S. salivarius*) were pelleted via centrifuge (10 minutes, 3K RPM) (Allegra 6R, Beckmann-Coulter), rinsed, and resuspended in antibiotic-free EMEM and an equal amount of their bacterial culture media to a concentration of 2-5 x 10^8 cells/mL. Mature Caco-2 or LS 174T monolayers were rinsed twice with warmed PBS. A 1 mL volume of resuspended bacterial sample was then applied to each well of the tissue culture plate. Plates were incubated at 37° C in a 5% CO_2 atmosphere for 2 hours with gentle intermittent rocking. After incubation, supernatant was removed and monolayers were rinsed 3 times with warmed PBS. The monolayers were then covered in 1 mL fresh PBS per well and vigorously agitated with micropipette until disrupted and fully resuspended. 10-fold serial dilutions were then plated on strain specific agar media to enumerate adherent cells.

Pathogen adhesion inhibition assay. Pathogen adhesion was determined by the method of Todoriki et al [58]. Overnight cultures of 3 potentially pathogenic strains (*E. coli, E. faecalis,* and *S. enterica*) and *Lactobacillus johnsonii* 456 were pelleted via centrifuge, rinsed, and resuspended in antibiotic-free EMEM to a concentration of 2 x 10^8 cells/mL, as determined by microscope count. Samples of this media were taken aside, diluted, and plated on specific agar media to control precisely for viable CFU plated. Mature Caco-2 or LS 174T monolayers were rinsed twice with warmed PBS. 0.5 mL of *L. johnsonii* in EMEM was added to each well. Monolayers were then incubated at 37° C in a 5% CO_2 atmosphere for an hour with gentle intermittent rocking. After initial incubation, wells were rinsed twice with warmed PBS to remove nonadherent LBJ 456. 0.5 mL of pathogen suspensions were then applied to experimental and control (no LBJ pretreatment) wells. Plates were returned to the incubator for an additional hour. After incubation, supernatant was removed and monolayers were rinsed 3 more times. The monolayers were then covered in 1 mL fresh PBS per well and vigorously agitated with micropipette until disrupted and fully resuspended. 10-fold serial dilutions were then plated on specific agar media to enumerate colonies from adherent bacteria of the test strain.

Co-culture inhibition assay. Cultures of 3 potentially pathogenic strains (*E. coli, E. faecalis,* and *S. enterica*) and *Lactobacillus johnsonii* 456 were grown up overnight as described earlier to concentrations of 2-10 x 10^8 cells/mL, by the method of Hsieh et al [98]. Cells were rinsed and pelleted via centrifuge, then 1 x 10^8 cells of each pathogenic strain were co-inoculated with 1 x 10^8 cells of LBJ 456 into TS (*E. coli* and *S. enterica*) or BH (*E. faecalis*). 1 x 10^8 cells of each test strain were also resuspended alone in their respective media as a control. Co-cultures were incubated for 18-20 hours at 37° C, then plated for enumeration. After 24 hours at 37° C, colonies of the pathogenic strain were enumerated, and easy to distinguish morphologically from the inhibited growth of *Lactobacillus* colonies under aerobic conditions. LBJ 456 controls were enumerated after 48 hours at 37° C on MRS agar.

Supernatant inhibition assay. A slight modification on the method used by Sgouras et al was used to determine whether an acellular factor could inhibit pathogen growth [83]. Overnight cultures of *Lactobacillus* strains *L. johnsonii* 456, *L. johnsonii* VPI 7960, *L. casei*, and *L. plantarum* were cultured in MRS broth for 18-20 hours at 37° C under microaerophilic conditions. The test strains *B. lactis, E. coli, E. faecalis, and S. enterica* were also inoculated into their respective growth media, and cultured 18-20 hours at 37° C. Spent supernatant from the *Lactobacillus* cultures was vacuum filtered via a 0.45 micron filter (Nalge Nunc; Rochester NY) to exclude cellular components. *B. lactis, E. coli, E. faecalis, and S. enterica* overnight growth cultures were rinsed and pelleted via centrifuge, then 1 x 10^8 CFU of each test strain were inoculated into 5 mL of their fresh respective growth media, and either 5 mL of filter sterilized supernatant (FS) from one of the *Lactobacillus* cultures or fresh MRS adjusted to pH 4 with lactic acid as a control. Cultures were grown for 18-20 hours at 37° C, then serially diluted and plated on each strain's respective growth agar for enumeration. All plates were incubated at 37° C under their respective growth conditions described above. *B. lactis* was grown for 48 hours under anaerobic conditions while *E. coli, S. enterica,* and *E. faecalis* were incubated for 24 hours aerobically.

Human gut survival trial and enumeration of viable lactic acid bacteria. Yogurt containing a starter culture of LBJ 456 was generated using commercially available whole fat milk. The yogurt was kept fermenting at room temperature until fully solidified, then refrigerated at 4° C. 11 mixed gender individuals in good health (no inflammatory gut conditions or known disease states) received a 7 day course of this yogurt,

and consumed 100mL, or roughly 1 x 10^{10} CFU, every morning over the course of the trial week. A baseline fecal sample was taken prior to first yogurt consumption, and then at 7, 30, and 60 days after study initiation. Fecal samples were stored at -20° C . 11 individuals supplied fecal samples for each time point, and the others were excluded. To determine viable LAB load at each timepoint, 0.1g of fecal matter was thawed and serially diluted in PBS, then plated on MRS agar to select for LAB. Plates were enumerated after 48 hours at 37° C. Volunteers were asked to refrain from consuming other probiotics for the duration of the study, but otherwise maintain a normal diet. Researchers were blinded to the identity of volunteers. Study design was reviewed and volunteer consent was obtained by MicroBio Pharma, Inc.

LBJ 456 DNA detection in human fecal samples by RT-qPCR. Fecal bacterial DNA was purified using a Zymo QuickDNA Fecal/Soil Microbe Miniprep Kit (Zymo; Irvine, CA) according to manufacturer instructions. DNA content was verified using a Nanodrop (Thermo Fischer; Canoga Park, CA). Real-Time quantitative Polymerase Chain Reaction (RT-qPCR) was performed on the CFX96 Touch Real-Time PCR Detection System (Bio-Rad) using PerfeCTa SYBR Green SuperMix Low ROX reagent (Quantabio; Beverly, MA). DNA was diluted to a working solution of 10 ng/uL and 1 μl was used per replicate of each sample. Samples were analyzed in technical triplicates. Presence of LBJ in each sample was normalized to 16S levels. Primer sequences used are listed in **Table S1**. Optimal qPCR temperature of 55° C was determined by temperature gradient. Specificity of primers was determined by melt curve analysis and comparison of strains (**Supp. Sig. S4**).

Genome Sequencing. Whole genome sequencing of *Lactobacillus johnsonii* 456 was performed by Genewiz (South Plainfield, NJ) on PacBio Sequel to an average coverage of 100X per sample.

Core genome comparison. We compared the genome of *Lactobacillus johnsonii* 456 (LBJ 456) with 23 other *L. johnsonii* genomes available from NCBI on September 7, 2017. We first calculated the core genomic regions shared by all 24 *L. johnsonii* strains, as described by Tomida et al [99]. Briefly, Nucmer was used to identify homologous regions between the genome of NCC 533 and each of the other 23 genomes. The set of core genomic regions was determined to be the regions homologous to NCC 533 that were present in the genomes of the 23 other strains. Single nucleotide polymorphisms (SNPs) were identified within core regions using Nucmer and were used to construct a phylogenetic tree in MEGA 7 using the Neighbor-Joining method on p-distances [100]. Bootstrapping was performed using 500 replicates.

Non-core genome comparison. Non-core genomic regions among the *L. johnsonii* genomes were also identified as described by Tomida et al [99]. Briefly, a pan-genome across all 24 *L. johnsonii* strains was constructed by first using Nucmer to compare the NCC 533 genome with one of the 23 other genomes. Regions in this genome without homology to NCC 533 were concatenated to the NCC 533 genome sequence. This concatenated sequence was then iteratively compared using the same method to each of the remaining genomes to construct the pan-genome. Finally, the pan-genome was compared to each of the 24 genomes individually to identify non-core regions ≥ 500 bp that were absent in at least one of the genomes.

Genome analysis. To determine whether the 24 *L. johnsonii* isolates, and LBJ 456 in particular, may possess distinct host-binding properties, we identified putative MBPs within the isolate genomes. A set of reference MBPs was compiled from amino acid sequences matching the search term "((((mucus[Title] OR mucin[Title])) AND binding[Title])) OR ((mucus-binding[Title] OR mucin-binding[Title]))", downloaded from the NCBI protein database as of September 9,

2017. A non-redundant set of reference MBPs was obtained by clustering sequences with ≥ 97% identity using CD-HIT [101], and all proteins from all 24 *L. johnsonii* strains were aligned to this reference set using BLASTP. Putative *L. johnsonii* MBPs were identified as sequences showing at least 60% identity to at least one reference MBP. *L. johnsonii* MBPs were further clustered by 70% identity using CD-HIT. Bacteriocin-encoding loci in the LBJ 456 genome were detected using BAGEL4.

Statistical Analyses. Statistical analyses were carried out using Graphpad Prism 5 software and Microsoft Excel. T tests were used to assess significance of differences in bacterial survival and adhesion assays. Changes within fecal CFU were carried out using the non-parametric Friedman test and Wilcoxon signed rank post-hoc analysis; *P* values were adjusted with a Bonferroni correction.

ACKNOWLEDGEMENTS. We thank Dr. Patrick Allard (University of California, Los Angeles) for generous facilities and supply sharing, MicroBio Pharma, Inc. (Los Angeles) for organizing the volunteer trial and providing us with fecal samples, and the lab of Dr. Huiying Li (University of California, Los Angeles) for equipment sharing. Jocelyn Castellanos was supported by an NIEHS Student to Scientist grant (5R25ES025505-02).

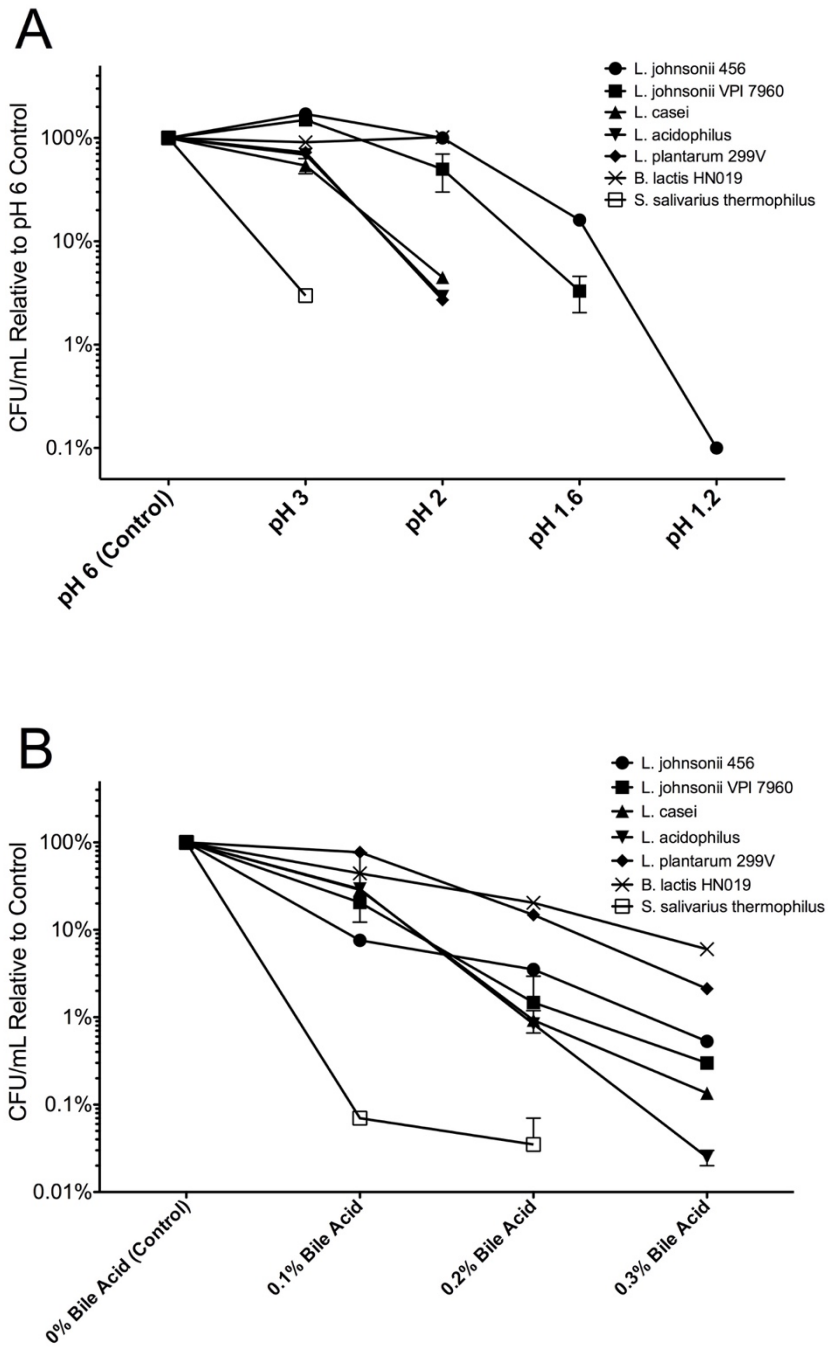

Fig 1. *L. johnsonii* 456 has exceptional resistance to gastric acidity and moderate bile acid tolerance. (A) Survival of *Lactobacillus* and other probiotic associated strains after 2 hours in SGA. (B) Relative growth capability of test strains after growth in media supplemented with bile acids. Results are expressed as means and SEMs (n = 2). Each experimental pH or bile acid concentration vs. control was run as a separate experiment, and all experiments were repeated at least twice. Specific representation at each pH reading by histogram is included in **Supplemental Figures S1 and S2**.

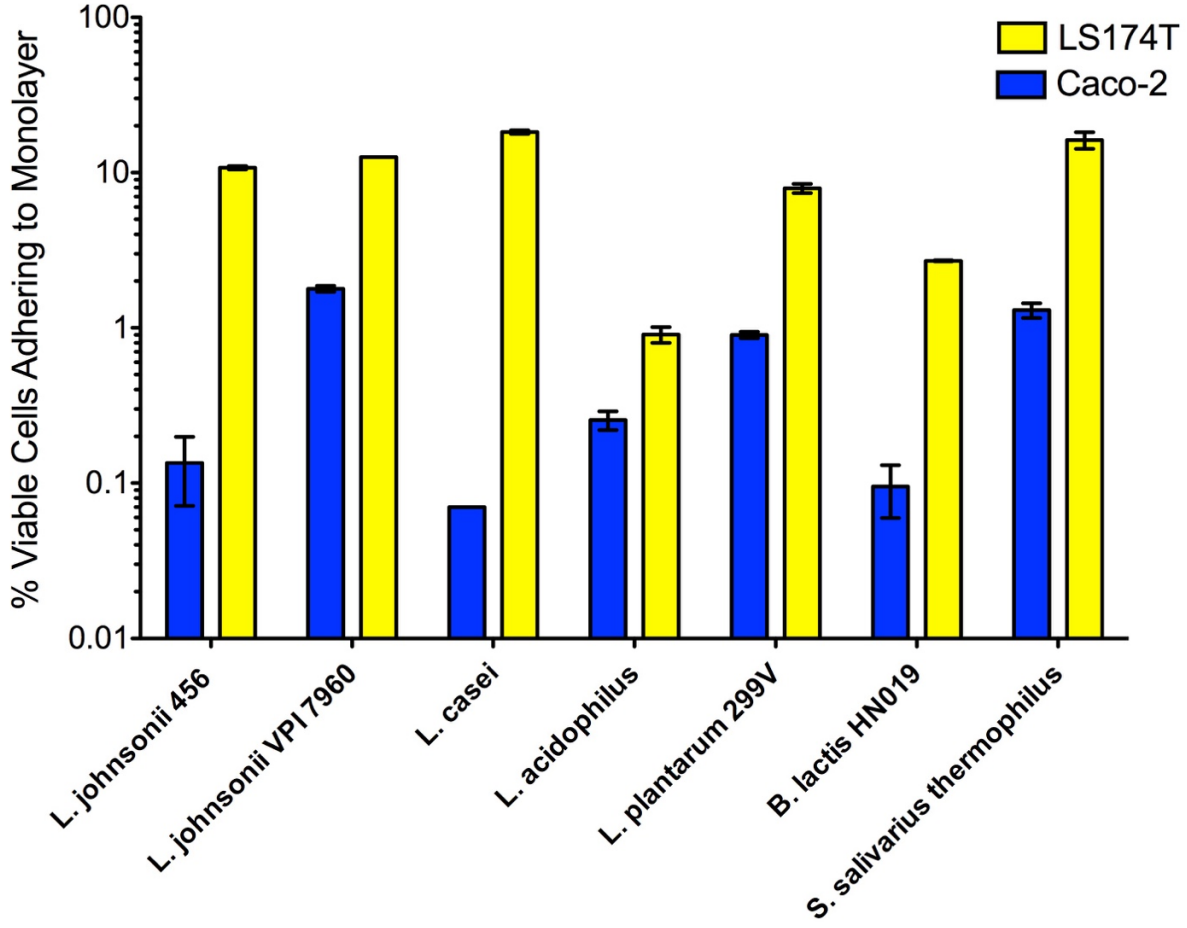

Fig. 2. *L. johnsonii* 456 adheres best to a goblet cell-like gut epithelial monolayer. Relative adhesion of viable cells shown as a percentage of viable cells plated (2-5 x 10^8 cells/well) (*n*=2). Data expressed as means and SEM. Experiment was repeated twice.

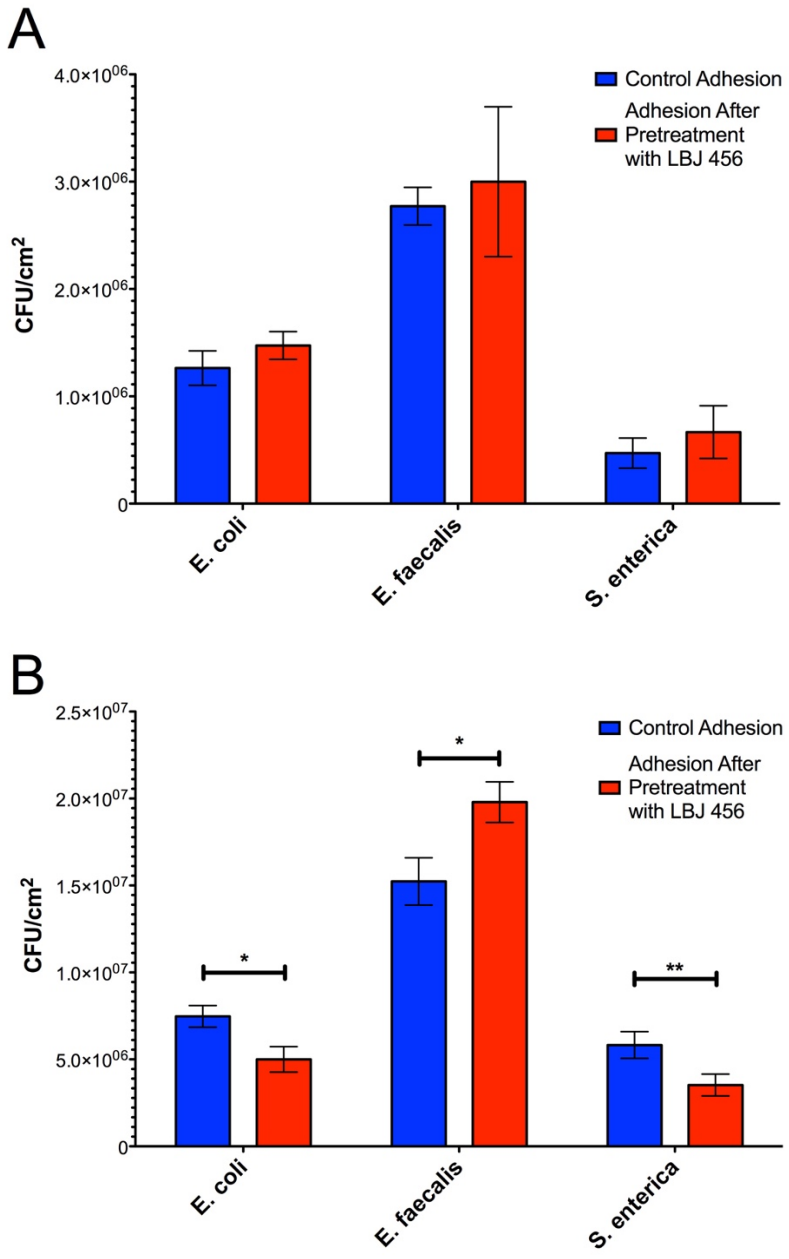

Fig. 3. *L. johnsonii* 456 significantly inhibits pathogenic strain adhesion to goblet cell-like gut epithelial monolayers, but not enterocyte-like monolayers. (A) Adhesion of pathogenic bacteria to a Caco-2 monolayer after 1 hour pre-exposure to LBJ 456. (B) Adhesion of pathogenic bacteria to an LS 174T monolayer after 1 hour pre-exposure to LBJ 456. Data expressed as means and SEM. Relevant statistically significant differences are indicated [* = $p < 0.05$, ** = $p < 0.1$ (t test); n = 4]. All experiments were performed twice.

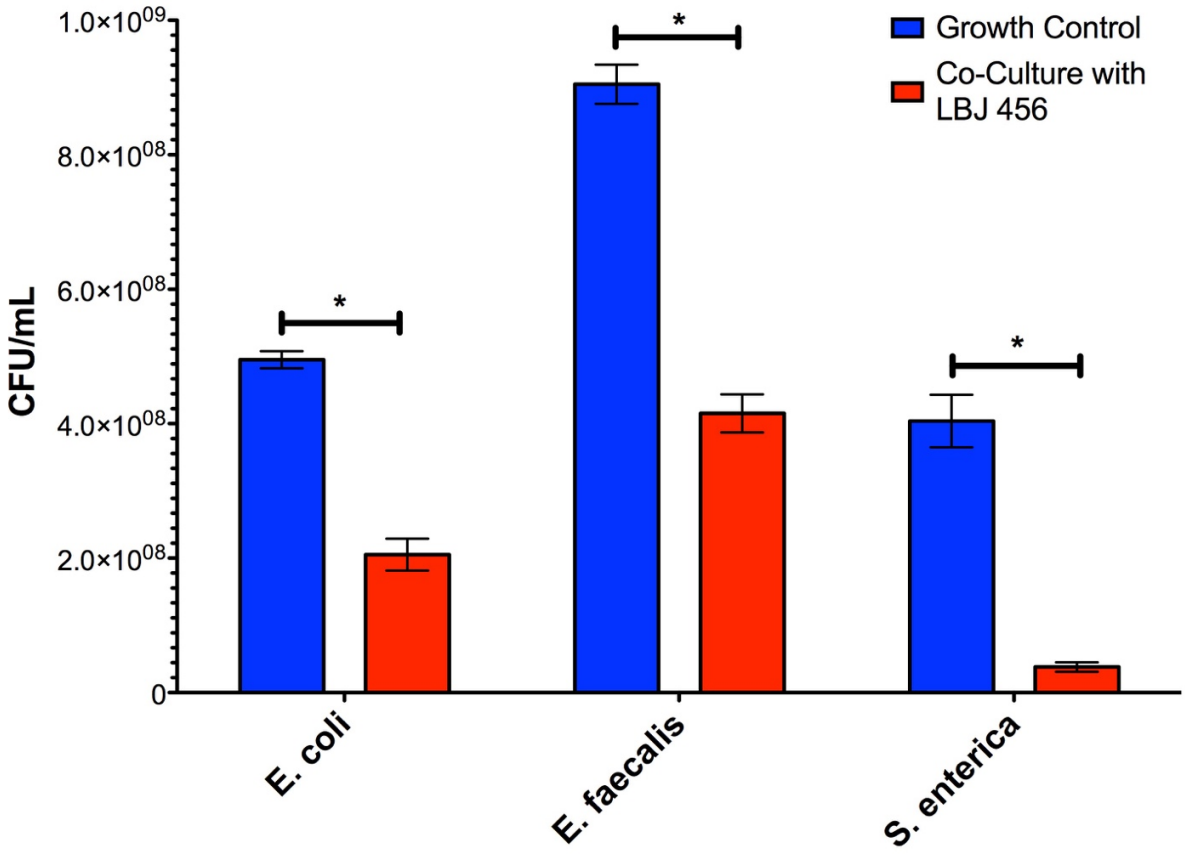

Fig. 4. Co-culture with *L. johnsonii* 456 significantly inhibits growth of pathogenic strains. Data expressed as means and SEM. Relevant statistically significant differences are indicated [* = $p < 0.05$ (t test); n = 6]. Experiment was repeated twice.

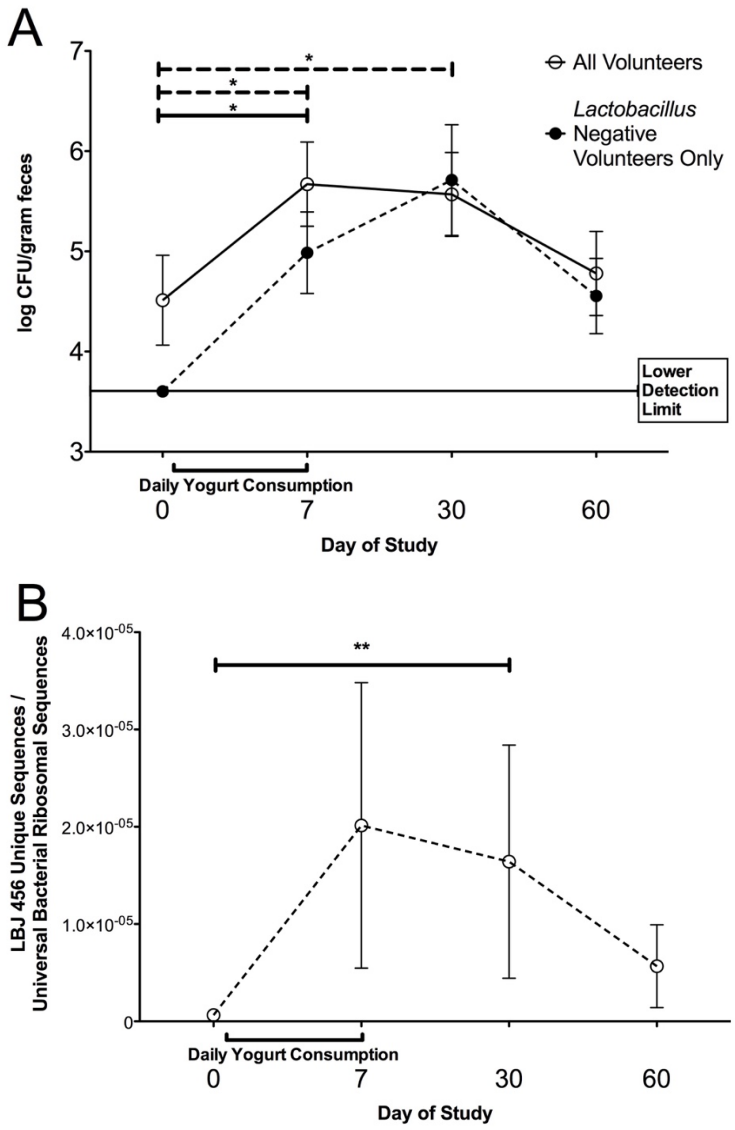

Fig. 5. A 7 day course of LBJ 456 yogurt leads to significant elevations in both total lactic acid bacteria (LAB) and LBJ 456 specific DNA. (A) Fecal load of viable LAB, as detectable by anaerobic growth on MRS agar, prior to and after 7 day course. Solid line: All volunteers that completed a full course and supplied all four fecal samples (*n* = 11). Dashed Line: individuals with no detectable LAB at day 0, prior to initiation of yogurt course (*n* = 6). All individuals with LAB negative backgrounds had detectable LAB at day 7. 5/6 still had detectable levels at 30 days, and half were still detectable at day 60. Lower detection limit of this assay = 4000 CFU/mL. * = $p < 0.05$ (Wilcoxon signed rank test) for Day 0-7 (all volunteers) and Day 0-7 and Day 0-30 (LBJ negative background volunteers only). (B) qPCR of detectable DNA sequences in fecal samples, expressed as ratio of LBJ 456 specific DNA sequence to 16sRNA universally detectable bacterial sequence. Ratio of LBJ 456 specific DNA to 16sRNA DNA sequence is approximately 1:1 in cultured LBJ 456, and undetectable in LBJ VPI 7960 control (control data not shown). ** = $p < 0.1$ (Wilcoxon signed rank test) Data expressed as means and SEM.

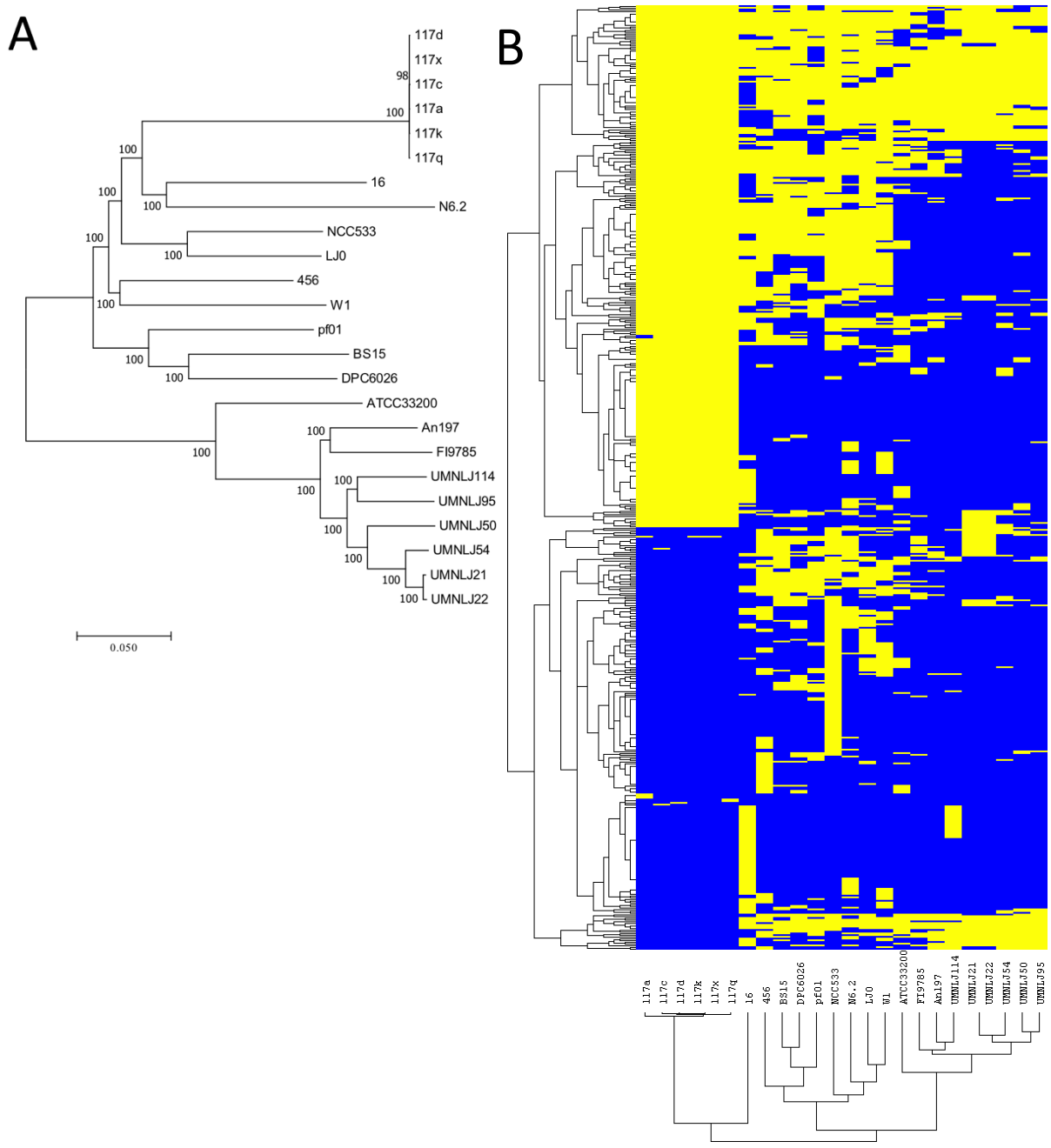

Fig. 6. *L. johnsonii* 456 is genetically distinct from other described *L. johnsonii* strains. (A) Phylogenetic tree of 24 *L. johnsonii* isolates based on 101,088 SNPs in core genomic regions. Distances represent percentage of SNP differences out of total compared SNPs. (B) Frequency of non-core regions among the 24 *L. johnsonii* strains. Yellow cells indicate presence of a non-core region (along columns) in a strain (along rows). Dendrograms based on complete linkage hierarchical clustering of strains or regions based on Euclideans distances. Non-core region lengths are not represented here.

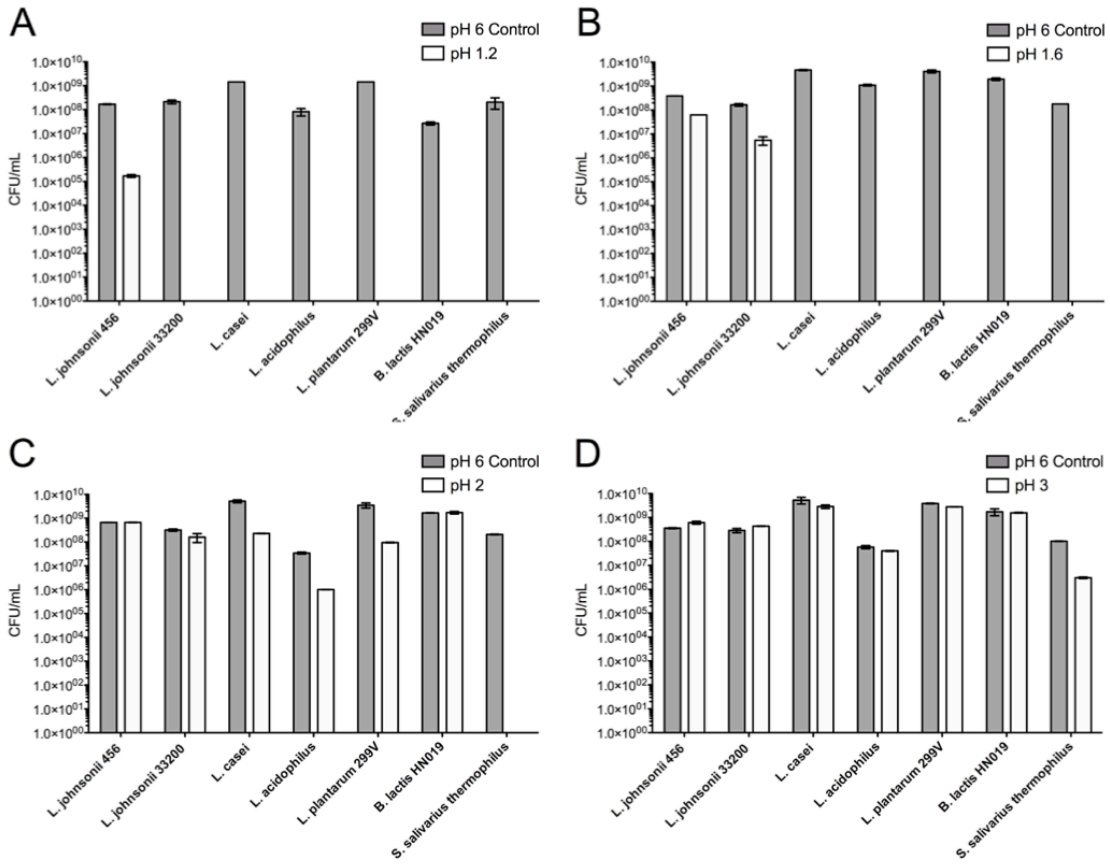

Supplemental Figure S1 Survival of *Lactobacillus* and other probiotic associated strains after 2 hours in SGA (Fig 1*A*), total CFU.

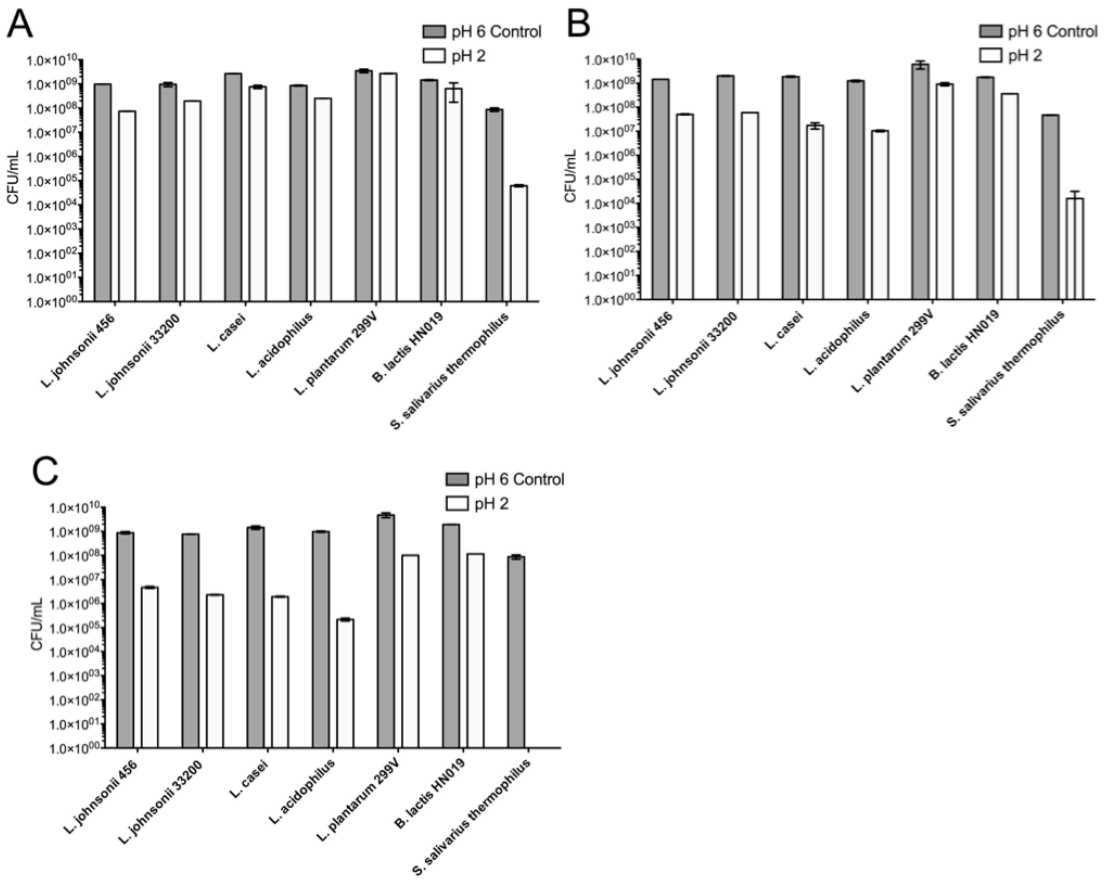

Supplemental Figure S2 Growth of *Lactobacillus* and other probiotic associated strains after 24 hours in various bile acid solutions (Fig 1*B*), total CFU.

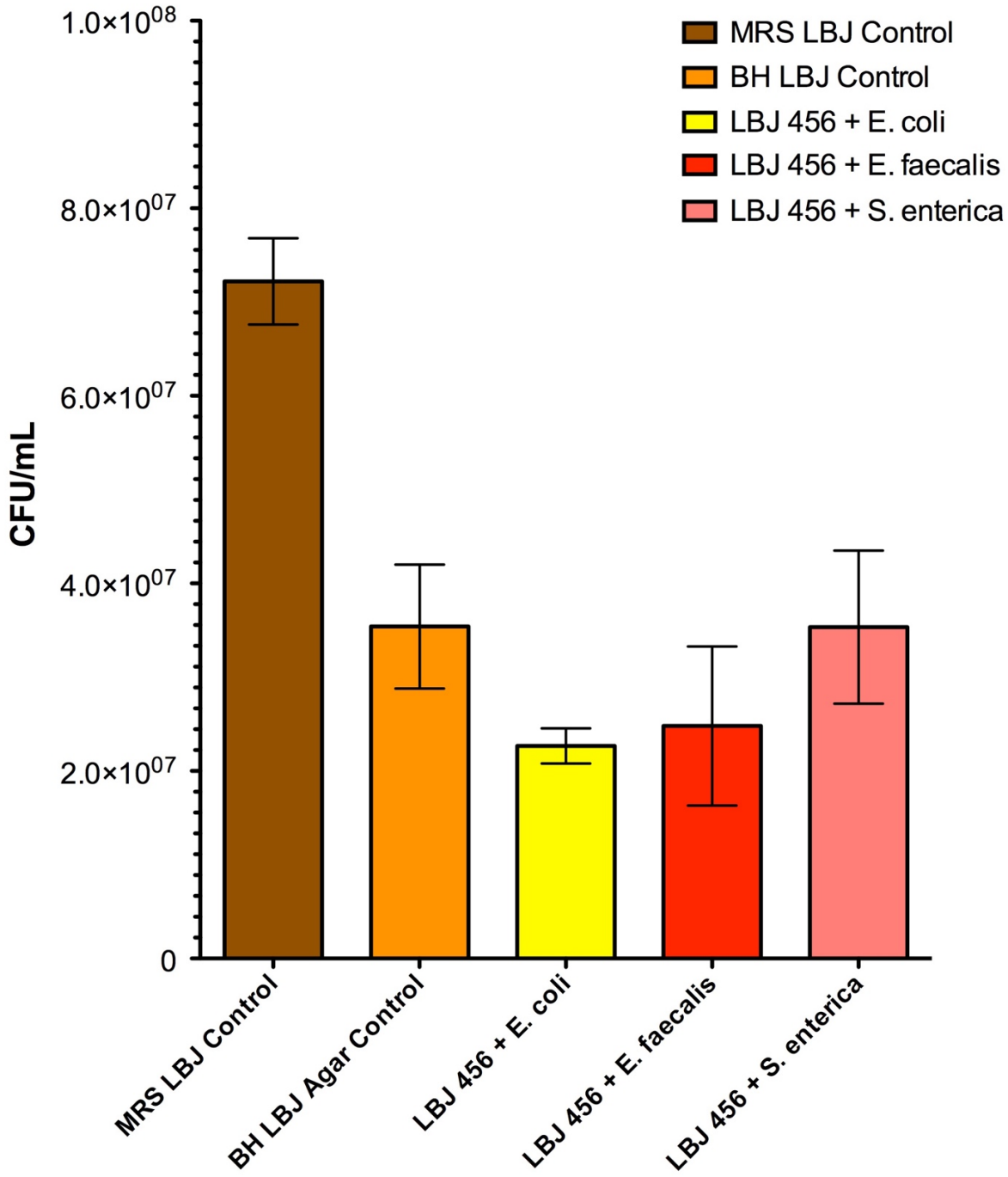

Supplemental Figure S3 *L. johnsonii* 456 CFU from co-culture experiment (Fig. 5). LBJ 456 grows in aerobic co-culture with pathogenic strains. Data expressed as means and SEM. [n = 3]. Experiment was repeated twice.

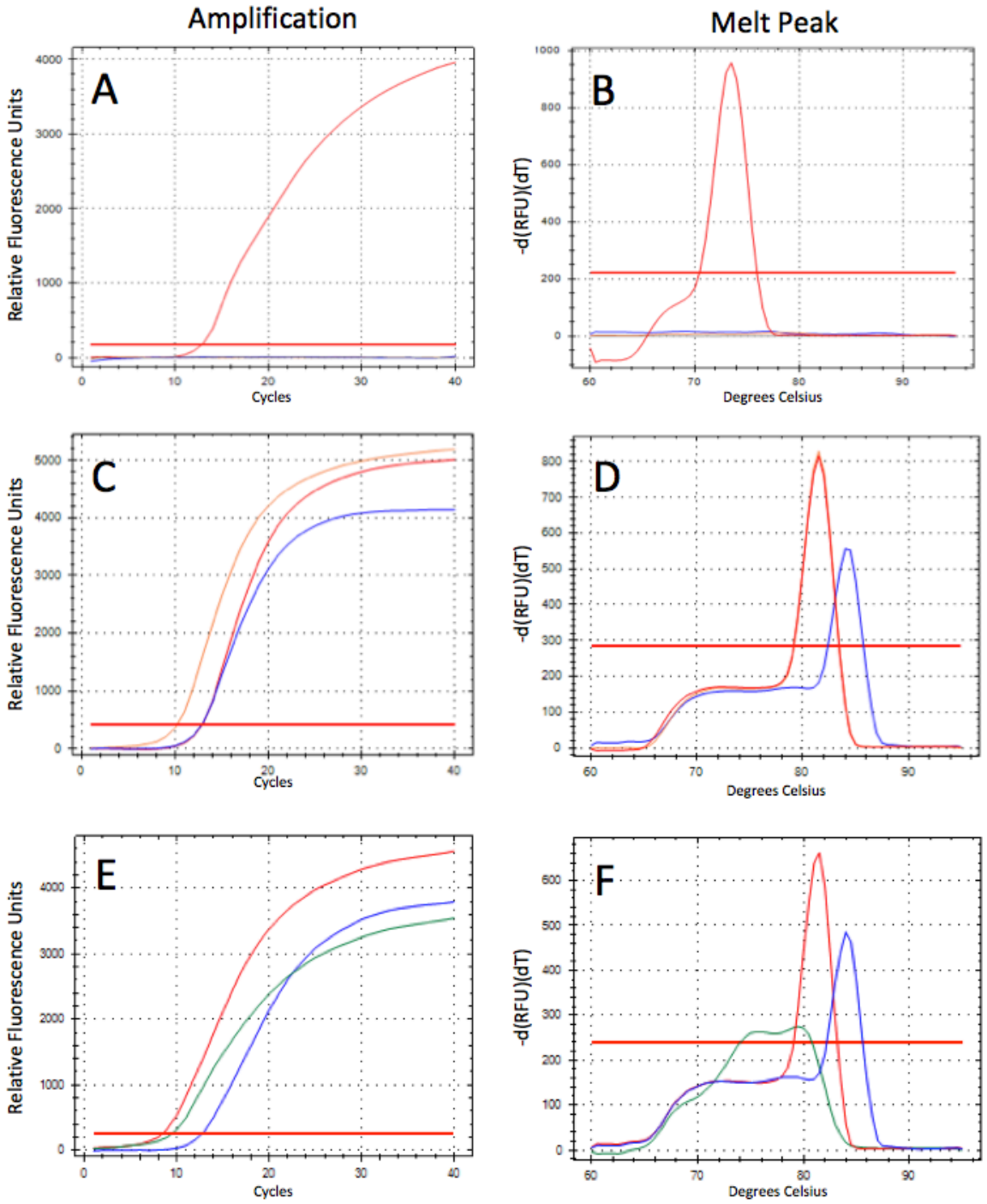

Supplemental Figure S4 Primer specificity for qPCR experiment. Red curves = *L. johnsonii* 456 DNA samples, orange curves = *L. johnsonii* VPI 7960 DNA samples, blue curves = *B. Lactis* DNA samples, green curves = feces derived mixed bacterial DNA samples. Bold red horizontal line denotes detection limit. (A) Specific amplification of LBJ 456 DNA using LJ4F/R primer set. (B) Single melt peak for LJ4F/R primer set, indicating single and specific PCR product. (C,E) Amplification of DNA using 16sRNA primer set. (D,F) Melt peaks for 16sRNA primer set, indicating single strain specific 16s amplification, and a varied amplification in the feces derived mixed bacterial DNA samples.

A

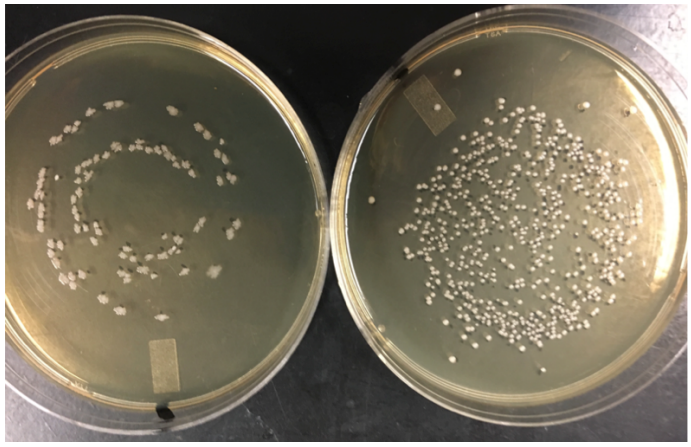

B

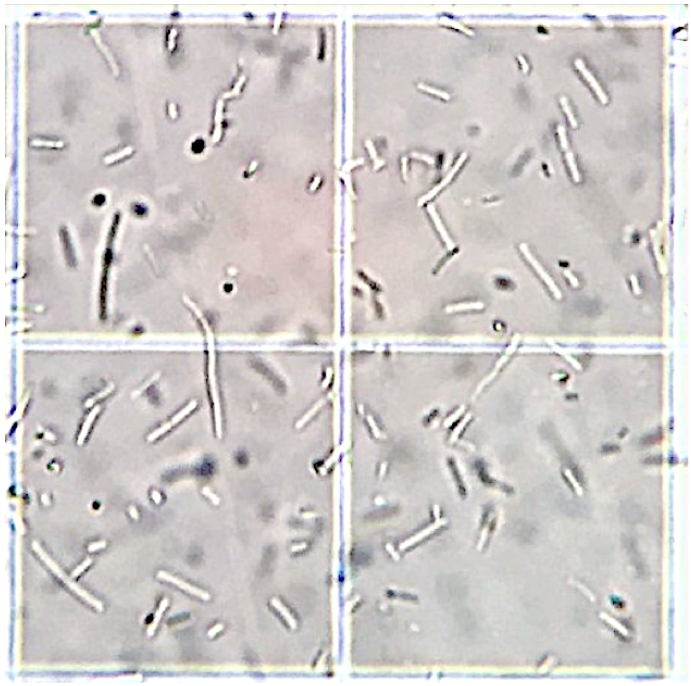

Supplemental Figure S5 *L. johnsonii* 456 has distinctive morphology. (A) *L. johnsonii* VPI 7960 (left, rough edges) colony morphology as compared to *L. johnsonii* 456 colony morphology (right, smooth edges) on MRS agar. (B) *L. johnsonii* 456 bacilli as viewed under a light microscope. Bordering squares are 0.1 x 0.1 mm. Sharpness of image enhanced for better visualization.

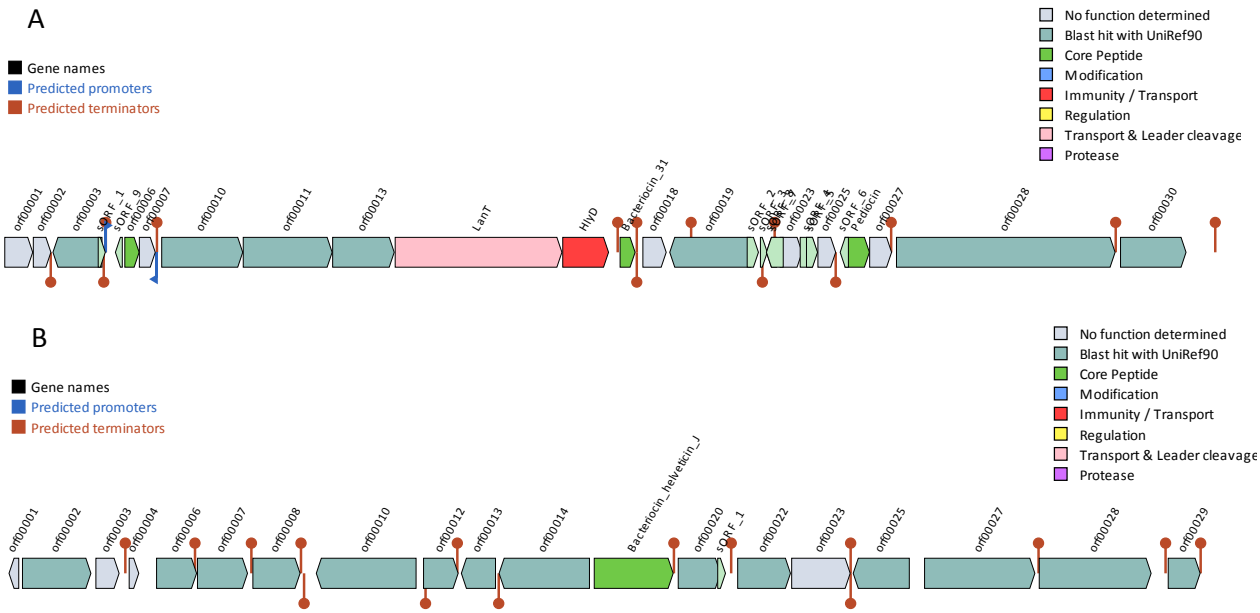

Supplemental Figure S6 Bacteriocin-encoding loci in the LBJ 456 genome identified by BAGEL4.

Table 1. Strains and Cell Lines Used

Bacterial Strain	Source and Description
Lactobacillus johnsonii 456	Mouse gut isolate, UCLA
Lactobacillus johnsonii VPI 7960	ATCC 33200 (type strain)
Lactobacillus casei 03	ATCC 393 (type strain)
Lactobacillus acidophilus ATCC 4356	ATCC 4356 (type strain)
Lactobacillus plantarum 299V	Purified from commercial product
Steptococcus salivarius thermophilus NCDO 573	ATCC 19258 (type strain)
Bifidobacterium lactis HN019	Purified from commercial product
Escherichia coli H10407	ATCC 35401 (enterotoxigenic)
Enterococcus faecalis NCTC775	ATCC 19433 (type strain)
Salmonella enterica enterica serovar *typhimurium*	ATCC 13311 (enteropathogenic)

Human Cancer Cell Line	Source and Description
Caco-2	ATCC HTB-37, human colorectal adenocarcinoma, enterocyte-like
LS 174T	ATCC CL-188, human colorectal adenocarcinoma, goblet cell-like

Table 2. Inhibition of growth by *Lactobacillus* filtered supernatant

Bacterial Strain	Source of Supernatant	CFU/mL*	% Relative to Control*	p Value**
E. coli H10407	MRS Control	1.92e+008 ± 1.90e+007	-	-
	L. johnsonii 456	1.94e+008 ± 1.00e+007	101.0 ± 5.21	0.9485
	L. johnsonii VPI 7960	1.54e+008 ± 3.00e+007	80.21 ± 15.6	0.3247
	L. casei 03	2.22e+008 ± 1.80e+007	115.6 ± 9.38	0.3813
	L. plantarum 299V	0	0%	**n/a**
E. faecalis NCTC775	MRS Control	6.41e+008 ± 7.67e+007	-	-
	L. johnsonii 456	3.00e+008 ± 2.80e+007	46.80 ± 4.37	**0.0427**
	L. johnsonii VPI 7960	3.34e+008 ± 6.60e+007	52.11 ± 10.30	0.0654
	L. casei 03	3.48e+008 ± 2.80e+007	54.29 ± 4.37	0.0653
	L. plantarum 299V	1.34e+006 ± 4200	0.205 ± 0.065	**0.0051**
S. enterica typhimurium	MRS Control	2.35e+008 ± 2.73e+007	-	-
	L. johnsonii 456	0	0%	**n/a**
	L. johnsonii VPI 7960	0	0%	**n/a**
	L. casei 03	2.80e+007 ± 8.00e+006	11.92 ± 3.41	**0.0074**
	L. plantarum 299V	0	0%	**n/a**
B. lactis HN019	MRS Control	1.37e+009 ± 9.60e+007	-	-
	L. johnsonii 456	5.12e+008 ± 1.20e+007	37.32 ± 0.875	**0.0124**
	L. johnsonii VPI 7960	5.64e+008 ± 4.40e+007	41.11 ± 3.21	**0.0167**
	L. casei 03	5.40e+008 ± 8.00e+007	39.36 ± 5.83	**0.0218**
	L. plantarum 299V	8.40e+008 ± 4.80e+007	61.23 ± 3.50	**0.0384**

* Numerical values are listed as the mean ± SEM

** p values of experimental groups against MRS control were calculated by two-tailed unpaired t test, except for instances of repeated zero values. **Bold entries** indicate a p values under 0.05. N=4

Table 3. Genes within noncore regions unique to *L. johnsonii* 456

Start	End	Strand	Function
125191	125331	-	hypothetical protein
125331	126032	-	Transposase DDE domain protein
126112	126417	-	hypothetical protein
234405	235364	-	hypothetical protein
235812	236573	+	FtsK/SpoIIIE family protein
237107	237385	+	hypothetical protein
237570	237938	+	Plasmid replication protein
238066	238638	+	RNA helicase
238731	238922	+	hypothetical protein
238985	239779	+	hypothetical protein
239776	240219	+	hypothetical protein
255022	256620	+	Lipid A export ATP-binding/permease
605765	609664	+	YSIRK type signal peptide
734735	751894	+	Serine-aspartate repeat-containing
939056	939733	+	Sortase family protein
940040	951076	+	MucBP domain protein
951317	952744	+	MucBP domain protein
1292897	1305865	-	Extracellular matrix-binding protein
1336160	1337077	-	Mrr restriction system protein
1337141	1338232	+	Type I restriction modification DNA
1338298	1339023	-	Type I restriction modification DNA
1386125	1386856	-	UvrD/REP helicase
1782742	1783119	+	hypothetical protein
1783116	1784315	-	Type I restriction modification DNA
1784293	1785915	-	Type I restriction enzyme EcoKI M
1785915	1788983	-	Type I restriction enzyme EcoR124II

Table S1. Primer sequences used

Primer Name	Description	
LJ4F	LBJ 456 specific forward primer	AGA CCC AAA GGC GCT TAT AGA
LJ4R	LBJ 456 specific reverse primer	TGT AAG TTC AGA AAA ATG TAT CCC G
907R	Universal 16s bacterial reverse primer	CCG TCA ATT CCT TTR* AGT TT
785F	Universal 16s bacterial forward primer	GGA TTA GAT ACC CTG GTA

Lactobacillus johnsonii 456 specific sequences were designed using the primerBLAST online tool to target a unique sequence upstream of an integrase.

* R denotes a degenerate base comprised of roughly equal amounts A and G in individual primer sequences

Table S2. Bacteriocin-encoding loci identified by BAGEL4 in the LBJ 456 genome

Putative bacteriocin locus 1					
BAGEL4 ORF	**start**	**end**	**strand**	**Gene ID**	**Description / Closest homolog**
orf00001	862506	862868	+	PROKKA_00790	N/A
orf00002	862876	863103	+	PROKKA_00791	N/A
orf00003	863130	863765	-	PROKKA_00792	Uridine kinase
orf00006	864061	864246	+	PROKKA_00793	ggmotif; Bacteriocin_IIc;
orf00007	864249	864455	+	PROKKA_00794	N/A
orf00010	864539	865588	+	PROKKA_00795	Uncharacterized 14.4 kDa protein in laf 3'region
orf00011	865595	866746	+	PROKKA_00796	Bacteriocin production related histidine kinase
orf00013	866753	867550	+	PROKKA_00797	AbpR [Lactobacillus salivarius subsp. salivarius]
LanT	867563	869722	+	PROKKA_00798	AbpT bacteriocin export accessory protein
HlyD	869733	870326	+	PROKKA_00799	Uncharacterized protein in laf 5'region (Fragment)
Bacteriocin_31	870476	870670	+	PROKKA_00800	Bacteriocin_II; Bacteriocin_IIc; 16.2;Bacteriocin_31
orf00018	870771	871073	+	PROKKA_00801	N/A
orf00019	871119	872168	-	PROKKA_00802	Uncharacterized 14.4 kDa protein in laf 3'region
orf00023	872549	872833	+	PROKKA_00803	N/A
orf00025	873038	873268	+	PROKKA_00805	N/A
Pediocin	873391	873705	+	PROKKA_00806	159.2;Pediocin
orf00027	873708	873992	+	PROKKA_00807	N/A
orf00028	874056	876887	+	PROKKA_00808	Calcium-transporting ATPase
orf00030	876958	877806	+	PROKKA_00809	Uncharacterized protein YjjU
Putative bacteriocin locus 2					
orf00001	788762	788893	-	N/A	
orf00002	788943	789860	+	PROKKA_00722	Fructose-bisphosphate aldolase
orf00003	789927	790238	+	PROKKA_00723	N/A
orf00004	790373	790501	+	PROKKA_00724	N/A
orf00006	790740	791276	+	PROKKA_00725	Hypoxanthine-guanine phosphoribosyltransferase
orf00007	791288	791959	+	PROKKA_00726	Putative glutamine amidotransferase-like protein YfeJ
orf00008	792031	792663	+	PROKKA_00727	Uncharacterized sugar epimerase YhfK
orf00010	792881	794218	-	PROKKA_00728	Putative transposase in snaA-snaB intergenic region
orf00012	794318	794782	+	PROKKA_00729	Transposase for insertion sequence element IS200
orf00013	794825	795283	-	PROKKA_00730	Protein YtsP
orf00014	795331	796542	-	PROKKA_00731	Putative ion-transport protein YfeO
Bacteriocin_helveticin_J	796606	797664	+	PROKKA_00732	Bacteriocin_helveticin_J
orf00020	797732	798298	+	PROKKA_00733	DNA-3-methyladenine glycosylase 1
orf00022	798529	799236	+	PROKKA_00734	Uncharacterized transporter MTH_1382
orf00023	799252	800037	+	PROKKA_00735	N/A
orf00025	800077	800829	-	PROKKA_00736	Glycerol uptake facilitator protein-like 5
orf00027	801034	802512	+	PROKKA_00737	Uncharacterized MFS-type transporter YusP
orf00028	802571	804070	+	PROKKA_00738	Multidrug resistance protein 3
orf00029	804299	804727	+	PROKKA_00739	Putative acetyltransferase YjbC

1. Ciorba, M.A., *A gastroenterologist's guide to probiotics.* Clinical gastroenterology and hepatology, 2012. **10**(9): p. 960-968.
2. Cho, I. and M.J. Blaser, *The human microbiome: at the interface of health and disease.* Nature Reviews Genetics, 2012. **13**(4): p. 260-270.
3. Sheehan, D., C. Moran, and F. Shanahan, *The microbiota in inflammatory bowel disease.* Journal of gastroenterology, 2015. **50**(5): p. 495-507.
4. Hooper, L.V., D.R. Littman, and A.J. Macpherson, *Interactions between the microbiota and the immune system.* Science, 2012. **336**(6086): p. 1268-1273.
5. Hamer, H.M., et al., *The role of butyrate on colonic function.* Alimentary pharmacology & therapeutics, 2008. **27**(2): p. 104-119.
6. Turnbaugh, P.J., et al., *The human microbiome project: exploring the microbial part of ourselves in a changing world.* Nature, 2007. **449**(7164): p. 804.
7. Turnbaugh, P.J., et al., *A core gut microbiome in obese and lean twins.* nature, 2009. **457**(7228): p. 480-484.
8. Jones, M.L., et al., *The human microbiome and bile acid metabolism: dysbiosis, dysmetabolism, disease and intervention.* Expert opinion on biological therapy, 2014. **14**(4): p. 467-482.
9. Hartstra, A.V., et al., *Insights into the role of the microbiome in obesity and type 2 diabetes.* Diabetes care, 2015. **38**(1): p. 159-165.
10. Foster, J.A. and K.-A.M. Neufeld, *Gut–brain axis: how the microbiome influences anxiety and depression.* Trends in neurosciences, 2013. **36**(5): p. 305-312.
11. Servin, A.L. and M.-H. Coconnier, *Adhesion of probiotic strains to the intestinal mucosa and interaction with pathogens.* Best Practice & Research Clinical Gastroenterology, 2003. **17**(5): p. 741-754.
12. Barefoot, S.F. and T.R. Klaenhammer, *Detection and activity of lactacin B, a bacteriocin produced by Lactobacillus acidophilus.* Applied and Environmental microbiology, 1983. **45**(6): p. 1808-1815.
13. Ocaña, V.S. and M.E. Nader-Macías, *Production of antimicrobial substances by lactic acid bacteria II: screening bacteriocin-producing strains with probiotic purposes and characterization of a Lactobacillus bacteriocin.* Public Health Microbiology: Methods and Protocols, 2004: p. 347-353.
14. Midolo, P., et al., *In vitro inhibition of Helicobacter pylori NCTC 11637 by organic acids and lactic acid bacteria.* Journal of Applied Bacteriology, 1995. **79**(4): p. 475-479.
15. Reid, G., et al., *Potential uses of probiotics in clinical practice.* Clinical microbiology reviews, 2003. **16**(4): p. 658-672.
16. Ghouri, Y.A., et al., *Systematic review of randomized controlled trials of probiotics, prebiotics, and synbiotics in inflammatory bowel disease.* Clinical and experimental gastroenterology, 2014. **7**: p. 473.
17. Di Cerbo, A. and B. Palmieri, *The market of probiotics.* Pakistan journal of pharmaceutical sciences, 2015. **28**(6).
18. Doron, S., et al., *Effect of Lactobacillus rhamnosus GG administration on vancomycin-resistant Enterococcus colonization in adults with comorbidities.* Antimicrobial agents and chemotherapy, 2015. **59**(8): p. 4593-4599.
19. Van Gossum, A., et al., *Multicenter randomized-controlled clinical trial of probiotics (Lactobacillus johnsonii, LA1) on early endoscopic recurrence of Crohn's disease after ileo-caecal resection.* Inflammatory bowel diseases, 2007. **13**(2): p. 135-142.
20. Mileti, E., et al., *Comparison of the immunomodulatory properties of three probiotic strains of Lactobacilli using complex culture systems: prediction for in vivo efficacy.* PloS one, 2009. **4**(9): p. e7056.

21. Klaenhammer, T.R., *Probiotic bacteria: today and tomorrow.* The Journal of nutrition, 2000. **130**(2): p. 415S-416S.
22. Yamamoto, M.L., et al., *Intestinal bacteria modify lymphoma incidence and latency by affecting systemic inflammatory state, oxidative stress, and leukocyte genotoxicity.* Cancer research, 2013. **73**(14): p. 4222-4232.
23. Hill, C., et al., *Expert consensus document: The International Scientific Association for Probiotics and Prebiotics consensus statement on the scope and appropriate use of the term probiotic.* Nature reviews Gastroenterology & hepatology, 2014. **11**(8): p. 506-514.
24. Brassart, D., et al., *The selection of dairy bacterial strains with probiotic properties based on their adhesion to human intestinal epithelial cells.* Proceedings Lactic, 1994. **94**.
25. Salminen, S., et al., *Development of selection criteria for probiotic strains to assess their potential in functional foods: a Nordic and European approach.* Bioscience and Microflora, 1996. **15**(2): p. 61-67.
26. Sender, R., S. Fuchs, and R. Milo, *Revised estimates for the number of human and bacteria cells in the body.* PLoS biology, 2016. **14**(8): p. e1002533.
27. Větrovský, T. and P. Baldrian, *The variability of the 16S rRNA gene in bacterial genomes and its consequences for bacterial community analyses.* PloS one, 2013. **8**(2): p. e57923.
28. Wu, X., et al., *Genome sequence of Lactobacillus johnsonii strain W1, isolated from mice.* Genome announcements, 2016. **4**(3): p. e00561-16.
29. Buhnik-Rosenblau, K., et al., *Indication for Co-evolution of Lactobacillus johnsonii with its hosts.* BMC microbiology, 2012. **12**(1): p. 149.
30. Kailasapathy, K. and J. Chin, *Survival and therapeutic potential of probiotic organisms with reference to Lactobacillus acidophilus and Bifidobacterium spp.* Immunology and cell Biology, 2000. **78**(1): p. 80-88.
31. Charteris, W., et al., *Development and application of an in vitro methodology to determine the transit tolerance of potentially probiotic Lactobacillus and Bifidobacterium species in the upper human gastrointestinal tract.* Journal of applied microbiology, 1998. **84**(5): p. 759-768.
32. Mudie, D.M., et al., *Quantification of gastrointestinal liquid volumes and distribution following a 240 mL dose of water in the fasted state.* Molecular pharmaceutics, 2014. **11**(9): p. 3039-3047.
33. Prasad, J., et al., *Selection and characterisation of Lactobacillus and Bifidobacterium strains for use as probiotics.* International Dairy Journal, 1998. **8**(12): p. 993-1002.
34. Liong, M. and N. Shah, *Acid and bile tolerance and cholesterol removal ability of lactobacilli strains.* Journal of dairy science, 2005. **88**(1): p. 55-66.
35. Hassanzadazar, H., et al. *Investigation of antibacterial, acid and bile tolerance properties of lactobacilli isolated from Koozeh cheese*. in *Veterinary Research Forum*. 2012. Faculty of Veterinary Medicine, Urmia University, Urmia, Iran.
36. Sahadeva, R., et al., *Survival of commercial probiotic strains to pH and bile.* International Food Research Journal, 2011. **18**(4).
37. Pan, X., et al., *The acid, bile tolerance and antimicrobial property of Lactobacillus acidophilus NIT.* Food Control, 2009. **20**(6): p. 598-602.
38. Aiba, Y., et al., *A highly acid-resistant novel strain of Lactobacillus johnsonii No. 1088 has antibacterial activity, including that against Helicobacter pylori, and inhibits gastrin-mediated acid production in mice.* Microbiologyopen, 2015. **4**(3): p. 465-474.
39. Corcoran, B., et al., *Survival of probiotic lactobacilli in acidic environments is enhanced in the presence of metabolizable sugars.* Applied and environmental microbiology, 2005. **71**(6): p. 3060-3067.
40. Maragkoudakis, P.A., et al., *Probiotic potential of Lactobacillus strains isolated from dairy products.* International Dairy Journal, 2006. **16**(3): p. 189-199.

41. Begley, M., C. Hill, and C.G. Gahan, *Bile salt hydrolase activity in probiotics.* Applied and environmental microbiology, 2006. **72**(3): p. 1729-1738.
42. Di Ciaula, A., et al., *Bile Acid Physiology.* Annals of Hepatology: Official Journal of the Mexican Association of Hepatology, 2017. **16**.
43. Northfield, T. and I. McColl, *Postprandial concentrations of free and conjugated bile acids down the length of the normal human small intestine.* Gut, 1973. **14**(7): p. 513-518.
44. Jalanka-Tuovinen, J., et al., *Intestinal microbiota in healthy adults: temporal analysis reveals individual and common core and relation to intestinal symptoms.* PloS one, 2011. **6**(7): p. e23035.
45. David, L.A., et al., *Diet rapidly and reproducibly alters the human gut microbiome.* Nature, 2014. **505**(7484): p. 559.
46. Bezkorovainy, A., *Probiotics: determinants of survival and growth in the gut.* The American journal of clinical nutrition, 2001. **73**(2): p. 399s-405s.
47. Yuki, N., et al., *Survival of a probiotic, Lactobacillus casei strain Shirota, in the gastrointestinal tract: selective isolation from faeces and identification using monoclonal antibodies.* International journal of food microbiology, 1999. **48**(1): p. 51-57.
48. Alander, M., et al., *Persistence of colonization of human colonic mucosa by a probiotic strain, Lactobacillus rhamnosusGG, after oral consumption.* Applied and Environmental Microbiology, 1999. **65**(1): p. 351-354.
49. Goossens, D., et al., *The effect of Lactobacillus plantarum 299v on the bacterial composition and metabolic activity in faeces of healthy volunteers: a placebo-controlled study on the onset and duration of effects.* Alimentary pharmacology & therapeutics, 2003. **18**(5): p. 495-505.
50. Juge, N., *Microbial adhesins to gastrointestinal mucus.* Trends in microbiology, 2012. **20**(1): p. 30-39.
51. Van Klinken, B.J.-W., et al., *Gastrointestinal expression and partial cDNA cloning of murine Muc2.* American Journal of Physiology-Gastrointestinal and Liver Physiology, 1999. **276**(1): p. G115-G124.
52. Tytgat, K.M., et al., *Biosynthesis of human colonic mucin: Muc2 is the prominent secretory mucin.* Gastroenterology, 1994. **107**(5): p. 1352-1363.
53. van Klinken, B.J.-W., et al., *The human intestinal cell lines Caco-2 and LS174T as models to study cell-type specific mucin expression.* Glycoconjugate journal, 1996. **13**(5): p. 757-768.
54. Johansson, M.E., J.M.H. Larsson, and G.C. Hansson, *The two mucus layers of colon are organized by the MUC2 mucin, whereas the outer layer is a legislator of host–microbial interactions.* Proceedings of the national academy of sciences, 2011. **108**(Supplement 1): p. 4659-4665.
55. Ouwehand, A.C. and S. Salminen, *In vitro adhesion assays for probiotics and their in vivo relevance: a review.* Microbial ecology in health and disease, 2003. **15**(4): p. 175-184.
56. Crociani, J., et al., *Adhesion of different bifidobacteria strains to human enterocyte-like Caco-2 cells and comparison with in vivo study.* Letters in Applied Microbiology, 1995. **21**(3): p. 146-148.
57. Chauviere, G., et al., *Adhesion of human Lactobacillus acidophilus strain LB to human enterocyte-like Caco-2 cells.* Microbiology, 1992. **138**(8): p. 1689-1696.
58. Todoriki, K., et al., *Inhibition of adhesion of food-borne pathogens to Caco-2 cells by Lactobacillus strains.* Journal of Applied Microbiology, 2001. **91**(1): p. 154-159.
59. Jung, T.-H., et al., *Butyrate modulates bacterial adherence on LS174T human colorectal cells by stimulating mucin secretion and MAPK signaling pathway.* Nutrition research and practice, 2015. **9**(4): p. 343-349.

60. Bernet, M.-F., et al., *Lactobacillus acidophilus LA 1 binds to cultured human intestinal cell lines and inhibits cell attachment and cell invasion by enterovirulent bacteria.* Gut, 1994. **35**(4): p. 483-489.
61. Luo, Q., et al., *Enterotoxigenic Escherichia coli secretes a highly conserved mucin-degrading metalloprotease to effectively engage intestinal epithelial cells.* Infection and immunity, 2014. **82**(2): p. 509-521.
62. Crossman, L.C., et al., *A commensal gone bad: complete genome sequence of the prototypical enterotoxigenic Escherichia coli strain H10407.* Journal of bacteriology, 2010. **192**(21): p. 5822-5831.
63. Taxt, A., et al., *Heat-stable enterotoxin of enterotoxigenic Escherichia coli as a vaccine target.* Infection and immunity, 2010. **78**(5): p. 1824-1831.
64. Gagnon, M., et al., *Comparison of the Caco-2, HT-29 and the mucus-secreting HT29-MTX intestinal cell models to investigate Salmonella adhesion and invasion.* Journal of microbiological methods, 2013. **94**(3): p. 274-279.
65. Moellering Jr, R.C., *Emergence of Enterococcus as a significant pathogen.* Clinical infectious diseases, 1992: p. 1173-1176.
66. Diep, D.B., et al., *An overview of the mosaic bacteriocin pln loci from Lactobacillus plantarum.* Peptides, 2009. **30**(8): p. 1562-1574.
67. da Silva Sabo, S., et al., *Overview of Lactobacillus plantarum as a promising bacteriocin producer among lactic acid bacteria.* Food Research International, 2014. **64**: p. 527-536.
68. Abee, T., T. Klaenhammer, and L. Letellier, *Kinetic studies of the action of lactacin F, a bacteriocin produced by Lactobacillus johnsonii that forms poration complexes in the cytoplasmic membrane.* Applied and Environmental Microbiology, 1994. **60**(3): p. 1006-1013.
69. Ouwehand, A.C., et al., *Assessment of adhesion properties of novel probiotic strains to human intestinal mucus.* International journal of food microbiology, 2001. **64**(1): p. 119-126.
70. Deplancke, B. and H.R. Gaskins, *Microbial modulation of innate defense: goblet cells and the intestinal mucus layer.* The American journal of clinical nutrition, 2001. **73**(6): p. 1131S-1141S.
71. Mack, D., et al., *Extracellular MUC3 mucin secretion follows adherence of Lactobacillus strains to intestinal epithelial cells in vitro.* Gut, 2003. **52**(6): p. 827-833.
72. Kumar, P., et al., *EatA, an immunogenic protective antigen of enterotoxigenic Escherichia coli, degrades intestinal mucin.* Infection and immunity, 2014. **82**(2): p. 500-508.
73. Van der Sluis, M., et al., *Muc2-deficient mice spontaneously develop colitis, indicating that MUC2 is critical for colonic protection.* Gastroenterology, 2006. **131**(1): p. 117-129.
74. Velcich, A., et al., *Colorectal cancer in mice genetically deficient in the mucin Muc2.* Science, 2002. **295**(5560): p. 1726-1729.
75. Kelly, C.P., C. Pothoulakis, and J.T. LaMont, *Clostridium difficile colitis.* New England Journal of Medicine, 1994. **330**(4): p. 257-262.
76. Louis, P., G.L. Hold, and H.J. Flint, *The gut microbiota, bacterial metabolites and colorectal cancer.* Nature Reviews Microbiology, 2014. **12**(10): p. 661.
77. van Baarlen, P., et al., *Human mucosal in vivo transcriptome responses to three lactobacilli indicate how probiotics may modulate human cellular pathways.* Proceedings of the National Academy of Sciences, 2011. **108**(Supplement 1): p. 4562-4569.
78. Smits, H.H., et al., *Selective probiotic bacteria induce IL-10–producing regulatory T cells in vitro by modulating dendritic cell function through dendritic cell–specific intercellular adhesion molecule 3–grabbing nonintegrin.* Journal of Allergy and Clinical Immunology, 2005. **115**(6): p. 1260-1267.

79. Roselli, M., et al., *Probiotic bacteria Bifidobacterium animalis MB5 and Lactobacillus rhamnosus GG protect intestinal Caco-2 cells from the inflammation-associated response induced by enterotoxigenic Escherichia coli K88.* British Journal of Nutrition, 2006. **95**(6): p. 1177-1184.
80. Isobe, H., et al., *Reduction of overall Helicobacter pylori colonization levels in the stomach of Mongolian gerbil by Lactobacillus johnsonii La1 (LC1) and its in vitro activities against H. pylori motility and adherence.* Bioscience, biotechnology, and biochemistry, 2012. **76**(4): p. 850-852.
81. Humen, M.A., et al., *Lactobacillus johnsonii La1 antagonizes Giardia intestinalis in vivo.* Infection and immunity, 2005. **73**(2): p. 1265-1269.
82. La Ragione, R., et al., *In vivo characterization of Lactobacillus johnsonii FI9785 for use as a defined competitive exclusion agent against bacterial pathogens in poultry.* Letters in Applied Microbiology, 2004. **38**(3): p. 197-205.
83. Sgouras, D., et al., *In vitro and in vivo inhibition of Helicobacter pylori by Lactobacillus casei strain Shirota.* Applied and environmental microbiology, 2004. **70**(1): p. 518-526.
84. Sgouras, D.N., et al., *Lactobacillus johnsonii La1 attenuates Helicobacter pylori-associated gastritis and reduces levels of proinflammatory chemokines in C57BL/6 mice.* Clinical and Diagnostic Laboratory Immunology, 2005. **12**(12): p. 1378-1386.
85. Bereswill, S., et al., *Lactobacillus johnsonii ameliorates intestinal, extra-intestinal and systemic pro-inflammatory immune responses following murine Campylobacter jejuni infection.* Scientific Reports, 2017. **7**.
86. Liu, Q., et al., *Lactobacillus plantarum BSGP201683 isolated from giant panda feces attenuated inflammation and improved gut microflora in mice challenged with enterotoxigenic Escherichia coli.* Frontiers in microbiology, 2017. **8**: p. 1885.
87. Saavedra, J., *Probiotics and infectious diarrhea.* The American journal of gastroenterology, 2000. **95**(1): p. S16-S18.
88. Huang, J.S., et al., *Efficacy of probiotic use in acute diarrhea in children: a meta-analysis.* Digestive diseases and sciences, 2002. **47**(11): p. 2625-2634.
89. Gao, X.W., et al., *Dose–response efficacy of a proprietary probiotic formula of Lactobacillus acidophilus CL1285 and Lactobacillus casei LBC80R for antibiotic-associated diarrhea and Clostridium difficile-associated diarrhea prophylaxis in adult patients.* The American journal of gastroenterology, 2010. **105**(7): p. 1636.
90. Kotloff, K.L., *The burden and etiology of diarrheal illness in developing countries.* Pediatric Clinics, 2017. **64**(4): p. 799-814.
91. Guandalini, S., et al., *Lactobacillus GG administered in oral rehydration solution to children with acute diarrhea: a multicenter European trial.* Journal of pediatric gastroenterology and nutrition, 2000. **30**(1): p. 54-60.
92. Isolauri, E., et al., *A human Lactobacillus strain (Lactobacillus casei sp strain GG) promotes recovery from acute diarrhea in children.* Pediatrics, 1991. **88**(1): p. 90-97.
93. Saavedra, J.M., et al., *Feeding of Bifidobacterium bifidum and Streptococcus thermophilus to infants in hospital for prevention of diarrhoea and shedding of rotavirus.* The lancet, 1994. **344**(8929): p. 1046-1049.
94. Szajewska, H., et al., *Meta-analysis: Lactobacillus GG for treating acute diarrhoea in children.* Alimentary pharmacology & therapeutics, 2007. **25**(8): p. 871-881.
95. Watson, J.T., M. Gayer, and M.A. Connolly, *Epidemics after natural disasters.* Emerging infectious diseases, 2007. **13**(1): p. 1.
96. Gilliland, S. and D. Walker, *Factors to consider when selecting a culture of Lactobacillus acidophilus as a dietary adjunct to produce a hypocholesterolemic effect in humans.* Journal of dairy science, 1990. **73**(4): p. 905-911.
97. Natoli, M., et al., *Good Caco-2 cell culture practices.* Toxicology in vitro, 2012. **26**(8): p. 1243-1246.

98. Hsieh, P.S., et al., *Eradication of Helicobacter pylori Infection by the Probiotic Strains Lactobacillus johnsonii MH-68 and L. salivarius ssp. salicinius AP-32.* Helicobacter, 2012. **17**(6): p. 466-477.
99. Tomida, S., et al., *Pan-genome and comparative genome analyses of propionibacterium acnes reveal its genomic diversity in the healthy and diseased human skin microbiome.* MBio, 2013. **4**(3): p. e00003-13.
100. Kumar, S., G. Stecher, and K. Tamura, *MEGA7: Molecular Evolutionary Genetics Analysis version 7.0 for bigger datasets.* Molecular biology and evolution, 2016. **33**(7): p. 1870-1874.
101. Li, W. and A. Godzik, *Cd-hit: a fast program for clustering and comparing large sets of protein or nucleotide sequences.* Bioinformatics, 2006. **22**(13): p. 1658-1659.

Chapter 4: Mouse Models for Radiation-Induced Cancers

Mutagenesis, 2016, 31, 491–509
doi:10.1093/mutage/gew019
Review
Advance Access publication 21 May 2016

OXFORD

Review

Mouse models for radiation-induced cancers

Leena Rivina[1,†], Michael J. Davoren[1,*,†] and Robert H. Schiestl[1–4]

[1]Department of Environmental Health Sciences, [2]Department of Pathology and Laboratory Medicine and [3]Department of Radiation Oncology, University of California, Los Angeles, 650 Charles E. Young Dr. South, CHS 71-295, Los Angeles, CA 90095, USA and [4]JCCC Healthy and At-Risk Populations Program Area, 650 Charles E. Young Dr. South, CHS 71-295, Los Angeles, CA 90095, USA

*To whom correspondence should be addressed. Tel: +1 310 267 2593; Fax: +1 310 267 2578; Email: mdavoren@g.ucla.edu
†These authors contributed equally to this work.

Received 23 May 2014; Revised 31 March 2016; Accepted 4 April 2016.

Abstract

Potential ionising radiation exposure scenarios are varied, but all bring risks beyond the simple issues of short-term survival. Whether accidentally exposed to a single, whole-body dose in an act of terrorism or purposefully exposed to fractionated doses as part of a therapeutic regimen, radiation exposure carries the consequence of elevated cancer risk. The long-term impact of both intentional and unintentional exposure could potentially be mitigated by treatments specifically developed to limit the mutations and precancerous replication that ensue in the wake of irradiation The development of such agents would undoubtedly require a substantial degree of *in vitro* testing, but in order to accurately recapitulate the complex process of radiation-induced carcinogenesis, well-understood animal models are necessary. Inbred strains of the laboratory mouse, *Mus musculus*, present the most logical choice due to the high number of molecular and physiological similarities they share with humans. Their small size, high rate of breeding and fully sequenced genome further increase its value for use in cancer research. This chapter will review relevant *m. musculus* inbred and F_1 hybrid animals of radiation-induced myeloid leukemia, thymic lymphoma, breast and lung cancers. Method of cancer induction and associated molecular pathologies will also be described for each model.

Introduction

Cancer is, at its core, a disease of time—the accumulation of the specific cocktail of mutations necessary to yield a population of cancerous cells usually takes many years. As the United States population ages, cancer rates increase and will only continue to increase for the forseeable future. The medical technology, drug regimens and techniques we use to treat cancer cases also continue to improve, leading to long-term survival of cancer patients at unprecedented rates. According to present models, 50% of US citizens will receive a cancer diagnosis in their lifetimes, and half of these will receive radiation therapy as a part of their course of treatment—a rate hardly unique among developed nations (1,2). Radiotherapy is sometimes used as the sole avenue of cancer therapy, but it is more commonly received in combination with as chemotherapeutic drugs, molecular targeted therapy or immunotherapy. The use of radiation therapy is not confined to the treatment of cancers, either: it is also routinely used for immunosuppression in the cases of bone marrow, stem cell and organ transplantation (3). The unparalleled ability of radiation to kill cancer cells, however, does not come without cost. It is impossible to completely prevent collateral damage to healthy tissues when irradiating a tumor site. This damage can result in acute radiation toxicity, but more insidiously can increase the risk of chronic secondary malignancies down the line, specifically radiation-induced cancer (4,5). Even the diagnostic use of radiation in medicine comes with a collateral cost. Indeed, epidemiology from fluoroscope-induced breast cancer rates contributed much to our knowledge of radiation-induced breast cancers (6). Despite much lower exposure times and dose-rates when compared with treatment-seeking radiation therapy, the use of diagnostic techniques such as CT scans and PET tracers also take their toll in terms of DNA damage (7,8).

Unnecessary exposure of healthy surrounding tissues continues to be reduced by advances in radiation delivery technology. This more targeted delivery leads to more effective tumor killing as well,

increasing the therapeutic ratio (9–12). Even so, the complexities of tumor growth and interactions between cancer and the body within the tumor microenvironment will always lead to some collateral exposure. The development of alternate cotherapies is therefore an imperative to reduce the risk of both secondary tumors and acute toxicities resulting from radiation therapy.

Potential interventions against the side effects of *purposeful* radiation exposure would not have their value limited to that sole avenue of application, either; a treatment with demonstrated effects against both primary and secondary radiation-induced malignancies in the clinical setting would prove invaluable in far uglier, less intentional scenarios as well. The risk of a terrorist attack utilising the release of radiation or radioactive material is considered to be a very real threat by the United States government (13), and the meltdown of the Fukushima Daiichi reactor in 2011 radiation release incident demonstrates that unintentional, massive amounts of radiation exposure are possible as well. Organisations like the National Cancer Institute (NCI) have recognised the gap in our medical capability to respond to radiation emergencies, and identified research priorities (14). Obviously, interventions that prevent immediate death from acute radiation injury take precedence, but the need for treatment plans that lessen the risk of eventual complications in survivors, like cancer, has also been recognised (15).

When discussing the potential types of compounds that could be administered to reduce radiation damage, whether to prevent damage to the healthy tissue surrounding the tumor site, or to reduce sustained genotoxicity after accidental exposure to radiation, it is helpful to divide them into three classes. A first class of radiation protectors would consist of agents applied prior to radiation exposure. An ideal radioprotector would offer differential protection to healthy tissue over tumor, and allow for higher, more effective tumor-killing doses—perhaps by taking advantage in differences of DNA repair function (16) Radiation mitigators, a second class, would maintain efficacy when applied post-exposure (PE), but prior to the onset of symptoms. Agents such as these could focus on treating organ failure-level effects, such as radiation-induced neuropathy (17) or nephropathy (18), or might ideally prevent cell-level damage after the insult. The third class, therapies, would be administered after the onset of symptoms, and likely focus on treating these symptoms rather than their causes (19). Currently, only a single agent is approved by the Food and Drug Administration (FDA) for the purpose of reducing radiation damage to healthy tissue. This agent, amifostine (20), falls into the first category, as intravenous administration is given a few minutes prior to radiotherapy in clinical practice. The medical research community recognises that a single, limited treatment is not sufficient to meet the needs of future radiation oncology—and comes up dreadfully short in a disaster exposure scenario. The NCI, in collaboration with National Institute of Allergy and Infectious Diseases (NIAID) has developed an algorithm to appraise agents designed to reduce the detrimental effects of cancer therapies, and prepare them for clinical development (21). In order for a candidate agent to meet these stringent standards, success in animal model is a mandatory prerequisite. Another workshop reached similar conclusions with regards to accidental radiation exposure (14). This chapter seeks to supply researchers developing these types of interventions with a comprehensive description of animal models relevant to the adverse effects of radiation, specifically the increased risk of cancers. Models specialised for the investigation of the more acute toxicities resulting from exposure to radiation have been covered previously to great effect by Williams and Colleagues (22).

Methods

Research strategy

Over the course of the last century of biological research, the laboratory mouse *Mus musculus* has been our ever present companion, a cornerstone of *in vivo* research and the go-to model for any study requiring the complex environment of a living mammalian body. Thousands of strains are now available for research use, and ever more specialised mice are constantly under development. The field of cancer research is no exception. Modern mouse strains are often specialised in order to mimic exceptionally precise or specific aspects of carcinogenesis or a corresponding pathology. Xenograft models or humanised mice can be used directly with human neoplastic cells or to express aberrant human proteins. Other engineered strains exist which develop a certain type of cancer, developing along an exact, planned path, after exposure to a specific carcinogen. Genetically engineered mice, or GEM, represent the pinnacle of *in vivo* modeling of highly focused research into narrow portions of carcinogenetic processes. They are often the most accurate way of recapitulating the peculiarities or underlying molecular mechanisms of the human disease (23). For this reason, GEM are often used in lieu of more traditional inbred mouse strains. They often develop tumors more quickly and at more predictable intervals.

However, the very same precision that characterises GEM as superior tools for answering highly specific questions about a cancer acts as a potential drawback when investigating alternative mechanisms of cancer formation. GEM are usually developed to follow an exact carcinogenesis pathway. While this can be helpful to many research projects, one would not be able to draw many general conclusions when testing novel compounds or hypothetical alternative mechanisms. The purview of GEM rests strongly in their powerful ability to refine existing disease pathways or test highly targeted interventions. In this way, inbred strains remain the best choice for 'ground-level' investigations into the process of cancer development, as well as agents that affect that process. The use of inbred mice was indispensable for the initial discoveries of the oncogenes and tumor suppressors that were later manipulated to derive dedicated strains of GEM, as well as the toxic and therapeutic effects of countless agents (24). The value of inbred strains is still apparent, especially when it comes to investigating interventions that may act through less well understood mechanisms, such as those against radiation-induced cancer risk.

The same reasoning for why inbred mouse models remain superior to GEM for general cancer induction and progression studies might also beg the question as to why *outbred* strains are not preferred. After all, outbred strains should show greater genetic heterogeneity than inbred strains, serving as a more accurate model of the genetic diversity in a human population. This very heterogeneity, though, can become a liability when it comes to running a carcinogenesis experiment. When examining any process with both environmental and genetic components, such as cancer development in response to radiation, minimising the genetic variance between individuals is critical to the ability to determine experimental significance with sufficient power. Greater variance between individual outbred mice often means that significantly more mice are required (25). The level of genetic heterogeneity in a given outbred stock can vary greatly in terms of the number of polymorphic loci present (26). Population bottlenecks in outbred stock can lead to genetic drift, an issue made worse between varying levels of quality control between suppliers (27). Indeed, the change in allele frequency of any outbred population over time can make it very difficult to make use of

previously published information regarding that strain, even if the mice are obtained from the same supplier. Each user must therefore recharacterise the strain of interest prior to beginning an experiment (25). Even if concerned about the potential for one strain's genetic resistance to a particular insult, it is generally more efficient to use multiple strains of inbred mice than a single outbred strain (28).

The purpose of this review is to identify and describe inbred mouse models of radiation-induced (RI) cancers, with a focus on using them to investigate interventions against their development. Central emphasis will be placed on myeloid leukemia, lung, and breast cancers as most common subtypes of cancer to arise after radiation therapy (5).

Inclusion criteria

Murine models discussed in this review are limited to those pertaining to radiation-induced carcinogenesis of lymphomas, leukemias, breast and lung cancers. In particular, focus will be placed on inbred models in which cancer is induced following exposures to 'Low LET' (linear energy transfer) gamma- and X-ray irradiations. These models are most relevant to the dose rates healthy tissue is exposed to during such radiotherapy procedures as the Gamma Knife (29). 'High-LET' radiation inductions, GEM and xenograft models are outside of the scope of this work. Most of the models described rely solely on radiation for tumor induction, with a few special exceptions (*SJL/J mice*). Models described include total body irradiation (TBI) and localised IR induction methods as well as fractionated and single dose schemes. When comparing mouse induction to human radiation treatment, mouse fractionation is often split to a far lesser degree, largely due to issues of practicality. Despite this difference, disease induction is often quite comparable in terms of relative latency and pathology. Although we hope to draw general conclusions that apply to both primary and secondary RI cancers, mouse exposure scenarios are limited to primary radiation induction of tumors due to experimental feasibility.

Another point should be clarified regarding the radiation induction of cancers. Cancer progression generally requires multiple successive mutations in order to be officially recognised. Oftentimes, 'initiating' mutations can lie dormant—on their own, they are insufficient to cause the cell to progress to metastatic disease. Only after a subsequent 'promoting' insult is sustained will a traditional progression model become applicable. While some mutagens characteristically act as one or the other, Ionising radiation is a 'complete carcinogen,' capable of both induction and promotion (30–32). In many of these models, the radiation induction we discuss actually functions as the inducer of a promoting mutation. In many cases, oncogenes may already be active in both experimental animals and humans from birth (33), and it is the factors that facilitate the expansion of these cells that can be said to induce carcinogenesis (34). Details on specific mechanisms of promotion can be found in the molecular pathology sections below.

The ultimate goal of research using these models will be to develop interventions for human disease. For this reason, the models chosen constitute those that most closely mimic the underlying molecular pathologies of each type of cancer as observed in humans, maximising clinical relevance.

Results and discussion

Radiation-induced myeloid leukemia

Leukemia was one of the first cancers to have its link with radiation well documented. In the infancy of radiation research, the long-term dangers posed by constant exposure were not well understood. Radiation safety standards were quite lax by today's standards, and many cases of leukemia likely arose in early scientists and radiologists working with unshielded sources of ionising radiation (35). This early link was, in fact, supported by experiments demonstrating that ionising radiation could lead to leukemia in laboratory mice as early as the 1930s (36). Unfortunately, it was decades before this correlation between radiation exposure and leukemia mortality was noted to be anything more than anecdotal. The first studies to truly lend significant epidemiological evidence to these risks were the Life Span Studies, following both Atomic Bomb survivors and therapeutic radiation patients, treated for such diseases as cervical cancer, tinea capitis and ankylosing spondylitis (37–42). A particularly incisive study by Boice and colleagues established a sharp increase in leukemia incidence following radiation treatment for the uterine cervix carcinoma (43). Additional data emerged in the wake of the Chernobyl disaster. Detailed records on the excess risk estimates for the development of leukemia in populations analyzed by such factors as age and estimated exposure level have come to light for analysis in the last few decades. For example, clear associations were drawn from people and cleanup workers exposed to higher doses of radiation (44), while the link is more tenuous for populations exposed to under ~0.5 mSv (45). Though the circumstances of the event were tragic, information garnered in its aftermath has provided a far more complete data set on age-dependence, doses and latencies (46–49).

These studies provide risk evidence from a wide range of exposure scenarios, irradiation rates, sources and doses. By comparing the data, scientists were able to identify salient features common to all irradiation induced leukemias. The two most commonly observed RI-induced cancers in an adult population are both myeloid leukemias, of the acute (AML) or chronic (CML) subtypes (39,40,42,50–52). The subtype of leukemia most commonly seen in children varies by age of exposure. Younger children exposed around 5–9 years of age more generally develop acute lymphocytic leukemia (ALL), while children exposed after the age of 10 are more likely to develop AML. A fourth type of leukemia risk, that of chronic lymphocytic leukemia (CLL) does not seem to correlate with radiation exposure in the same manner as the others, exhibiting only a weak link if any (53,54). Leukemia after radiation exposure can arise relatively rapidly, with the highest risk observed in the decade immediately following initial exposure. After this period, relative risk decreases, albeit never returning to the baseline level of an unirradiated individual (39,40,46,51,55). Relative risk for developing different subtypes of leukemia has also been observed to vary by other factors, including the sex of the patient (40,42,46,50). The relative risk of contracting leukemia roughly doubled in one study following women receiving radiation treatment for endometrial cancer, whether exposed to low, constant dose rates or high, fractionated ones. This study estimated about 14 excess cancers per 10 000 IR-treated individuals (56).

Epidemiological data is a valuable starting point for any study of radiation-induced cancer, as it provides a background against which any experimental data from models can be checked for relevance. Interventions, however, demand the use of models for preliminary testing. Clinical trials in patients undergoing radiation therapy can provide primary human data, but only after extensive vetting as part of FDA approval. Similarly, an experimental intervention in humans *could* potentially be justified in the aftermath of a radiation catastrophe, but even in such a case an intervention must at least be partially understood before use. Murine models, therefore, are absolutely essentially for the process of understanding the mechanisms of induction of RI-induced carcinogenesis, improving risk diagnostics and especially furthering the development of radiation protection

and mitigation efforts. Several well-characterised mouse models of leukemia are available, including RF (57,58), SJL/J (59), CBA (60,61) and C3H/He (62). The following table, adapted from our previous review, summarises the optimal induction method, associated ML frequencies and other relevant features of each model (63) (Table 1).

RF mouse

The RF mouse was developed at the Rockefeller Institute for use as a general-purpose stock from the A, R and S strains (25,58). The strain has a relatively high proclivity for IR-induced leukemogenesis, as studied by Upton and colleagues (64). Some of the earliest accounts of radiation-induced leukemia took place using this strain, from observations in mice exposed to nuclear detonations in experiments conducted by Furth and colleagues (65,66). Myelogenous leukemia (ML) is induced in this strain with a single unfractionated dose of ionising radiation. This method of induction is generally considered to closely mimic human disease progression, exhibiting diagnosable tissue lesions during a prolonged preclinical period (58).

A low background rate of leukemic development is present in this strain. Between 18–24 months of age, roughly 2–4% of even unirradiated RF mice develop myeloid leukemia (68). This lifetime incidence rate is boosted up to 40% upon exposure of 8-week-old RF males to 1.5 Gy of ionising radiation. Paradoxically, *in utero* and neonatal irradiations actually *decrease* ML induction (57,64). Higher doses of IR (4.25 Gy) increases disease penetrance further to between 50 and 90% of animals, with a latency period of 4–6 months (58,68,69). Useful elements of disease progression can be observed in this model as well. The accumulation of immature myeloid cells in the spleen and liver of progressing animals can be measured as early as 12 weeks post exposure. The infiltration of leukemic cells can be observed in peribronchial areas, lymph nodes and gastrointestinal lymphoid organs. One potential confounding drawback of this model is that thymic lymphoma is also induced in 25% of mice irradiated at the dose necessary to induce myeloid leukemia, which could interfere with accurate ML diagnosis and disease modelling (58). Sex differences in susceptibility were also demonstrated by Upton and colleagues. Thymic lymphoma is more common in female mice, while males are more likely to develop ML. This gives the possibility of mixed hematopoietic tumors of both myeloid leukemic and thymic lymphoma origin presenting in the model, limiting its utility (57).

Characteristic chromosomal rearrangements are visible in the karyotypes of cells undergoing leukemic progression in this strain. According to Hayata *et al.*, ML in the RF model typically exhibits partial deletion of chromosome 2 and total loss of the Y-chromosome (although he regards this loss of Y as a mere artifact of cell proliferation rather than involved in leukemogenesis) (70), similarly to the SJL/J mouse discussed next (71). One of the strengths of this model is that the several month latency of ML in RF mice correlates well with human data. As stated previously, the peak incidence of leukemia diagnoses occurred 5–10 years post exposure in both Japanese atomic bomb survivors and children exposed to the Chernobyl disaster (40,46,50,72). Radiotherapy induced leukemia occurs on a slightly shorter, but still similar, latency period of 2.5–7 years (73).

SJL/J mouse

The SJL/J strain was developed in 1960 by Murphy and colleagues. It is known for the high spontaneous frequency of reticulum cell neoplasms (type B, RCN B) occurring in one third of mice roughly a year after birth in both sexes (74–76). This strain has also been proposed as a model for the study of Hodgkin's Lymphoma, as the histological pattern of these RCNs presents quite similarly to that of human Hodgkin's disease (77).

One whole body 3–3.5 Gy exposure in 8–10-week-old female SJL/J mice induces myeloid leukemia in 10–30% of animals. Fractionated X-ray doses have been observes to induce lymphosarcomas as well (77). Leukemic infiltration can be observed in the bone marrow, lymph nodes, spleen and liver, consistent with observation of human AML (59). The percentage of animals that develop radiation-induced acute myeloid leukemia actually increases the later the age to exposure, up until 12 weeks. This increase in susceptibility is likely explained by the maturation of the mouse's mononuclear phagocytic system, which occurs at this time (76).

Radiation alone is sufficient to initiate RI-AML in this strain. In order to better recapitulate all aspects of this complex, multiphase malignancy, though, additional promoting factors are generally administered (78). In the overwhelming majority of irradiated mice, preleukemic cells exhibiting characteristic chromosome 2 deletions can be observed in the bone marrow early on. Clinical presentation of overt AML occurs at 90–120 days (79,80). As stated previously, however, this only occurs in 10–30% of IR-treated mice. A follow-up administration of corticosteroids increases RI-AML incidence to 50–70% (59). Further reduced latencies and increased frequencies of ~75% can be reached by co-administration of growth factors such as colony stimulating factor-1 (CSF-1) (78,81). The decision to investigate this particular factor was based on the observation that, 2–4 months prior to onset, mice that would go on to develop AML solely after radiation had significantly elevated CSF-1 levels as compared to those that developed RCN-B or no cancer at all. RI-AML cells *in vitro* can also be observed to synthesise significant amounts of CSF-1, further supporting the hypothesis that high CSF-1 is correlated with leukemia progression (76).

The presentation of RI-AML in the SJL/J mouse strongly resembles that observed in humans (59). AML is diagnosed at relatively high frequencies in patients with Hodgkin's Disease in remission after receiving radiotherapy and steroid regimens—mimicking the combination induction in the mouse quite closely (82,83). This correlation between a Hodgkin's Disease/RCN B background state and the induction of RI-AML afterwards makes SJL/J an extremely valid RI-AML model for this particular set of circumstances. Both this strain of mice and Hodgkin's Disease patients tend to develop

Table 1. Induction of myeloid leukemia in mice with low-LET ionising radiation

Mouse strain	Age	Sex	Dosage	Fractionation	Latency	Spontaneous frequency	Induced frequency	Ref.
RF (RF/J, RFM)	8 weeks	Male	4.25 Gy	Single dose	4–12 months	2–4%	50–90%	(57,58)
SJL/J	8–10 weeks	Female	3–3.5 Gy	Single dose	12 months	0%	10–30%	(59)
C3H/He	8–10 weeks	Male	2.84 Gy	Single dose	1.5–18 months	<1%	25%	(60,61)
CBA (CBA/Ca, CBA/Cne, CBA/H)	12–15 weeks	Male	3 Gy	Single dose	18–24 months	<1%	25%	(62)

myeloid leukemias of the acute rather than the chronic type (84). Elevated serum CSF-1 has also been reported in some neoplastic malignancies, including AML and appears to be associated with poor prognosis (85–88).

C3H mouse

The C3H strain is one of biology's oldest and most widely used, developed by Strong in 1920 from a cross of the Bragg Albino mouse and the DBA mouse. Dams in the strain were specifically selected for elevated incidence of mammary tumors (MT). Ninety percent of unfostered pups develop mammary tumors by 11 months of age. This peculiarity of cancer incidence is due to the transfer of mouse mammary tumor virus (MMTV) into the offspring via the mother's milk. Fostering newborn animals or transferring fertilised ova to a surrogate free of MTV significantly reduces the tumor development frequency (25). However, the fostered C3H/He substrain exhibits a high incidence of spontaneous hepatomas later in life (62,89).

A total of 23.9% of 8–10-week-old male C3H/He mice develop myeloid leukemia after a single whole body X-irradiation of 3 Gy. Myelomonocytic leukemia is by far the most prevalent subtype. Female mice are significantly less susceptible to induction (90). The dose-response curves of C3H mice appear quite similar to those of RFM and the CBA strains. Leukemic induction frequency increases proportionally with level of radiation received until a critical dose at around 3 Gy, after which the incidence of ML drops rapidly (60). The administration of the synthetic glucocorticoid prednisolone following irradiation increases the incidence of ML to 38.5%, a scenario similar to promotion with corticosteroids in SJL/J mice (59). Unirradiated C3H mice have a spontaneous leukemia incidence under 1%, and that rate can be entirely eliminating with caloric restriction to 2/3 of a normal diet (62). Caloric restriction is even effective at reducing the incidence of RI-ML down to 7.9% if restriction is started prior to 6 weeks of age, or as low as 10.7% if CR begins after irradiation, at 10 weeks of age (91). Caloric restriction's effectiveness likely involves the suppression of pro-growth signaling via insulin pathway modulation (92). Chronic inflammation is also implicated as an exacerbating factor in the promotion of leukemogenesis. They also demonstrated that chronic low-level inflammation, induced by insertion of a cellulose acetate membrane, increases RI-ML incidence to 35.9% (90).

In the C3H/He strain, just as in RFM and SJL/J mice, the partial deletion of chromosome 2 is observed in RI-AML development (70,93). Chromosome 2 deletions can be detected in the bone marrow as early as the first metaphase occurring post irradiation, suggesting a critical initiating role in the process of leukemogenesis (94). The Ph^1 chromosome transformation common to human chronic myeloid leukemia, can be compared to these murine chromosome 2 aberrations in terms of both incidence and disease specificity (95,96).

CBA mouse

CBA mice, like C3H mice, were developed by Strong around 1920. They too are derived from crossing brag Albino and DBA mice, but in this case while specifically selecting for low background mammary tumor incidence. The two major substrains, CBA/Ca and CBA/H, encompass the majority of descendants of the original mice from the UK (97,98). Male CBA/Ca mice have a shorter lifespan then females (25).

Irradiating 12-week-old male CBA/H mice with 3 Gy of X or Gamma spectrum radiation induces myeloid leukemia in 25% of mice. As the disease progresses after a long latency period (generally over 1.5 years), metastases occur in sternal bone marrow, liver and splenic tissue, serving as a diagnostic endpoint (60,61). As in the previously discussed models, the induction kinetics of RI-induced leukemia are curvilinear, implying a threshold dose is necessary to initiate. Furthermore, much higher doses do not induce leukemia at all. This fact correlates well with human epidemiology (99,100).

Again, abnormalities in the structure of chromosome 2 can be observed in over 20% of the mice irradiated at this level (98,101,102). Such abnormalities can be observed from as early as 20 h after IR, to as late as 24 months after (103). Although presentation of chromosome 2 defects would be consistent with leukemic progression in that clone of cells, Bouffler *et al.* were unable to prove that the presence of an aberrant chromosome 2 clone will conclusively predict eventual development of RI-AML in CBA mice (104). Abnormalities of chromosome 4 can also be observed in half of cases of AML in this strain. The loss of *Lyr2*/TLSR5 via deletion or translocation was identified as a likely event in disease progression by Cleary *et al.* (105). Epigenetic changes can be observed as well. After irradiation in this model, an 8% decrease in in DNA-methylation is present. As this decrease is not observed in AML-resistant C57Bl/6, this change could be associated with the CBA/H mouse's greater RI-AML susceptibility (106).

The CBA mouse is the preferred genetically unmodified mouse model for RI-AML. Advantages include a low spontaneous frequency of AML and a close resemblance to human RI-AML in disease morphology (97,107). Based on extrapolation of induction kinetics by X-ray and neutron exposure, Dekkers *et al* have suggested that a "two-hit" model of RI-AML induction in CBA/H. This requirement of multiple mutations for progression makes for a more useful model of human RI-AML (108).

ML-associated molecular pathologies

As previously mentioned, the development of chromosome 2 anomalies are a common observation in multiple mouse models (RF, C3H/He, CBA and SJL/J) and tend to associate with their development of acute myelogenous leukemia (70,71,93). Rodents have high rates of chromosomal recombination when compared with humans, so determining the directly corresponding piece human chromosome for a given mouse segment is often a daunting task (109). Amongst the genes present on mouse chromosome 2 is the Abl gene, famous for its fusion into the Bcr-Abl fusion protein in the Philadelphia chromosome. Although the Philadelphia chromosome is usually associated with CML, it can also be found in ALL and other leukemic lineages (110,111). The involvement of this gene could be considered as a factor in these mice, but in mice, the lesion here generally takes the form of a deletion. Because of this, it was already assumed that the gene responsible for leukemia initiation was likely a tumor suppressor rather than a proto-oncogene, like Abl (112). The guilty party was identified by Cook and colleagues as the *sfpi*1 gene in 2004 after identifying the general location as a common region of loss of heterozygosity (LOH) (112,113). This gene, found in the 2Mbp region commonly missing in AML mice, encodes the transcription factor PU.1 (114).

PU.1 is a key transcription factor in normal hematopoiesis, involved in promotion, differentiation and regulation of every hematopoietic lineage. It is essential for both proper stem cell maintenance and the terminal differentiation of macrophages and neutrophils (115–119). The PU.1 protein includes multiple domains including DNA binding, protein–protein interaction and regulatory phosphorylation domains imperative for controlled function (120). In developing hematopoietic cells, lower levels of PU.1 lead to lymphocyte fates, while higher levels lead to myeloid fates.

Proper function is required for successful development in both cases (121,122). However, its importance in equivalent human transformations is still a subject of active debate (114,123,124).

Primary allelic loss is often caused by a deletion of the aforementioned 2Mbp region from chromosome 2; the second copy of *sfpi1* is often inactivated via point mutations in its DNA binding region, yielding a nonfunctional protein (114,123). Homozygous conditional knockdown of PU.1 in the bone marrow, reducing expression levels to only 20% of wild type, induces AML in mice inactivated from birth by 3–8 months of age (125). Induction can be achieved via inactivation in adult mice as well (126). Also not sufficient for leukemic transformation alone, the malfunction of this gene is commonly found paired with other mutations and gene losses in leukemia. The loss of PU.1 function via a chromosome 2 deletion is a common 'second hit' leukemogenesis event in transgenic mice already expressing the oncoprotein PML-PAR (127). Upregulation of *c-myc* has also been reported accompanying PU.1 deficiencies in AML cells (128). Interestingly, the forced expression of PU.1 at normal levels in promyelocitic leukemia cells inhibited clonogenic growth, forced monocytic differentiation and induced apoptosis, supporting the hypothesis that the suboptimal expression of PU.1 can promote leukemogenesis by blocking proper maturation of the cell (114,119). Peng *et al.* (129) have suggested the quantification of PU.1-deleted bone marrow cells as a surrogate marker for RI-AML.

Given these data, it would be tempting to declare PU.1 a tumor suppressor. However, other studies have shown that *over*expression of the very same transcription factor can lead to other cancers, in particular erythroleukemias (130). It would be more correct to argue that PU.1 is a critical transcription factor involved in the differentiation of multiple hematopoietic lineages, the dysregulation of which serves the development of many leukemic variants.

The human ortholog of PU.1, encoded by the *SPI1* gene, is on chromosome 11 (119), and is expressed at low levels in most AML cases, as might be predicted from the mouse models (131). In contrast with mouse models, though, its inactivation by deletion is comparatively rare in humans (123,124). Other mechanisms of PU.1 deactivation have been suggested to take precedence in human AML. The gene could be epigenetically silenced, or inactivated through interaction with a mutated receptor (i.e. the Flt3 cytokine receptor found in 25% of human AML) or another protein (114). The aberrant expression of certain miRNAs, specifically miR-155, has also been suggested as a cause of reduced PU.1 expression (132). Finnon *et al*. supported this possibility with the observation that *Flt3*-ITD and *Sfpi1*/PU.1 mutations are mutually exclusive in murine radiation-induced AML. Regardless of which gene is mutated, there is no overt phenotypic difference, suggesting that the two are capable of playing an equivalent role in the oncogenesis process (133).

As stated previously, the kinetics of IR-induction of myeloid leukemia in these models suggests that two hits are necessary. It remains to be proven, however, whether radiation is generally responsible for both of these events. Current understanding points strongly towards irradiation as the source of *Spfi1* deletions (80,93,129). The deletion could result from direct damage such as breaks in the DNA induced by ionising radiation itself, or secondary genomic instability such as that caused by IR-induced free radicals (135–137). For the loss of the second allele, however, radiation is not the most likely candidate, as IR does not induce the point mutations often observed in *Spfi1* (114,123,128). That type of mutation is more likely to be of spontaneous origin, and would generally be rectified via homologous repair mechanisms if not for its deleted counterpart (137,139).

Ban and Kai demonstrated that hematopoietic stem cells (HCS) surviving 3Gy of radiation are subjected to replicative stress, contributing to their accelerated senescence. This increased rate of replication decreases replicative fidelity and increases the rate of mutation accumulation, increasing the chance of a point mutation in the remaining copy of the *Spfi1* gene. Mathematical models fitted to experimental data from cobblestone area forming cells (CAFC) and colony forming unit-granulocyte/macrophages (CFU-G/M) on *ex vivo* bone marrows revealed that irradiated HSCs cycle as much as 10 times more quickly than HSCs in unexposed animals (138).

Hirouchi *et al.* (107) challenged the commonly accepted paradigm that HSCs are the sole genitors of RI-AML, concluding that the cancer can arise from long-lived HSCs, short-lived multipotent progenitors (MPPs) and even common myeloid progenitors (CMPs) that have acquired self-renewal potential. They postulate that the inactivation of *Dusp2* on chromosome 2 is another likely contributor. Cell surface phenotypes and gene expression profiles of the AML stem cells isolated in their study often resembled CMPs more closely than they did HSCs (139).

Even though mouse chromosomes do not directly correlate with human chromosomes, it is useful to identify commonly deleted or otherwise aberrant regions, as genes that *are* directly correlated with the human disease are often found in these 'trouble spots'. Chromosome 2 has been identified as a particular trouble spot in RI-AML, as stated several times before. Other loci on chromosomes 8, 13 and 18 have also been identified as involved in leukemogenesis. RBBP8, a BRCA1 modulator present on chromosome 18, is upregulated in response to X-ray exposure in RI-AML-sensitive CBA mice but not the RI-AML-resistant strain C57BL/6 (140).

Radiation-induced lymphoma

Although readily inducible in rodents, the link between lymphoma and exposure to ionising radiation in humans is not as strong as that between IR and leukemia. Evidence supports at least minor correlation between radiotherapy and certain types of lymphomas, according to Hartge and colleagues (141,142). Other investigators have cautioned that found the link between non-Hodgkin's lymphoma (NHL) and radiation exposure is excessively weak, and that there may be no association at all between IR and Hodgkin's disease (40,143–145). Certain epidemiological studies, however, tip the scales of evidence in favor of an association. Richardson *et al* showed a strong link between ionising radiation and lymphoma mortality among men exposed to irradiation at the Savannah River Site in South Carolina. Skepticism over the strength of the IR-lymphoma link is probably due to the disease's protracted latency and obscure mechanism of induction, which make it more difficult to point to IR as the directly responsible agent (146).

In rodent pathological classification, no difference has been historically drawn between lymphomas and lymphocytic leukemias. Malignant lymphomas have traditionally been subdivided into six classifications, and described further based on the tumor site as thymic, mesenteric or leukemic (147). Prior to necropsy, researchers must often turn to indirect observations of animal symptoms to diagnose lymphoma. Generic moribund symptoms such as labored breathing and hunched posture, taken along with the specific lymphomic elements of spleen and lymph node enlargement, are indications of fulminant malignancy. When enlarged spleens or lymph nodes are not readily visible in moribund mice, animals are usually suspected to have a thymic lymphoma, but it is difficult to conclusively prove location via simple visual observation (148). Immunological markers and analysis of morphologic criteria is sampled cells are more useful

for diagnosis (149–151). The immunophenotypes of murine lymphomas often closely resemble those of their human counterparts, despite the fact that a direct human analog of thymic lymphoma does not exist (151).

Since its first description in 1953 by Kaplan *et al.*, the induction of thymic lymphoma (TL) in mice has been extensively studied as a model radiation-induced cancer (142). C57BL substrains, BALB/c and NSF mice are all susceptible to RI-TL (153). Table 2 summarises the induction methods and details of the thymic lymphoma models described below.

C57BL mouse

C57BL mice, developed in 1921, are one of the most widely used mouse strains in the laboratory. They are derived from a simple cross between female 57 and male 52 of the same Miss Abbie Lanthrop stock. Spontaneous leukemia develops in almost 7% of C57BL/6 mice (154).

The induction of thymic lymphomas in mice by radiation has been accomplished for many years. Sacher and Brues (155) were able to induce thymic lymphomas with X-irradiation as early as 1949. In 1952, Kaplan *et al.* published a seminal paper identifying the optimal dose fractionation period for TL induction. Irradiating C57BL mice just four times at weekly intervals results in 93% disease penetrance within roughly 250 days of the initial irradiation. When taking into account all of Kaplan's fractionation experiments, even those with lower degrees of penetrance, female C57BL mice are significantly more susceptible in developing thymic lymphoma, with 58% of females dying of lymphomas versus 47% of males. TL can also be induced in many substrains with similar frequencies and induction periods, including C57BL/6, C57BL/10 and C57BL/Ka (156–158). The primary sites of metastasis in most murine lymphoma cases are the lungs and peripheral lymph nodes (159).

The presence of MEL-14^{hi} (lymphocyte homing receptor), H-2K^{hi} (histocompatibility antigen) and IL-2R^{+} (interleukin 2 receptor) surface markers on thymus cortical cells is often a hallmark of nascent lymphoma development. In a healthy adult thymus, less than 3% of the cells in the cortex express these surface antigens (160–162). Most TL tumors also bear the T-lymphocyte specific antigens Thy-1, Lyt-1 and Lyt-2 (163,164).

In C57/BL mice, the most commonly detected chromosomal abnormality in IR-induced thymic lymphomas is trisomy 15, seen in 65–71% of cases (165,166). Duplication of a chromosome 15 leads to a third copy of the oncogene *myc* (167,168). This aneuploidy has a human parallel, making it highly relevant to human disease progression. In nearly all Burkitt's lymphoma (BL) cases, a translocation between *myc*'s home region and an immunoglobin regulatory region lead to similar increased protein expression. *Myc* is one of the best known oncogenes; as a transcription factor downregulating apoptosis and upregulating mitosis, its dysregulation has been observed in many cancers besides BL (169). N-*ras* or K-*ras* activation is another common oncogene to be activated, reported in just over 50% of RI-TL cases in the C57BL/6J strain (161,170). Inactivation of tumor suppressor *p53* does not seem to be a hallmark of this model's RI-TL progression, although transgenic *p53* knockout mice do exhibit higher frequency of RI-TL (168,171).

BALB/c mouse

BALB mice were originally bred by Bagg in 1913. In 1932 Snell expanded the strain and added the '/c' appellation to reflect their homozygous 'color' locus (172). BALB/c mice are sensitive to radiation-induced lethality, but have not been shown to develop RI lymphatic leukemia. Radiosensitivity of the BALB/c strain is at least partially due to low levels of DNA-PKcs expression, leading to diminished double-strand break repair capacity (173).

However, thymic lymphoma can be readily induced according to the methodology introduced by Kaplan *et al.* Just as in C57/BL6 mice, 1.7 Gy of fractionated radiation beginning at 4 weeks of age induces this cancer in 86% of males and 77% of females, with a mean latency of about 5 months. Although their induced rate is lower, only females spontaneously develop lymphoma in 5.5% of animals (148,153).

Most studies of lymphomagenesis mechanisms were conducted in either C57BL/6 and its substrains, or in hybrid models comprised of a BALB/c parent mated to a radiation-induced lymphoma-resistant strain. More recently, inbred BALB/c mice have been used in studies investigating the role of microRNAs (miRNA) in radiation-induced lymphomagenesis. Liu *et al.* have concluded that the expression of the tumor suppressor gene *Big-h3* is downregulated while miR-21 is upregulated in RI-TL. It is likely that miR-21 suppresses *Big-h3* expression by binding to specific target sequences in the 3′ untranslated region of the mRNA (a 3'UTR dependent manner) (174,175).

NFS mouse

Inbred NFS mice were derived from outbred NIH Swiss-Webster mice introduced to Japan in 1972. The strain is maintained by sibling mating. It is currently referred to as either NFS or NIH Swiss/S (176).

In NFS mice, induction of thymic lymphoma is performed with four weekly irradiations of 1.7 Gy beginning at 1 month of age, much like induction in BALB/c and C57BL mice. In this strain, males and females have nearly identical susceptibility rates. The latency period, thought, is longer in males, at 208 days versus 167 in females. Spontaneous thymic lymphoma occurs in roughly 10% of mice by 600 days of age (176). The incidence of IR-TL can be reduced by performing a thymectomy prior to irradation. Completing this procedure before irradiating *increases* the incidence of nonthymic lymphomas and leukemias, leading to alternative cancers in 67% of treated mice. This athymic induction potentially provides a murine

Table 2. Induction of thymic lymphoma in mice with low-LET ionising radiation

Malignancy	Mouse strain	Age	Sex	Dosage	Fractionation	Latency	spontaneous frequency	Induced frequency	Ref.
Thymic Lymphoma	C57BL (C57BL/6, C57BL/6J)	4–6 weeks	Male, Female	~1.7 Gy	4× once weekly	3–6 months	<1%	> 90%	(159)
Thymic Lymphoma	BALB/c (BALB/cHeA)	4 weeks	Male, Female	~1.7 Gy	4× once weekly	2.5–9.5 months	5–6% females; 0% males	77% (Females) 86% (Males)	(148,153)
Thymic Lymphoma	NFS	4 weeks	Male, Female	~1.7 Gy	4× once weekly	3–6 months	>1% within 12 months	90% (females) 89% (males)	(176,177)

lymphoma model more in line with human lymphomagenesis by eliminating the distinctly murine thymic lymphoma. In athymic animals, the latency period for hematopoietic malignancies lasted up to 10 months following IR, 2 months longer than the equivalent TL induction period. These nonthymic lymphomas are most likely to be of B-cell origin, and can be predominantly found in the spleen or mesenteric lymph nodes (177).

TL-associated molecular pathologies

In thymic lymphoma research, hybrid models are often used over inbred strains due to simpler detection of underlying molecular pathologies. Commonly used hybrids include (C57BL/6J × BALB/c)F_1, B6C3F1 (C57BL/6J × C3H)F_1, C3B6F1 (C3H × C57BL/6)F_1, (BALB/c × MSM)F_1 (178), (C57BL/6J × RF/J)F_1 (179), (C57BL/6J × DBA)F_1 and CBA/H × C57BL/6 (180,181) as well as the CXS series of recombinant inbred strains derived from TL-susceptible BALB/cHeA and TL-resistant STS/A (148). As one might expect, when inducing thymic lymphoma in hybrids between strains with low susceptibilities and those with high susceptibilities, like BALB/c × MSM, RI-TL frequencies usually lie between those of the parental strains. These particular hybrids will require higher radiation doses to be used during their four weekly fractions when compared to the TL-susceptible strains discussed above, such as the use of 2.5 Gy rather than 1.7 Gy (178). Studies involving hybrid mice have elucidated the importance of tumor suppressor inactivation in TL progression, with such genes as *Ikaros/Znf1a1* (182,183), *Bcl11b/Rit1* (184), *p73* (185), *p19/ARF* (186), *p15/INK4b(Cdkn2b)* and *p16/INK4a(Cdkn2a)* (187) commonly deleted or suppressed in radiation-induced lymphomagenesis. Transgenic expression of *Notch1* in murine lymphocytes also induces lymphomagenesis (188). As with any cancer, the combination of tumor suppressor inactivation with oncogene activation drastically increases progression. *Notch1* activation coupled with inactivation of *Notch2*, overexpression of *c-Myc* and defective *Znfn1a1/Ikaros* binding has been reported in 81.25% of RI-TLs, suggesting their molecular collaboration in the lymphomagenesis process (189). Hybrid experiments also confirm the roles of the common chromosome abnormalities of chromosomes 4, 11 and 12, although such aberrations do not appear ubiquitously in all hybrids. BALB/C × MSM does not often show LOH on chromosome 4, while the same event is commonly observed in C57BL/6J × RF/J hybrids (181). Observations like this underscore that genetically inherited predisposition for damaging events to occur at certain gene loci plays an important role in the differences in disease susceptibility and molecular pathology between strains. Saito *et al* report multiple susceptibility loci, pointing to areas near *D4Mit12* on chromosome 4, *D2Mit15* on chromosome 2 and *D5Mit15* on chromosome 5 (178). Additional, sex-dependent susceptibility loci have been identified by Piskorowska and colleagues on chromosome 10 (*D10Mit134*), and chromosome 12 (*D12Mit52I*) (190).

The C57BL/6 and C3H hybrid strains C3B6F1 and B6C3F1 present similar chromosome aberrations, exhibiting copy-number reduction and allelic loss at *Ikaros* and *Bcl1b,* but not at *Cdkn2a/Cdk2b* and *Pten* loci, when compared to their parental strains. Alterations of *Ikaros* and *Bcl1b* are usually due to multilocus deletions, while *Cdkn2a/Cdk2b* and *Pten* show uniparental disomy. In this strain *Ikaros* appears to be lost first, followed by the loss of *Bcl11l* at a later time. This pattern contrasts with that observed in BALB/c × MSM hybrids, where the order is reversed (166). In C57BL/6 and C3H hybrids rearrangements in *Tcra* (T-Cell Receptor Alpha) are more common than *Tcrb* (T-Cell Receptor Beta) rearrangements, although both aberrations are observed *Tcrb* is more strictly regulated than *Tcra*, so this disparity is to be expected, but the fact that *Tcrb* allelic loss is observed suggests that increased aberrant V(D)J rearrangement or increases in illegitimate V(D)J recombination may be important events in IR-induced lymphomagenesis. Divergence in the rates of these particular events may be other factors responsible for differences in susceptibility to RI-TL between strains (166). V(D)J recombination deficiencies are also associated with intragenic deletions in *Bcl11b* and *Notch1*. These phenomena have been observed in human lymphoid malignancies as well (191–193).

The idea that the major contribution of radiation to IR-TL is by the indirect mechanism of inducing genomic instability was expanded upon by Kominami and Niwa (194). Their hypothesis suggests that the main result of fractionated total body irradiation is widespread apoptosis in the thymus gland, rather than minor, mutation inducing damage to the larger population of cells. The high casualty rate leaves a void in that cell niche, stimulating differentiation arrest and population regeneration by surviving thymocytes. The replicative stress of this event both reduces replicative fidelity and crafts a progrowth environment for those cells possessing tumorigenic potential (157,195–197). The observation that transplantation or intravenous infusion of unirradiated donor marrow into the irradiated host reduces subsequent lymphomagenesis is consistent with this model. By restoring the thymic microenvironment, the clonal expansion of irradiated T-cell precursors is prevented. Shielding the bone marrow of the irradiated host protects against RI-TL through the same microenvironment-preserving mechanism. Inversely, the transplantation of an unirradiated thymus into an irradiated animal leads to the development of full TL, again suggesting that the replicative stress is most responsible for lymphoma progression rather than direct radiation damage (196,198–200). Muto and colleagues demonstrated that intrathymic and intraperitoneal injections of thymocytes from donors irradiated 4 months previously also resulted in T-type lymphomas derived from donor cells. However, when donor cells were taken only one month post irradiation, only intrathymic injections developed into donor-type lymphomas in the recipient host. This suggests that the thymus is important in the further promotion of these 'prelymphoma' cells. Injecting bone marrow cells rather than thymocytes failed to induce lymphomas in the recipient, suggesting that the bone marrow is a less likely origin site of this prelymphoma cell (201). Furthermore, subjecting RF mice to thymectomy prior to irradiation drastically reduced the incidence of TL, from 32% to just 1% (57). Lymphoma progression, therefore, likely follows the body's attempt to repopulate after massive induction of apoptosis after IR. The importance of apoptosis as a key first step in thymic leukemogenesis is further supported by the finding that manipulation of apoptotic susceptibility in GEM can impair or even accelerate the process (202,203). Mori *et al* point to the region containing *prkdc* as a quantitative trait locus determining susceptibility to both radiation-induced apoptosis and cancer (204). The irradiation of supporting cells and tissues, rather than only thymocytes, plays a critical role in the origination of this malignancy. After catastrophic damage is taken by the thymic microenvironment, it is the thymus' own desperate attempts to stimulate thymocyte repopulation that prime the replicatively stressed cells for development into TL.

The interactions between thymus tissues and hematopoietic progenitors which lead to lymphoma appear to be at least partially mediated by Notch receptors and their ligands (194). Alterations in the management of reactive oxygen species (ROS) that would accompany a state of rapid replication would lead to the accumulation of further pro-lymphomic mutations in repopulating thymocytes

(31,205). The presence of a variant of *Mtf-1* (metal responsive transcription factor-1), identified in TL-susceptible BALB/c mice by Tamura *et al.*, was linked to both higher proliferation levels of premature thymocytes and higher levels of ROS when compared to RI-TL resistant strains lacking this variant (206,207). MTF-1 is involved in post-radiation signaling pathways regulating intracellular ROS (208).

Although thymic lymphoma itself is not specifically observed in humans, the radiation-induced lymphomagenesis mouse model offers important insight into the progression of related human hematopoietic neoplasias. The *Ikaros* gene, identified in the RI-TL mouse model, is implicated in human acute lymphoblastic leukemia (ALL), the most common hematopoietic malignancy in children (182,209–212). Tsuji *et al.* used the RI-TL model to demonstrate the contribution of illegitimate V(D)J recombination to *Notch1* 5′-deletions, deregulation of which is thought to be involved in the etiology of both B- and T-cell human lymphomagenesis (213). *Notch1,* a diverse master regulator responsible for a plethora of cellular processes, is itself an important player in both RI-TL and T-cell acute lymphoblastic leukemia (213). *PTEN* (215) and *CDKN2A/CDKN2B* have similarly been proposed as potential oncogenes in human ALL (216,217). *EPHA7*, inactivated in 100% of TL in mice, is also inactivated in 95.23% of human T-cell lymphoblastic leukemia/lymphomas (T-LBL) via loss of heterozygosity, promoter hypermethylation, or a combination of the two (218).

Radiation-induced lung cancer

Lung carcinoma is the deadliest cancer type in industrialised nations, responsible for over a quarter of all cancer deaths. Smoking remains the single greatest risk factor behind this disease (219). Despite this, lung cancers were one of the first to be linked with radiation exposure because of their high rate of mortality (220). The vast majority of data on the link between radiation exposure and development of lung cancer can be attributed to epidemiology from three groups: underground miners, exposed to internal alpha radiation via radon-222 and radon-220 inhalation; Patients who have undergone radiotherapy patients to treat neoplastic and non-neoplastic malignancies; and Japanese atomic bomb survivors (4,221,222). The latency period after induction from gamma or X-ray exposure is particularly long for lung cancer, taking a minimum of 9–10 years, with an increased risk persisting in survivors for over 25 years. After correcting for gender based differences in smoking rates, females are considerably more susceptible to radiation-induced lung cancer than males. Adenocarcinoma appears to be the most common type of lung cancer in a population exposed to large amounts of radiation. No correlation exists between age of exposure and development of this malignancy (4,223,224). Travis and colleagues have reported that, in Hodgkin's disease patients treated with total radiation doses of 40Gy or more, a significant increase in all histopathological types of lung cancer can be observed even after controlling for smoking. Incidence of radiotherapy-induced lung cancer in Hodgkin's Disease patients peaks 5–9 years after radiation therapy (225–227). Evidence of the link between lung cancer and irradiation is further supported by studies reporting increased rates of lung cancer in radiation treated breast cancer survivors as well (228,229). One study of such irradiation treated breast cancer patients showed a relative lung cancer risk of 1.5 over 10 years when compared to surgery only controls (230).

Localised radiation exposure, like whole body exposure, can result in health effects with varying degrees of severity. In both mice and humans these consequences include pulmonary fibrosis and carcinogenesis. Whether radiation exposure will result in primarily pulmonary fibrosis or increased cancer risk appears to be a function of dose. Fibrosis occurs when cells are killed outright, so it is actually lower doses of IR that are more likely to cause the initiation of carcinogenesis (220). Williams *et al* provide an extensive guide for the selection of radiation-induced fibrosis animals models (22). The table below summarises three models of radiation-induced lung cancer, generated by employing both whole body irradiations and targeted thoracic exposures in C3H, BALB/c and RFM mice.

C3H mouse

C3H/He mice are moderately sensitive to the induction of lung cancers via IR, and also develop spontaneous lung tumors at a low frequency (231). Multiple regimens are viable in this mouse depending on the goal of the researcher. A single 7.5 Gy irradiation to the thorax followed by three 3 Gy whole body irradiations at 3 month intervals afterward yields the highest induction frequency, at 62%. The great

Table 3. Induction of lung cancer in mice with low-LET ionising radiation

Malignancy	Mouse strain	Age	Sex	Dosage	Fractionation	Latency	Spontaneous frequency	Induced frequency	Ref.
Lung Cancer	C3H (C3H/HeSlc)	6 weeks	Male	7.5 Gy thoracic	2 doses, 12-h interval	12 months	3.5–9.5%	40%	(232,233)
Lung Cancer	RFM (RFM/Un)	10–12 weeks	Female	9 Gy thoracic	single	9 months	~28%	87%	(235,236)
Lung Cancer	BALB/c (BALB/c/An)	12 weeks	Female	2 Gy TBI	single	12 months	~12%	~37%	(237,238)

Table 4. Induction of breast cancer in mice with low-LET ionising radiation

Malignancy	Mouse strain	Age	Sex	Dosage	Fractionation	Latency	Spontaneous frequency	Induced frequency	Ref.
Breast cancer	BALB/c	12 weeks	Female	2.0 Gy TBI	Single	~24 months	8%	22%	(237)
Breast cancer	BALB/c orthograft	12 weeks	Female	1.0 Gy TBI of donor cells	Single	10 weeks	<1%	Dysplasia ~75% Tumors ~25% (dependent upon donor cell passage)	(271)
Breast cancer	BALB/c chimera	12 weeks	Female	4.0 Gy TBI of host	Single	6 weeks	~19%	~81%	(30)

expanse of time between exposures, however, makes this model less relevant to researchers trying to closely model a human exposure scenario. Another plan, two 7.5 Gy thoracic irradiations around a 12 hour interval, yields roughly 40% induction in males exposed at 6 weeks of age, and is generally considered to be more relevant clinically. Mice irradiated in this fashion develop alveologenic adenomas and adenocarcinomas after a latency period of 12 months. Tubular or papillary form tumors are observed only rarely (232). In whole body irradiation dose response studies, Hashimoto and colleagues showed that tumor incidence increased with dose to a peak at 5.0 Gy, but decreased at 10Gy. This observation demonstrates the competitive dynamics between opposing inductive and suppressive effects of radiation with regards to the initiation of cancer and fibrosis. Comparatively lower doses induce DNA strand breaks, deletions and recombinations that can push a cell into cancer development, but higher doses can kill affected cells outright and lead to their replacement by less cancer-prone fibrotic tissue (233).

Even factors as ostensibly distant as circadian rhythm have measureable effects on induction rates. An irradiation at night is a far more potent inducer of RI-LC in C3H mice than an equivalent daytime dose. In this strain, a full 5 Gy of irradiation during the day is required to match the tumor induction frequency seen with just 1.25 Gy at night (232). This response does not seem to be an artifact of the murine model, as circadian variations have been reported in human cancer therapy responses as well (234). As stated previously, dual thoracic irradiation is the most clinically relevant method of induction for this strain, and also carries the lowest rate of inducing other, obfuscating cancer types along with the lung tumors to be studied (220).

RFM mouse

Lung adenomas are inducible in both male and female RFM/Un mice exposed to IR at 10–12 weeks old (235,236). Following a single 9.0 Gy thoracic irradiation, roughly 87% of females develop lung cancer within 6–9 months, with an average of 1.8 tumors per mouse. Males are slightly more resilient. A dose of 10.0 Gy causes the same malignancy roughly 54% of the time within 11 months, with a tumor multiplicity of 0.8 tumors per mouse. A potential downside of this strain is its high rate of spontaneous lung carcinogenesis, arising in 28% of unirradiated females and 32% of males (235,236).

BALB/c mouse

A single 2.0 Gy whole body irradiation at a dose rate of .35 Gy/min administered to a 12-week-old female BALB/c/An mouse results in a 37% induction rate of lung adenocarcinoma, with an average latency of 12 months. The spontaneous rate of these mice developing this cancer is between 11 and 14 % (237). Fractionation of the 2.0 Gy dose does not increase lung cancer incidence relative to the single irradiation (238).

Lung cancer-associated molecular pathologies

Though the effects of dose, dose-rate, fractionation and radiation quality on murine lung carcinogenesis have been studied extensively for some time, the mechanisms of lung cancer induction are notoriously difficult to discern in animal models. The underlying molecular and pathophysiological mechanisms remained largely elusive until GEM achieved widespread use. Some molecular mechanisms identified still have yet to be definitively correlated with observed pathologies in inbred strains (233–238,239). A great deal of data, though, was able to be obtained retroactively from massive radiation studies involving 40,000 $B6CF_1$ hybrid mice (C57BL/6 females × BALB/c male) at Argonne National Laboratory between 1971 and 1986 (240,241). Genetic material was extracted for PCR-amplification from the paraffin-preserved lung tissues of animals with adenocarcinomas and their controls. A significant percentage of the samples derived from radiation-induced or spontaneous lung adenocarcinomas from this study showed deletions of the tumor suppressor *Rb*. Deletion of this gene appeared to cut across all adenocarcinomas regardless of their mechanism of induction, suggesting that its loss is critical to lung cancer progression. No statistically significant differences in *Rb* deletion frequency were observed in adenocarcinomas whether animals received 60 weekly doses of 0.1 Gy, single doses of 5.69 Gy, or were so unfortunate as to develop adenocarcinomas spontaneously. Furthermore, 97% of samples containing *Rb* deletions also carried *p53* deletions, suggesting that mutation of *p53* is likely a predominant step in radiation-induced lung carcinogenesis in $B6CF_1$ mice (241). A separate study on the same preserved tissues also uncovered a high rate of point mutations in the *K-ras* gene, again regardless of whether the cancer arose spontaneously or after 24 or 60 weekly irradiations (242).

Dysregulation of *p53*, *K-ras* and *Rb* are commonly observed in both human and murine lung cancers (243–245). The *p53* tumor suppressor is so commonly mutated in cancers of all that it has accumulated a variety of nicknames like 'the guardian of the genome'. Lung cancer is certainly no exception, with its inactivation by either deletion or mutation occuring in 80% of primary lung tumors (244–249). The loss of *p53* is associated with poor clinical outcome (243). *Rb* is another tumor suppressor inactivated either directly or indirectly in a wide variety of tumors, including 90% of human small cell carcinomas (250,251). *K-ras* is a proto-oncogene involved in cell differentiation, growth and anti-apoptosis, but it also widely modified in many cancers (252). A total of 20–30% of human lung adenocarcinomas possess a mutation in the *RAS* gene (253). Activated *K-ras* is also associated with a poor clinical prognosis (254).

Although much of the molecular pathology of lung cancer was teased out of GEM, inbred mice provide a more versatile platform for the testing of therapeutic agents directed against secondary cancers, including those induced or promoted by radiation therapy. Mice genetically engineered to mimic human cancers, such as mice with *K-ras* knockout of lung adenocarcinoma (23), are useful and sophisticated models for answering specific questions of molecular biology, but are purposefully self-limiting and biased by nature. These models are predisposed to develop only one type of malignancy along a designated progression route. As such, they do not permit the study of alternative mechanisms of carcinogenesis. If radiation-induced lung carcinogenesis, or interventions against it, act outside of precisely pre-programmed initiation and progression pathways, GEM studies are much less relevant. Inbred mice present a more unbiased approach to discovery studies.

Radiation-induced breast cancer

As with lung cancer, three massive groups are responsible for most epidemiological data on the link between radiation exposure and breast cancer. These three groups are Japanese female survivors of the atomic bomb attacks, females subjected to diagnostic fluoroscopes in Massachusetts tuberculosis sanatoria and women treated for postpartum mastitis in New York (6,255,256). Data from the Japanese atomic bomb cohort demonstrates that breast carcinoma risk increases by a greater extent than all other solid tumor risks upon exposure to IR (4). In the Massachusetts study, females exposed to over a hundred separate instances of diagnostic x-rays were shown to be 80% more likely to develop breast tumors than controls (255). Radiation therapy is implicated as a causative agent

in secondary breast cancers, and demonstrate dependency on age at exposure. Up to 35% of women treated for Hodgkin's disease with radiation therapy early in life developed breast cancer by the age of forty. According to Bhatia and Sankila, the latency period of IR-induced breast cancer is roughly 10 years (257,258). Stovall and colleagues report that an absorbed radiotherapy doses over 1Gy to the contralateral breast during treatment of a primary breast tumor is linked to a high risk of secondary *de novo* contralateral breast cancer (CBC) (259). Reproductive history is also a factor in CBC risk. Women childless at first cancer diagnosis were more likely to develop CBC after radiotherapy than age-matched mothers (260). According to Boice, women treated with radiation therapy for existing breast cancer can have up to 1.5 times the risk of developing a second, contralateral cancer, especially if irradiated before age 45. As a total population, about 2.7% of secondary breast tumors can be attributable to radiation (261).

Ionising radiation is well-established as an etiological agent in both murine and human breast cancer (223,233,262–267). Mammary cancer mouse models are absolutely invaluable to the study of chemotherapeutic interventions and modeling molecular pathologies, despite differences such as differences in precise site of origination and low hormonal dependence frequencies (264). The BALB/c mouse is an extensively used model of mammary cancer, which can be induced with either full body irradiation or the implantation of irradiated tissues into syngenic mice (268). As detailed below, much of the radiation sensitivity that contributes to the convenience of the BALB/c model for IR breast cancer induction can be attributed to rather languid PKcs protein activity, which leads to lower levels of NHEJ repair (269). Importantly, this maintains the model's relevance to human breast cancer induction, as the human ortholog of this same gene has a particularly low level of differential expression in human breast tissue (270). Table 4 summarises the most commonly used BALB/c models.

BALB/c whole-body exposure model

Studies in the BALB/c female whole-body irradiation model show an increase in mammary carcinogenesis from a background frequency of around 8% to about 22% over the mouse's entire lifetime. This mammary adenocarcinoma induction method consists of irradiating 12 week old females with a total dose of 2.0 Gy, at the dose-rate of 0.35Gy/min. Irradiation with the same total dose at the lower dose-rate of 0.083 Gy/day results in only half the induction frequency, around ~13% (237). The high dose rate seems to be key rather than the total dose; even a dose of 0.25Gy at 0.35Gy/min is capable of inducing mammary tumors in about 20% of mice (238). While irradiation increases the incidence of breast adenocarcinomas, it does not decrease disease latency relative to spontaneously arising tumors. Hyperplastic lesions in the mammary ducts are generally detected 12–14 months after IR exposure, prior to appearance of the tumor proper (272). Radiation-induced breast adenocarcinoma sensitivity in the BALB/c female has been attributed to polymorphisms of *Prkdc*, a DNA-dependent protein kinase gene, involved in DNA repair and post-IR cell signaling (269). An unfortunate drawback of this model, despite its simplicity, is its high rate of concurrent ovarian tumor development, detected in over 90% of autopsied mice (237).

BALB/c syngenic transplant model

In 1959, a great advance was made in the field of breast cancer biology when DeOme and colleagues introduced a murine orthograft breast cancer model. This model consists of clearing the mammary fat pad from a 3-week-old female virgin mouse and subsequently transplanting a 1mm duct fragment from a donor mouse with hyperplastic lesions (273,274). Ethier and Ullrich successfully adopted this model from the original strain into BALB/c mice and used it extensively to demonstrate differences in sensitivity between strains and associated molecular mechanisms (269,271,275,276). Barcellos-Hoff and colleagues employed this model to demonstrate the importance of tissue microenvironment in the breast carcinogenesis process (277–280).

Ethier and Ullrich also employed the 'cell dissociation assay,' a combined *in vitro*/ cell culture model in which 12 week old virgin donor BALB/c females are whole body irradiated with a total dose of 1.0 Gy, with mammary tissues removed at 24 h post-exposure. A single-cell suspension of 10^4 cells from these donor animals is then injected into 3-week-old virgin BALB/c females with cleared mammary fat pads. 10 weeks post procedure, recipient mice are sacrificed and outgrowths removed and analyzed for anomalies in ductal architecture. Normal duct outgrowths contain 2–3 terminal ducts, and are capped by end buds in the fat pad. Abnormal outgrowths, on the other hand, can have 10 or more terminal ducts capped with hyperplastic end buds. These abnormal architectures are classified between Classes I and III, with Class III being most severe (275,281,282).

In another series of experiments, Ullrich and colleagues demonstrated that cells harvested from an irradiated donor, passaged *in vitro* and finally transplanted into unirradiated recipient mice develop into either dysplasia or adenocarcinomas. The degree of dysplasia exhibited in the host mouse depends upon time of harvesting and number of passages in culture prior to implantation. Cells harvested 52 weeks post-IR tended to generate dysplastic outgrowths in 75% of mice and develop into full tumors in 25% of cases. Cells harvested at up to 16 weeks IR only develop into normal outgrowths unless subjected to extensive *in vitro* passaging. This observation suggests that the irradiated ductal microenvironment plays a critical role in the initiation of oncogenesis. The dysplasia and tumors observed in the host mouse resemble *in situ* tumorigenesis, complete with leukocyte infiltrations and angiogenesis (272).

BALB/c chimeric model

Barcellos-Hoff and Ravi established a chimeric radiation model in which the fat pads of a BALB/c mouse host are cleared at 3 weeks of age. The same mouse is then whole body irradiated with 4.0 Gy at 10–12 weeks of age (30). Three days later, these hosts receive a transplant of immortalised but non-malignant COMMA-D mouse epithelial cells, derived from midpregnancy BALB/c females (283). Six weeks post-IR the cells injected into irradiated host develop into tumors with 81% penetrance, compared to only 19% of cells injected into an unirradiated host. This syngenic model further demonstrates that radiation causes changes in the stromal microenvironment which contribute to carcinogenicity (30). Whole implantation of a 1 mm^3 formed duct epithelial fragment acquired from either a wildtype donor or a donor primed for neoplastic development also works as an alternative model to injection of cell suspension (284).

Breast cancer-associated molecular pathologies

Cell lines harvested from female BALB/C mice 4 weeks (EF42) or 16 weeks (EF137) after 1 Gy whole body irradiation are a common investigative platform for the molecular pathologies of breast cancer tumorigenesis. Cell culture studies point to a number of familiar players in the oncogenic protein scene. Reduced or absent Rb can be detected after 11 passages in EF42 cells, and after only six passages

in the EF137 line. Mutant *p53* is present in 95% of these cells after 20 passages and even as early as passage 6 in 1–5% of cultures, supplying more evidence that *p53* mutation is an initiating transformation event in preneoplastic cells. Expression of angiogenesis markers can usually be detected after about 20 passages (272). In *in vivo* transplantation studies, Ethier and Ullrich reported that introducing 10 times the usual amount of cells (10^5) actually decreased both the frequency and severity of observed dysplasia, compared to a standard injection of 10^4 cells (275,281). This suggests that replicative stress may be contributing to faster and more prominent progression into ductal dysplasia.

Barcellos-Hoff and colleagues link the rapid remodeling of the irradiated mammary gland microenvironment to changes in both the extracellular matrix and increases in Transforming growth factor beta (TGF-β) expression (277,285–287). The compensatory expression of this growth factor is likely increased to encourage replacement of cells forced to undergo apoptosis in the original irradiation, but high expression brings with it the dangers of progrowth signaling and replicative stress (284). TGF-β is involved in the regulation of a variety of cell processes, including cell cycle control, apoptosis and cell differentiation (286,288). Activation of TGF-β as a result of radiation has also been implicated to influence cell fate decisions and DNA-repair kinetics in an ATM-dependent manner (289,290).

Importantly, chimeric models are able to capture prominent features of breast cancers thought to arise following irradiation even though the transplanted epithelium itself has not been irradiated. IR-associated human breast cancer arises from the duct cells and often infiltrates the rest of the breast tissue, a progression similar to that observed in transplantation mouse models (5). Tumors induced from transplanted epithelium that test negative for P53 expression are estrogen receptor (ER) negative as well, much like the phenotype observed in secondary IR derived human breast cancers (284,291). The *Rb* deficiencies observed by Ullrich and Preston in neoplastic duct cells are also often reported in human breast cancer, and correlate with a highly invasive tumor phenotype (292).

Conclusions

An absolutely ideal radiation-induced carcinogenesis mouse model possesses a low spontaneous background frequency of the desired malignancy, has a short latency period, avoids the co-development of cancers at alternative sites, and produces tumors nearly identical to the corresponding human cancer in terms of onset, progression and underlying pathology. As a perfect model does not exist, researchers are inevitably forced to compromise on some of these features. It is generally more feasible to compromise on features such as cancer latency and induction frequency, as these can be compensated for by study design and sheer subject volume. The most care should be taken to best emulate molecular and pathophysiological features of human radiation-induced malignancies, as these features are key to a model's relevance. No model reflects the human condition completely, however, even on a single factor. The use of mouse models must always be realised as part of a toolkit containing other experimental platforms as well. Radiation-induced secondary cancers can still be difficult to discern from primary tumors in both humans and mouse models. Further research into identifying and differentiating these cancers based on differences in their respective molecular signatures is a difficult challenge, but one that brings great potential reward.

Radiation mitigation, with the aim of reducing cancer risk in irradiated individuals is a developing but promising field. Administration of antioxidants appears to reduce damage from irradiation, likely by quenching ROS generated. The administration of antioxidants generally shows the best effect via protection, not mitigation. However, there is evidence that some medium to long-term radiation-induced injury may come about due to chronic oxidative stress—in which case, the correct application of antioxidants may have a measurable effect in the mitigation window after all (293). Kuefner et al. observed a significant reduction of H2AX foci, markers of DNA damage, upon *in vitro* preincubation of human lymphocytes with glutathione before irradiation, but this effect did not extend to post-irradiation incubation, nor is it clear whether this effect might carry over to *in vivo* experimentation (294). As mentioned previously, Amifostine and its active metabolite, WR-1065, have been shown to have some promise differentially protecting healthy tissue over tumor cells during radiotherapy when administered beforehand (20,295). The use of other micronutrients, such as DNA cofactors and selenium, has also been suggested (296). No clear agent stands out yet, however, as the perfect agent to protect against both radiation-induced toxicity and subsequent cancer risk. As with all complex drug/disease interactions, the use of mouse models to determine an effective treatment is an imperative. If a compound can be conclusively shown to effect the myeloid leukemia rates in these establish models, it would have an extraordinary impact on the field of oncology.

The mouse models presented are often a compromise on the background frequencies and rates of induction, but all demonstrate strong molecular and phenotypic correlations to salient features of the human cancers they are meant to represent. These models provide a powerful tool for testing the therapeutic benefit of candidate drugs and other interventions against radiation-induced carcinogenesis.

Acknowledgements

The authors wish to thank the NIEHS Training Grant in Molecular Toxicology for funding provided to Michael J. Davoren.

Conflict of interest statement: None declared.

References

1. Howlader N, Noone AM, Krapcho M, *et al.* (eds). (2012) *SEER Cancer Statistics Review, 1975–2009 (Vintage 2009 Populations)*. National Cancer Institute.
2. Ringborg, U., Bergqvist, D., Brorsson, B., *et al.* (2003) The Swedish Council on Technology Assessment in Health Care (SBU) systematic overview of radiotherapy for cancer including a prospective survey of radiotherapy practice in Sweden 2001–summary and conclusions. *Acta Oncol.*, 42, 357–365.
3. Prasanna, P. G., Stone, H. B., Wong, R. S., Capala, J., Bernhard, E. J., Vikram, B. and Coleman, C. N. (2012) Normal tissue protection for improving radiotherapy: Where are the Gaps? *Transl. Cancer Res.*, 1, 35–48.
4. Fajardo, L. F., Berthrong, M. and Anderson, R. E. (2001) *Radiation Pathology*. Oxford University Press, New York.
5. Hall, E. J. and Giaccia, A. J. (2012) *Radiobiology for the Radiologist*, 7th edn. Wolters Kluwer Health/Lippincott Williams & Wilkins, Philadelphia.
6. Boice, J. D. Jr and Monson, R. R. (1977) Breast cancer in women after repeated fluoroscopic examinations of the chest. *J. Natl. Cancer Inst.*, 59, 823–832.
7. Mathews, J. D., Forsythe, A. V., Brady, Z., *et al.* (2013) Cancer risk in 680,000 people exposed to computed tomography scans in childhood or adolescence: data linkage study of 11 million Australians. *BMJ*, 346, f2360.
8. Pearce, M. S., Salotti, J. A., Little, M. P., *et al.* (2012) Radiation exposure from CT scans in childhood and subsequent risk of leukaemia and brain tumours: a retrospective cohort study. *Lancet*, 380, 499–505.

9. Zelefsky, M. J., Fuks, Z. and Leibel, S. A. (2002) Intensity-modulated radiation therapy for prostate cancer. *Semin. Radiat. Oncol.*, 12, 229–237.
10. de Arruda, F. F., Puri, D. R., Zhung, J., *et al.* (2006) Intensity-modulated radiation therapy for the treatment of oropharyngeal carcinoma: the Memorial Sloan-Kettering Cancer Center experience. *Int. J. Radiat. Oncol. Biol. Phys.*, 64, 363–373.
11. Chen, J., Morin, O., Aubin, M., Bucci, M. K., Chuang, C. F. and Pouliot, J. (2014) Dose-guided radiation therapy with megavoltage cone-beam CT. *Br. J. Radiol*, 79, 87–98.
12. Timmerman, R., Paulus, R., Galvin, J., *et al.* (2010) Stereotactic body radiation therapy for inoperable early stage lung cancer. *JAMA*, 303, 1070–1076.
13. Hogan, D. E. and Kellison, T. (2002) Nuclear terrorism. *Am. J. Med. Sci.*, 323, 341–349.
14. Stone, H. B., Moulder, J. E., Coleman, C. N., *et al.* (2004) Models for evaluating agents intended for the prophylaxis, mitigation and treatment of radiation injuries. Report of an NCI Workshop, December 3-4, 2003. *Radiat. Res.*, 162, 711–728.
15. Pellmar, T. C. and Rockwell, S.; Radiological/Nuclear Threat Countermeasures Working Group. (2005) Priority list of research areas for radiological nuclear threat countermeasures. *Radiat. Res.*, 163, 115–123.
16. Moulder, J. E. and Cohen, E. P. (2007) Future strategies for mitigation and treatment of chronic radiation-induced normal tissue injury. *Semin. Radiat. Oncol.*, 17, 141–148.
17. Kim, J. H., Brown, S. L., Kolozsvary, A., Jenrow, K. A., Ryu, S., Rosenblum, M. L. and Carretero, O. A. (2004) Modificatiossn of radiation injury by ramipril, inhibitor of angiotensin-converting enzyme, on optic neuropathy in the rat. *Radiat. Res.*, 161, 137–142.
18. Moulder, J. E., Fish, B. L. and Cohen, E. P. (2003) ACE inhibitors and AII receptor antagonists in the treatment and prevention of bone marrow transplant nephropathy. *Curr. Pharm. Des.*, 9, 737–749.
19. Kim, K., Damoiseaux, R., Norris, A. J., Rivina, L., Bradley, K., Jung, M. E., Gatti, R. A., Schiestl, R. H. and McBride, W. H. (2011) High throughput screening of small molecule libraries for modifiers of radiation responses. *Int. J. Radiat. Biol.*, 87, 839–845.
20. Rubin, P. (2008) *Late Effects of Cancer Treatment on Normal Tissues: CURED I, LENT*. Springer, Berlin.
21. Ryan, J. L., Krishnan, S., Movsas, B., Coleman, C. N., Vikram, B. and Yoo, S. S. (2011) Decreasing the adverse effects of cancer therapy: an NCI Workshop on the preclinical development of radiation injury mitigators/protectors. *Radiat. Res.*, 176, 688–691.
22. Williams, J. P., Brown, S. L., Georges, G. E., *et al.* (2010) Animal models for medical countermeasures to radiation exposure. *Radiat. Res.*, 173, 557–578.
23. Jackson, E. L., Willis, N., Mercer, K., Bronson, R. T., Crowley, D., Montoya, R., Jacks, T. and Tuveson, D. A. (2001) Analysis of lung tumor initiation and progression using conditional expression of oncogenic K-ras. *Genes Dev.*, 15, 3243–3248.
24. Frese, K. K. and Tuveson, D. A. (2007) Maximizing mouse cancer models. *Nat. Rev. Cancer*, 7, 645–658.
25. Chia, R., Achilli, F., Festing, M. F. and Fisher, E. M. (2005) The origins and uses of mouse outbred stocks. *Nat. Genet.*, 37, 1181–1186.
26. Cui, S., Chesson, C. and Hope, R. (1993) Genetic variation within and between strains of outbred Swiss mice. *Lab. Anim.*, 27, 116–123.
27. Papaioannou, V. E. and Festing, M. F. (1980) Genetic drift in a stock of laboratory mice. *Lab. Anim.*, 14, 11–13.
28. Felton, R. P. and Gaylor, D. W. (1989) Multistrain experiments for screening toxic substances. *J. Toxicol. Environ. Health*, 26, 399–411.
29. Wu, A. (1992) Physics and dosimetry of the gamma knife. *Neurosurg. Clin. N. Am.*, 3, 35–50.
30. Barcellos-Hoff, M. H. and Ravani, S. A. (2000) Irradiated mammary gland stroma promotes the expression of tumorigenic potential by unirradiated epithelial cells. *Cancer Res.*, 60, 1254–1260.
31. Little, J. B. (2000) Radiation carcinogenesis. *Carcinogenesis*, 21, 397–404.
32. Fry, R. J., Ley, R. D., Grube, D. and Staffeldt, E. (1982) Studies on the multistage nature of radiation carcinogenesis. *Carcinog. Compr. Surv.*, 7, 155–165.
33. Kumar, R., Sukumar, S. and Barbacid, M. (1990) Activation of ras oncogenes preceding the onset of neoplasia. *Science*, 248, 1101–1104.
34. Mori, H., Colman, S. M., Xiao, Z., Ford, A. M., Healy, L. E., Donaldson, C., Hows, J. M., Navarrete, C. and Greaves, M. (2002) Chromosome translocations and covert leukemic clones are generated during normal fetal development. *Proc. Natl. Acad. Sci. USA*, 99, 8242–8247.
35. March, H. C. (1944) Leukemia in radiologists. *Radiology*, 43, 275–278.
36. Krebs, C., Rask-Nielsen, H. C. and Wagner, A. (1930) The origin of Lymphosarcomatosis and its relation to other forms of Leucosis in white mice Lymphomatosis infiltrans leucemica et aleucemica. *Acta Radiologica*, 1–72.
37. Shore, R. E., Moseson, M., Harley, N. and Pasternack, B. S. (2003) Tumors and other diseases following childhood x-ray treatment for ringworm of the scalp (Tinea capitis). *Health Phys.*, 85, 404–408.
38. Hall, E. J. and Giaccia, A. J. (2006) *Radiobiology for the Radiologist*, 6th edn. Lippincott Williams & Wilkins, Philadelphia.
39. Little, M. P., Weiss, H. A., Boice, J. D. Jr, Darby, S. C., Day, N. E. and Muirhead, C. R. (1999) Risks of leukemia in Japanese atomic bomb survivors, in women treated for cervical cancer, and in patients treated for ankylosing spondylitis. *Radiat. Res.*, 152, 280–292.
40. Preston, D. L., Kusumi, S., Tomonaga, M., *et al.* (1994) Cancer incidence in atomic bomb survivors. Part III. Leukemia, lymphoma and multiple myeloma, 1950-1987. *Radiat. Res.*, 137, S68–S97.
41. Weiss, H. A., Darby, S. C. and Doll, R. (1994) Cancer mortality following X-ray treatment for ankylosing spondylitis. *Int. J. Cancer*, 59, 327–338.
42. Weiss, H. A., Darby, S. C., Fearn, T. and Doll, R. (1995) Leukemia mortality after X-ray treatment for ankylosing spondylitis. *Radiat. Res.*, 142, 1–11.
43. Boice, J. D. Jr, Engholm, G., Kleinerman, R. A., *et al.* (1988) Radiation dose and second cancer risk in patients treated for cancer of the cervix. *Radiat. Res.*, 116, 3–55.
44. Zablotska, L. B., Bazyka, D., Lubin, J. H., *et al.* (2013) Radiation and the risk of chronic lymphocytic and other leukemias among chornobyl cleanup workers. *Environ. Health Perspect.*, 121, 59–65.
45. Auvinen, A., Seppä, K., Pasanen, K., *et al.* (2014) Chernobyl fallout and cancer incidence in Finland. *Int. J. Cancer*, 134, 2253–2263.
46. Noshchenko, A. G., Bondar, O. Y. and Drozdova, V. D. (2010) Radiation-induced leukemia among children aged 0-5 years at the time of the Chernobyl accident. *Int. J. Cancer*, 127, 412–426.
47. Ivanov, V. K., Tsyb, A. F., Gorsky, A. I., Maksyutov, M. A., Rastopchin, E. M., Konogorov, A. P., Korelo, A. M., Biryukov, A. P. and Matyash, V. A. (1997) Leukaemia and thyroid cancer in emergency workers of the Chernobyl accident: estimation of radiation risks (1986-1995). *Radiat. Environ. Biophys.*, 36, 9–16.
48. Ivanov, V. K., Gorskiĭ, A. I., Tsyb, A. F. and Khaut, S. E. (2003) Incidence of post-Chernobyl leukemia and thyroid cancer in children and adolescents in the Briansk region: evaluation of radiation risks. *Vopr. Onkol.*, 49, 445–449.
49. Ivanov, V. K., Gorski, A. I., Maksioutov, M. A., Vlasov, O. K., Godko, A. M., Tsyb, A. F., Tirmarche, M., Valenty, M. and Verger, P. (2003) Thyroid cancer incidence among adolescents and adults in the Bryansk region of Russia following the Chernobyl accident. *Health Phys.*, 84, 46–60.
50. Preston, D. L., Pierce, D. A., Shimizu, Y., Cullings, H. M., Fujita, S., Funamoto, S. and Kodama, K. (2004) Effect of recent changes in atomic bomb survivor dosimetry on cancer mortality risk estimates. *Radiat. Res.*, 162, 377–389.
51. Little, M. P., Wakeford, R., Tawn, E. J., Bouffler, S. D. and Berrington de Gonzalez, A. (2009) Risks associated with low doses and low dose rates of ionizing radiation: why linearity may be (almost) the best we can do. *Radiology*, 251, 6–12.
52. Tomonaga, M. (1962) Leukaemia in Nagasaki atomic bomb survivors from 1945 through 1959. *Bull. World Health Organ.*, 26, 619–631.
53. Cardis, E., Gilbert, E. S., Carpenter, L., *et al.* (1995) Effects of low doses and low dose rates of external ionizing radiation: cancer mortality among nuclear industry workers in three countries. *Radiat. Res.*, 142, 117–132.
54. Richardson, D. B., Wing, S., Schroeder, J., Schmitz-Feuerhake, I. and Hoffmann, W. (2005) Ionizing radiation and chronic lymphocytic leukemia. *Environ. Health Perspect.*, 113, 1–5.

55. Little, M. P., Wakeford, R. and Kendall, G. M. (2009) Updated estimates of the proportion of childhood leukaemia incidence in Great Britain that may be caused by natural background ionising radiation. *J. Radiol. Prot*., 29, 467–482.
56. Curtis, R. E., Boice, J. D. Jr, Stovall, M., *et al.* (1994) Relationship of leukemia risk to radiation dose following cancer of the uterine corpus. *J. Natl. Cancer Inst*., 86, 1315–1324.
57. Upton, A. C., Wolff, F. F., Furth, J. and Kimball, A. W. (1958) A comparison of the induction of myeloid and lymphoid leukemias in x-radiated RF mice. *Cancer Res*., 18, 842–848.
58. Wolman, S. R., McMorrow, L. E. and Cohen, M. W. (1982) Animal model of human disease: myelogenous leukemia in the RF mouse. *Am. J. Pathol*., 107, 280–284.
59. Resnitzky, P., Estrov, Z. and Haran-Ghera, N. (1985) High incidence of acute myeloid leukemia in SJL/J mice after X-irradiation and corticosteroids. *Leuk. Res*., 9, 1519–1528.
60. Major, I. R. and Mole, R. H. (1978) Myeloid leukaemia in X-ray irradiated CBA mice. *Nature*, 272, 455–456.
61. Major, I. R. (1979) Induction of myeloid leukaemia by whole-body single exposure of CBA male mice to x-rays. *Br. J. Cancer*, 40, 903–913.
62. Seki, M., Yoshida, K., Nishimura, M. and Nemoto, K. (1991) Radiation-induced myeloid leukemia in C3H/He mice and the effect of prednisolone acetate on leukemogenesis. *Radiat. Res*., 127, 146–149.
63. Rivina, L., Davoren, M. and Schiestl, R. H. (2014) Radiation-induced myeloid leukemia in murine models. *Hum. Genomics*, 8, 13.
64. Upton, A. C., Jenkins, V. K. and Conklin, J. W. (1964) Myeloid leukemia in the mouse. *Ann. N. Y. Acad. Sci*., 114, 189–202.
65. Furth, J., Upton, A. C., Christenberry, K. W., Benedict, W. H. and Moshman, J. (1954) Some late effects in mice of ionizing radiation from an experimental nuclear detonation. *Radiology*, 63, 562–570.
66. Furth, J. (1946) Recent experimental studies on leukemia. *Physiol. Rev*., 26, 47–76.
67. Cole, R. K. and Furth, J. (1941) Experimental studies on the genetics of spontaneous leukamia in mice. *Cancer Res*., 1, 957–965.
68. Ullrich, R. L. and Preston, R. J. (1987) Myeloid leukemia in male RFM mice following irradiation with fission spectrum neutrons or gamma rays. *Radiat. Res*., 109, 165–170.
69. Upton, A. C., Buffett, R. F., Furth, J. and Doherty, D. G. (1958) Radiation-induced dental death in mice. *Radiat. Res*., 8, 475–479.
70. Hayata, I., Ishihara, T., Hirashima, K., Sado, T. and Yamagiwa, J. (1979) Partial deletion of chromosome No. 2 in myelocytic leukemias of irradiated C3H/He and RFM mice. *J. Natl. Cancer Inst*., 63, 843–848.
71. Azumi, J. I. and Sachs, L. (1977) Chromosome mapping of the genes that control differentiation and malignancy in myeloid leukemic cells. *Proc. Natl. Acad. Sci. U. S. A*., 74, 253–257.
72. Morgan, C. (1980) Hiroshima, Nagasaki and the RERF. *Am. J. Pathol*., 98, 843–856.
73. Smith, S. M., Le Beau, M. M., Huo, D., Karrison, T., Sobecks, R. M., Anastasi, J., Vardiman, J. W., Rowley, J. D. and Larson, R. A. (2003) Clinical-cytogenetic associations in 306 patients with therapy-related myelodysplasia and myeloid leukemia: the University of Chicago series. *Blood*, 102, 43–52.
74. Murphy, E. D. (1963) SJL/J, a new inbred strain of mouse with a high, early incedence of reticulum cell neoplasms. *Proc. Am. Assoc. Cancer Res*., 464.
75. Dunn, T. B. (1954) Normal and pathologic anatomy of the reticular tissue in laboratory mice, with a classification and discussion of neoplasms. *J. Natl. Cancer Inst*., 14, 1281–1433.
76. Haran-Ghera, N., Krautghamer, R., Lapidot, T., Peled, A., Dominguez, M. G. and Stanley, E. R. (1997) Increased circulating colony-stimulating factor-1 (CSF-1) in SJL/J mice with radiation-induced acute myeloid leukemia (AML) is associated with autocrine regulation of AML cells by CSF-1. *Blood*, 89, 2537–2545.
77. Haran-Ghera, N., Kotler, M. and Meshorer, A. (1967) Studies on leukemia development in the SJL/J strain of mice. *J. Natl. Cancer Inst*., 39, 653–661.
78. Haran-Ghera, N., Resnitzky, P., Krautghamer, R. and Tartakovsky, B. (1992) Multiphase process involved in radiation induced murine AML. *Leukemia*, 6, 123S–125S.
79. Haran-Ghera, N., Trakhtenbrot, L., Resnitzky, P. and Peled, A. (1989) Preleukemia in experimental leukemogenesis. *Haematol. Blood Transfus*., 32, 243–249.
80. Trakhtenbrot, L., Krauthgamer, R., Resnitzky, P. and Haran-Ghera, N. (1988) Deletion of chromosome 2 is an early event in the development of radiation-induced myeloid leukemia in SJL/J mice. *Leukemia*, 2, 545–550.
81. Tartakovsky, B., Goldstein, O., Krautghamer, R. and Haran-Ghera, N. (1993) Low doses of radiation induce systemic production of cytokines: possible contribution to leukemogenesis. *Int. J. Cancer*, 55, 269–274.
82. Cadman, E. C., Capizzi, R. L. and Bertino, J. R. (1977) Acute nonlymphocytic leukemia: a delayed complication of Hodgkin's disease therapy: analysis of 109 cases. *Cancer*, 40, 1280–1296.
83. Coleman, C. N., Williams, C. J., Flint, A., Glatstein, E. J., Rosenberg, S. A. and Kaplan, H. S. (1977) Hematologic neoplasia in patients treated for Hodgkin's disease. *N. Engl. J. Med*., 297, 1249–1252.
84. Pedersen-Bjergaard, J., Philip, P., Pedersen, N. T., Hou-Jensen, K., Svejgaard, A., Jensen, G. and Nissen, N. I. (1984) Acute nonlymphocytic leukemia, preleukemia, and acute myeloproliferative syndrome secondary to treatment of other malignant diseases. II. Bone marrow cytology, cytogenetics, results of HLA typing, response to antileukemic chemotherapy, and survival in a total series of 55 patients. *Cancer*, 54, 452–462.
85. Scholl, S. M., Bascou, C. H., Mosseri, V., *et al.* (1994) Circulating levels of colony-stimulating factor 1 as a prognostic indicator in 82 patients with epithelial ovarian cancer. *Br. J. Cancer*, 69, 342–346.
86. Hakala, A., Kacinski, B. M., Stanley, E. R., Kohorn, E. I., Puistola, U., Risteli, J., Risteli, L., Tomás, C. and Kauppila, A. (1995) Macrophage colony-stimulating factor 1, a clinically useful tumor marker in endometrial adenocarcinoma: comparison with CA 125 and the aminoterminal propeptide of type III procollagen. *Am. J. Obstet. Gynecol*., 173, 112–119.
87. Scholl, S. M., Lidereau, R., de la Rochefordière, A., Le-Nir, C. C., Mosseri, V., Noguès, C., Pouillart, P. and Stanley, F. R. (1996) Circulating levels of the macrophage colony stimulating factor CSF-1 in primary and metastatic breast cancer patients. A pilot study. *Breast Cancer Res. Treat*., 39, 275–283.
88. Toy, E. P., Chambers, J. T., Kacinski, B. M., Flick, M. B. and Chambers, S. K. (2001) The activated macrophage colony-stimulating factor (CSF-1) receptor as a predictor of poor outcome in advanced epithelial ovarian carcinoma. *Gynecol. Oncol*., 80, 194–200.
89. Festing, M. F. and Blackmore, D. K. (1971) Life span of specified-pathogen-free (MRC category 4) mice and rats. *Lab. Anim*., 5, 179–192.
90. Yoshida, K., Nemoto, K., Nishimura, M. and Seki, M. (1993) Exacerbating factors of radiation-induced myeloid leukemogenesis. *Leuk. Res*., 17, 437–440.
91. Yoshida, K., Inoue, T., Nojima, K., Hirabayashi, Y. and Sado, T. (1997) Calorie restriction reduces the incidence of myeloid leukemia induced by a single whole-body radiation in C3H/He mice. *Proc. Natl. Acad. Sci. USA*, 94, 2615–2619.
92. Yoshida, K., Hirabayashi, Y., Watanabe, F., Sado, T. and Inoue, T. (2006) Caloric restriction prevents radiation-induced myeloid leukemia in C3H/HeMs mice and inversely increases incidence of tumor-free death: implications in changes in number of hemopoietic progenitor cells. *Exp. Hematol*., 34, 274–283.
93. Hayata, I., Seki, M., Yoshida, K., Hirashima, K., Sado, T., Yamagiwa, J. and Ishihara, T. (1983) Chromosomal aberrations observed in 52 mouse myeloid leukemias. *Cancer Res*., 43, 367–373.
94. Ban, N., Kai, M. and Kusama, T. (1997) Chromosome aberrations in bone marrow cells of C3H/He mice at an early stage after whole-body irradiation. *J. Radiat. Res*., 38, 219–231.
95. Coupland, L. A., Jammu, V. and Pidcock, M. E. (2002) Partial deletion of chromosome 1 in a case of acute myelocytic leukemia. *Cancer Genet. Cytogenet*., 139, 60–62.
96. Finger, L. R., Kagan, J., Christopher, G., Kurtzberg, J., Hershfield, M. S., Nowell, P. C. and Croce, C. M. (1989) Involvement of the TCL5 gene on human chromosome 1 in T-cell leukemia and melanoma. *Proc. Natl. Acad. Sci. USA*, 86, 5039–5043.
97. Rithidech, K. N., Cronkite, E. P. and Bond, V. P. (1999) Advantages of the CBA mouse in leukemogenesis research. *Blood Cells Mol. Dis*., 25, 38–45.

98. Rithidech, K., Dunn, J. J., Bond, V. P., Gordon, C. R. and Cronkite, E. P. (1999) Characterization of genetic instability in radiation- and benzene-induced murine acute leukemia. *Mutat. Res*., 428, 33–39.
99. Mole, R. H. and Major, I. R. (1983) Myeloid leukaemia frequency after protracted exposure to ionizing radiation: experimental confirmation of the flat dose-response found in ankylosing spondylitis after a single treatment course with X-rays. *Leuk. Res*., 7, 295–300.
100. Smith, I. E., Powles, R., Clink, H. M., Jameson, B., Kay, H. E. and McElwain, T. J. (1977) Early deaths in acute myelogenous leukemia. *Cancer*, 39, 1710–1714.
101. Rithidech, K. N., Bond, V. P., Cronkite, E. P. and Thompson, M. H. (1993) A specific chromosomal deletion in murine leukemic cells induced by radiation with different qualities. *Exp. Hematol*., 21, 427–431.
102. Rithidech, K., Dunn, J. J., Roe, B. A., Gordon, C. R. and Cronkite, E. P. (2002) Evidence for two commonly deleted regions on mouse chromosome 2 in gamma ray-induced acute myeloid leukemic cells. *Exp. Hematol*., 30, 564–570.
103. Rithidech, K., Bond, V. P., Cronkite, E. P., Thompson, M. H. and Bullis, J. E. (1995) Hypermutability of mouse chromosome 2 during the development of x-ray-induced murine myeloid leukemia. *Proc. Natl. Acad. Sci. USA*, 92, 1152–1156.
104. Bouffler, S. D., Meijne, E. I., Morris, D. J. and Papworth, D. (1997) Chromosome 2 hypersensitivity and clonal development in murine radiation acute myeloid leukaemia. *Int. J. Radiat. Biol*., 72, 181–189.
105. Cleary, H., Boulton, E. and Plumb, M. (2001) Allelic loss on chromosome 4 (Lyr2/TLSR5) is associated with myeloid, B-lympho-myeloid, and lymphoid (B and T) mouse radiation-induced leukemias. *Blood*, 98, 1549–1554.
106. Giotopoulos, G., McCormick, C., Cole, C., Zanker, A., Jawad, M., Brown, R. and Plumb, M. (2006) DNA methylation during mouse hemopoietic differentiation and radiation-induced leukemia. *Exp. Hematol*., 34, 1462–1470.
107. Jawad, M., Giotopoulos, G., Fitch, S., Cole, C., Plumb, M. and Talbot, C. J. (2007) Mouse bone marrow and peripheral blood erythroid cell counts are regulated by different autosomal genetic loci. *Blood Cells. Mol. Dis*., 38, 69–77.
108. Dekkers, F., Bijwaard, H., Bouffler, S., Ellender, M., Huiskamp, R., Kowalczuk, C., Meijne, E. and Sutmuller, M. (2011) A two-mutation model of radiation-induced acute myeloid leukemia using historical mouse data. *Radiat. Environ. Biophys*., 50, 37–45.
109. Graves, J. A. (1996) Mammals that break the rules: genetics of marsupials and monotremes. *Annu. Rev. Genet*., 30, 233–260.
110. Carver, E. A. and Stubbs, L. (1997) Zooming in on the human-mouse comparative map: genome conservation re-examined on a high-resolution scale. *Genome Res*., 7, 1123–1137.
111. Talpaz, M., Shah, N. P., Kantarjian, H., *et al.* (2006) Dasatinib in imatinib-resistant Philadelphia chromosome-positive leukemias. *N. Engl. J. Med*., 354, 2531–2541.
112. Alexander, B. J., Rasko, J. E., Morahan, G. and Cook, W. D. (1995) Gene deletion explains both in vivo and in vitro generated chromosome 2 aberrations associated with murine myeloid leukemia. *Leukemia*, 9, 2009–2015.
113. Silver, A., Moody, J., Dunford, R., *et al.* (1999) Molecular mapping of chromosome 2 deletions in murine radiation-induced AML localizes a putative tumor suppressor gene to a 1.0 cM region homologous to human chromosome segment 11p11-12. *Genes Chromosomes Cancer*, 24, 95–104.
114. Cook, W. D., McCaw, B. J., Herring, C., John, D. L., Foote, S. J., Nutt, S. L. and Adams, J. M. (2004) PU.1 is a suppressor of myeloid leukemia, inactivated in mice by gene deletion and mutation of its DNA binding domain. *Blood*, 104, 3437–3444.
115. Moreau-Gachelin, F., Tavitian, A. and Tambourin, P. (1988) Spi-1 is a putative oncogene in virally induced murine erythroleukaemias. *Nature*, 331, 277–280.
116. Scott, E. W., Simon, M. C., Anastasi, J. and Singh, H. (1994) Requirement of transcription factor PU.1 in the development of multiple hematopoietic lineages. *Science*, 265, 1573–1577.
117. Simon, M. C., Olson, M., Scott, E., Hack, A., Su, G. and Singh, H. (1996) Terminal myeloid gene expression and differentiation requires the transcription factor PU.1. *Curr. Top. Microbiol. Immunol*., 211, 113–119.
118. McKercher, S. R., Torbett, B. E., Anderson, K. L., *et al.* (1996) Targeted disruption of the PU.1 gene results in multiple hematopoietic abnormalities. *EMBO J*., 15, 5647–5658.
119. Kastner, P. and Chan, S. (2008) PU.1: a crucial and versatile player in hematopoiesis and leukemia. *Int. J. Biochem. Cell Biol*., 40, 22–27.
120. Joo, M., Park, G. Y., Wright, J. G., Blackwell, T. S., Atchison, M. L. and Christman, J. W. (2004) Transcriptional regulation of the cyclooxygenase-2 gene in macrophages by PU.1. *J. Biol. Chem*., 279, 6658–6665.
121. Owen, J.A., Punt, J., Stranford, S. A., and Jones, P. P. (2013) *Kuby Immunology*. WH Freeman, New York.
122. Scott, E. W., Simon, M. C., Anastasi, J. and Singh, H. (1994) Requirement of transcription factor PU.1 in the development of multiple hematopoietic lineages. *Science*, 265, 1573–1577.
123. Suraweera, N., Meijne, E., Moody, J., *et al.* (2005) Mutations of the PU.1 Ets domain are specifically associated with murine radiation-induced, but not human therapy-related, acute myeloid leukaemia. *Oncogene*, 24, 3678–3683.
124. Mueller, B. U., Pabst, T., Osato, M., *et al.* (2002) Heterozygous PU.1 mutations are associated with acute myeloid leukemia. *Blood*, 100, 998–1007.
125. Rosenbauer, F., Wagner, K., Kutok, J. L., Iwasaki, H., Le Beau, M. M., Okuno, Y., Akashi, K., Fiering, S. and Tenen, D. G. (2004) Acute myeloid leukemia induced by graded reduction of a lineage-specific transcription factor, PU.1. *Nat. Genet*., 36, 624–630.
126. Metcalf, D., Dakic, A., Mifsud, S., Di Rago, L., Wu, L. and Nutt, S. (2006) Inactivation of PU.1 in adult mice leads to the development of myeloid leukemia. *Proc. Natl. Acad. Sci. U. S. A*., 103, 1486–1491.
127. Walter, M. J., Park, J. S., Ries, R. E., Lau, S. K., McLellan, M., Jaeger, S., Wilson, R. K., Mardis, E. R. and Ley, T. J. (2005) Reduced PU.1 expression causes myeloid progenitor expansion and increased leukemia penetrance in mice expressing PML-RARalpha. *Proc. Natl. Acad. Sci. USA*, 102, 12513–12518.
128. Hirouchi, T., Takabatake, T., Yoshida, K., Nitta, Y., Nakamura, M., Tanaka, S., Ichinohe, K., Oghiso, Y. and Tanaka, K. (2008) Upregulation of c-myc gene accompanied by PU.1 deficiency in radiation-induced acute myeloid leukemia in mice. *Exp. Hematol*., 36, 871–885.
129. Peng, Y., Brown, N., Finnon, R., *et al.* (2009) Radiation leukemogenesis in mice: loss of PU.1 on chromosome 2 in CBA and C57BL/6 mice after irradiation with 1 GeV/nucleon 56Fe ions, X rays or gamma rays. Part I. Experimental observations. *Radiat. Res*., 171, 474–483.
130. Moreau-Gachelin, F., Wendling, F., Molina, T., Denis, N., Titeux, M., Grimber, G., Briand, P., Vainchenker, W. and Tavitian, A. (1996) Spi-1/PU.1 transgenic mice develop multistep erythroleukemias. *Mol. Cell. Biol*., 16, 2453–2463.
131. Steidl, U., Rosenbauer, F., Verhaak, R. G., *et al.* (2006) Essential role of Jun family transcription factors in PU.1 knockdown-induced leukemic stem cells. *Nat. Genet*., 38, 1269–1277.
132. Fernando, T. R., Rodriguez-Malave, N. I. and Rao, D. S. (2012) MicroRNAs in B cell development and malignancy. *J. Hematol. Oncol*., 5, 7.
133. Finnon, R., Brown, N., Moody, J., *et al.* (2012) Flt3-ITD mutations in a mouse model of radiation-induced acute myeloid leukaemia. *Leukemia*, 26, 1445–1446.
134. Plumb, M., Cleary, H. and Wright, E. (1998) Genetic instability in radiation-induced leukaemias: mouse models. *Int. J. Radiat. Biol*., 74, 711–720.
135. Boulton, E., Cleary, H., Papworth, D. and Plumb, M. (2001) Susceptibility to radiation-induced leukaemia/lymphoma is genetically separable from sensitivity to radiation-induced genomic instability. *Int. J. Radiat. Biol*., 77, 21–29.
136. Morgan, W. F. (2003) Is there a common mechanism underlying genomic instability, bystander effects and other nontargeted effects of exposure to ionizing radiation? *Oncogene*, 22, 7094–7099.
137. Busuttil, R. A., Rubio, M., Dollé, M. E., Campisi, J. and Vijg, J. (2003) Oxygen accelerates the accumulation of mutations during the senescence and immortalization of murine cells in culture. *Aging Cell*, 2, 287–294.

138. Ban, N. and Kai, M. (2009) Implication of replicative stress-related stem cell ageing in radiation-induced murine leukaemia. *Br. J. Cancer*, 101, 363–371.
139. Hirouchi, T., Akabane, M., Tanaka, S., Braga-Tanaka, I. 3rd, Todate, A., Ichinohe, K., Oghiso, Y. and Tanaka, K. (2011) Cell surface marker phenotypes and gene expression profiles of murine radiation-induced acute myeloid leukemia stem cells are similar to those of common myeloid progenitors. *Radiat. Res*., 176, 311–322.
140. Darakhshan, F., Badie, C., Moody, J., *et al.* (2006) Evidence for complex multigenic inheritance of radiation AML susceptibility in mice revealed using a surrogate phenotypic assay. *Carcinogenesis*, 27, 311–318.
141. Schottenfeld, D., and Fraumeni, J.F. (2006) *Cancer Epidemiology and Prevention*, 3rd edn. Oxford University Press, Oxford.
142. Hartge, P. and Smith, M. T. (2007) Environmental and behavioral factors and the risk of non-Hodgkin lymphoma. *Cancer Epidemiol. Biomarkers Prev*., 16, 367–368.
143. Boice, J. D. Jr. (1992) Radiation and non-Hodgkin's lymphoma. *Cancer Res*., 52, 5489s–5491s.
144. United Nations. Scientific Committee on the Effects of Atomic Radiation. (2000) *Sources and effects of ionizing radiation: United Nations Scientific Committee on the Effects of Atomic Radiation: UNSCEAR 2000 report to the General Assembly, with scientific annexes*. United Nations, New York.
145. Adami, H. -O., Hunter, D. J., and Trichopoulos, D. (2002) *Textbook of cancer epidemiology*. Oxford University Press, Oxford.
146. Richardson, D. B., Sugiyama, H., Wing, S., *et al.* (2009) Positive associations between ionizing radiation and lymphoma mortality among men. *Am. J. Epidemiol*., 169, 969–976.
147. Waalkes, M. P. and Ward, J. M. (1994) *Carcinogenesis*. Raven Press, New York.
148. Okumoto, M., Nishikawa, R., Imai, S. and Hilgers, J. (1990) Genetic analysis of resistance to radiation lymphomagenesis with recombinant inbred strains of mice. *Cancer Res*., 50, 3848–3850.
149. Pattengale, P. K. and Taylor, C. R. (1983) Experimental models of lymphoproliferative disease. The mouse as a model for human non-Hodgkin's lymphomas and related leukemias. *Am. J. Pathol*., 113, 237–265.
150. Pattengale, P. K. and Frith, C. H. (1983) Immunomorphologic classification of spontaneous lymphoid cell neoplasms occurring in female BALB/c mice. *J. Natl. Cancer Inst*., 70, 169–179.
151. Pattengale, P., Leder, A., Kuo, A., Stewart, T. and Leder, P. (1986) Lymphohematopoietic and other malignant neoplasms occurring spontaneously in transgenic mice carrying and expressing MTV/myc fusion genes. *Curr. Top. Microbiol. Immunol*., 132, 9–16.
152. Kaplan, H. S., Brown, M. B. and Paull, J. (1953) Influence of postirradiation thymectomy and of thymic implants on lymphoid tumor incidence in C57BL mice. *Cancer Res*., 13, 677–680.
153. Okumoto, M., Nishikawa, R., Imai, S. and Hilgers, J. (1989) Resistance of STS/A mice to lymphoma induction by X-irradiation. *J. Radiat. Res*., 30, 135–139.
154. Meier, H., Myers, D. D. and Huebner, R. J. (1970) Differential effect of a synthetic polyribonucleotide complex on spontaneous and transplanted leukemia in mice. *Life Sci. II*., 9, 653–659.
155. Sacher, G. A. and Brues A. M. (1949) Analysis of lymphoma induction by X rays in mice. *Cancer Res*., 1.
156. Muto, M., Sado, T., Hayata, I., Nagasawa, F., Kamisaku, H. and Kubo, E. (1983) Reconfirmation of indirect induction of radiogenic lymphomas using thymectomized, irradiated B10 mice grafted with neonatal thymuses from Thy 1 congenic donors. *Cancer Res*., 43, 3822–3827.
157. Boniver, J., Humblet, C., Rongy, A. M., Delvenne, C., Delvenne, P., Greimers, R., Thiry, A., Courtoy, R. and Defresne, M. P. (1990) Cellular aspects of the pathogenesis of radiation–induced thymic lymphomas in C57 BL mice (review). *In Vivo*, 4, 41–43.
158. Humblet, C., Greimers, R., Boniver, J. and Defrense, M. P. (1997) Stages in the development of radiation-induced thymic lymphomas in C57 BL/Ka mice: preleukemic cells become progressively resistant to the tumor preventing effects of a bone marrow graft. *Exp. Hematol*., 25, 109–113.
159. Kaplan, H. S. (1952) Radiation-induced lymphoid tumors of mice. *Acta Unio Int. Contra Cancrum*, 7, 849–859.
160. Reichert, W., Buselmaier, W. and Vogel, F. (1984) Elimination of X-ray-induced chromosomal aberrations in the progeny of female mice. *Mutat. Res*., 139, 87–94.
161. Newcomb, E. W., Steinberg, J. J. and Pellicer, A. (1988) ras oncogenes and phenotypic staging in N-methylnitrosourea- and gamma-irradiation-induced thymic lymphomas in C57BL/6J mice. *Cancer Res*., 48, 5514–5521.
162. Amari, N. M. and Meruelo, D. (1987) Murine thymomas induced by fractionated-X-irradiation have specific T-cell receptor rearrangements and characteristics associated with day-15 to -16 fetal thymocytes. *Mol. Cell. Biol*., 7, 4159–4168.
163. Hogarth, P. M., Henning, M. M. and McKenzie, I. F. (1982) Alloantigenic phenotype of radiation-induced thymomas in the mouse. *J. Natl. Cancer Inst*., 69, 619–626.
164. Hogarth, P. M., Edwards, J., McKenzie, I. F., Goding, J. W. and Liew, F. Y. (1982) Monoclonal antibodies to the murine Ly-2.1 cell surface antigen. *Immunology*, 46, 135–144.
165. McMorrow, L. E., Newcomb, E. W. and Pellicer, A. (1988) Identification of a specific marker chromosome early in tumor development in gammairradiated C57BL/6J mice. *Leukemia*, 2, 115–119.
166. Takabatake, T., Kakinuma, S., Hirouchi, T., Nakamura, M. M., Fujikawa, K., Nishimura, M., Oghiso, Y., Shimada, Y. and Tanaka, K. (2008) Analysis of changes in DNA copy number in radiation-induced thymic lymphomas of susceptible C57BL/6, resistant C3H and hybrid F1 Mice. *Radiat. Res*., 169, 426–436.
167. Sasaki, M. (1982) Current status of cytogenetic studies in animal tumors with special reference to nonrandom chromosome changes. *Cancer Genet. Cytogenet*., 5, 153–172.
168. Brathwaite, O., Bayona, W. and Newcomb, E. W. (1992) p53 mutations in C57BL/6J murine thymic lymphomas induced by gamma-irradiation and N-methylnitrosourea. *Cancer Res*., 52, 3791–3795.
169. Tomita, N. (2011) BCL2 and MYC dual-hit lymphoma/leukemia. *J. Clin. Exp. Hematopathol*., 51, 7–12.
170. Newcomb, E. W., Corominas, M., Bayona, W. and Pellicer, A. (1989) Multistage carcinogenesis in murine thymocytes: involvement of oncogenes, chromosomal imbalances and T cell growth factor receptor. *Anticancer Res*., 9, 1407–1415.
171. Mao, J. H., Wu, D., Perez-Losada, J., Nagase, H., DelRosario, R. and Balmain, A. (2003) Genetic interactions between Pten and p53 in radiation-induced lymphoma development. *Oncogene*, 22, 8379–8385.
172. Potter, M. (1985) History of the BALB/c family. In The BALB/c Mouse. Springer Berlin, Heidelberg, pp. 1–5.
173. Okayasu, R., Suetomi, K., Yu, Y., Silver, A., Bedford, J. S., Cox, R. and Ullrich, R. L. (2000) A deficiency in DNA repair and DNA-PKcs expression in the radiosensitive BALB/c mouse. *Cancer Res*., 60, 4342–4345.
174. Liu, C., Li, B., Cheng, Y., *et al.* (2011) MiR-21 plays an important role in radiation induced carcinogenesis in BALB/c mice by directly targeting the tumor suppressor gene Big-h3. *Int. J. Biol. Sci*., 7, 347–363.
175. Lewis, B. P., Shih, I. H., Jones-Rhoades, M. W., Bartel, D. P. and Burge, C. B. (2003) Prediction of mammalian microRNA targets. *Cell*, 115, 787–798.
176. Okumoto, M., Nishikawa, R., Takamori, Y., Iwai, Y., Iwai, M. and Tsubura, Y. (1985) Endogenous type-C viral expression during lymphoma development in irradiated NFS mice. *Radiat. Res*., 104, 153–165.
177. Mori, N. and Takamori, Y. (1990) Development of nonthymic lymphomas in thymectomized NFS mice exposed to split-dose X-irradiation. *J. Radiat. Res*., 31, 389–395.
178. Saito, Y., Ochiai, Y., Kodama, Y., *et al.* (2001) Genetic loci controlling susceptibility to gamma-ray-induced thymic lymphoma. *Oncogene*, 20, 5243–5247.
179. Santos, J., Pérez de Castro, I., Herranz, M., Pellicer, A. and Fernández-Piqueras, J. (1996) Allelic losses on chromosome 4 suggest the existence of a candidate tumor suppressor gene region of about 0.6 cM in gamma-radiation-induced mouse primary thymic lymphomas. *Oncogene*, 12, 669–676.

180. Cleary, H. J., Boulton, E. and Plumb, M. (1999) Allelic loss and promoter hypermethylation of the p15INK4b gene features in mouse radiation-induced lymphoid - but not myeloid - leukaemias. *Leukemia*, 13, 2049–2052.
181. Cleary, H. J., Wright, E. and Plumb, M. (1999) Specificity of loss of heterozygosity in radiation-induced mouse myeloid and lymphoid leukaemias. *Int. J. Radiat. Biol.*, 75, 1223–1230.
182. Okano, H., Saito, Y., Miyazawa, T., *et al.* (1999) Homozygous deletions and point mutations of the Ikaros gene in gamma-ray-induced mouse thymic lymphomas. *Oncogene*, 18, 6677–6683.
183. Shimada, Y., Nishimura, M., Kakinuma, S., Okumoto, M., Shiroishi, T., Clifton, K. H. and Wakana, S. (2000) Radiation-associated loss of heterozygosity at the Znfn1a1 (Ikaros) locus on chromosome 11 in murine thymic lymphomas. *Radiat. Res.*, 154, 293–300.
184. Shinbo, T., Matsuki, A., Matsumoto, Y., Kosugi, S., Takahashi, Y., Niwa, O. and Kominami, R. (1999) Allelic loss mapping and physical delineation of a region harboring a putative thymic lymphoma suppressor gene on mouse chromosome 12. *Oncogene*, 18, 4131–4136.
185. Herranz, M., Santos, J., Salido, E., Fernández-Piqueras, J. and Serrano, M. (1999) Mouse p73 gene maps to the distal part of chromosome 4 and might be involved in the progression of gamma-radiation-induced T-cell lymphomas. *Cancer Res.*, 59, 2068–2071.
186. Meléndez, B., Malumbres, M., Pérez de Castro, I., Santos, J., Pellicer, A. and Fernández-Piqueras, J. (2000) Characterization of the murine p19(ARF) promoter CpG island and its methylation pattern in primary lymphomas. *Carcinogenesis*, 21, 817–821.
187. Malumbres, M., Pérez de Castro, I., Santos, J., Fernández Piqueras, J. and Pellicer, A. (1999) Hypermethylation of the cell cycle inhibitor p15INK4b 3'-untranslated region interferes with its transcriptional regulation in primary lymphomas. *Oncogene*, 18, 385–396.
188. Pear, W. S., Aster, J. C., Scott, M. L., Hasserjian, R. P., Soffer, B., Sklar, J. and Baltimore, D. (1996) Exclusive development of T cell neoplasms in mice transplanted with bone marrow expressing activated Notch alleles. *J. Exp. Med.*, 183, 2283–2291.
189. López-Nieva, P., Santos, J. and Fernández-Piqueras, J. (2004) Defective expression of Notch1 and Notch2 in connection to alterations of c-Myc and Ikaros in gamma-radiation-induced mouse thymic lymphomas. *Carcinogenesis*, 25, 1299–1304.
190. Piskorowska, J., Gajewska, M., Szymańska, H., *et al.* (2011) Susceptibility loci and chromosomal abnormalities in radiation induced hematopoietic neoplasms in mice. *J. Radiat. Res.*, 52, 147–158.
191. Davila, M., Foster, S., Kelsoe, G. and Yang, K. (2001) A role for secondary V(D)J recombination in oncogenic chromosomal translocations? *Adv. Cancer Res.*, 81, 61–92.
192. Marculescu, R., Le, T., Böcskör, S., Mitterbauer, G., Chott, A., Mannhalter, C., Jaeger, U. and Nadel, B. (2002) Alternative end-joining in follicular lymphomas' t(14;18) translocation. *Leukemia*, 16, 120–126.
193. Marculescu, R., Le, T., Simon, P., Jaeger, U. and Nadel, B. (2002) V(D)J-mediated translocations in lymphoid neoplasms: a functional assessment of genomic instability by cryptic sites. *J. Exp. Med.*, 195, 85–98.
194. Kominami, R. and Niwa, O. (2006) Radiation carcinogenesis in mouse thymic lymphomas. *Cancer Sci.*, 97, 575–581.
195. Kaplan, H. S. (1964) The role of radiation on experimental leukemogenesis. *Natl. Cancer Inst. Monogr.*, 14, 207–220.
196. Sado, T., Kamisaku, H. and Kubo, E. (1991) Bone marrow-thymus interactions during thymic lymphomagenesis induced by fractionated radiation exposure in B10 mice: analysis using bone marrow transplantation between Thy 1 congenic mice. *J. Radiat. Res.*, 32, 168–180.
197. Boniver, J., Humblet, C., Rongy, A. M., Delvenne, C., Delvenne, P., Greimers, R., Thiry, A., Courtoy, R. and Defresne, M. P. (1990) Cellular events in radiation-induced lymphomagenesis. *Int. J. Radiat. Biol.*, 57, 693–698.
198. Kaplan, H. S., Hirsch, B. B. and Brown, M. B. (1956) Indirect induction of lymphomas in irradiated mice. IV. Genetic evidence of the origin of the tumor cells from the thymic grafts. *Cancer Res.*, 16, 434–436.
199. Kaplan, H. S., Carnes, W. H., Brown, M. B. and Hirsch, B. B. (1956) Indirect induction of lymphomas in irradiated mice. I. Tumor incidence and morphology in mice bearing nonirradiated thymic grafts. *Cancer Res.*, 16, 422–425.
200. Kaplan, H. S., Brown, M. B., Hirsch, B. B. and Carnes, W. H. (1956) Indirect induction of lymphomas in irradiated mice. II. Factor of irradiation of the host. *Cancer Res.*, 16, 426–428.
201. Muto, M., Kubo, E. and Sado, T. (1987) Development of prelymphoma cells committed to thymic lymphomas during radiation-induced thymic lymphomagenesis in B10 mice. *Cancer Res.*, 47, 3469–3472.
202. Michalak, E. M., Vandenberg, C. J., Delbridge, A. R., Wu, L., Scott, C. L., Adams, J. M. and Strasser, A. (2010) Apoptosis-promoted tumorigenesis: gamma-irradiation-induced thymic lymphomagenesis requires Puma-driven leukocyte death. *Genes Dev.*, 24, 1608–1613.
203. Labi, V., Erlacher, M., Krumschnabel, G., Manzl, C., Tzankov, A., Pinon, J., Egle, A. and Villunger, A. (2010) Apoptosis of leukocytes triggered by acute DNA damage promotes lymphoma formation. *Genes Dev.*, 24, 1602–1607.
204. Mori, N., Matsumoto, Y., Okumoto, M., Suzuki, N. and Yamate, J. (2001) Variations in Prkdc encoding the catalytic subunit of DNA-dependent protein kinase (DNA-PKcs) and susceptibility to radiation-induced apoptosis and lymphomagenesis. *Oncogene*, 20, 3609–3619.
205. Redpath, J. L. and Gutierrez, M. (2001) Kinetics of induction of reactive oxygen species during the post-irradiation expression of neoplastic transformation in vitro. *Int. J. Radiat. Biol.*, 77, 1081–1085.
206. Tamura, Y., Maruyama, M., Mishima, Y., *et al.* (2005) Predisposition to mouse thymic lymphomas in response to ionizing radiation depends on variant alleles encoding metal-responsive transcription factor-1 (Mtf-1). *Oncogene*, 24, 399–406.
207. Maruyama, M., Yamamoto, T., Kohara, Y., Katsuragi, Y., Mishima, Y., Aoyagi, Y. and Kominami, R. (2007) Mtf-1 lymphoma-susceptibility locus affects retention of large thymocytes with high ROS levels in mice after gamma-irradiation. *Biochem. Biophys. Res. Commun.*, 354, 209–215.
208. Lichtlen, P., Wang, Y., Belser, T., Georgiev, O., Certa, U., Sack, R. and Schaffner, W. (2001) Target gene search for the metal-responsive transcription factor MTF-1. *Nucleic Acids Res.*, 29, 1514–1523.
209. Sun, L., Goodman, P. A., Wood, C. M., *et al.* (1999) Expression of aberrantly spliced oncogenic ikaros isoforms in childhood acute lymphoblastic leukemia. *J. Clin. Oncol.*, 17, 3753–3766.
210. Sun, L., Crotty, M. L., Sensel, M., *et al.* (1999) Expression of dominant-negative Ikaros isoforms in T-cell acute lymphoblastic leukemia. *Clin. Cancer Res.*, 5, 2112–2120.
211. Ruiz, A., Jiang, J., Kempski, H. and Brady, H. J. (2004) Overexpression of the Ikaros 6 isoform is restricted to t(4;11) acute lymphoblastic leukaemia in children and infants and has a role in B-cell survival. *Br. J. Haematol.*, 125, 31–37.
212. Mullighan, C. G., Miller, C. B., Radtke, I., *et al.* (2008) BCR-ABL1 lymphoblastic leukaemia is characterized by the deletion of Ikaros. *Nature*, 453, 110–114.
213. Tsuji, H., Ishii-Ohba, H., Katsube, T., Ukai, H., Aizawa, S., Doi, M., Hioki, K. and Ogiu, T. (2004) Involvement of illegitimate V(D)J recombination or microhomology-mediated nonhomologous end-joining in the formation of intragenic deletions of the Notch1 gene in mouse thymic lymphomas. *Cancer Res.*, 64, 8882–8890.
214. Weng, A. P., Ferrando, A. A., Lee, W., Morris, J. P. 4th, Silverman, L. B., Sanchez-Irizarry, C., Blacklow, S. C., Look, A. T. and Aster, J. C. (2004) Activating mutations of NOTCH1 in human T cell acute lymphoblastic leukemia. *Science*, 306, 269–271.
215. Zuurbier, L., Petricoin, E. F. 3rd, Vuerhard, M. J., *et al.* (2012) The significance of PTEN and AKT aberrations in pediatric T-cell acute lymphoblastic leukemia. *Haematologica*, 97, 1405–1413.
216. Mulligan, C. S., Best, O. G. and Mulligan, S. P.; Chronic Lymphocytic Leukaemia Australian Research Consortium. (2009) The precursor of chronic lymphocytic leukemia. *N. Engl. J. Med.*, 360, 2575.
217. Okuda, T., Shurtleff, S. A., Valentine, M. B., *et al.* (1995) Frequent deletion of p16INK4a/MTS1 and p15INK4b/MTS2 in pediatric acute lymphoblastic leukemia. *Blood*, 85, 2321–2330.
218. López-Nieva, P., Vaquero, C., Fernández-Navarro, P., González-Sánchez, L., Villa-Morales, M., Santos, J., Esteller, M. and Fernández-Piqueras, J.

(2012) EPHA7, a new target gene for 6q deletion in T-cell lymphoblastic lymphomas. *Carcinogenesis*, 33, 452–458.
219. Carbone, D. (1992) Smoking and cancer. *Am. J. Med.*, 93, 13S–17S.
220. Coggle, J. E., Lambert, B. E. and Moores, S. R. (1986) Radiation effects in the lung. *Environ. Health Perspect.*, 70, 261–291.
221. Griem, M. L., Kleinerman, R. A., Boice, J. D. Jr, Stovall, M., Shefner, D. and Lubin, J. H. (1994) Cancer following radiotherapy for peptic ulcer. *J. Natl. Cancer Inst.*, 86, 842–849.
222. Darby, S. C., Doll, R., Gill, S. K. and Smith, P. G. (1987) Long term mortality after a single treatment course with X-rays in patients treated for ankylosing spondylitis. *Br. J. Cancer*, 55, 179–190.
223. Preston, D. L., Ron, E., Tokuoka, S., Funamoto, S., Nishi, N., Soda, M., Mabuchi, K. and Kodama, K. (2007) Solid cancer incidence in atomic bomb survivors: 1958-1998. *Radiat. Res.*, 168, 1–64.
224. Egawa, H., Furukawa, K., Preston, D., *et al.* (2012) Radiation and smoking effects on lung cancer incidence by histological types among atomic bomb survivors. *Radiat. Res.*, 178, 191–201.
225. Travis, L. B. (2002) Therapy-associated solid tumors. *Acta Oncol.*, 41, 323–333.
226. Travis, L. B., Gospodarowicz, M., Curtis, R. E., *et al.* (2002) Lung cancer following chemotherapy and radiotherapy for Hodgkin's disease. *J. Natl. Cancer Inst.*, 94, 182–192.
227. Travis, L. B., Curtis, R. E. and Boice, J. D. Jr. (1996) Late effects of treatment for childhood Hodgkin's disease. *N. Engl. J. Med.*, 335, 352–353.
228. Prochazka, M., Granath, F., Ekbom, A., Shields, P. G. and Hall, P. (2002) Lung cancer risks in women with previous breast cancer. *Eur. J. Cancer*, 38, 1520–1525.
229. Kirova, Y. M., Gambotti, L., De Rycke, Y., Vilcoq, J. R., Asselain, B. and Fourquet, A. (2007) Risk of second malignancies after adjuvant radiotherapy for breast cancer: a large-scale, single-institution review. *Int. J. Radiat. Oncol. Biol. Phys.*, 68, 359–363.
230. Roychoudhuri, R., Evans, H., Robinson, D. and Møller, H. (2004) Radiation-induced malignancies following radiotherapy for breast cancer. *Br. J. Cancer*, 91, 868–872.
231. Endoh, D., Suzuki, A., Kuwabara, M., Satoh, H. and Sato, F. (1987) Circadian variation in lung tumor induction with X-rays in mice. *J. Radiat. Res.*, 28, 186–189.
232. Hashimoto, N., Endoh, D., Kuwabara, M., Satoh, H. and Sato, F. (1994) Induction of lung tumors in C3H strain mice after single or fractionated irradiation with X-rays. *J. Vet. Med. Sci.*, 56, 493–498.
233. Hashimoto, N., Endoh, D., Kuwabara, M., Satoh, H. and Sato, F. (1990) Dose and dose-splitting effects of X-rays on lung tumour induction in mice. *Int. J. Radiat. Biol.*, 58, 351–360.
234. Focan, C. (2002) Chronobiological concepts underlying the chronotherapy of human lung cancer. *Chronobiol. Int.*, 19, 253–273.
235. Yuhas, J. M. and Walker, A. E. (1973) Exposure-response curve for radiation-induced lung tumors in the mouse. *Radiat. Res.*, 54, 261–273.
236. Ullrich, R. L., Jernigan, M. C. and Adams, L. M. (1979) Induction of lung tumors in RFM mice after localized exposures to X rays or neutrons. *Radiat. Res.*, 80, 464–473.
237. Ullrich, R. L. (1983) Tumor induction in BALB/c female mice after fission neutron or gamma irradiation. *Radiat. Res.*, 93, 506–515.
238. Ullrich, R. L., Jernigan, M. C., Satterfield, L. C. and Bowles, N. D. (1987) Radiation carcinogenesis: time-dose relationships. *Radiat. Res.*, 111, 179–184.
239. Coggle, J. E. (1991) The role of animal models in radiation lung carcinogenesis. *Radiat. Environ. Biophys.*, 30, 239–241.
240. Grahn, D., Lombard, L. S. and Carnes, B. A. (1992) The comparative tumorigenic effects of fission neutrons and cobalt-60 gamma rays in the B6CF1 mouse. *Radiat. Res.*, 129, 19–36.
241. Zhang, Y. and Woloschak, G. E. (1997) Rb and p53 gene deletions in lung adenocarcinomas from irradiated and control mice. *Radiat. Res.*, 148, 81–89.
242. Zhang, Y. and Woloschak, G. E. (1998) Detection of codon 12 point mutations of the K-ras gene from mouse lung adenocarcinoma by 'enriched' PCR. *Int. J. Radiat. Biol.*, 74, 43–51.
243. Tuveson, D. A. and Jacks, T. (1999) Modeling human lung cancer in mice: similarities and shortcomings. *Oncogene*, 18, 5318–5324.
244. Salgia, R. and Skarin, A. T. (1998) Molecular abnormalities in lung cancer. *J. Clin. Oncol.*, 16, 1207–1217.
245. Sekido, Y., Fong, K. M. and Minna, J. D. (1998) Progress in understanding the molecular pathogenesis of human lung cancer. *Biochim. Biophys. Acta*, 1378, F21–F59.
246. D'Amico, D., Carbone, D., Mitsudomi, T., *et al.* (1992) High frequency of somatically acquired p53 mutations in small-cell lung cancer cell lines and tumors. *Oncogene*, 7, 339–346.
247. Hensel, C. H., Xiang, R. H., Sakaguchi, A. Y. and Naylor, S. L. (1991) Use of the single strand conformation polymorphism technique and PCR to detect p53 gene mutations in small cell lung cancer. *Oncogene*, 6, 1067–1071.
248. Takahashi, T., Takahashi, T., Suzuki, H., Hida, T., Sekido, Y., Ariyoshi, Y. and Ueda, R. (1991) The p53 gene is very frequently mutated in small-cell lung cancer with a distinct nucleotide substitution pattern. *Oncogene*, 6, 1775–1778.
249. Sameshima, Y., Matsuno, Y., Hirohashi, S., Shimosato, Y., Mizoguchi, H., Sugimura, T., Terada, M. and Yokota, J. (1992) Alterations of the p53 gene are common and critical events for the maintenance of malignant phenotypes in small-cell lung carcinoma. *Oncogene*, 7, 451–457.
250. Sherr, C. J. and McCormick, F. (2002) The RB and p53 pathways in cancer. *Cancer Cell*, 2, 103–112.
251. Olsson, A. Y., Feber, A., Edwards, S., Te Poele, R., Giddings, I., Merson, S. and Cooper, C. S. (2007) Role of E2F3 expression in modulating cellular proliferation rate in human bladder and prostate cancer cells. *Oncogene*, 26, 1028–1037.
252. Vojtek, A. B. and Der, C. J. (1998) Increasing complexity of the Ras signaling pathway. *J. Biol. Chem.*, 273, 19925–19928.
253. Califano, R., Landi, L. and Cappuzzo, F. (2012) Prognostic and predictive value of K-RAS mutations in non-small cell lung cancer. *Drugs*, 72, 28–36.
254. Bongiorno, P. F., Whyte, R. I., Lesser, E. J., Moore, J. H., Orringer, M. B. and Beer, D. G. (1994) Alterations of K-ras, p53, and erbB-2/neu in human lung adenocarcinomas. *J. Thorac. Cardiovasc. Surg.*, 107, 590–595.
255. Boice, J. D. Jr, Preston, D., Davis, F. G. and Monson, R. R. (1991) Frequent chest X-ray fluoroscopy and breast cancer incidence among tuberculosis patients in Massachusetts. *Radiat. Res.*, 125, 214–222.
256. Land, C. E., Tokunaga, M., Koyama, K., Soda, M., Preston, D. L., Nishimori, I. and Tokuoka, S. (2003) Incidence of female breast cancer among atomic bomb survivors, Hiroshima and Nagasaki, 1950-1990. *Radiat. Res.*, 160, 707–717.
257. Bhatia, S., Robison, L. L., Oberlin, O., Greenberg, M., Bunin, G., Fossati-Bellani, F. and Meadows, A. T. (1996) Breast cancer and other second neoplasms after childhood Hodgkin's disease. *N. Engl. J. Med.*, 334, 745–751.
258. Sankila, R., Garwicz, S., Olsen, J. H., *et al.* (1996) Risk of subsequent malignant neoplasms among 1,641 Hodgkin's disease patients diagnosed in childhood and adolescence: a population-based cohort study in the five Nordic countries. Association of the Nordic Cancer Registries and the Nordic Society of Pediatric Hematology and Oncology. *J. Clin. Oncol.*, 14, 1442–1446.
259. Stovall, M., Smith, S. A., Langholz, B. M., *et al.*; Women's Environmental, Cancer, and Radiation Epidemiology Study Collaborative Group. (2008) Dose to the contralateral breast from radiotherapy and risk of second primary breast cancer in the WECARE study. *Int. J. Radiat. Oncol. Biol. Phys.*, 72, 1021–1030.
260. Brooks, J. D., Bernstein, L., Teraoka, S. N., *et al.*; WECARE Study Collaborative Group. (2012) Variation in genes related to obesity, weight, and weight change and risk of contralateral breast cancer in the WECARE Study population. *Cancer Epidemiol. Biomarkers Prev.*, 21, 2261–2267.
261. Boice, J. D. Jr, Harvey, E. B., Blettner, M., Stovall, M. and Flannery, J. T. (1992) Cancer in the contralateral breast after radiotherapy for breast cancer. *N. Engl. J. Med.*, 326, 781–785.
262. Thomas, D. B., Rosenblatt, K., Jimenez, L. M., *et al.* (1994) Ionizing radiation and breast cancer in men (United States). *Cancer Causes Control*, 5, 9–14.

263. Ronckers, C. M., Erdmann, C. A. and Land, C. E. (2005) Radiation and breast cancer: a review of current evidence. *Breast Cancer Res.*, 7, 21–32.
264. Imaoka, T., Nishimura, M., Iizuka, D., Daino, K., Takabatake, T., Okamoto, M., Kakinuma, S. and Shimada, Y. (2009) Radiation-induced mammary carcinogenesis in rodent models: what's different from chemical carcinogenesis? *J. Radiat. Res.*, 50, 281–293.
265. Medina, D. (2000) The preneoplastic phenotype in murine mammary tumorigenesis. *J. Mammary Gland Biol. Neoplasia*, 5, 393–407.
266. Finerty, J. C., Binhammer, R. T., Schneider, M. and Cunningham, A. W. (1953) Neoplasms in rats exposed to single-dose total-body X radiation. *J. Natl. Cancer Inst.*, 14, 149–157.
267. shellabarger, C. J., Cronkite, E. P., Bond, V. P. and Lippincott, S. W. (1957) The occurrence of mammary tumors in the rat after sublethal whole-body irradiation. *Radiat. Res.*, 6, 501–512.
268. Medina, D. (2010) Of mice and women: A short history of mouse mammary cancer research with an emphasis on the paradigms inspired by the transplantation method. *Cold Spring Harb. Perspect. Biol.*, 2, a004523.
269. Yu, Y., Okayasu, R., Weil, M. M., Silver, A., McCarthy, M., Zabriskie, R., Long, S., Cox, R. and Ullrich, R. L. (2001) Elevated breast cancer risk in irradiated BALB/c mice associates with unique functional polymorphism of the Prkdc (DNA-dependent protein kinase catalytic subunit) gene. *Cancer Res.*, 61, 1820–1824.
270. Moll, U., Lau, R., Sypes, M. A., Gupta, M. M. and Anderson, C. W. (1999) DNA-PK, the DNA-activated protein kinase, is differentially expressed in normal and malignant human tissues. *Oncogene*, 18, 3114–3126.
271. Ethier, S. P. and Ullrich, R. L. (1984) Factors influencing expression of mammary ductal dysplasia in cell dissociation-derived murine mammary outgrowths. *Cancer Res.*, 44, 4523–4527.
272. Ullrich, R. L. and Preston, R. J. (1991) Radiation induced mammary cancer. *J. Radiat. Res.*, 32, 104–109.
273. Deome, K. B., Faulkin, L. J. Jr, Bern, H. A. and Blair, P. B. (1959) Development of mammary tumors from hyperplastic alveolar nodules transplanted into gland-free mammary fat pads of female C3H mice. *Cancer Res.*, 19, 515–520.
274. Deome, K. B., Miyamoto, M. J., Osborn, R. C., Guzman, R. C. and Lum, K. (1978) Detection of inapparent nodule-transformed cells in the mammary gland tissues of virgin female BALB/cfC3H mice. *Cancer Res.*, 38, 2103–2111.
275. Ethier, S. P. and Ullrich, R. L. (1982) Detection of ductal dysplasia in mammary outgrowths derived from carcinogen-treated virgin female BALB/c mice. *Cancer Res.*, 42, 1753–1760.
276. Ethier, S. P., Adams, L. M. and Ullrich, R. L. (1984) Morphological and histological characteristics of mammary dysplasias occurring in cell dissociation-derived murine mammary outgrowths. *Cancer Res.*, 44, 4517–4522.
277. Barcellos-Hoff, M. H. (1993) Radiation-induced transforming growth factor beta and subsequent extracellular matrix reorganization in murine mammary gland. *Cancer Res.*, 53, 3880–3886.
278. Barcellos-Hoff, M. H. (1998) The potential influence of radiation-induced microenvironments in neoplastic progression. *J. Mamm. Gland Biol. Neoplasia*, 3, 165–175.
279. Barcellos-Hoff, M.H. (2005) How tissues respond to damage at the cellular level: orchestration by transforming growth factor-{beta} (TGF-{beta}). *BJR Suppl/BIR*, 27, 123–127.
280. Barcellos-Hoff, M. H. (2005) Integrative radiation carcinogenesis: interactions between cell and tissue responses to DNA damage. *Semin. Cancer Biol.*, 15, 138–148.
281. Ethier, S. P. and Ullrich, R. L. (1982) Induction of mammary tumors in virgin female BALB/c mice by single low doses of 7,12-dimethylbenz[a] anthracene. *J. Natl. Cancer Inst.*, 69, 1199–1203.
282. Ullrich, R. L., Bowles, N. D., Satterfield, L. C. and Davis, C. M. (1996) Strain-dependent susceptibility to radiation-induced mammary cancer is a result of differences in epithelial cell sensitivity to transformation. *Radiat. Res.*, 146, 353–355.
283. Danielson, M. (1984) Hemodynamic effects of diuretic therapy in hypertension. *Acta Pharmacol. Toxicol. (Copenh).*, 54, 33–36.
284. Nguyen, D. H., Oketch-Rabah, H. A., Illa-Bochaca, I., *et al.* (2011) Radiation acts on the microenvironment to affect breast carcinogenesis by distinct mechanisms that decrease cancer latency and affect tumor type. *Cancer Cell*, 19, 640–651.
285. Barcellos-Hoff, M. H. and Brooks, A. L. (2001) Extracellular signaling through the microenvironment: a hypothesis relating carcinogenesis, bystander effects, and genomic instability. *Radiat. Res.*, 156, 618–627.
286. Barcellos-Hoff, M. H., Park, C. and Wright, E. G. (2005) Radiation and the microenvironment - tumorigenesis and therapy. *Nat. Rev. Cancer*, 5, 867–875.
287. Barcellos-Hoff, M. H. and Medina, D. (2005) New highlights on stroma-epithelial interactions in breast cancer. *Breast Cancer Res.*, 7, 33–36.
288. Alberts, B. (2008) *Molecular Biology of the Cell*, 5th edn. Garland Science, New York.
289. Andarawewa, K. L., Paupert, J., Pal, A. and Barcellos-Hoff, M. H. (2007) New rationales for using TGFbeta inhibitors in radiotherapy. *Int. J. Radiat. Biol.*, 83, 803–811.
290. Andarawewa, K. L., Erickson, A. C., Chou, W. S., Costes, S. V., Gascard, P., Mott, J. D., Bissell, M. J. and Barcellos-Hoff, M. H. (2007) Ionizing radiation predisposes nonmalignant human mammary epithelial cells to undergo transforming growth factor beta induced epithelial to mesenchymal transition. *Cancer Res.*, 67, 8662–8670.
291. Castiglioni, F., Terenziani, M., Carcangiu, M. L., *et al.* (2007) Radiation effects on development of HER2-positive breast carcinomas. *Clin. Cancer Res.*, 13, 46–51.
292. Arima, Y., Hayashi, H., Sasaki, M., *et al.* (2012) Induction of ZEB proteins by inactivation of RB protein is key determinant of mesenchymal phenotype of breast cancer. *J. Biol. Chem.*, 287, 7896–7906.
293. Robbins, M. E. and Zhao, W. (2004) Chronic oxidative stress and radiation-induced late normal tissue injury: a review. *Int. J. Radiat. Biol.*, 80, 251–259.
294. Kuefner, M. A., Brand, M., Ehrlich, J., Braga, L., Uder, M. and Semelka, R. C. (2012) Effect of antioxidants on X-ray-induced γ-H2AX foci in human blood lymphocytes: preliminary observations. *Radiology*, 264, 59–67.
295. Margulies, B. S., Damron, T. A. and Allen, M. J. (2008) The differential effects of the radioprotectant drugs amifostine and sodium selenite treatment in combination with radiation therapy on constituent bone cells, Ewing's sarcoma of bone tumor cells, and rhabdomyosarcoma tumor cells in vitro. *J. Orthop. Res.*, 26, 1512–1519.
296. Sieber, F., Muir, S. A., Cohen, E. P., North, P. E., Fish, B. L., Irving, A. A., Mäder, M. and Moulder, J. E. (2009) High-dose selenium for the mitigation of radiation injury: a pilot study in a rat model. *Radiat. Res.*, 171, 368–373.

Chapter 5: Conclusions and Future Directions

CONCLUSIONS

In developed countries, cancer is the second largest cause of death after cardiovascular disease. In many ways, though, cancer can be more intimidating. Cardiovascular disease can be managed once progression is detected. Active management of blood pressure, cholesterol levels, and inflammation is all possible, and yields real benefits in reduced risk. Cancer progression, however, is largely unable to be mitigated until the mature disease itself is detected. In many cases, prognoses are poor by the time it is caught [1]. Known sources of genotoxicity and carcinogens can be avoided, but there are very few reliable ways to actively mitigate the accumulation of DNA damage.

The development of agents capable of mitigating genotoxic damage immediately after a causal event, but prior to the onset of anything recognizable as carcinogenic progression, represents a new opportunity for therapeutic intervention. In chapter 2, we investigated the efficacy and mechanism of Yel002, a molecule uncovered via a high throughput screen for agents capable of mitigating lethality and genotoxicity in a yeast model. The focal intent of Yel002 was the mitigation of acute radiation syndrome (ARS) in subjects irradiated at near lethal levels, and the compound was very effective in this regard. Yel002 exposure promoted the rapid re-expansion of the hematopoietic stem cell niche to replenish depleted white blood cells and platelets following irradiation in animal models. However, the yeast screen alone could not have predicted the impressive litany of secondary effects we observed in different experimental models. Yel002 promoted continued cell cycle progression in irradiated cells and delayed senescence. Importantly, the compound was capable of interfering with leukemic progression in the DBA/2 model even in the absence of radiation. Many questions and challenges still remain for the further development of Yel002 as a pharmaceutical, including quality control and stability, but these results show potential worth future inquiry.

We are only just beginning to understand the importance and potential of the human microbiome. Through the microbiota, aspects of our environment we never thought could affect

us directly, such as glyphosate pesticides as detailed in Appendix I, might have far-reaching effects on our health. Direct management of this bacterial community presents a novel way for us to influence that health positively, as well. Although much of the topic is diluted by pseudoscientific claims in the popular sphere, probiotic bacteria can have real, measurable, and beneficial effects, including the inhibition of pathogenic gut bacteria [2-4]. In Chapter 3, we elucidated the antipathogen effects of the *Lactobacillus johnsonii* strain 456. LBJ 456 inhibited both growth and adhesion of known diarrheal, inflammation inducing strains like enterotoxigenic *E. coli* and *Salmonella*. We also assessed the survival of LBJ 456 in the gut, and determined that it was a viable colonizer that fit the profile for a human probiotic strain. If future experiments show that LBJ 456's cytokine and antigenotoxic effects in mice translate to humans, the strain may become one of the first probiotics clinically approved for the mitigation of gut-derived inflammation.

Cancer is a disease with a complex process of development. It is impossible to completely recapitulate risk and progression through *in vitro* experimentation alone. Before any conclusions can be drawn as to whether an intervention aimed at reducing genotoxicity or inflammation in the short term has any real effect on cancer risk, it must be tested in an animal model. In Chapter 4, we presented our article *Mouse models for radiation-induced cancers*, as originally published in *Mutagenesis* [5]. The models we delineated here recapitulate the development and pathologies of radiation induced breast cancer, lung cancer, leukemia and lymphoma. Laboratory mice present a number of advantages for the modeling of radiation induced cancer progression, and will be indispensable for the testing of agents designed to interfere with that progression.

This thesis detailed two different points of intervention for the active management and mitigation of genotoxicity that might lead to increased cancer risk, as well as methods by which related future treatments might be discovered. Both interventions require additional inquiry and refinement before being used in humans, but the potential to reduce cancer risk

prior to actual carcinogenesis is worth additional experimentation. More is revealed about carcinogenic progression and initiation every day, and each discovery offers a new point for intervention. I am confident that in the future active mitigation, rather than just avoidance of carcinogens, will become part of the cancer avoidance paradigm.

FUTURE DIRECTIONS

Identification of Yel002 binding target

Yel002 was shown to affect cell cycling, likely through a mechanism with an effect on pRb, and potentially affects relative DNA repair pathway preference in irradiated cells. However, the specific binding partner was not identified. After the establishment of more consistent quality control for Yel002 synthesis, we will aim to precisely identify of cell components necessary for Yel002 function. This process will involve the use of knockouts and inducible inhibition of cell cycle components and repair pathways, as well as sequence analysis to look for markers of particular types of genomic rearrangements and repair. The evaluation of changes in relative repair pathway preference should be a high priority for testing, as new, cell-free assays have been developed to measure differential pathway choice since the original experiments in this thesis were performed [6, 7].

Differential DNA damage mitigation and repair

Beyond their application in mitigating damage from accidental radiation exposure, DNA damage mitigators and protectors could be used with purposeful irradiation if, by virtue of their specific mechanisms, they provide different levels of mitigation to different cell types. If a mitigator's capacity for rescue relies upon a particular cell pathway, it may not function in cancer cells that have disabled that pathway. This use has already been observed with existing mitigators under development. The TLR 5 agonist CBLB502 gave differential

radioprotection in an *in vivo* tumor model, allowing mice to survive higher therapeutic radiation doses for more effective tumor clearance, without protecting the tumor [8]. After mitigators are tested against tumors lacking the repair or survival mechanisms they act through, gene sequencing in clinical cancer cases could identify which mitigators are compatible with its mutation profile, allowing for better radiotherapy indices with personalized medicine.

There is some evidence that Yel002 functions via shunting the competitive DNA repair profile of a treated cell to favor NHEJ over other DSB repair mechanisms. Over the course of their development, many cancers come to rely more heavily on particular repair pathways, sometimes to the extent that others are nonfunctional [9, 10]. For this reason, it might be possible to induce a "synthetic lethality" by inhibiting the specific DNA repair method a cancer cell relies on, or pushing it towards using one that is defective [11, 12]. This effect could potentially be artificially induced by co-treatment with other compounds known to disrupt DNA repair mechanisms, like Olaparib, inhibitor of PARP1, which is involved in MMEJ [6, 13].

Testing of antigenotoxic interventions in animal and human models of advanced age

As the body ages, DNA repair functionality decreases [14]. In particular, the capacity of hematopoietic precursors to repair themselves in response to high levels of stress or other genotoxic insult is significantly reduced [15]. Yel002's capacity to promote NHEJ repair and reduce senescence-associated effects may ameliorate some of these effects *in vivo*. In addition, the radiation studies performed in chapter 2 focused solely on radiation rescue in young mice. In a real exposure scenario, individuals of all ages would be exposed. In the future, experiments with exposed animals at different ages will be necessary to accurately predict levels of rescue at older ages.

Development of future DNA damage mitigators

Yel002 showed activity as a mitigator of both acute radiation syndrome and double-strand break induction with a variety of models. Importantly, this further validates the use of the DEL assay as a predictor of carcinogenesis rates. The DEL assay has already been validated as a strong predictor of potentially carcinogenic substances, greatly outperforming such popular tests as the Ames assay in terms of precision and human relevance [16-19]. The results shown here are evidence that this assay functions as a detector of compounds that *reduce* the risk of carcinogenesis as well. Its low cost and high-throughput capability make the DEL assay an excellent choice for future mitigator and protector screens.

Identification of LBJ 456 antipathogen factors

Our experiments revealed strong inhibition of certain pathogens by both LBJ 456 itself and a factor that persists in the strain's supernatant after filter sterilization. Gene sequencing and comparison to characterized genes suggest that the active factor may be a bacteriocin, a protein inhibitor of competing bacterial species. The isolation and characterization of this factor will help to elucidate the mechanisms by which LBJ 456 interferes with the growth of pathogenic species in the gut. The nature of the competing factor can be confirmed by the addition of proteinases to the sterile supernatant, leading to rescue of pathogen growth. The bacteriocin itself can also be characterized via precipitation and purification [20, 21]. Identification of an acellular factor responsible for some of LBJ 456's effects will also speed testing for activity against a wider variety of pathogenic species. Pathogen growth can be tested in the presence of bacteriocin-containing supernatant or purified bacteriocin, rather than needing to employ co-culture techniques.

Human clinical studies with LBJ 456

In a small pilot study, LBJ 456 was shown to persist in the human gut after ingestion for roughly a month. However, resource limitations kept the size of this initial study very

small. A future, larger trial, with a greater number pre-ingestion baseline samples and placebo control will precisely determine the relative efficacy in human gut colonization, and a more accurate average duration [22]. In addition, LBJ 456's *in vitro* results suggest the capacity to inhibit diarrhea causing pathogen growth. Eventually, application of the strain in larger, disease specific clinical trials could determine whether the use of this strain can prevent or reduce duration of specific pathogen infections, including those associated with long-term inflammatory risks like *H. pylori [23].*

Isolation and development of future anti-inflammatory strains

LBJ 456 was originally isolated from mice in an environmentally restricted facility, an approach that had a number of benefits. The strain only came to our original attention because of its association with lower levels of genotoxicity, as measured by a specific genetic reporter system [24]. We were able to rapidly test the strain's efficacy as an inducer of anti-inflammatory outcomes in its host species based on perturbations of cytokine and cancer levels, which are difficult to measure without genetically and environmentally homogenous test subjects. However, this approach also has its drawbacks. The composition of the mouse gut microbiome is radically different from that of a human, with some 85% of murine bacterial genera absent in the human gut [25]. Inflammatory responses against microbes in the mouse gut do not necessarily recapitulate those observed in humans [26, 27]. For future candidate strains, the human gut may be a better source of potentially probiotic bacteria. With "native" bacteria, the likelihood of survival through the human gastrointestinal tract and its barriers would already be all but assured. However, association with strong anti-inflammatory or antipathogen outcomes would be difficult to associate and study due to human environmental and genetic heterogeneity. Rather than looking for a strain associated with a difficult to normalize parameter like inflammatory cytokine level or genotoxicity, it may be more useful to first look for human populations associated with a broad beneficial trait likely to be associated

with diet and microbiome, then work backwards to isolate strains from those populations. “Blue Zones,” or areas associated with an exceptional number of healthy individuals of advanced age, have been suggested as a potential source of such probiotic species [28].

1. Iqbal, J., et al., *Differences in breast cancer stage at diagnosis and cancer-specific survival by race and ethnicity in the United States.* Jama, 2015. **313**(2): p. 165-173.
2. Saavedra, J., *Probiotics and infectious diarrhea.* The American journal of gastroenterology, 2000. **95**(1): p. S16-S18.
3. Huang, J.S., et al., *Efficacy of probiotic use in acute diarrhea in children: a meta-analysis.* Digestive diseases and sciences, 2002. **47**(11): p. 2625-2634.
4. Bickston, S.J., L.W. Comerford, and F. Cominelli, *Future therapies for inflammatory bowel disease.* Current gastroenterology reports, 2003. **5**(6): p. 518-523.
5. Rivina, L., M.J. Davoren, and R.H. Schiestl, *Mouse models for radiation-induced cancers.* Mutagenesis, 2016. **31**(5): p. 491-509.
6. Sharma, S., et al., *Homology and enzymatic requirements of microhomology-dependent alternative end joining.* Cell death & disease, 2016. **6**(3): p. e1697.
7. Nagel, Z.D., et al., *Multiplexed DNA repair assays for multiple lesions and multiple doses via transcription inhibition and transcriptional mutagenesis.* Proceedings of the National Academy of Sciences, 2014. **111**(18): p. E1823-E1832.
8. Burdelya, L.G., et al., *An agonist of toll-like receptor 5 has radioprotective activity in mouse and primate models.* Science, 2008. **320**(5873): p. 226-230.
9. Ceccaldi, R., et al., *Homologous-recombination-deficient tumours are dependent on Polϑ-mediated repair.* Nature, 2015. **518**(7538): p. 258.
10. Aparicio, T., R. Baer, and J. Gautier, *DNA double-strand break repair pathway choice and cancer.* DNA repair, 2014. **19**: p. 169-175.
11. Santivasi, W.L. and F. Xia, *Ionizing radiation-induced DNA damage, response, and repair.* Antioxidants & redox signaling, 2014. **21**(2): p. 251-259.
12. Brough, R., et al., *Searching for synthetic lethality in cancer.* Current opinion in genetics & development, 2011. **21**(1): p. 34-41.
13. Tutt, A., et al., *Oral poly (ADP-ribose) polymerase inhibitor olaparib in patients with BRCA1 or BRCA2 mutations and advanced breast cancer: a proof-of-concept trial.* The Lancet, 2010. **376**(9737): p. 235-244.
14. Goukassian, D., et al., *Mechanisms and implications of the age-associated decrease in DNA repair capacity.* The FASEB journal, 2000. **14**(10): p. 1325-1334.
15. Rossi, D.J., et al., *Deficiencies in DNA damage repair limit the function of haematopoietic stem cells with age.* Nature, 2007. **447**(7145): p. 725.
16. Carls, N. and R.H. Schiestl, *Evaluation of the yeast DEL assay with 10 compounds selected by the International Program on Chemical Safety for the evaluation of short-term tests for carcinogens.* Mutation Research/Genetic Toxicology, 1994. **320**(4): p. 293-303.
17. Brennan, R.J. and R.H. Schiestl, *Detecting carcinogens with the yeast DEL assay.* Genetic Recombination: Reviews and Protocols, 2004: p. 111-124.
18. Galli, A. and R.H. Schiestl, *Effect of Salmonella assay negative and positive carcinogens on intrachromosomal recombination in S-phase arrested yeast cells.* Mutation Research/Genetic Toxicology and Environmental Mutagenesis, 1998. **419**(1): p. 53-68.

19. Kirpnick, Z., et al., *Yeast DEL assay detects clastogens.* Mutation Research/Genetic Toxicology and Environmental Mutagenesis, 2005. **582**(1): p. 116-134.
20. Maldonado-Barragán, A., et al., *Purification and genetic characterization of gassericin E, a novel co-culture inducible bacteriocin from Lactobacillus gasseri EV1461 isolated from the vagina of a healthy woman.* BMC microbiology, 2016. **16**(1): p. 37.
21. Akimaru, G., et al., *Characterization and purification of a bacteriocin-like substance produced by Lactobacillus crispatus LBS 17-11 isolated from an oral cavity of human subject.* Asian Pacific journal of dentistry: APJD, 2017. **17**(1): p. 9-14.
22. Goossens, D., et al., *The effect of Lactobacillus plantarum 299v on the bacterial composition and metabolic activity in faeces of healthy volunteers: a placebo-controlled study on the onset and duration of effects.* Alimentary pharmacology & therapeutics, 2003. **18**(5): p. 495-505.
23. Wang, F., et al., *Helicobacter pylori-induced gastric inflammation and gastric cancer.* Cancer letters, 2014. **345**(2): p. 196-202.
24. Yamamoto, M.L., et al., *Intestinal bacteria modify lymphoma incidence and latency by affecting systemic inflammatory state, oxidative stress, and leukocyte genotoxicity.* Cancer research, 2013. **73**(14): p. 4222-4232.
25. Ley, R.E., et al., *Obesity alters gut microbial ecology.* Proceedings of the National Academy of Sciences of the United States of America, 2005. **102**(31): p. 11070-11075.
26. Nell, S., S. Suerbaum, and C. Josenhans, *The impact of the microbiota on the pathogenesis of IBD: lessons from mouse infection models.* Nature Reviews Microbiology, 2010. **8**(8): p. 564.
27. Nguyen, T.L.A., et al., *How informative is the mouse for human gut microbiota research?* Disease models & mechanisms, 2015. **8**(1): p. 1-16.
28. Yang, H.-y., et al., *Oral administration of live Bifidobacterium substrains isolated from healthy centenarians enhanced immune function in BALB/c mice.* Nutrition research, 2009. **29**(4): p. 281-289.

Appendix I: Glyphosate Based Herbicides and Cancer Risk: A Post IARC Decision Review of Potential Mechanisms, Policy, and Avenues of Research

Glyphosate Based Herbicides and Cancer Risk: A Post IARC Decision Review of Potential Mechanisms, Policy, and Avenues of Research

Michael J. Davoren and Robert H. Schiestl

Molecular Toxicology Interdepartmental Program, University of California, Los Angeles, Los Angeles, California, USA

Background: Since its initial sales in the 1970s, the herbicide glyphosate attained widespread use in modern agriculture. As of 2016, this compound was the most commercially successful and widely used herbicide of all time. Despite a primary mechanism action that targets a pathway absent in animal cells, and regulatory studies showing safety margins orders of magnitude better than many other, more directly toxic herbicidal compounds, the long-held view of glyphosate as a perfectly safe chemical compound has been eroded by the slow accumulation of studies evincing more insidious health risks. Current, official views of respected international regulatory and health bodies remain divided on glyphosate's status as a human carcinogen, but the 2015 IARC decision to reclassify the compound as Category 2a (probably carcinogenic to humans) marked a sea change in the scientific community's consensus view.
Objectives: The goal of this review is to consider the state of science regarding glyphosate's potential as a human carcinogen and genotoxin, with particular focus on studies suggesting mechanisms which would go largely undetected in traditional toxicology studies.
Methods: We examine the current regulatory limits on and environmental concentrations of this compound, discuss studies suggesting toxicity that could directly or indirectly affect human cancer rates, and assess their relevance in light of exposure levels.
Discussion: Many traditional carcinogenesis studies do not demonstrate significant elevations in cancer risk. However, other studies suggest that complex mechanisms, such as nonmonotonic endocrine disruption and microbiome perturbation, may respond to low doses of glyphosate and affect total cancer risk over a lifetime.
Conclusion: Considering the near-universal exposure to this compound on a population level, large-scale studies on these mechanisms are important for public health. Public exposure should be limited in light of modern understanding of subtle mechanisms of carcinogenesis.

Background

Glyphosate's herbicidal capacity was initially discovered by John Franz in 1970 [1]. The patent

Address correspondence to M. J. Davoren, 650 Charles E. Young Dr. S, CHS 71-295, Los Angeles, CA 90095. Email: mdavoren@g.ucla.edu
Competing Financial Interest Declaration: Robert H. Schiestl is a consultant with Baum, Hedlund, Aristei, and Goldman, P.C. This work was not funded by this group; it was the authors' sole decision to write and publish this review.
Acknowledgements and Funding: The writing of this review was self funded by the authors. This work is not associated with any grant, academic or private.

was assigned to his employing corporation, Monsanto, in 1974, and first introduced to market under the brand name formulation Roundup. Usage of glyphosate-based herbicides (GBHs) only increased with the introduction of glyphosate resistant genetically modified (GM) crops. By the turn of the century, glyphosate resistance was the most common GM trait in agriculture [2]. GBHs, now manufactured by many chemical companies beyond the original patent holder, are the most commonly used herbicide class worldwide, accounting for more than half of agricultural herbicide use in the United States alone [3, 4]. A GBH contains an aqueous solution of glyphosate salt as well as other adjuvant compounds, including surfactants, that increase penetration and efficacy but may carry their own effects [5]. GBHs, through their synergy with glyphosate tolerant GM crops, are major contributors to the economic benefits GM crops provide in the US agricultural sector. Farmers utilizing these combinations see crop yield increases of up to 22%, and profit increases of up to 68% over non-GM crops [6].

Glyphosate's mechanism of herbicidal action is the inhibition of the shikimate pathway, an aromatic amino acid metabolism pathway absent in animal cells but critical to the growth of most plants [7]. Specifically, glyphosate inhibits the enzyme enolpyruvylshikimate-3-phosphate synthase (EPSP) [8, 9]. This pathway is also present and needed for growth in some bacteria and fungi [10]. At face value, this kingdom-exclusive mechanism should make glyphosate the closest thing to an ideal herbicide. The proprietary data submitted to regulators in the 1970s for initial registration of the compound suggested low toxicity and no significant risk of long term effects like elevated cancer risks, and many studies in the intervening decades concurred with that assessment [11, 12]. However, the last several years have seen the accumulation of evidence that long term risks, especially from chronic exposure, may in fact exist. The resulting discordance between toxicity proponents and skeptics has divided the scientific community in one of the most heated scientific debates in recent memory.

One of the most controversial studies to report carcinogenic effects from glyphosate in mice was published by Giles-Éric Séralini in 2012 [13]. The study was widely criticized on a number of different fronts, including animal welfare noncompliance, particularly anomalous conclusions regarding GM plants themselves (rather than glyphosate), and gross mistakes regarding pathology [14]. Other groups took issue with Séralini's statistical methods, and claim that no significant elevation in tumor incidence is observed if more traditional statistical analysis is used with the data [15]. In the end, the Séralini affair concluded with the original journal retracting the paper, despite finding no evidence of misconduct, largely due to significant concerns raised regarding the statistical methods, although the author raised some legitimate concerns about enforcement of double standards [16]. The Séralini group republished their manuscript without further review in a second journal [17].

The results of the Séralini group's 2012 paper are now generally discounted by mainstream scientists, but allegations of bias have been aimed at their detractors as well. The fast-tracked appointment of a former Monsanto employee to a newly created position on the editorial board of *Food and Chemical Toxicology* immediately preceding the Séralini retraction raised questions of potential impropriety [18]. Many authors writing leading reviews that push a toxicity-skeptic viewpoint acknowledge funding from corporate entities with a vested interest in glyphosate as well [12]. Other researchers point out that much of the original data supplied by manufacturers during the regulatory process, upon which initial safety assessments were based, is still considered to be proprietary and not open to public review [19]. Another

controversial author, Stephanie Seneff, claims that these initial assessments were based on improperly combined experimental and historical control data [20].
The International Agency for Research on Cancer's (IARC) 2015 reclassification of glyphosate as a Category 2a (probable carcinogen) belies the continued debate around the status of this compound [21]. Critiquing groups maintain that the overall weight of evidence still shows no significant risks [22]. Another subdivision of the World Health Organization (WHO) , the Joint Food and Agriculture Organization, maintained in 2016 that glyphosate was unlikely to pose a carcinogenic risk [23]. Many regulatory agencies, including the European Food Safety Authority (EFSA) and European Chemicals Agency (EChA) continue to hold the official viewpoint that glyphosate does not pose a genotoxic or carcinogenic risk to humans [24]. Concerned scientists contended that the IARC evaluation was in fact more rigorous by relying solely on publicly available, peer-reviewed data to make its assessment, while EFSA and EChA regulators factored in proprietary information from registrants closed to comment from the wider scientific community [25]. Other groups expressed concern with these agencies bias towards registrant entities [26].
In the United States as of early 2018, glyphosate is currently undergoing a re-registration review process in accordance with the Federal Insecticide, Fungicide, and Rodenticide Act (FIFRA), but the EPA still maintains that there is no demonstrable link to carcinogenicity [27, 28]. The studies cited in the their recently released, *Revised Glyphosate Issue Paper,* though, give a mixed message. Of the three occupational exposure epidemiology studies given a "High Quality" ranking, one reports a strong statistically significant association with lymphoma incidence [29]. Another suggests a strong trend towards association with multiple myeloma in the initial study, with a 10 year followup study showing a trend towards association with acute myeloid leukemia in the same cohort [30, 31].The third, an investigation into the effects of many pesticides, finds no association with prostate cancer, but does not focus on glyphosate or even mention the compound outside of supplemental data tables [31].

Review Methods

A great number of reviews have sought to aggregate the information available about glyphosate's long term toxic potential, often drawing conflicting conclusions based on interpretations about the validity of the studies they examined [19, 22, 28, 32]. Acute toxicity studies were excluded from our search. For this review, we sought to focus largely on more subtle mechanisms that could operate to promote carcinogenesis through low dose exposure. Literature searches were conducting using the Science Direct, PubMed, and Google Scholar platforms. Keyword combinations were used ("glyphosate AND keyword") to screen articles for each section. For the exposure limits section, co-keywords included "regulation", "environmental AND exposure", and "application". For the direct carcinogenesis section, co-keywords included "carcinogen", "cancer", and "genotoxicity". For nonmonotonic effects, we used "nonmonotonic" and "endocrine", while for microbiome effects we used "microbiome", "bacteria" and "microbiota". Articles that were not available in full to our institution or not available in English were not used.

Exposure Methods, Levels, and Limits

Glyphosate remains the most widely used herbicide both in the U.S. and the world. Rates of use continue to increase each year. Grube estimates that in 2007, 180 million pounds were applied to U.S. crops, while Benbrook estimates that that amount increased to 270 million pounds by 2014 [33, 34]. Nearly 93% of the soy crop and 85% of the U.S. corn crop are treated with GBHs, with 2 pounds of the active ingredient applied on average to each treated acre of corn [35]. Multiple factors, beyond simple expansion of the agriculture industry, drive this great increase in applied glyphosate. The growing emergence of glyphosate resistant weeds demands increased herbicide levels to maintain the same level of control [36]. The compound itself is being used in new roles, as well. The process of pre-harvest crop desiccation, for example, involves the deliberate spraying of glyphosate sensitive crops with the chemical to speed cessation of growth and prepare the crop for harvest in a more controlled manner – a process that often leaves glyphosate residue on the desiccated crops. As of 2009, glyphosate was the only herbicide registered to be used in this manner in the U.S. [37]. Some 250,000 to 300,000 acres of sugarcane were desiccated in this manner across the state of Louisiana in 2005 [38]. Glyphosate accumulates in treated plants, so the EPA has set allowable levels (shown in **Table 1**) for most food products [39]. The chronic reference dose (CrfD), also set by the EPA, is currently 1.75 mg/kg/day for the U.S., although the E.U.'s acceptable daily intake (ADI) is set much lower, at 0.3 mg/kg/day [19].

Fortunately, most experimentally measured environmental concentrations fall below both of these hard limits. Bøhn, for example, reports 3.3 mg/kg of glyphosate and 5.7 mg/kg of its metabolite aminomethylphosphonic acid (AMPA) in GM soybeans [40]. Seneff reports levels up to 1 mg/kg in rat chow and 0.3 mg/kg in dog food – well within regulated levels, although the endogenous levels in rat chow should merit special consideration from animal researchers [20]. Glyphosate's water-soluble nature does present a runoff risk. The compound can accumulate in streams and especially irrigation ditches near to treated areas. In areas directly adjacent to treated fields, Coupe et al. measured water concentrations of glyphosate as high as 0.86% (~5 x 10^{-5} M) [41]. Areas further from treatment sites are still at risk as well. Over a third of tested U.S. lakes, ponds, and wetlands tested positive for glyphosate and AMPA, with concentrations up to 0.3 ppm (~1.77 x 10^{-9} M) [42].

Most human and animal studies also show detectable amounts of glyphosate eliminated via the primary pathway of urination. Krüger et al. found an average concentration of 15 µg/mL (~8.87 x 10^{-8} M) in the urine of European human volunteers eating a conventional diet [43]. In a review of 8 studies, Niemann et al. estimate an average intake between 0.1 and 3.3 µg/kg of body weight per person per day, well below limits currently imposed by regulators [44].

Evidence of Direct Carcinogenic Effects

The IARC decision to reclassify glyphosate as a category 2A (probable carcinogen) was largely based on four studies showing elevated rates of Non-Hodgkins's Lymphoma (NHL) in occupationally exposed workers. [21, 29, 30, 45]. The exact mechanism by which damage is induced, though, is still unclear. Bolognesi et al. demonstrated slightly increased levels of micronuclei derived from chromosome breakage events (MN) in exposed workers from Colombia [46]. These events might not result from direct genotoxic effects from glyphosate

itself, though. Many common genotoxicity assays, such as the Ames assay, show no significant induction of DNA damage by glyphosate exposure alone [47]. A stronger association is seen with the application of complete GBHs. A decade before his population study, Bolognesi showed an increase in MN in a mouse model exposed at 300 mg/kg and single strand chromosome breaks induced in human lymphocytes. Glyphosate alone induced measurable breaks, but the full Roundup formulation was far more potent [48]. When it comes to induction of direct carcinogenic effects, evidence suggests that the surfactants present in the application mixture, especially POE-15, are a major component of GBH toxicity. This adjuvant alone is toxic to human embryonic and placental cells at levels as low as 1 ppm [49]. The full Roundup formulation was more than twice as effective at inducing lethal toxicity in human placental cell lines, albeit at levels much higher than environmental concentrations [50]. Guilherme et al. showed increases in DSB-detecting Comet Assay and MN assay lesions after 1 day at 56 µg/L Roundup in eels (0.05 ppm), which is well within environmental exposure levels [51]. Çavaş and Könen showed dose dependent increases in the same criteria in goldfish, but starting at the higher dose of 5ppm [52]. These data suggest that it is crucial to analyze and regulate GBHs as a mixture, rather than assume no synergy and set levels based on each component's toxicology alone.

Glyphosate's main degradation product, AMPA, seems to induce genotoxicity as well. Guilherme et al. showed DSB induction for this compound in the eel model at just 11.8 µg/L [53]. Mañas et al. showed that this compound induces measurable breaks at 2.5 mM in human lymphocyte culture, and at 200 mg/kg in mice[54]. Studies seeking to measure glyphosate residues both in organisms and the environment must also take this degradation product into account when calculating total exposure.

The IARC also cited animal cancer studies showing elevated risk of hemangiosarcoma, renal tubule carcinoma, and pancreatic cell islet adenoma, as well as skin tumor promotion in a 2-hit mouse model [21]. At the same time, many other studies demonstrate no direct increase in risk of carcinogenesis [22]. In most observations, direct toxicity is not well observed until above current regulatory levels. If glyphosate and its metabolites are carcinogenic, it is likely that much of this risk can only be measured outside of the standard Paracelsian dose-response model.

Endocrine Disruption and Nonmonotonic Effects

The majority of toxicology characterization studies used by worldwide regulatory agencies assume that the agent in question will behave monotonically. Testing of a compound at many doses is used to define an upper toxicity effect level (E_{max}) and a no or lowest observed adverse effect level (NOAEL or LOAEL), between which a gradation of effects is usually assumed [55]. However, for a growing variety of compounds, particularly those which mimic or disrupt aspects of the endocrine system, this classical dose-response assumption is no longer sufficient to fully characterize risk. For example, the well-known estrogen mimic bisphenol A decreases tumor latency and metastasis only at very low doses in a mouse breast cancer model [56]. The nonmonotonic dose-reponse relationships of these compounds mean that effects may be present **below** a previously set NOAEL [57, 58].

Cell line studies give different results depending on the line, dose, and formula used. The full roundup formulation is often associated with a more linear dose profile, suggesting that toxicity from adjuvant compounds is largely monotonic. In estrogen receptor-reporter transfected HepG2 cells, glyphosate alone had a nonlinear effect at under 0.05% concentration, while the full Roundup formulation reduced androgen receptor-induced transcription linearly at lower doses [59]. Testosterone-producing Leydig cells provide another model for endocrine disruption effects both *in* and *ex vivo* [60]. Walsh reported significantly disrupted progesterone production, with no parallel decrease in total protein synthesis, linearly from 25 μg/mL, but only for the complete Roundup formulation [61]. Full Roundup formulation significantly changed progression of puberty and decreased serum testosterone in prepubertal Wistar rats exposed from 5mg/kg once per day.

Thongprakaisang et al. noted the nonmonotonicity of glyphosate alone on human hormone-dependent breast cancer cell line proliferation, observing a greater effect at concentrations of 10^{-8} -10^{-9} rather than 10^{-6} M. This effect was mediated by the estrogen response element (ERE) and could be blocked by the addition of an estrogen receptor antagonist [62].

Jin et al. recently observed a nonmonotonic effect on estradiol levels in male Delta Smelt, with significant elevations after exposure to 0.46 and 4.2, but not 45 and 570 μM glyphosate [63]. Armiliato et. Al detected significantly increased expression of steroidogenic factor-1 and oocyte growth in zebrafish exposed to water concentrations as low as 65 μg/L [64]. In other fish, like trout, no significant association with endocrine disruption has been shown. Glyphosate did not show any estrogenic activity in yeast with a recombinant trout estrogen receptor at concentrations of 10^{-8} – 10^{-4}, nor did it increase levels of plasma vitellogenin in young rainbow trout themselves at 0.11 mg/L [65, 66]. In larval amphibians, environmentally relevant aqueous concentrations of glyphosate induce greater perturbation of behaviors such as movement frequency than higher concentrations, suggesting that subtle effects on their nervous systems may also be possible at very low doses [67]. Despite these recent observations, the effects of glyphosate at very low concentrations is still underinvestigated. Via endocrine mimicry, very low levels of glyphosate might potentiate human carcinogenesis, even if under regulatory limits currently considered to be safe.

Microbiome Disruption

In recent decades, the microbiome has grown to be a major new frontier in the field of human health. The composition of our gut microbiota has been compared to a “second genome” due to its far-reaching effects on nearly every aspect of human health. Determination of the species inhabiting the human GI tract, and their relative numbers, is multifactorial and dynamic. Even within an individual, this composition can change greatly over a lifetime in response to health, diet, and antibiotic exposure, among other factors [68].

Probiotic, or beneficial, bacteria, benefit human health via a number of mechanisms from the GI tract. Pathogenic bacterial adhesion and toxin efficacy are inhibited both by antimicrobial compounds generated on site, as well as direct competition for real estate. For example, the presence of *Bifidobacteria* directly inhibits the ability of *Salmonella* species to bind and cause disease [69]. Beneficial bacteria balance the gut’s immune response by modulating the ratio of inflammatory to anti-inflammatory cytokine production, which effects levels of inflammation

both in the gut and systemically [70]. Lactic acid bacteria (LAB), although they represent a very small portion of the total microbiome, have been demonstrated to be of particular importance with regards to gut homeostasis [71, 72]. The acidic pH products that they generate as waste inhibit the growth of many strains of pathogenic bacteria, and the short-chain fatty acids (SCFAs) they produce are a direct source of energy for human gut epithelial cells, improving gut integrity and colonic function [73, 74]. Probiotic production of the SCFA acetate is capable of directly reducing adhesion and toxin translocation by enterohemorrhagic *E. coli.* SCFAs are generally derived from the ability of LABs and other beneficial bacteria to metabolize otherwise indigestible dietary fiber [75]. Deficiency in these strains is often associated with inflammatory states such as Celiac Disease [76, 77]. The loss of gut homeostasis associated with increases in pathogenic strains, decreases in beneficial strains, and inflammation is termed gut dysbiosis.

Inflammatory states associated with gut dysbiosis lead to decreased integrity between epithelial cells junctions, making the barrier "leaky" and creating a feedback loop by impairing nutrient uptake and pathogen defense [78]. The "leaky gut" dysbiotic phenotype has been linked to negative effects ranging from inflammatory bowel disease to depression [79, 80]. All chronic inflammatory diseases of the gut have been strongly linked to increased risk of cancer [81, 82]. Pathogen-induced inflammation in particular is closely associated with cancers of local tissues. For example, mucosal associated tissue lymphomas are associated with bacterial inflammation and colitis [83], while the stomach pathogen *H. pylori* is especially well linked to stomach inflammation and gastric cancers [84, 85].

Glyphosate has long been known to have antibiotic function through its inhibition of EPSP [10, 86]. The fact that the accepted primary mechanism clearly affects species present in the human gut makes microbiome disruption, and subsequent inflammation, one of the most likely candidates for glyphosate carcinogenicity. One of the most concerning details about glyphosate's antimicrobial potential on the microbiome is that, in general, it seems to have a greater effect on strains generally considered to be "beneficial" than those considered to be "pathogenic". Shehata et al. investigated glyphosate's inhibitory effect on many species considered to be pathogenic or beneficial in the chicken microbiome, revealing over 50 times greater tolerance in disease causing *Clostridium* species than beneficial *Bifidobacteria* [87]. The potential effects of glyphosate are more disruptive than simple differential growth inhibition, as well. At levels under application concentrations, but lower than regulatory limits, glyphosate induced antibiotic resistance mechanisms in *Salmonella* species [88]. *Enterococcus* species can inhibit the production of *Clostridium* toxins like botulinum toxin, but this inhibition is itself inhibited at glyphosate concentrations that do not inhibit *Clostridium* growth [89]. *Staphylococcus aureus's* EPSP is insensitive to glyphosate inhibition [90]. **Table 2** describes growth-inhibitory levels of glyphosate on different pathogenic and beneficial gut bacteria. Although most inhibitory concentrations appear to be well above regulatory limits, differential sensitivity, and the multifactorial nature of microbiome composition stability, means that the slight advantage glyphosate appears to offer pathogenic strains leaves open the possibility that chronic exposure to low levels might have insidious effects. For example, Nielsen et al. report that a brief two-week exposure of young mice to food containing glyphosate had no effect on the microbiome based on DNA sequencing. However, a significant, dose dependent decrease in fecal pH was observed, suggesting impaired short-chain fatty acid production by beneficial

strains [91]. As longer studies are completed, it will be interesting to determine whether these short-term effects measurably impact long term health outcomes.
The shikimate pathway inhibited by glyphosate is important for bacterial folate production [92]. Probiotic bacteria are a major source of folate, producing the vitamin on site in the gut [93]. Folate deficiency in humans has been directly linked to genotoxicity, carcinogenicity, and chromosome breakage events [94, 95]. Deficiency increases the rate of IR-induced DNA strand breakage in human lymphocytes [96].
GBHs, with their adjuvant surfactants and emulsifiers, are more disruptive than glyphosate alone. Clair et al. report that Roundup inhibits the growth of the LAB *Lactococcis cremoris* at concentrations of 200ppm, while glyphosate alone does not [97]. Emulsifiers and surfactants alone have been shown to induce colitis in a mouse model, a condition which directly increases rates of colon carcinogenesis [98, 99]. Interestingly, one of the mechanisms by which emulsifiers like Tween 80 appear to cause dysbiosis is by creating an environment favorable to flagellin-expressing pathogenic bacteria, rather than directly harming beneficial strains [100]. Dietary grade emulsifier exposure in this model led to population increases in bacteria directly associated with chronic, low-grade inflammation [101]. Results from these surfactant studies raise the interesting possibility that GBHs could potentially have a synergetic, two-pronged effect on the gut microbiome from the action of their ingredients in tandem. Emulsifying agents could be inducing a pro-pathogen environment, while at the same time glyphosate itself inhibits the growth and antipathogen properties of beneficial strains.
Most existing studies show strong inhibition of beneficial bacteria by glyphosate only at levels above that to which the gut would be exposed, based on current regulation and exposure estimates – although the ruminant fermenter *Ruminococcus's* inhibitory sensitivity falls very close to some predictions of dietary intake [102]. Observed differential inhibition, even at levels an order of magnitude higher than those expected in the gut, should still be a cause of concern. The gut microbiome, all in its complexity, exists in a state of dynamic equilibrium. An external push from even a small factor, like a change in diet, can change the relative ratios of strains and move the ecosystem closer to a dysbiotic state [103]. Future studies should investigate whether relative ratios of gut bacteria, dysbiosis, inflammation, or even diarrhea associated with such glyphosate resistant bacteria as *Clostridia* are associated with occupational or dietary glyphosate exposure.

Recommendations

The IARC has classified glyphosate as a probable human carcinogen, but its status as one is far from decided in the eyes of the international scientific community. There is much work to be done in the foreseeable future in order to elucidate the mechanisms by which it may cause human health risks. Despite the economic benefits these compounds provide to the agriculture industry, we feel that the potential risks glyphosate and GBHs present to public health merit the following policy recommendations:

1. In light of the continued uncertainty with regards to possible genotoxic, and especially developmental, effects of glyphosate on the human body, we suggest the United States invoke the Food Quality Protection Act's enforcement of a tenfold safety margin for

pesticides or herbicides without reliable data showing no risk to children [104]. Current glyphosate cRfD levels of 1.75 mg/kg/day should be reduced to 0.175 mg/kg/day, bringing the value beneath the 0.3 mg/kg/day level used by the E.U. and closer to that recommended by multiple research groups [19, 105]. The vast majority of human urine samples collected from herbicide workers still fall well below this level, so enforcement to this standard is not unreasonable [44]. Debate over the E.U.'s re-approval of glyphosate, and whether to change the ADI levels, is still ongoing near the close of 2017.

2. Much of the debate over glyphosate's safety is marred by accusations of politically and economically motivated study findings. Each party has accused the other of disregarding and withholding data that does not fit the set of conclusions they seek to promote. We hold the opinion that the principle of free and open peer review is the best method to put these issues to rest. We call on researchers of glyphosate toxicity and carcinogenicity to place extra effort into keeping all raw data publically available for perusal and comment. In particular, we call on corporate entities that maintain proprietary datasets, especially those used to comply with government registration and regulation processes, to voluntarily make this information freely available for independent review.
3. Given that the accepted mechanism of glyphosate action involves the disruption of the shikimate pathway, and that this pathway is present and critical to the metabolism of many species in the human gut microbiome, both direct toxicity and epidemiology studies diets effected by or contaminated with GBHs must be initiated and expanded immediately. Studies should include the effects of GBH-treated and GBH-free food diets on the composition of the human microbiome, as well as the secondary gut and systemic inflammatory conditions that might result from perturbations therein.
4. Human epidemiology studies should be performed to examine the putative link between a GBH exposed diet and micronutrient and vitamin deficiencies, which could result from both inhibition of bacterial synthesis pathways as well as direct mineral chelation [106, 107].
5. The testing of different formulations of GBHs must occur alongside and in addition to the testing of glyphosate alone at every level, and especially at the regulatory stage. Many regulatory agencies do not require retesting of chemical combinations, especially those at levels deemed "safe" on their own [108]. Despite this policy, it is well accepted that surfactant compounds applied along with glyphosate can act synergistically, increasing the potentially toxic compounds rate of cell entry or systemic absorption [49].
6. If glyphosate is a human carcinogen, the mechanisms by which it acts are likely obfuscated behind such complex mechanisms as nonmonotonic endocrine mimicry, indirect initiation of inflammation and genotoxicity through microbiome mediators, and slow accumulations over many years of exposure. These events can require large studies to elucidate with significant statistical power. Therefore, relying solely on the often used, three-tier system for genotoxicity risk assessment (generally Ames test, *in vitro* mammalian cell mutation, and *in vivo* chromosomal aberration) is insufficient. This approach is currently favored by such bodies as the OECD and the US EPA [109]. Results that do not adhere to this accepted framework are given less weight by both regulatory agencies and scientists associated with glyphosate-registering corporations. Additional

investigations of glyphosate with regards to specific mechanisms of toxicity in specialized models must be completed. For example, the DEL assay, a yeast-based test that drastically outperforms the traditional Ames test in carcinogen detection, could be used to examine induction of DSBs in exposed cells [110, 111].

7. With regards to carcinogenesis itself, animal results are often taken less seriously if they do not adhere to standard dose and number criteria such as those advanced by the OECD [112]. These criteria often give undue emphasis to traditional dose-responses at higher doses of the potential carcinogen, near to toxic levels. Low-dose, endocrine response mediated effects can remain overlooked. New regulatory testing protocols must be established taking into account low-dose interactions, especially those that establish whether a compound has a nonmonotonic dose response [57, 58, 113]. In addition, the scientific community should continue to critically examine every carcinogenesis study by its own merits, rather than disregarding studies with necessarily lower samples sizes based on arbitrary criteria such as the Klimisch score [114].

Conclusions

Economically, glyphosate is one of the most important chemical compounds in use worldwide, with increased agricultural yields resulting from its use. From this perspective, the skepticism shown towards results suggesting that its use carries long term risks to public health is both rational and reasonable. The use of glyphosate, and restrictions placed upon that use, must be carefully measured against economic, environmental, and health repercussions.

Over the last two decades, evidence has mounted that points towards significant potential risk associated with its use – use which only grows more widespread with each passing year. Farmers are now using greater amounts of glyphosates than in the past, at more time points during year, and in new roles, such as pre-harvest desiccation. As a result, levels of glyphosate and its degradation product AMPA continue to increase in both our food and our water supply. Glyphosate's potential for carcinogenic effects is complex in nature. Likely mechanisms of action, such as endocrine and microbiome disruption, appear to function outside traditional direct mechanisms of toxicity, which means that the establishment of past NOAELs may no longer be relevant. Unfortunately, much of the framework used by international regulatory agencies is still tailored to set "safe" levels only for compounds that function via classical dose-response mechanisms. Regardless of the results of further research, these agencies must modernize their standards of testing and regulation in order to properly respond to new science.

The potential ramifications of glyphosate use are significant enough that careful, measured, and unbiased peer-reviewed research is necessary to ascertain the magnitude of its effects. All possible mechanisms of action should be under investigation. In no cases should we assume that relying solely on past data is acceptable, especially when such data was gathered while understanding of the far-reaching effects of hormone mimicry and the microbiome was incomplete. The scientific and regulatory communities must reach consensus in an open manner that results in an appropriate response to any risk posed by glyphosate, as well as establishes a better, more comprehensive framework for herbicide safety assessment in the future.

Table 1 – EPA Allowable Glyphosate Residue for Selected Crops [115]

Crop	Tolerated ppm (mg/kg)
Sugarcane (cane)	2 ppm
Sugarcane (molasses)	30 ppm
Nongrass animal feed	400 ppm
Barley Bran	30 ppm
Soy	20 ppm

Table 2 - Studies Demonstrating Differential Effect of Glyphosate on Gut Microbiota

Study	Bacterial Strains	Role	Glyphosate Tolerance (MIC)	Notes
Shehata 2013 [87]	*Clostridium* sp.	pathogen	high, 5 mg/mL	chicken gut isolates
	Salmonella sp.	pathogen	high, 5 mg/mL	
	Escherichia Coli	commensal/pathogen	high, 1.2 mg/mL	
	Staphylococcus sp.	commensal/pathogen	med, 0.3 mg/mL	
	Lactobacillus sp.	beneficial	med, 0.6 mg/mL	
	Bifidobacterium sp.	beneficial	low, 0.075 mg/mL	
	Enterococcus sp.	commensal/beneficial	low, 0.15 mg/mL	
Schulz 1985 [116]	*Pseudomonas aeruginosa*	pathogen	high, ~ 1 mg/mL	
Ackermann 2015 [102]	*Clostridium botulinum*	pathogen	high, >1 mg/mL	Botulism toxin production increased at this level
	Ruminococcus sp.	ruminant fermenter	low , 0.01 mg/mL	
Krüger 2013 [89]	*Enterococcus* sp.	commensal/beneficial	low, 0.1 mg/mL	Capacity to inhibit *C. botulinum* toxin production decreased at this level
	Clostridium botulinum	pathogen	High, >1 mg/mL	

1. John, F., *N-phosphonomethyl-glycine phytotoxicant compositions*. 1974, Google Patents.
2. Carpenter, J. and L. Gianessi, *Herbicide tolerant soybeans: Why growers are adopting Roundup Ready varieties.* 1999.
3. Coupe, R.H. and P.D. Capel, *Trends in pesticide use on soybean, corn and cotton since the introduction of major genetically modified crops in the United States.* Pest management science, 2016. **72**(5): p. 1013-1022.
4. Atwood, D. and C. Paisley-Jones, *Pesticides industry sales and usage: 2008-2012 market estimates.* Biological and Economic Analysis Division. Office of Pesticide Programs. Office of Chemical Safety and Pollution Prevention. Washington, DC: US Environmental Protection Agency, 2017: p. 1-24.
5. Folmar, L.C., H. Sanders, and A. Julin, *Toxicity of the herbicide glyphosate and several of its formulations to fish and aquatic invertebrates.* Archives of Environmental Contamination and Toxicology, 1979. **8**(3): p. 269-278.
6. Klümper, W. and M. Qaim, *A meta-analysis of the impacts of genetically modified crops.* PloS one, 2014. **9**(11): p. e111629.
7. Holländer, H. and N. Amrhein, *The site of the inhibition of the shikimate pathway by glyphosate I. Inhibition by glyphosate of phenylpropanoid synthesis in buckwheat (Fagopyrum esculentum Moench).* Plant physiology, 1980. **66**(5): p. 823-829.
8. Steinrücken, H. and N. Amrhein, *The herbicide glyphosate is a potent inhibitor of 5-enolpyruvylshikimic acid-3-phosphate synthase.* Biochemical and biophysical research communications, 1980. **94**(4): p. 1207-1212.
9. Boocock, M.R. and J.R. Coggins, *Kinetics of 5-enolpyruvylshikimate-3-phosphate synthase inhibition by glyphosate.* Febs Letters, 1983. **154**(1): p. 127-133.
10. Amrhein, N., et al., *The site of the inhibition of the shikimate pathway by glyphosate II. Interference of glyphosate with chorismate formation in vivo and in vitro.* Plant physiology, 1980. **66**(5): p. 830-834.
11. Greim, H., et al., *Evaluation of carcinogenic potential of the herbicide glyphosate, drawing on tumor incidence data from fourteen chronic/carcinogenicity rodent studies.* Critical reviews in toxicology, 2015. **45**(3): p. 185-208.
12. Williams, A.L., R.E. Watson, and J.M. DeSesso, *Developmental and reproductive outcomes in humans and animals after glyphosate exposure: a critical analysis.* Journal of Toxicology and Environmental Health, Part B, 2012. **15**(1): p. 39-96.
13. Séralini, G.-E., et al., *RETRACTED: Long term toxicity of a Roundup herbicide and a Roundup-tolerant genetically modified maize.* Food and chemical toxicology, 2012. **50**(11): p. 4221-4231.
14. Schorsch, F., *Serious inadequacies regarding the pathology data presented in the paper by Séralini et al.(2012).* Food and Chemical Toxicology, 2013(53): p. 465-466.
15. Panchin, A.Y. and A.I. Tuzhikov, *Published GMO studies find no evidence of harm when corrected for multiple comparisons.* Critical reviews in biotechnology, 2017. **37**(2): p. 213-217.
16. Séralini, G., et al., *Conclusiveness of toxicity data and double standards.* Food and Chemical Toxicology, 2014. **69**: p. 357-359.

17. Séralini, G.-E., et al., *Republished study: long-term toxicity of a Roundup herbicide and a Roundup-tolerantgenetically modified maize.* Environmental Sciences Europe, 2014. **26**(1): p. 14.
18. Robinson, C., J. Latham, and R. Smith, *The Goodman affair: Monsanto targets the heart of science.* Independent Science News, 2013. **20**.
19. Myers, J.P., et al., *Concerns over use of glyphosate-based herbicides and risks associated with exposures: a consensus statement.* Environmental Health, 2016. **15**(1): p. 19.
20. Samsel, A. and S. Seneff, *Glyphosate, pathways to modern diseases IV: cancer and related pathologies.* J. Biol. Phys. Chem, 2015. **15**: p. 121-159.
21. Fritschi, L., et al., *Carcinogenicity of tetrachlorvinphos, parathion, malathion, diazinon, and glyphosate.* Red, 2015. **114**(2).
22. Williams, G.M., et al., *A review of the carcinogenic potential of glyphosate by four independent expert panels and comparison to the IARC assessment.* Critical reviews in toxicology, 2016. **46**(sup1): p. 3-20.
23. FAO, W., *Pesticide Residues in Food.* Joint FAO/WHO Meeting on Pesticide Residues, 2016.
24. Juncker, J.C., *Open letter: Review of the Carcinogenicity of Glyphosate by EChA, EFSA and BfR.* 2017.
25. Portier, C.J., et al., *Differences in the carcinogenic evaluation of glyphosate between the International Agency for Research on Cancer (IARC) and the European Food Safety Authority (EFSA).* J Epidemiol Community Health, 2016: p. jech-2015-207005.
26. Robinson, C., et al., *Conflicts of interest at the European Food Safety Authority erode public confidence.* J Epidemiol Community Health, 2013: p. jech-2012-202185.
27. Code, U.S., *Federal Insecticide, Fungicide, and Rodenticide Act*, in *7 USC 136*. 1985: United States.
28. EPA, *Revised Glyphosate Issue Paper: Evaluation of Carcinogenic Potential*, EPA, Editor. 2017, EPA Office of Pesticide Programs.
29. Eriksson, M., et al., *Pesticide exposure as risk factor for non-Hodgkin lymphoma including histopathological subgroup analysis.* International Journal of Cancer, 2008. **123**(7): p. 1657-1663.
30. De Roos, A.J., et al., *Cancer incidence among glyphosate-exposed pesticide applicators in the Agricultural Health Study.* Environmental Health Perspectives, 2005. **113**(1): p. 49.
31. Andreotti, G., et al., *Glyphosate use and cancer incidence in the Agricultural Health Study.* JNCI: Journal of the National Cancer Institute, 2018.
32. Mesnage, R., et al., *Potential toxic effects of glyphosate and its commercial formulations below regulatory limits.* Food and Chemical Toxicology, 2015. **84**: p. 133-153.
33. Grube, A., et al., *Pesticides industry sales and usage.* US EPA, Washington, DC, 2011.
34. Benbrook, C.M., *Trends in glyphosate herbicide use in the United States and globally.* Environmental Sciences Europe, 2016. **28**(1): p. 3.
35. Fernandez-Cornejo, J., et al., *Genetically engineered crops in the United States.* 2014.
36. Powles, S.B. and C. Preston, *Evolved glyphosate resistance in plants: biochemical and genetic basis of resistance.* Weed Technology, 2006. **20**(2): p. 282-289.
37. Dalley, C.D. and E.P. Richard Jr, *Herbicides as ripeners for sugarcane.* Weed science, 2010. **58**(3): p. 329-333.

38. Legendre, B., et al., *Timing of glyphosate applications, alternatives to the use of glyphosate and response of new varieties to glyphosate in maximizing the yield of sugar per acre of Louisiana sugarcane in 2005.* SUGARCANE RESEARCH ANNUAL PROGRESS REPORT, 2005: p. 182.
39. Johal, G. and D. Huber, *Glyphosate effects on diseases of plants.* European Journal of agronomy, 2009. **31**(3): p. 144-152.
40. Bøhn, T., et al., *Compositional differences in soybeans on the market: glyphosate accumulates in Roundup Ready GM soybeans.* Food chemistry, 2014. **153**: p. 207-215.
41. Coupe, R.H., et al., *Fate and transport of glyphosate and aminomethylphosphonic acid in surface waters of agricultural basins.* Pest management science, 2012. **68**(1): p. 16-30.
42. Battaglin, W., et al., *Glyphosate and its degradation product AMPA occur frequently and widely in US soils, surface water, groundwater, and precipitation.* JAWRA Journal of the American Water Resources Association, 2014. **50**(2): p. 275-290.
43. Krüger, M., et al., *Detection of glyphosate residues in animals and humans.* Journal of Environmental & Analytical Toxicology, 2014. **4**(2): p. 1.
44. Niemann, L., et al., *A critical review of glyphosate findings in human urine samples and comparison with the exposure of operators and consumers.* Journal für Verbraucherschutz und Lebensmittelsicherheit, 2015. **10**(1): p. 3-12.
45. Karunanayake, C.P., et al., *Hodgkin lymphoma and pesticides exposure in men: a Canadian case-control study.* Journal of agromedicine, 2012. **17**(1): p. 30-39.
46. Bolognesi, C., et al., *Biomonitoring of genotoxic risk in agricultural workers from five Colombian regions: association to occupational exposure to glyphosate.* Journal of Toxicology and Environmental Health, Part A, 2009. **72**(15-16): p. 986-997.
47. Kier, L.D. and D.J. Kirkland, *Review of genotoxicity studies of glyphosate and glyphosate-based formulations.* Critical reviews in toxicology, 2013. **43**(4): p. 283-315.
48. Bolognesi, C., et al., *Genotoxic activity of glyphosate and its technical formulation Roundup.* Journal of Agricultural and food chemistry, 1997. **45**(5): p. 1957-1962.
49. Mesnage, R., B. Bernay, and G.-E. Séralini, *Ethoxylated adjuvants of glyphosate-based herbicides are active principles of human cell toxicity.* Toxicology, 2013. **313**(2): p. 122-128.
50. Richard, S., et al., *Differential effects of glyphosate and roundup on human placental cells and aromatase.* Environmental health perspectives, 2005. **113**(6): p. 716.
51. Guilherme, S., et al., *European eel (Anguilla anguilla) genotoxic and pro-oxidant responses following short-term exposure to Roundup®—a glyphosate-based herbicide.* Mutagenesis, 2010. **25**(5): p. 523-530.
52. Çavaş, T. and S. Könen, *Detection of cytogenetic and DNA damage in peripheral erythrocytes of goldfish (Carassius auratus) exposed to a glyphosate formulation using the micronucleus test and the comet assay.* Mutagenesis, 2007. **22**(4): p. 263-268.
53. Guilherme, S., et al., *DNA and chromosomal damage induced in fish (Anguilla anguilla L.) by aminomethylphosphonic acid (AMPA)—the major environmental breakdown product of glyphosate.* Environmental Science and Pollution Research, 2014. **21**(14): p. 8730-8739.

54. Mañas, F., et al., *Genotoxicity of AMPA, the environmental metabolite of glyphosate, assessed by the Comet assay and cytogenetic tests.* Ecotoxicology and Environmental Safety, 2009. **72**(3): p. 834-837.
55. Council, N.R., *Risk assessment in the federal government: managing the process*. 1983: National Academies Press.
56. Jenkins, S., et al., *Chronic oral exposure to bisphenol A results in a nonmonotonic dose response in mammary carcinogenesis and metastasis in MMTV-erbB2 mice.* Environmental health perspectives, 2011. **119**(11): p. 1604.
57. Lagarde, F., et al., *Non-monotonic dose-response relationships and endocrine disruptors: a qualitative method of assessment.* Environmental Health, 2015. **14**(1): p. 13.
58. Vandenberg, L.N., et al., *Hormones and endocrine-disrupting chemicals: low-dose effects and nonmonotonic dose responses.* Endocrine reviews, 2012. **33**(3): p. 378-455.
59. Gasnier, C., et al., *Glyphosate-based herbicides are toxic and endocrine disruptors in human cell lines.* Toxicology, 2009. **262**(3): p. 184-191.
60. Akingbemi, B.T., et al., *Inhibition of testicular steroidogenesis by the xenoestrogen bisphenol A is associated with reduced pituitary luteinizing hormone secretion and decreased steroidogenic enzyme gene expression in rat Leydig cells.* Endocrinology, 2004. **145**(2): p. 592-603.
61. Walsh, L.P., et al., *Roundup inhibits steroidogenesis by disrupting steroidogenic acute regulatory (StAR) protein expression.* Environmental Health Perspectives, 2000. **108**(8): p. 769.
62. Thongprakaisang, S., et al., *Glyphosate induces human breast cancer cells growth via estrogen receptors.* Food and Chemical Toxicology, 2013. **59**: p. 129-136.
63. Jin, J., et al., *Sub-lethal effects of herbicides penoxsulam, imazamox, fluridone and glyphosate on Delta Smelt (Hypomesus transpacificus).* Aquatic Toxicology, 2018.
64. Armiliato, N., et al., *Changes in ultrastructure and expression of steroidogenic factor-1 in ovaries of zebrafish Danio rerio exposed to glyphosate.* Journal of Toxicology and Environmental Health, Part A, 2014. **77**(7): p. 405-414.
65. Petit, F., et al., *Two complementary bioassays for screening the estrogenic potency of xenobiotics: recombinant yeast for trout estrogen receptor and trout hepatocyte cultures.* Journal of Molecular Endocrinology, 1997. **19**(3): p. 321-335.
66. Xie, L., et al., *Evaluation of estrogenic activities of aquatic herbicides and surfactants using an rainbow trout vitellogenin assay.* Toxicological Sciences, 2005. **87**(2): p. 391-398.
67. Gandhi, J.S. and K.K. Cecala, *Interactive effects of temperature and glyphosate on the behavior of blue ridge two-lined salamanders (Eurycea wilderae).* Environmental toxicology and chemistry, 2016. **35**(9): p. 2297-2303.
68. Havenaar, R. and J.H. Huis, *Probiotics: a general view*, in *The Lactic Acid Bacteria Volume 1*. 1992, Springer. p. 151-170.
69. Isolauri, E., et al., *Probiotics: effects on immunity.* The American journal of clinical nutrition, 2001. **73**(2): p. 444s-450s.
70. Mulder, R., R. Havenaar, and J. Huis, *Intervention strategies: the use of probiotics and competitive exclusion microfloras against contamination with pathogens in pigs and poultry*, in *Probiotics 2*. 1997, Springer. p. 187-207.

71. Bezkorovainy, A., *Probiotics: determinants of survival and growth in the gut.* The American journal of clinical nutrition, 2001. **73**(2): p. 399s-405s.
72. Hsieh, P.-S., et al., *Potential of probiotic strains to modulate the inflammatory responses of epithelial and immune cells in vitro.* New Microbiol, 2013. **36**(2): p. 167-79.
73. Hamer, H.M., et al., *The role of butyrate on colonic function.* Alimentary pharmacology & therapeutics, 2008. **27**(2): p. 104-119.
74. Russell, W.R., et al., *Colonic bacterial metabolites and human health.* Current opinion in microbiology, 2013. **16**(3): p. 246-254.
75. Brüssow, H. and S.J. Parkinson, *You are what you eat.* Nature biotechnology, 2014. **32**(3): p. 243-245.
76. Di Cagno, R., et al., *Different fecal microbiotas and volatile organic compounds in treated and untreated children with celiac disease.* Applied and environmental microbiology, 2009. **75**(12): p. 3963-3971.
77. Di Cagno, R., et al., *Duodenal and faecal microbiota of celiac children: molecular, phenotype and metabolome characterization.* BMC microbiology, 2011. **11**(1): p. 219.
78. Jiang, W., et al., *Dysbiosis gut microbiota associated with inflammation and impaired mucosal immune function in intestine of humans with non-alcoholic fatty liver disease.* Scientific reports, 2015. **5**.
79. Mass, M., M. Kubera, and J.-C. Leunis, *The gut-brain barrier in major depression: intestinal mucosal dysfunction with an increased translocation of LPS from gram negative enterobacteria (leaky gut) plays a role in the inflammatory pathophysiology of depression.* Neuroendocrinology Letters, 2008. **29**(1): p. 117-124.
80. Sheehan, D., C. Moran, and F. Shanahan, *The microbiota in inflammatory bowel disease.* Journal of gastroenterology, 2015. **50**(5): p. 495-507.
81. Balkwill, F., K.A. Charles, and A. Mantovani, *Smoldering and polarized inflammation in the initiation and promotion of malignant disease.* Cancer cell, 2005. **7**(3): p. 211-217.
82. Tsuei, J., et al., *Bile acid dysregulation, gut dysbiosis, and gastrointestinal cancer.* Experimental Biology and Medicine, 2014. **239**(11): p. 1489-1504.
83. Yamamoto, M.L. and R.H. Schiestl, *Intestinal microbiome and lymphoma development.* Cancer journal (Sudbury, Mass.), 2014. **20**(3): p. 190.
84. Smoot, D.T., et al., *Influence of Helicobacter pylori on reactive oxygen-induced gastric epithelial cell injury.* Carcinogenesis, 2000. **21**(11): p. 2091-2095.
85. Group, E.S., *An international association between Helicobacter pylori infection and gastric cancer.* The Lancet, 1993. **341**(8857): p. 1359-1363.
86. Schönbrunn, E., et al., *Interaction of the herbicide glyphosate with its target enzyme 5-enolpyruvylshikimate 3-phosphate synthase in atomic detail.* Proceedings of the National Academy of Sciences, 2001. **98**(4): p. 1376-1380.
87. Shehata, A.A., et al., *The effect of glyphosate on potential pathogens and beneficial members of poultry microbiota in vitro.* Current microbiology, 2013. **66**(4): p. 350-358.
88. Kurenbach, B., et al., *Sublethal exposure to commercial formulations of the herbicides Dicamba, 2, 4-Dichlorophenoxyacetic acid, and Glyphosate cause changes in antibiotic susceptibility in Escherichia coli and Salmonella enterica serovar Typhimurium.* MBio, 2015. **6**(2): p. e00009-15.

89. Krüger, M., et al., *Glyphosate suppresses the antagonistic effect of Enterococcus spp. on Clostridium botulinum.* Anaerobe, 2013. **20**: p. 74-78.
90. Priestman, M.A., et al., *5-Enolpyruvylshikimate-3-phosphate synthase from Staphylococcus aureus is insensitive to glyphosate.* FEBS letters, 2005. **579**(3): p. 728-732.
91. Nielsen, L.N., et al., *Glyphosate has limited short-term effects on commensal bacterial community composition in the gut environment due to sufficient aromatic amino acid levels.* Environmental Pollution, 2018. **233**: p. 364-376.
92. Dosselaere, F. and J. Vanderleyden, *A metabolic node in action: chorismate-utilizing enzymes in microorganisms.* Critical reviews in microbiology, 2001. **27**(2): p. 75-131.
93. Rossi, M., A. Amaretti, and S. Raimondi, *Folate production by probiotic bacteria.* Nutrients, 2011. **3**(1): p. 118-134.
94. Ames, B.N., *DNA damage from micronutrient deficiencies is likely to be a major cause of cancer.* Mutation Research/Fundamental and Molecular Mechanisms of Mutagenesis, 2001. **475**(1): p. 7-20.
95. Blount, B.C., et al., *Folate deficiency causes uracil misincorporation into human DNA and chromosome breakage: implications for cancer and neuronal damage.* Proceedings of the National Academy of Sciences, 1997. **94**(7): p. 3290-3295.
96. Courtemanche, C., et al., *Folate deficiency and ionizing radiation cause DNA breaks in primary human lymphocytes: a comparison.* The FASEB journal, 2004. **18**(1): p. 209-211.
97. Clair, E., et al., *Effects of Roundup® and Glyphosate on Three Food Microorganisms: Geotrichum candidum, Lactococcus lactis subsp. cremoris and Lactobacillus delbrueckii subsp. bulgaricus.* Current microbiology, 2012. **64**(5): p. 486-491.
98. Chassaing, B., et al., *Dietary emulsifiers impact the mouse gut microbiota promoting colitis and metabolic syndrome.* Nature, 2015. **519**(7541): p. 92-96.
99. Viennois, E., et al., *Dietary emulsifier-induced low-grade inflammation promotes colon carcinogenesis.* Cancer research, 2016: p. canres. 1359.2016.
100. Chassaing, B., T. Van de Wiele, and A. Gewirtz, *O-013 Dietary Emulsifiers Directly Impact the Human Gut Microbiota Increasing Its Pro-inflammatory Potential and Ability to Induce Intestinal Inflammation.* Inflammatory bowel diseases, 2017. **23**: p. S5.
101. Chassaing, B., et al., *Dietary emulsifiers directly alter human microbiota composition and gene expression ex vivo potentiating intestinal inflammation.* Gut, 2017: p. gutjnl-2016-313099.
102. Ackermann, W., et al., *The influence of glyphosate on the microbiota and production of botulinum neurotoxin during ruminal fermentation.* Current microbiology, 2015. **70**(3): p. 374-382.
103. David, L.A., et al., *Diet rapidly and reproducibly alters the human gut microbiome.* Nature, 2014. **505**(7484): p. 559.
104. Code, U.S., *Food Quality Protection Act*, in *5 U.S.C. 554 Chapter 7*. 1996: U.S.A.
105. Antoniou, M., et al., *Teratogenic effects of glyphosate-based herbicides: divergence of regulatory decisions from scientific evidence.* J Environ Anal Toxicol S, 2012. **4**(006): p. 2161-0525.

106. Cakmak, I., et al., *Glyphosate reduced seed and leaf concentrations of calcium, manganese, magnesium, and iron in non-glyphosate resistant soybean.* European Journal of Agronomy, 2009. **31**(3): p. 114-119.
107. Mertens, M., et al., *Glyphosate, a chelating agent—relevant for ecological risk assessment?* Environmental Science and Pollution Research, 2018: p. 1-20.
108. Mesnage, R., et al., *Major pesticides are more toxic to human cells than their declared active principles.* BioMed research international, 2014. **2014**.
109. Cimino, M.C., *Comparative overview of current international strategies and guidelines for genetic toxicology testing for regulatory purposes.* Environmental and molecular mutagenesis, 2006. **47**(5): p. 362-390.
110. Brennan, R.J. and R.H. Schiestl, *Detecting carcinogens with the yeast DEL assay.* Genetic Recombination: Reviews and Protocols, 2004: p. 111-124.
111. Carls, N. and R.H. Schiestl, *Evaluation of the yeast DEL assay with 10 compounds selected by the International Program on Chemical Safety for the evaluation of short-term tests for carcinogens.* Mutation Research/Genetic Toxicology, 1994. **320**(4): p. 293-303.
112. Hsu, C.-H. and T. Stedeford, *Cancer risk assessment: chemical carcinogenesis, hazard evaluation, and risk quantification*. 2010: John Wiley & Sons.
113. vom Saal, F.S., et al., *Flawed experimental design reveals the need for guidelines requiring appropriate positive controls in endocrine disruption research.* Toxicological Sciences, 2010. **115**(2): p. 612-613.
114. Zoeller, R.T. and L.N. Vandenberg, *Assessing dose–response relationships for endocrine disrupting chemicals (EDCs): a focus on non-monotonicity.* Environmental Health, 2015. **14**(1): p. 42.
115. EPA, *Glyphosate; Tolerances for residues*, in *40 CFR 180.364*. 1980.
116. Schulz, A., A. Krüper, and N. Amrhein, *Differential sensitivity of bacterial 5-enolpyruvylshikimate-3-phosphate synthases to the herbicide glyphosate.* FEMS Microbiology Letters, 1985. **28**(3): p. 297-301.

Appendix II: BALR-6 Regulates Cell Growth and Cell Survival in B-Lymphoblastic Lymphoma

Rodríguez-Malavé et al. Molecular Cancer (2015) 14:214
DOI 10.1186/s12943-015-0485-z

Molecular Cancer

RESEARCH Open Access

BALR-6 regulates cell growth and cell survival in B-lymphoblastic leukemia

Norma I. Rodríguez-Malavé[1,2], Thilini R. Fernando[1], Parth C. Patel[1], Jorge R. Contreras[1,2], Jayanth Kumar Palanichamy[1,7], Tiffany M. Tran[1], Jaime Anguiano[1], Michael J. Davoren[5,6], Michael O. Alberti[1], Kimanh T. Pioli[1], Salemiz Sandoval[1], Gay M. Crooks[1,2,3,4] and Dinesh S. Rao[1,2,3,4*]

Abstract

Background: A new class of non-coding RNAs, known as long non-coding RNAs (lncRNAs), has been recently described. These lncRNAs are implicated to play pivotal roles in various molecular processes, including development and oncogenesis. Gene expression profiling of human B-ALL samples showed differential lncRNA expression in samples with particular cytogenetic abnormalities. One of the most promising lncRNAs identified, designated B-ALL associated long RNA-6 (BALR-6), had the highest expression in patient samples carrying the MLL rearrangement, and is the focus of this study.

Results: Here, we performed a series of experiments to define the function of BALR-6, including several novel splice forms that we identified. Functionally, siRNA-mediated knockdown of BALR-6 in human B-ALL cell lines caused reduced cell proliferation and increased cell death. Conversely, overexpression of BALR-6 isoforms in both human and mouse cell lines caused increased proliferation and decreased apoptosis. Overexpression of BALR-6 in murine bone marrow transplantation experiments caused a significant increase in early hematopoietic progenitor populations, suggesting that its dysregulation may cause developmental changes. Notably, the knockdown of BALR-6 resulted in global dysregulation of gene expression. The gene set was enriched for leukemia-associated genes, as well as for the transcriptome regulated by Specificity Protein 1 (SP1). We confirmed changes in the expression of SP1, as well as its known interactor and downstream target CREB1. Luciferase reporter assays demonstrated an enhancement of SP1-mediated transcription in the presence of BALR-6. These data provide a putative mechanism for regulation by BALR-6 in B-ALL.

Conclusions: Our findings support a role for the novel lncRNA BALR-6 in promoting cell survival in B-ALL. Furthermore, this lncRNA influences gene expression in B-ALL in a manner consistent with a function in transcriptional regulation. Specifically, our findings suggest that BALR-6 expression regulates the transcriptome downstream of SP1, and that this may underlie the function of BALR-6 in B-ALL.

Keywords: lncRNA, B-ALL, MLL, SP1, Microarray, Leukemia, RNA, Non-coding RNA

Background

The human genome produces thousands of non-coding transcripts [1]. These include the recently described class of long non-coding RNAs (lncRNAs), which have distinct chromatin signatures and epigenetic marks, designating them as unique structures that are conserved in mammals [2, 3]. More recently, comparison of lncRNA expression in zebrafish to that of mammals has suggested that although these structures retain limited overall sequence conservation among vertebrates, they show strong conservation of short stretches of sequence, chromosomal synteny and functional conservation [4]. Prior studies have shown that lncRNAs play a variety of roles in the regulation of transcription, splicing and miRNA function [5–7]. This may not be an exhaustive description of the functions of lncRNAs, as new functions are being discovered in other cellular processes [8, 9]. As might be expected, considering their roles in critical cellular functions, lncRNAs have been found to be dysregulated in cancer, with

* Correspondence: drao@mednet.ucla.edu
[1]Department of Pathology and Laboratory Medicine, UCLA, Los Angeles, USA
[2]Cellular and Molecular Pathology Ph.D. Program, UCLA, Los Angeles, USA
Full list of author information is available at the end of the article

functional roles in oncogenesis described for a handful of lncRNAs so far [10–13].

B-lymphoblastic leukemia (B-acute lymphoblastic leukemia, B-ALL) is a malignancy of precursor B-cells harboring mutations and translocations that result in dysregulated gene expression [14, 15]. We have recently completed a comprehensive description of lncRNAs in B-ALL and analyzed the association of lncRNA expression with clinicopathologic parameters. Our study showed differential lncRNA expression in samples with particular cytogenetic abnormalities [16]. One of the lncRNAs from our study, designated B-ALL associated long RNA-6 (BALR-6), was significantly upregulated in all subsets of patient samples when compared to normal CD19+ cells. Interestingly, the highest expression of BALR-6 was seen in patient samples carrying the MLL rearrangement [16]. MLL rearranged B-ALL cases have a very poor prognosis and occur in infants, making them particularly hard to treat [17].

Located on chromosome 3p24.3 in humans, *BALR-6* exists in a syntenic gene block with neighboring genes *SATB1* and *TBC1D5* that is conserved in several vertebrate species (Fig. 1a, b and d) [16]. Analysis of publically available data from the Broad Institute/ENCODE shows H3K4m3 and H3K36m3 modifications along the promoter and gene body at *LOC339862*, where BALR-6 resides, indicating that it is a transcriptional element (Fig. 1a) [4, 16, 18–20]. Alternative splicing analysis by the Swiss Institute of Bioinformatics predicted multiple transcripts expressed at this gene locus (Additional file 1: Figure S1A) [21]. Moreover, 100 Vertebrate PhastCons analyses of the *BALR-6* locus demonstrated significant conservation of the gene body, suggesting a functional transcript (Fig. 1b) [22].

To further study this lncRNA we undertook loss-of-function analyses in B-ALL cell lines and gain-of-function analyses in vivo. We found that BALR-6 is a pro-survival factor for B-ALL cell lines, and that its knockdown led to decreased growth and increased apoptosis of these cells. In vivo, overexpression of BALR-6 led to an alteration of hematopoiesis with a shift to more immature progenitor populations. Gene expression analyses of knockdown cell lines showed a differentially expressed gene set in BALR-6 knockdown cells, with enrichment for SP1 transcriptional targets and leukemogenic genes. Finally, luciferase assays demonstrated an increase in transcriptional activity when SP1 and BALR-6 were co-expressed. Together, these findings point to a role for BALR-6 in cellular survival, leukemogenesis and highlight the role of novel elements of gene regulation in B-ALL.

Results

BALR-6 knockdown inhibits proliferation of human B-ALL cell lines

To comprehensively study the function for this novel lncRNA, we first characterized the transcripts originating at the genomic locus corresponding to *BALR-6*. Using RS4;11 cell line mRNA, Rapid Amplification of cDNA Ends (RACE) uncovered multiple isoforms; from these, three were cloned and sequenced corresponding to the genomic locus as shown (Additional file 1: Figure S1A-B). Northern Blot analysis of RS4;11 DNAse treated RNA revealed the expression of two isoforms containing exon 3 and exon 5 sequences, one sized at ~3.8 Kb and the other at ~1.2 Kb (Additional file 1: Figure S1C). The annotated mRNA and new alternative splice forms, including unannotated exons, were confirmed as depicted in Fig. 1c. Isoform 1 contains several small open reading frames (ORFs), however no Kozak sequences are found in their initial ATG region, and the predicted ORFs do not resemble any known functional proteins or peptide [23]. Isoforms 2 and 3 lacked open reading frames and translation initiation sites as evaluated by EMBOSS Transeq, predicting them to be non-coding transcripts (Additional file 1: Figure S1D).

To map the murine homologous transcript, we carried out 5′RACE and 3′RACE using mRNA extracted from murine pre B-ALL cell line 70Z/3. The sequences uncovered matched the human BALR-6 sequence, confirming that there is a murine transcript originating from this same locus (Additional file 1: Figure S1E). Further analysis by BLAT showed genomic conservation of syntenic blocks in a variety of vertebrates, including *Xenopus tropicalis* (Fig. 1d). Together, these data demonstrate a highly conserved, functional and complex gene locus that expresses multiple non-coding transcripts, some yet to be discovered. During normal B cell development, BALR-6 is dynamically expressed, with high expression in pre-B cells and subsequent downregulation (Fig. 2a). This suggests that the high expression of BALR-6 in B-ALL could represent a stage-specific expression pattern in leukemia derived from early stages of B-cell development. To elucidate a cellular function for BALR-6, we first evaluated the expression levels of the transcripts in human B-ALL cell lines. BALR-6 expression was highest in RS4;11 cells and MV(411) cells, which carry the MLL-AF4 rearrangement, when compared to other lines (Fig. 2b). Additionally, RS4;11 cells treated with bromodomain and extra-terminal (BET) motif binding protein inhibitor I-BET151 [24] showed decreased levels of BALR-6 in a dose-dependent manner (Fig. 2c). Given that I-BET151 has previously been shown to inhibit transcription downstream of MLL, we propose that BALR-6 expression is induced by MLL, although this effect may not be entirely specific to MLL-AF4.

Using the approach described previously, siRNAs against the splice junctions between exons of BALR-6 were cloned into a mmu-miR-155 expression cassette (Additional file 1: Figure S2A) [4, 16, 25, 26]. We observed knockdown of all the identified transcripts in

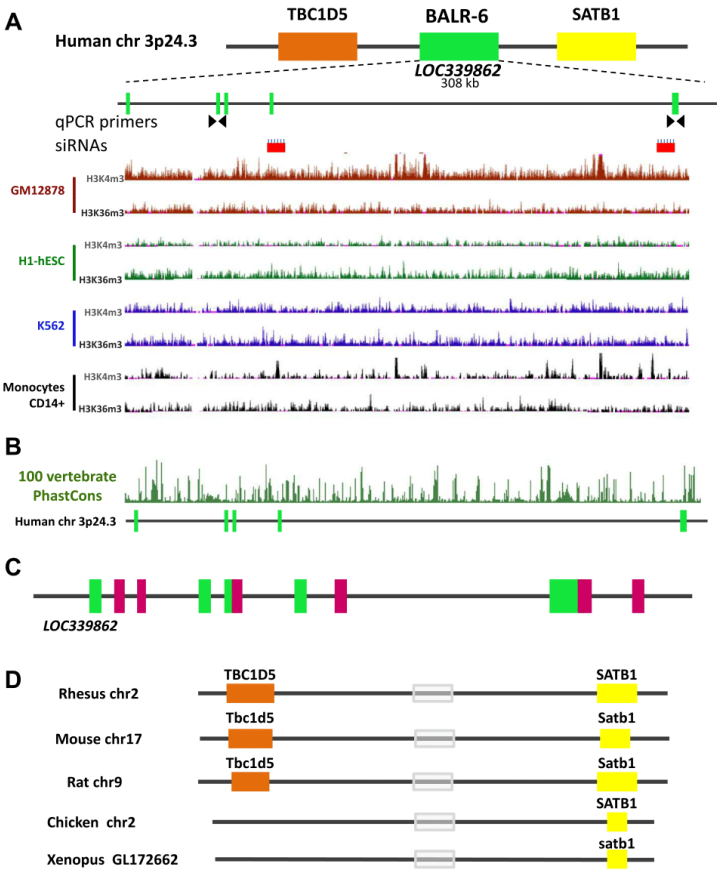

Fig. 1 Molecular characterization of *BALR-6*. **a** Top: Chromosomal location of *BALR-6* in the human genome, surrounding genes, qPCR primers, siRNAs, known annotated exons (*green boxes*), known introns (*black lines*) are shown. Bottom: Chip-Seq histone modification map from the Broad institute/ENCODE, taken from UCSC genome browser, shows H3K4m3 and H3K36m3 patterns at *LOC339862* in four different cell types indicating active transcription of the lncRNA. **b** The 100 Vertebrate PhastCons plot from the UCSC whole-genome shows conserved regions among 98 vertebrates including mice and zebrafish throughout the locus. **c** RACE discovered unannotated exons (*magenta*) depicted with known annotated exons (*green*) at *LOC339862*. **d** Schematic depicting genomic conservation of the syntenic block among multiple vertebrates, as analyzed by BLAT. Grey box indicates location of homology to *BALR-6*

multiple B-ALL cell lines (Fig. 2d and Additional file 1: Figure S2B). Transduced B-ALL cells showed a reduction in proliferation as early as 48 h after plating, with consistent reduction in proliferation observed over the full duration of the assay (up to 144 h) (Fig. 2e, f and Additional file 1: Figure S2C). siRNA-transduced B-ALL cells had significantly higher levels of apoptosis, as measured by AnnexinV, when compared with vector-transduced lines (Fig. 2g, h and Additional file 1: Figure S2D). Flow cytometry demonstrated that the siRNA2-transduced RS4;11 cell lines had an increase in Sub-G0 cells and a decrease in all other cell stages, consistent with increased apoptosis and decreased flux through the cell cycle (Fig. 2i). Together, these findings suggest a modest yet conserved role for BALR-6 in the regulation of B-ALL cell survival and proliferation.

Constitutively expressed BALR-6 supports cell survival and proliferation

To examine the effects of BALR-6 gain of function, we overexpressed the previously identified isoforms in the human B-ALL cell line Nalm-6, which has relatively low

endogenous levels of the transcript (Figs. 2b and 3a). Gene transfer was conducted via a lentiviral expression system that has proven successful in our previous studies (Additional file 1: Figure S2E) [16]. Constitutive overexpression of BALR-6 Isoforms 2 and 3 led to a significant increase in proliferation as measured by MTS (Fig. 3c). In addition to an observed increase in overall growth rate, BALR-6 Isoforms 2 and 3 caused an increase in S phase cells and G2-M cells (Fig. 3d). Furthermore, AnnexinV staining showed significantly lower numbers of apoptotic cells under basal growth conditions in cell lines overexpressing any of the BALR-6 isoforms (Additional file 1: Figure S2G).

To overexpress BALR-6 in mouse cells, we constructed a set of MSCV-based bicistronic vectors (Fig. 3b, Additional file 1: Figure S2F). Successful overexpression of these constructs in murine pre B-ALL 70Z/3 cells led to a modest increase in proliferation (Fig. 3e and f). Cell cycle analysis of these lines showed an increase of S phase cells, G2-M cells (in Isoform 3 overexpressing lines) and a reduction in Sub-G0 cells, similar to the effects in Nalm-6 cells (Fig. 3g and h). Analysis by AnnexinV staining confirmed the lower number of apoptotic cells in Isoform 3 expressing cell lines (Additional file 1: Figure S2H). Moreover, these 70Z/3 Isoform 3 overexpression lines were less vulnerable to prednisolone-induced apoptosis (Additional file 1: Figure S2I). Conversely, siRNA-transduced RS4;11 cells were more prone to prednisolone-induced apoptosis (Additional file 1: Figure S2I). Therefore, knockdown and overexpression of BALR-6 had opposing phenotypes in B-ALL cell lines, and gain-of-function phenotypes were conserved in both human and mouse cells.

Enforced BALR-6 expression promotes expansion of hematopoietic progenitor populations in vivo

Since BALR-6 is highly expressed in B-ALL, we tested the effects of constitutive expression in an in vivo model [16]. 5-FU enriched bone marrow was transduced with retrovirus expressing the BALR-6 Isoform 3 and transplanted into lethally irradiated hosts (Fig. 3 and Additional file 1: Figure S2F, 2H). Mice were followed with peripheral bleeds for 16 weeks and then sacrificed for analysis. Peripheral white blood cell counts were not statistically different between the control and experimental groups. However, mice with enforced expression of BALR-6 showed a trend towards lower red blood cell counts, hematocrit and platelet counts (Additional file 1: Figure S3A). Flow cytometry revealed a lower percentage of CD11b + myeloid cells and a higher percentage of B220+ B-cells, but no difference in CD3ε + T-cell percentage in the eGFP+ population of experimental mice (Additional file 1: Figure S3B-C).

Mice were sacrificed following 4 months of reconstitution. Gross analysis showed no changes in the thymus, spleen, livers or kidneys. Microscopic inspection of hematoxylin and eosin – stained tissues did not reveal any differences (Additional file 1: Figure S3D). In the bone marrow, qRT-PCR confirmed successful overexpression of BALR-6 (Additional file 1: Figure S4A-B). Analysis by flow cytometry revealed an increase in precursor cell populations in the eGFP+ population of the experimental mice, when compared to the control group (Fig. 4a and b, Additional file 1: Figure S5C). After exclusion of differentiated cells in the bone marrow, we observed increased relative proportion of Lin-Sca1 + c-Kit + (LSK) cells, hematopoietic stem cells (HSCs) and lymphoid-primed multipotent progenitors (LMPPs) in mice overexpressing BALR-6 (Fig. 4a and b). An increase in the relative population of Lin-Sca1^{lo}c-Kit^{lo} cells and a trend towards increased relative population of common lymphoid progenitors (CLPs) was also observed (Additional file 1: Figure S4C). The developmental pathway of B-cells in the bone marrow was investigated by the method of Hardy et al. [27]. Once again, trends towards higher relative proportions of these B-cell developmental stages were observed (fractions A-F, Additional file 1: Figure S4D). Taken together, these results suggest that BALR-6 overexpression leads to an enrichment of early developmental stage cells in murine bone marrow, indicating that its expression confers a survival advantage or increased proliferation for cells in these earlier stages.

BALR-6 regulates expression of genes involved in multiple biological processes

At the molecular level, several studies have demonstrated that many lncRNAs act as transcriptional regulators [5, 11, 23, 28, 29]. To explore whether or not BALR-6 regulates gene expression, RNA isolated from knockdown cell lines was analyzed by microarray [30, 31]. Upon siRNA mediated knockdown of BALR-6, 2499 probes showed differential expression. Of these, 1862 unambiguously mapped to 1608 unique Entrez Gene IDs. Unsupervised hierarchical clustering analysis identified differentially expressed genes in the siRNA-expressing cell lines (Fig. 5a).

Further data analysis was carried out using WebGESTALT [32, 33]. Gene Ontology (GO) slim classification of differentially expressed genes by molecular function was utilized to provide insight into the pathways in which BALR-6 is involved, with protein binding function category having the most dysregulated genes (Fig. 5b). A number of biological processes, as annotated in the GO database, were significantly dysregulated in BALR-6 knockdown cell lines, including cell death and cell proliferation (Fig. 5c). Disease associated enrichment analysis, which was inferred using GLAD4U, showed an enrichment of genes known to be dysregulated in various disease states (Fig. 5e). Of the 38 significantly associated

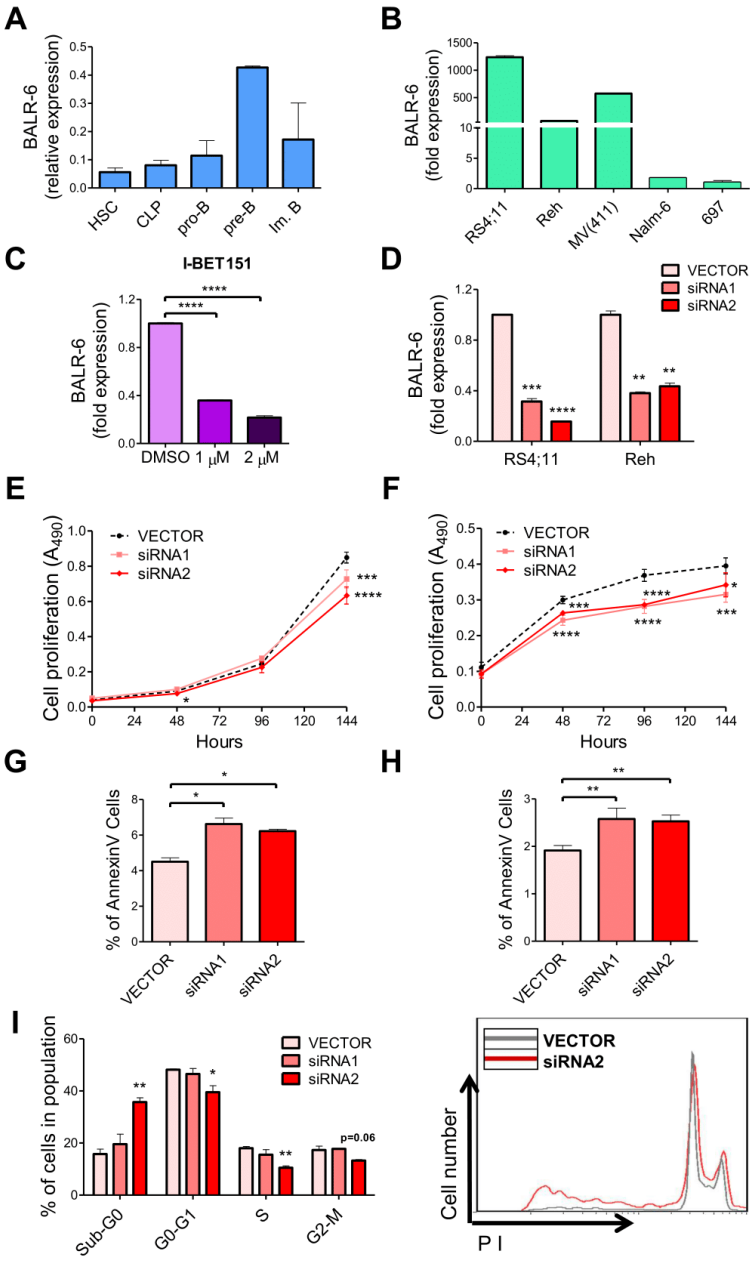

Fig. 2 (See legend on next page.)

(See figure on previous page.)
Fig. 2 BALR-6 knockdown reduces cell proliferation and increases apoptosis in human B-ALL cells. **a** BALR-6 expression in human bone marrow B-cell subsets by qRT-PCR. Normalized to ACTIN. **b** Quantitation of BALR-6 expression in human B-ALL cell lines by qRT-PCR confirming elevated levels in MLL translocated cell lines RS4;11, and MV(411). Normalized to ACTIN. **c** RS4;11 cell lines treated with 1 μM, and 2 μM of I-BET151 inhibitor for 36 h, presented a decrease in BALR-6 expression levels. Normalized to ACTIN. **d** qRT-PCR quantification of BALR-6 in RS4;11 and Reh cell lines transduced with vector control, siRNA1 or siRNA2. Normalized to ACTIN. **e**, **f** Decreased cell proliferation, upon siRNA mediated knockdown of BALR-6 in RS4;11 cells **e**, and Reh cells **f** as measured by MTS. **g**, **h** AnnexinV staining showed that siRNA mediated knockdown of BALR-6 in RS4;11 cells **g**, and Reh cells **h** resulted in an increase of apoptosis. **i** Propidium iodide staining of RS4;11 knockdown cell lines showed an increase in Sub-G0 and a decrease in G0-G1, S and G2-M cells. Representative histogram of (**i**) confirms cell cycle changes by siRNA2, shown to the right. HSC, hematopoietic stem cell; CLP, common lymphoid progenitor; pro-B, progenitor B; pre-B, precursor B; DMSO, dimethyl sulfoxide. Evaluations were made using a two-tailed *T*-test, $p < 0.05$ (*); $p < 0.005$ (**); $p < 0.0005$ (***); $p < 0.0001$ (****)

disease states, 14 were of leukemic origin. Transcription factor enrichment analysis showed a significant enrichment of genes that are predicted targets of SP1, among other transcription factors (Fig. 5d). Taken together, these data revealed the biological importance of BALR-6. A detailed description of the microarray analyses can be found in the methods.

SP1 transcriptome is modulated by BALR-6

As indicated by the transcription factor enrichment analysis, we confirmed that the expression SP1 and CREB1, a target and interactor of SP1, were dysregulated upon BALR-6 knockdown (Fig. 6a). The strongest phenotype was seen in the siRNA2-mediated knockdown, which also showed the strongest cellular phenotypes in the majority of pre B-ALL cell lines (Figs. 2d, i and 6a, Additional file 1: Figure S2B-D and Figure S5A-B). Conversely, increased levels of SP1 and CREB1 correlated with overexpression of BALR-6 isoforms in both human and murine cell lines (Nalm-6 and 70Z/3) (Fig. 6b).

To confirm our findings, a second microarray analysis was carried out with technical duplicates of RS4;11 cell lines transduced with empty vector or siRNA2. 2756 probes showed differential expression. Of these, 2280 unambiguously mapped to 2128 Entrez Gene IDs and were analyzed by hierarchical clustering (Additional file 1: Figure S6A). Enrichment analysis in WebGESTALT revealed similar GO slim classifications (Additional file 1: Figure S6B-C), and transcription factor target enrichment analysis confirmed the significant enrichment of SP1 targets seen previously (Fig. 5d, Additional file 1: Figure S6D). Additionally, enrichment of CREB1 targets was significant (Additional file 1: Figure S6D). Notably, leukemic diseases were the only ones significantly enriched in the disease association analysis (Additional file 1: Figure S6E). Together, these findings indicated a consistent change in the transcriptome, particularly downstream of SP1, upon knockdown of BALR-6 in MLL rearranged B-ALL.

To further understand the relationship of BALR-6 and SP1, we examined promoter regions of known SP1 targets (CREB1 and p21) and cloned these sequences into the luciferase reporter vector, pGL4.11 (Fig. 6c). The CREB1 promoter contained 7 putative SP1 binding sites, while the p21 promoter contained 6 such sites (Additional file 1: Figure S5C-D). Luciferase reporter assays in HEK 293 T cells with constitutive expression of SP1, Isoform 1, Isoform 3 or a combination of these vectors, revealed increased luciferase activity in both promoters (Fig. 6d and e). Notably, when SP1 and BALR-6 were co-overexpressed, we noted a strong increase in transcriptional activity with both the CREB1 and p21 promoter.

Discussion

The discovery of lncRNAs has revolutionized how we think about gene expression. The genomic organization of many lncRNAs is indeed complex. Some are found in regions overlapping with protein coding genes, while others that are exclusively intergenic [2, 4]. Some lncRNAs contain microRNAs within either their exonic or intronic sequence [34, 35]. Here, we have characterized several isoforms of a lncRNA that is overexpressed in leukemia and shows dynamic expression in hematopoietic development [16]. Expressed from a locus adjacent to genes important in lymphocyte development, BALR-6 itself is dynamically regulated during human B-cell development [36–38]. Our work significantly adds to the known repertoire of RNA molecules that are expressed from this locus, and several of these appear to be functional within a cellular context.

In this manuscript, we describe the cellular function of a second lncRNA that was discovered as being overexpressed in MLL-translocated B-ALL. In some ways, BALR-6 shows some similarities with the other lncRNA we studied, BALR-2 [16]. Indeed, knockdown of both lncRNAs led to decreased cell growth and increased apoptosis, and overexpression led to increased growth and a partial resistance to prednisolone treatment. These findings are not altogether surprising given that these lncRNAs may be contributing to the poor clinical behavior of an aggressive cytogenetic subtype of B-ALL [17]. However, there are important differences between these lncRNAs—the genomic locus for BALR-6 is more complex, there are multiple isoforms and no comparable murine transcript is described in publically available databases. Nonetheless, we have obtained fragments of a

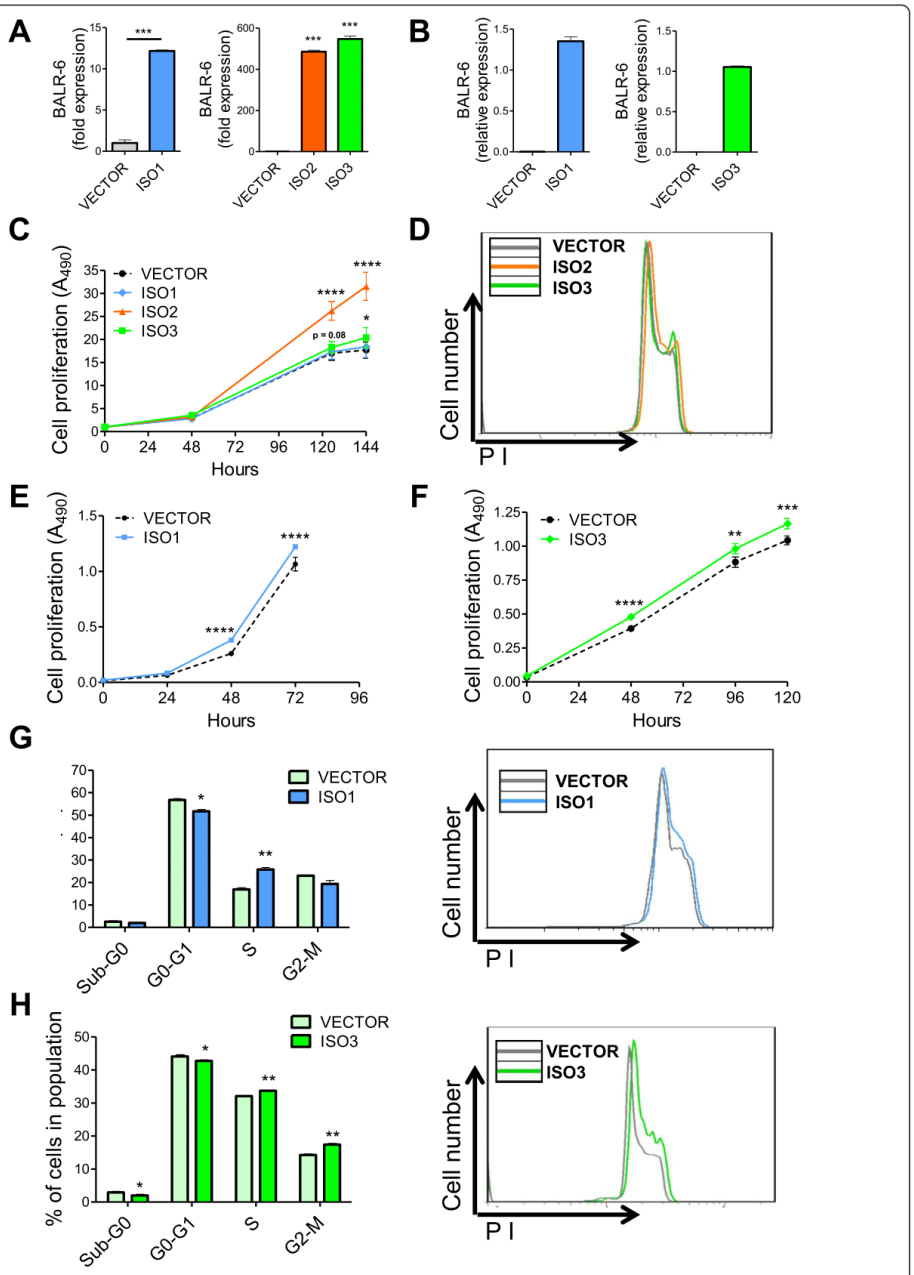

Fig. 3 (See legend on next page.)

(See figure on previous page.)
Fig. 3 BALR-6 overexpression increases proliferation in human Nalm-6 and murine 70Z/3 cells. **a** qRT-PCR quantitation of BALR-6 isoform expression in Nalm-6 human pre B-ALL cell line. Normalized to ACTIN. **b** qRT-PCR quantification of BALR-6 isoforms in 70Z/3 mouse pre B-ALL cell line. Normalized to Actin (ISO1) or L32 (ISO3). **c** Increased cell proliferation in BALR-6 overexpressing Nalm-6 cell lines, as measured by MTS. **d** Representative histogram of Nalm-6 overexpression lines, stained with propidium iodide, shows an increase in S phase cells and G2-M cells. **e**, **f** Increased cell proliferation in BALR-6 Isoform 1 (**e**) and Isoform 3 (**f**) overexpressing 70Z/3 cell lines, as measured by MTS. **g**, **h** Propidium iodide staining of 70Z/3 cells overexpressing BALR-6 Isoform 1 (**g**) and Isoform 3 (**h**), shows a consistent increase in G2-M cells, and a decrease in Sub-G0 cells. Representative histogram of figures (**g-h**) confirmed the increase in cells in the G2-M when compared to the empty vector, shown to the right. ISO1, Isoform 1; ISO2, Isoform 2; ISO3, Isoform 3. Evaluations were made using a two-tailed *T*-test, $p < 0.05$ (*); $p < 0.005$ (**); $p < 0.0005$ (***); $p < 0.0001$ (****)

low-expression transcript from murine hematopoietic cell lines that encoded portions homologous to human BALR-6. Further characterization of the murine transcripts will be the goal of future studies.

Significantly, our study is amongst the few characterizations of lncRNA dysregulation in the hematopoietic system [16, 39–41]. LncRNAs have been ascribed functions in lymphopoiesis, myelopoiesis and erythropoiesis [42–45]. Additionally, their differential expression has been described in peripheral T-cell subsets [46]. Here, we discovered the effect of BALR-6 overexpression on early hematopoietic progenitors in the marrow, including LSK cells, HSCs and LMPPs. Constitutive expression of BALR-6 isoforms led to increased survival or proliferation of normally transient bone marrow progenitor cells. Furthermore, Hardy fractions showed a trend towards being increased when compared to control, particularly those that developmentally precede the large pre B-cell stage (fraction C', early pre-B). The relative percentages of more mature B-lineage cells downstream of these developmental stages are largely normal. Despite increased proportions of early progenitor cells, passage through a checkpoint (such as the pre-BCR checkpoint) may reduce cell numbers back to baseline. This suggests that the function of BALR-6 in vivo may be in directing differentiation and adequate lymphoid cell development. The upregulation of this lncRNA causes a survival or proliferative advantage, a hallmark of leukemogenesis. Coupling BALR-6 overexpression with an appropriate oncogenic co-stimulus may lead to full-blown leukemogenesis or enhancement thereof, and this is currently an active area of investigation in the laboratory.

In line with a function in promoting the survival of early hematopoietic progenitors, BALR-6 clearly affects proliferation in cell line experiments. Upon siRNA mediated knockdown, we saw reduced cell proliferation and increased cell death. We observed the opposite effect when we constitutively expressed BALR-6 in human and murine B-ALL cell lines. Moreover, similar mechanisms may be operant in B-ALL with MLL translocations, and loss-of-function experiments in primary patient samples and mouse models of MLL-driven leukemia are areas for further investigation.

Given prior reports of lncRNAs serving to regulate transcriptional complexes, our finding that BALR-6 knockdown causes changes in the SP1 transcriptome is compelling. SP1 is a transcriptional regulator that is associated with dysregulated cell cycle arrest in multiple myeloma [47–49]. CREB1 is a well-known proto-oncogene that promotes cellular proliferation in hematopoietic cells [50, 51]. Here we demonstrate that SP1-mediated transcription at the CREB1 and p21 promoters are positively regulated by BALR-6, providing a putative mechanism for our observations of BALR-6's role in B-ALL.

Conclusions

In this study, we demonstrate that the MLL-AF4-dysregulated lncRNA, BALR-6, plays a role in cell survival and regulates hematopoietic progenitors. At the molecular level, BALR-6 regulates the transcriptome of B-ALL cell lines, likely through regulating SP1-mediated transcription. In summary, our study has several novel and unique findings that help uncover a role for a poorly understood class of molecules in a pathogenetic process. This will undoubtedly have impacts on our understanding of molecular biology within cancer cells.

Methods

Cloning and cell culture

mmu-miR-155 formatted siRNAs were cloned into BamHI and XhoI sites in the pHAGE2-CMV-ZsGreen-WPRE vector using the strategy that we have previously described to generate knockdown vectors [16, 25, 26, 52]. Using the sequence information from 5′ and 3′ RACE products we cloned full length transcripts into an MSCV-based bicistronic viral vector between the BamHI and XhoI sites, as described previously and into a pHAGE6-UBC-ZsGreen-CMV-LNC (P6UZCL) variant of the third generation lentiviral vector system, between the NotI and BamHI sites [16, 52]. Primer sequences used are listed in Additional file 2: Table S1 or mentioned previously [16]. RS4;11 and MV(411), (MLL-AF4-translocated; ATCC CRL-1873 and CRL-9591), Reh (TEL-AML1-translocated; CRL-8286), 697 (E2A-PBX1-translocated), Nalm-6, 70Z/3 (ATCC TIB-158) murine pre B-cell leukemic cell line, and the HEK 293 T cell line (ATCC CRL-11268) were grown

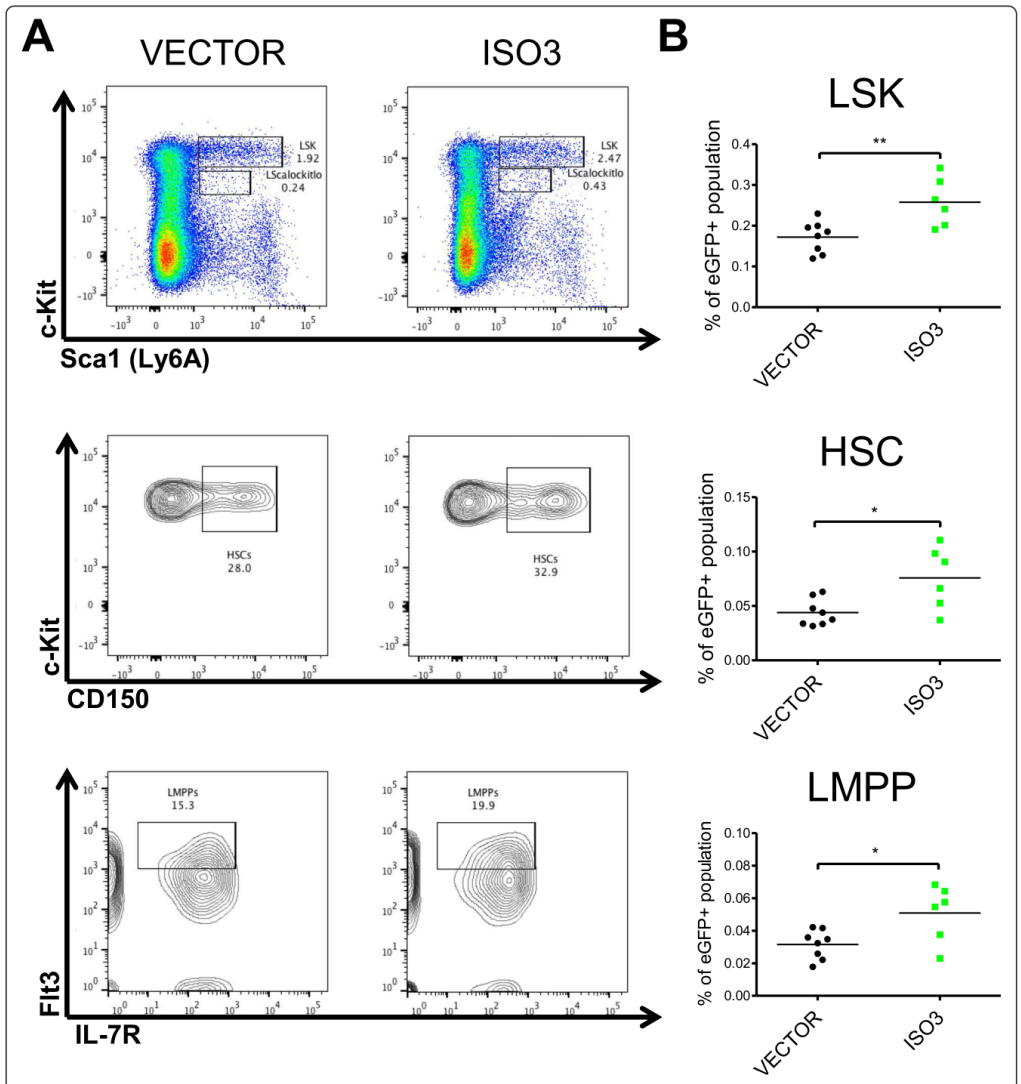

Fig. 4 BALR-6 overexpression causes an increase in hematopoietic precursor cells in vivo. **a** Representative FACS plots of hematopoietic progenitor populations LSK, HSC and LMPP in bone marrow transfer mice. **b** Quantitation of progenitor populations showing a significant increase in experimental mice when compared to control. Number of mice used in this analysis: VECTOR, $n = 8$; ISO3, $n = 6$. ISO3, Isoform 3; HSC, hematopoietic stem cell; LMPP, lymphoid primed multipotent progenitor; LSK, lineage- Sca1+ c-Kit+. Evaluations made using a two-tailed *T*-test, $p < 0.05$ (*); $p < 0.005$ (**)

in their corresponding media at 37 °C in a 5 % CO_2 incubator as previously described [16, 53].

Rapid amplification of cDNA ends (RACE)

To determine the 5′ and 3′ transcript ends of the lncRNAs, we performed RACE using First Choice RLM-RACE kit (Ambion). Using the sequence information from 5′ and 3′ RACE products, we cloned full length transcripts into P6UZCL, and into the MSCV viral vector. Primer sequences used and isoform sequences obtained are listed in Additional file 2: Table S1.

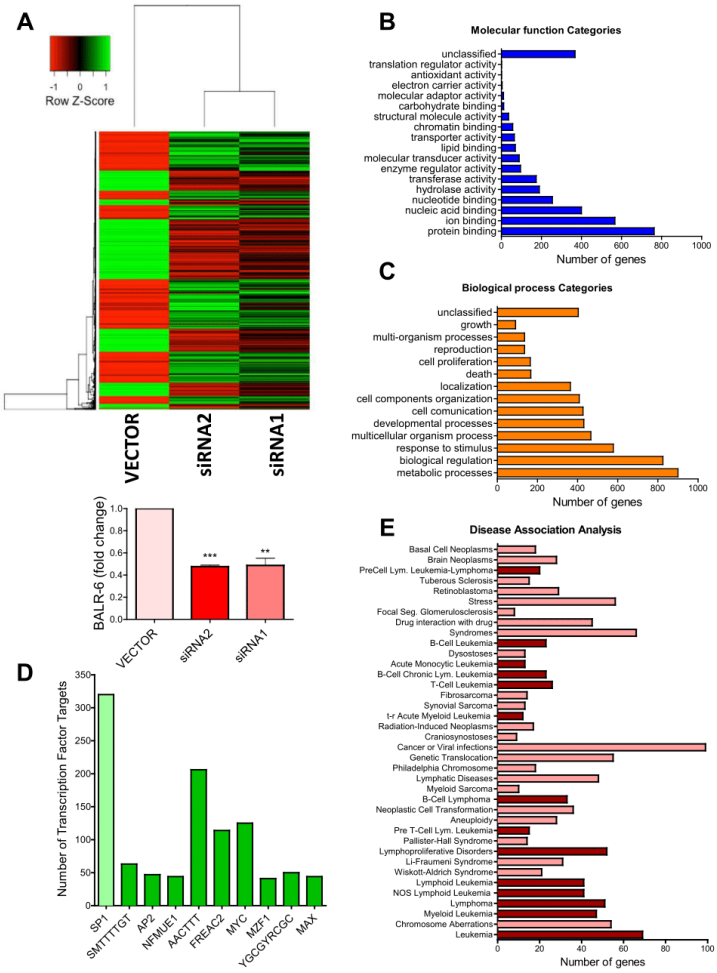

Fig. 5 BALR-6 knockdown leads to global differential expression of genes. **a** Unsupervised hierarchical gene clustering of differentially expressed genes upon BALR-6 siRNA mediated knockdown in RS4;11 cells (PPDE ≥ 95 %, fold change ≥ 1.5). qRT-PCR confirmation of BALR-6 knockdown shown below. Normalized to ACTIN. **b**, **c** Bar graphs of GO Slim classification enrichment analysis of differentially expressed genes by molecular function (**b**), and biological processes (**c**). **d** Enrichment analysis of transcription factor targets. Top ten transcription factors with a *p*-value ≤ 0.0001 are shown. SP1 had the highest number if dysregulated targets, highlighted in light green. For unknown transcription factors, binding site sequence is shown. **e** Disease association analysis by GLAD4U, revealing enrichment of genes associated to various malignancies, in particular, hematological malignancies (*dark red*). Diseases with a *p*-value ≤ 0.05 are shown.; PPDE, posterior probability of differential expression. Evaluations were made using a two-tailed *T*-test, $p < 0.005$ (**); $p < 0.0005$ (***)

Transduction and sorting of cell lines

Lentiviruses and MSCV-based retroviruses were produced to generate knockdown constructs as previously described [16, 25, 26, 52]. In brief, 5.0×10^5 cells were spin-infected at 30 °C for 90 min in the presence polybrene (4 μg/mL). Transduced cell lines were sorted for high green expression using a BD FACSAriaII cell sorter, and analysis was performed using BD FACSDiva software.

Biological assays

For pharmaco-induced assays, cells were cultured at a concentration of 1.0×10^6 cells per mL and treated for

36 h. I-BET151 was dissolved in dimethyl sulfoxide to desired concentrations. After treatment, cells were harvested for RNA extraction. For MTS proliferation assays, cells were cultured for at least 5 days before plating. Cells were plated at a density of 2500 cells per 100 μl of media in each well of a 96 well plate. Reagents were added according to the manufacturer's instructions (Promega CellTiter 96 Aqueous Non-Radioactive Cell Proliferation Assay kit) and cells were incubated at 37 °C, 5 % CO_2 for 4 h before absorbance was measured at 490 nm. For apoptosis assays, cells were plated at 5.0×10^5 cells/mL for 24 h with or without prednisolone treatment. Prednisolone (TCI America) was dissolved in dimethyl sulfoxide to desired concentrations. Cells were harvested after 24 h and stained with APC-tagged AnnexinV. For cell cycle analysis, cells were synchronized by serum starvation for 12 h (human cell lines) or 4 h (murine cell lines) then plated at 5.0×10^5 cells/mL and incubated at 37 °C, 5 % CO_2 for 24 h. Cells were harvested, fixed with EtOH and then stained with propidium iodide. AnnexinV stained and PI stained samples were analyzed using a BD FACS HTLSRII flow cytometer and further analysis was performed using FlowJo.

Luciferase assays

Promoter sequences for CREB1 and p21 were cloned upstream of synthetic firefly luciferase (luc2p) in the pGL4.11 vector. Renilla luciferase is expressed in the pGL4.75 vector downstream of the PGK promoter. HEK 293 T cells were transfected with the pGL4.75 and pGL4.11 containing reporter vectors at a 1:20 ratio (5 ng:100 ng), along with a combination of MSCV vector (empty, Isoform-1 or Isoform-3) and pCMV3 (empty or SP1-HA, Sino Biological Inc.) vector at a 1:1 ratio (200 ng:200 ng). For the last condition SP1, Isoform1 and Isoform 3 were transfected together at a ratio of 2:1:1 (200 ng:100 ng:100 ng). Co-transfections were performed with BioT (Bioland Scientific LLC) in 24 well plates as per the manufacturer's instructions. Cells were lysed after 32 h and supernatant lysate was collected as per manufacturer's instructions (Promega). The dual luciferase assay kit (Promega) was used as substrates for Renilla and firefly luciferase activity. Luminescence was measured on a Glomax-Multi Jr (Promega). The ratio of firefly to Renilla luciferase activity was calculated for all samples. The luminescence for the sample co-transfected with MSCV empty vector and pCMV3 empty vector, was used as a normalization control.

qRT-PCR and PCR

RNA from cell lines was reverse transcribed using qScript (Quantas Biosciences). Real Time quantitative PCR was performed with the StepOnePlus Real-Time PCR System (Applied Biosystems) using PerfeCTa SYBR Green FastMix reagent (Quantas Biosciences). cDNA from mice samples was amplified using KOD Master Mix (EMD Millipore) and ran on a 1.2 % agarose gel stained with ethidium bromide. Primer sequences used are listed in Additional file 2: Table S1.

Northern blot

Total RNA was separated on a 1.2 % (w/v) formaldehyde agarose gel and then blotted onto Hybond N+ nylon membranes (Amersham Biosciences) by semi-dry transfer (Bio-Rad,

Trans-Blot SD Semi-Dry Transfer Cell). DNA probes were ordered from Integrated DNA Technologies (IDT, San Diego, CA) with digoxigenin incorporated at 3′end. For ACTIN we used the RNA probe provided in the DIG Northern Starter Kit (Roche). Membranes were hybridized overnight using ULTRAhyb-Oligo Buffer (Ambion) at 37 or 42 °C with probes. Visualization was done by X-Ray film using CDP-Star reagents (Roche). X-Ray film was scanned and saved as jpeg files. Brightness and contrast was increased by 20 % for ease of visualization.

Data sources

Human genome assembly GRCh37/hg19 and the mouse genome assembly GRCm38/mm10 were used. Methylation patterns for the four cell lines were obtained from Chip-Seq data available in the UCSC genome browser generated by the Broad/ENCODE group [18–20]. Peak viewing range set from 1–50 for H3K4m3 modifications, and 1–15 for H3K36m3 modifications. Alternative splice form information was obtained from the Swiss Institute of Bioinformatics, via UCSC Genome Browser [21]. Genome alignments of RefSeq transcripts from human, mouse and other vertebrates, GenBank mRNAs and ESTs, as well as PhastCons scores were obtained from the UCSC Genome Browser [22].

Microarray data analysis

Microarray data was generated from samples of 3 different transduced RS4;11 cell lines with siRNAs against BALR-6, or the control empty vector. Samples were hybridized at the UCLA Clinical Microarray Core facility using Affymetrix HG-U133_Plus_2 microarray. The Affymetrix raw data files (.cel files) were loaded into the R program for quality control analysis. Additionally, raw hybridization intensities were normalized using the MAS5 method with the affy package in R. Normalized values were sorted by detection p-value ≤ 0.05. Differential expression analysis was performed using unpaired Bayesian comparison model (CyberT Website) [30, 31]. Data was then sorted for genes with a posterior probability of deferential expression (PPDE) ≥ 95 % and a fold change ≥ 1.5. Analysis of differentially expressed genes was carried

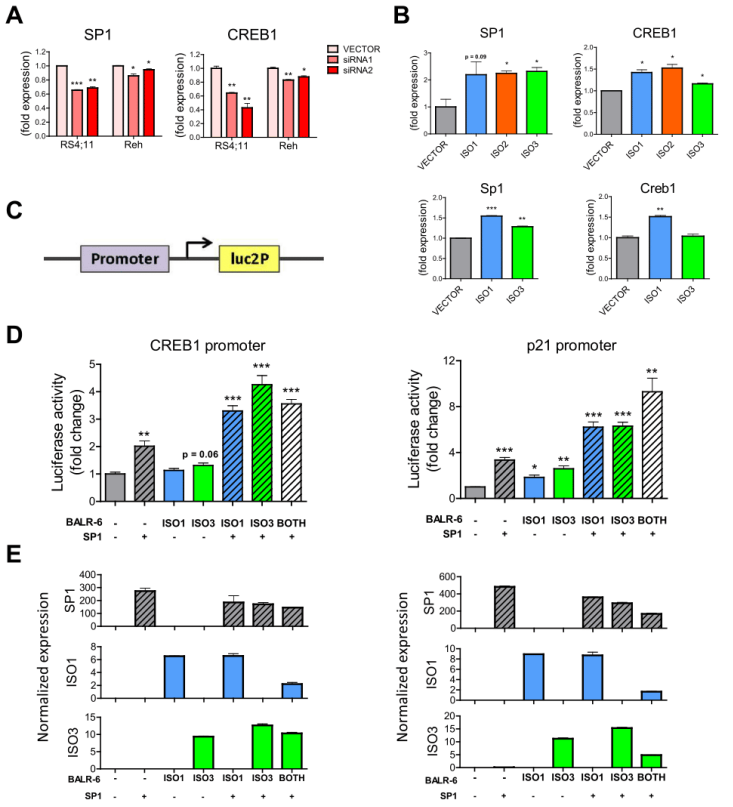

Fig. 6 SP1 transcriptome is modulated by BALR-6. **a** Confirmation of SP1 and CREB1 expression in RS4;11 microarray samples, as well as Reh knockdown cell lines. Normalized to ACTIN. (**b**) SP1 and CREB1 transcript level increase correlates with overexpression of BALR-6 in Nalm-6 cells (*top*) and 70Z/3 cells (*bottom*). Quantitation by qRT-PCR, normalized to ACTIN (Nalm-6 cells) or L32 (70Z/3 cells). **c** Schematic depicting location of cloned promoter sequences in the pGL4.11 vector system for luciferase assays. **d** Transcriptional activity at CREB1 (*left*) and p21 (*right*) promoter regions upon SP1 and/or BALR-6 overexpression, as measured by luciferase activity. **e** Quantitation of overexpression in luciferase assays (as seen in (**d**)) by qRT-PCR of respective transcripts, normalized to ACTIN. Evaluations were made using a two-tailed *T*-test, $p < 0.05$ (*); $p < 0.005$ (**); $p < 0.0005$ (***). luc2p, synthetic firefly luciferase

out using the WEB-based GEne SeT AnaLysis Toolkit (WebGESTALT, http://bioinfo.vanderbilt.edu/webgestalt/) [32, 33]. This online tool uses information from different public data sources for enrichment analysis, including the Gene Ontology data base, and GLAD4U. A second (validation) microarray was carried out, as described above, with technical duplicates for RS4;11 cell lines transduced with siRNA2 or the empty vector. For differential analysis the raw data files were loaded into the R environment and analyzed using the R library of Linear Models for Microarray Data (LIMMA). Pairwise comparison and eBayes fit was carried out. Data was then sorted for genes with a p-value ≤ 0.05. Further analysis was done as described above, using WebGESTALT.

Mice and bone marrow transplantation

Mice were housed under pathogen free conditions at the University of California, Los Angeles (UCLA). Donor mice were injected intraperitoneally with 200 mg/kg of 5-fluorouracil. After 5 days the mice were sacrificed. The bone marrow was collected under sterile conditions and plated in media enriched with IL-3, IL-6 and mSCF (Gibco). 24 h after plating, the bone marrow was spin infected twice, at 30 °C for 90 min in the presence polybrene (4 μg/mL), with retroviruses expressing the empty

MSCV vector or BALR-6 Isoform 3. Recipient mice were lethally irradiated and injected with donor bone marrow 6 h after irradiation. 8 mice were used per group. One mouse in the ISO3 group died due to engraftment failure after 2 weeks post injection. These mice were bled at 8, 12 and 16 weeks post bone marrow injection. At 16 weeks the mice were sacrificed for full analysis. For statistical analysis, one mouse was excluded due to low eGFP expression. This experiment was repeated, and had similar results. All animal studies were approved by the UCLA Animal Research Committee (ARC).

Flow cytometry of samples

At 16 weeks post bone marrow transplant, blood, bone marrow, thymus and spleen were collected from the mice under sterile conditions [53]. Single cell suspensions were lysed in red blood cell lysis buffer. Fluorochrome conjugated antibodies were used for staining (antibodies were obtained from eBiosciences, and Biolegend). Cells were stained with surface marker antibodies for 30 min at 4 °C, washed twice with 1X PBS, and finally fixed with 1 % PFA. Flow cytometry was performed at the UCLA Jonsson Comprehensive Cancer Center (JCCC) and at the BROAD Stem Cell Research Flow Core. Analysis was performed using FlowJo software. The lists of antibodies used and gating schematics are provided in Additional file 2: Table S2. Normal adult human bone marrow was obtained commercially from healthy adults (All Cells, Inc.) as previously described [51]. CD34 enrichment from human bone marrow was performed using the magnetic activated cell sorting (MACS) system (Miltenyi Biotec, San Diego, CA) prior to isolation of CD34+ subsets by flow cytometry. Bone marrow CD34 selected cells were incubated with a cocktail of antibodies as well as FITC-labeled lineage depletion antibodies (Additional file 2: Table S3). CD19 was not included in the lineage depletion cocktail used for sorting the progenitor B population. The immunophenotypic definitions used to isolate progenitors from human bone marrow CD34 selected cells are described in Additional file 2: Table S3. All populations were purified using fluorescence-activated cell sorting on a FACSAria (355, 405, 488, 561 and 633 nm lasers) (BD Immunocytometry Systems).

Additional files

Additional file 1: Figure S1. BALR-6 locus encodes numerous alternative splice forms. **Figure S2.** Knockdown and overexpression of full length BALR-6 isoforms in mammalian cell lines. **Figure S3.** Constitutive expression of BALR-6 in mice periphery. **Figure S4.** Elevated levels of immature B cell populations in mice with BALR-6 overexpression. **Figure S5.** SP1 targets in siRNA mediated knockdown cell lines. **Figure S6.** Confirmation of global differential expression findings seen in initial microarray. (PDF 1.19 mb)

Additional file 2: Tables S1. Primers and RACE sequences for BALR-6. **Table S2.** Antibodies used for bone marrow transplant flow cytometry analysis, and population gating schematics. **Tables S3.** Antibodies used for CD34 enrichment of human bone marrow flow cytometry analysis, and population gating schematics. (PDF 125 kb)

Abbreviations

BALR: B-ALL associated long RNA; chr: chromosome; CLP: common lymphoid progenitor; CMV: cytomegalovirus promoter; DMSO: dimethyl sulfoxide; eGFP: enhanced green fluorescent protein; HSC: hematopoietic stem cell; ISO1: Isoform 1; ISO2: Isoform 2; ISO3: Isoform 3; LMPP: lymphoid primed multipotent progenitor; LSK: lineage- $Sca1^+$ $c\text{-}Kit^+$; LTR: long terminal repeats; ORF: open reading frame; PFA: paraformaldehyde; PGK: phosphoglycerate kinase promoter; PPDE: posterior probability of differential expression luc2p, synthetic firefly luciferase; pre-B: precursor B; pro-B: progenitor B; UBC: ubiquitin C promoter; ZsGreen: Zoanthus green fluorescent protein.

Competing interests

The authors have no relevant competing interests.

Authors' contributions

DSR designed research, analyzed data and prepared the manuscript. GMC designed research and prepared the manuscript. NIRM designed research, performed research, analyzed data and prepared manuscript. TRF, PCP, JRC, JKP, TMT, JA, MOA, KP and SS performed research, and prepared manuscript. MJD analyzed data, and prepared manuscript. All authors read and approved the final manuscript.

Acknowledgements

We would like to thank the UCLA Clinical Microarray Core for performing the microarray hybridization experiments, Alejandro Balazs at Caltech for lentiviral vector backbones, and Ken Dorshkind for helpful discussions. Also, we thank Neha Goswami, Ella Waters, Jasmine Gajeton, Peter D. Pioli, Nolan Ung, Jennifer King and May Paing for their technical support. Very special thanks to Diana C. Márquez-Garbán at Dr. Richard Pietras lab (UCLA) for use of their facilities for some of the experiments. This research was supported by the Graduate Research Fellowship Program from the National Science Foundation DGE-1144087 (N.I.R.M.), the Eugene V. Cota-Robles Fellowship from UCLA (N.I.R.M., J.R.C.), Tumor Biology Training Grant T32 CA009056 from the National Institute of Health (NIH) (T.R.F.), the institutional Tumor Immunology Training Grants NIH T32CA009120 (J.R.C.) and NIH T32009056 (T.R.F.), the Eli and Edythe Broad Center of Regenerative Medicine and Stem Cell Research at UCLA Training Program (M.O.A.), a Career Development Award K08CA133521 (D.S.R.), the Sidney Kimmel Translational Scholar Award SKF-11-013 (D.S.R), the Irving Feintech Family Foundation/Tower Cancer Research Foundation Research Grant (D.S.R), the University of California Cancer Research Coordinating Committee (D.S.R), the Stein-Oppenheimer Endowment Award (D.S.R), NIH P01 HL073104 (G.M.C.), UCLA Broad Stem Cell Research Center (BSCRC) (D.S.R., G.M.C), NIH T32 HL086345 (S.S.) and California Institute for Regenerative Medicine (CIRM) Training Grant TG2-01169 (S.S.). Flow cytometry was performed in the BSCRC FACS Core facility, and UCLA Jonsson Comprehensive Cancer Center (JCCC) and Center for AIDS Research Flow Cytometry Core Facility that is supported by National Institutes of Health awards CA-16042 and AI-28697, and by the JCCC, the UCLA AIDS Institute, the UCLA Council of Bioscience Resources, and the David Geffen School of Medicine at UCLA.

Author details

[1]Department of Pathology and Laboratory Medicine, UCLA, Los Angeles, USA. [2]Cellular and Molecular Pathology Ph.D. Program, UCLA, Los Angeles, USA. [3]Jonsson Comprehensive Cancer Center, UCLA, Los Angeles, USA. [4]Broad Stem Cell Research Center, UCLA, 650 Charles E. Young Drive, Factor 12-272, Los Angeles, CA 90095, USA. [5]Department of Environmental Health Sciences, UCLA, Los Angeles, USA. [6]Molecular Toxicology Interdepartmental Ph.D. Program, UCLA, Los Angeles, USA. [7]All India Institute of Medical Sciences (AIIMS), New Delhi, India.

Received: 25 July 2015 Accepted: 11 December 2015
Published online: 22 December 2015

References

1. Kapranov P, Cheng J, Dike S, Nix DA, Duttagupta R, Willingham AT, et al. RNA maps reveal new RNA classes and a possible function for pervasive transcription. Science. 2007;316:1484–8.
2. Guttman M, Amit I, Garber M, French C, Lin MF, Feldser D, et al. Chromatin signature reveals over a thousand highly conserved large non-coding RNAs in mammals. Nature. 2009;458:223–7.
3. Niazi F, Valadkhan S. Computational analysis of functional long noncoding RNAs reveals lack of peptide-coding capacity and parallels with 3′ UTRs. RNA. 2012;18:825–43.
4. Ulitsky I, Shkumatava A, Jan CH, Sive H, Bartel DP. Conserved function of lincRNAs in vertebrate embryonic development despite rapid sequence evolution. Cell. 2011;147:1537–50.
5. Rinn JL, Kertesz M, Wang JK, Squazzo SL, Xu X, Brugmann SA, et al. Functional demarcation of active and silent chromatin domains in human HOX loci by noncoding RNAs. Cell. 2007;129:1311–23.
6. Tripathi V, Ellis JD, Shen Z, Song DY, Pan Q, Watt AT, et al. The nuclear-retained noncoding RNA MALAT1 regulates alternative splicing by modulating SR splicing factor phosphorylation. Mol Cell. 2010;39:925–38.
7. Cesana M, Cacchiarelli D, Legnini I, Santini T, Sthandier O, Chinappi M, et al. A long noncoding RNA controls muscle differentiation by functioning as a competing endogenous RNA. Cell. 2011;147:358–69.
8. Carrieri C, Cimatti L, Biagioli M, Beugnet A, Zucchelli S, Fedele S, et al. Long non-coding antisense RNA controls Uchl1 translation through an embedded SINEB2 repeat. Nature. 2012;491:454–7.
9. Gong C, Maquat LE. lncRNAs transactivate STAU1-mediated mRNA decay by duplexing with 3' UTRs via Alu elements. Nature. 2011;470:284–8.
10. Gupta RA, Shah N, Wang KC, Kim J, Horlings HM, Wong DJ, et al. Long non-coding RNA HOTAIR reprograms chromatin state to promote cancer metastasis. Nature. 2010;464:1071–6.
11. Prensner JR, Iyer MK, Balbin OA, Dhanasekaran SM, Cao Q, Brenner JC, et al. Transcriptome sequencing across a prostate cancer cohort identifies PCAT-1, an unannotated lincRNA implicated in disease progression. Nat Biotechnol. 2011;29:742–9.
12. Gutschner T, Hammerle M, Eissmann M, Hsu J, Kim Y, Hung G, et al. The noncoding RNA MALAT1 is a critical regulator of the metastasis phenotype of lung cancer cells. Cancer Res. 2013;73:1180–9.
13. Isin M, Dalay N. LncRNAs and neoplasia. Clin Chim Acta. 2015;444:280–8.
14. Mullighan CG, Downing JR. Global genomic characterization of acute lymphoblastic leukemia. Semin Hematol. 2009;46:3–15.
15. Mullighan CG. Molecular genetics of B-precursor acute lymphoblastic leukemia. J Clin Invest. 2012;122:3407–15.
16. Fernando TR, Rodriguez-Malave NI, Waters EV, Yan W, Casero D, Basso G, et al. LncRNA Expression Discriminates Karyotype and Predicts Survival in B-Lymphoblastic Leukemia. Mol Cancer Res. 2015;13:839–51.
17. Pui CH, Behm FG, Downing JR, Hancock ML, Shurtleff SA, Ribeiro RC, et al. 11q23/MLL rearrangement confers a poor prognosis in infants with acute lymphoblastic leukemia. J Clin Oncol. 1994;12:909–15.
18. Bernstein BE, Kamal M, Lindblad-Toh K, Bekiranov S, Bailey DK, Huebert DJ, et al. Genomic maps and comparative analysis of histone modifications in human and mouse. Cell. 2005;120:169–81.
19. Ernst J, Kheradpour P, Mikkelsen TS, Shoresh N, Ward LD, Epstein CB, et al. Mapping and analysis of chromatin state dynamics in nine human cell types. Nature. 2011;473:43–9.
20. Ram O, Goren A, Amit I, Shoresh N, Yosef N, Ernst J, et al. Combinatorial patterning of chromatin regulators uncovered by genome-wide location analysis in human cells. Cell. 2011;147:1628–39.
21. Benson DA, Karsch-Mizrachi I, Lipman DJ, Ostell J, Wheeler DL. GenBank: update. Nucleic Acids Res. 2004;32:D23–6.
22. Siepel A, Bejerano G, Pedersen JS, Hinrichs AS, Hou M, Rosenbloom K, et al. Evolutionarily conserved elements in vertebrate, insect, worm, and yeast genomes. Genome Res. 2005;15:1034–50.
23. Zhou Y, Zhong Y, Wang Y, Zhang X, Batista DL, Gejman R, et al. Activation of p53 by MEG3 non-coding RNA. J Biol Chem. 2007;282:24731–42.
24. Dawson MA, Prinjha RK, Dittmann A, Giotopoulos G, Bantscheff M, Chan WI, et al. Inhibition of BET recruitment to chromatin as an effective treatment for MLL-fusion leukaemia. Nature. 2011;478:529–33.
25. O'Connell RM, Chaudhuri AA, Rao DS, Baltimore D. Inositol phosphatase SHIP1 is a primary target of miR-155. Proc Natl Acad Sci U S A. 2009;106:7113–8.
26. Rao DS, O'Connell RM, Chaudhuri AA, Garcia-Flores Y, Geiger TL, Baltimore D. MicroRNA-34a perturbs B lymphocyte development by repressing the forkhead box transcription factor Foxp1. Immunity. 2010;33:48–59.
27. Hardy RR, Hayakawa K. B cell development pathways. Annu Rev Immunol. 2001;19:595–621.
28. Yap KL, Li S, Munoz-Cabello AM, Raguz S, Zeng L, Mujtaba S, et al. Molecular interplay of the noncoding RNA ANRIL and methylated histone H3 lysine 27 by polycomb CBX7 in transcriptional silencing of INK4a. Mol Cell. 2010;38:662–74.
29. Khalil AM, Guttman M, Huarte M, Garber M, Raj A, Rivea Morales D, et al. Many human large intergenic noncoding RNAs associate with chromatin-modifying complexes and affect gene expression. Proc Natl Acad Sci U S A. 2009;106:11667–72.
30. Baldi P, Long AD. A Bayesian framework for the analysis of microarray expression data: regularized t -test and statistical inferences of gene changes. Bioinformatics. 2001;17:509–19.
31. Kayala MA, Baldi P. Cyber-T web server: differential analysis of high-throughput data. Nucleic Acids Res. 2012;40:W553–9.
32. Zhang B, Kirov S, Snoddy J. WebGestalt: an integrated system for exploring gene sets in various biological contexts. Nucleic Acids Res. 2005;33:W741–8.
33. Wang J, Duncan D, Shi Z, Zhang B. WEB-based GEne SeT AnaLysis Toolkit (WebGestalt): update 2013. Nucleic Acids Res. 2013;41:W77–83.
34. Lerner M, Harada M, Loven J, Castro J, Davis Z, Oscier D, et al. DLEU2, frequently deleted in malignancy, functions as a critical host gene of the cell cycle inhibitory microRNAs miR-15a and miR-16-1. Exp Cell Res. 2009;315:2941–52.
35. Cai X, Cullen BR. The imprinted H19 noncoding RNA is a primary microRNA precursor. RNA. 2007;13:313–6.
36. Dickinson LA, Joh T, Kohwi Y, Kohwi-Shigematsu T. A tissue-specific MAR/SAR DNA-binding protein with unusual binding site recognition. Cell. 1992;70:631–45.
37. Will B, Vogler TO, Bartholdy B, Garrett-Bakelman F, Mayer J, Barreyro L, et al. Satb1 regulates the self-renewal of hematopoietic stem cells by promoting quiescence and repressing differentiation commitment. Nat Immunol. 2013;14:437–45.
38. Kohwi-Shigematsu T, Poterlowicz K, Ordinario E, Han HJ, Botchkarev VA, Kohwi Y. Genome organizing function of SATB1 in tumor progression. Semin Cancer Biol. 2013;23:72–9.
39. Fang K, Han BW, Chen ZH, Lin KY, Zeng CW, Li XJ, et al. A distinct set of long non-coding RNAs in childhood MLL-rearranged acute lymphoblastic leukemia: biology and epigenetic target. Hum Mol Genet. 2014;23:3278–88.
40. Garitano-Trojaola A, Agirre X, Prosper F, Fortes P. Long non-coding RNAs in haematological malignancies. Int J Mol Sci. 2013;14:15386–422.
41. Alvarez-Dominguez JR, Hu W, Gromatzky AA, Lodish HF. Long noncoding RNAs during normal and malignant hematopoiesis. Int J Hematol. 2014;99:531–41.
42. Venkatraman A, He XC, Thorvaldsen JL, Sugimura R, Perry JM, Tao F, et al. Maternal imprinting at the H19-Igf2 locus maintains adult haematopoietic stem cell quiescence. Nature. 2013;500:345–9.
43. Aoki K, Harashima A, Sano M, Yokoi T, Nakamura S, Kibata M, et al. A thymus-specific noncoding RNA, Thy-ncR1, is a cytoplasmic riboregulator of MFAP4 mRNA in immature T-cell lines. BMC Mol Biol. 2010;11:99.
44. Zhang X, Lian Z, Padden C, Gerstein MB, Rozowsky J, Snyder M, et al. A myelopoiesis-associated regulatory intergenic noncoding RNA transcript within the human HOXA cluster. Blood. 2009;113:2526–34.
45. Hu W, Yuan B, Flygare J, Lodish HF. Long noncoding RNA-mediated anti-apoptotic activity in murine erythroid terminal differentiation. Genes Dev. 2011;25:2573–8.
46. Xia F, Dong F, Yang Y, Huang A, Chen S, Sun D, et al. Dynamic transcription of long non-coding RNA genes during CD4+ T cell development and activation. PLoS One. 2014;9:e101588.
47. Fulciniti M, Amin S, Nanjappa P, Rodig S, Prabhala R, Li C, et al. Significant biological role of sp1 transactivation in multiple myeloma. Clin Cancer Res. 2011;17:6500–9.
48. Amodio N, Di Martino MT, Foresta U, Leone E, Lionetti M, Leotta M, et al. miR-29b sensitizes multiple myeloma cells to bortezomib-induced apoptosis through the activation of a feedback loop with the transcription factor Sp1. Cell Death Dis. 2012;3:e436.
49. Wang X, Yan Z, Fulciniti M, Li Y, Gkotzamanidou M, Amin SB, et al. Transcription factor-pathway coexpression analysis reveals cooperation

between SP1 and ESR1 on dysregulating cell cycle arrest in non-hyperdiploid multiple myeloma. Leukemia. 2014;28:894–903.
50. Shankar DB, Cheng JC, Kinjo K, Federman N, Moore TB, Gill A, et al. The role of CREB as a proto-oncogene in hematopoiesis and in acute myeloid leukemia. Cancer Cell. 2005;7:351–62.
51. Esparza SD, Chang J, Shankar DB, Zhang B, Nelson SF, Sakamoto KM. CREB regulates Meis1 expression in normal and malignant hematopoietic cells. Leukemia. 2008;22:665–7.
52. O'Connell RM, Balazs AB, Rao DS, Kivork C, Yang L, Baltimore D. Lentiviral vector delivery of human interleukin-7 (hIL-7) to human immune system (HIS) mice expands T lymphocyte populations. PLoS One. 2010;5:e12009.
53. Contreras JR, Palanichamy JK, Tran TM, Fernando TR, Rodriguez-Malave NI, Goswami N. MicroRNA-146a modulates B-cell oncogenesis by regulating Egr1. Oncotarget. 2015;6:11023–37.

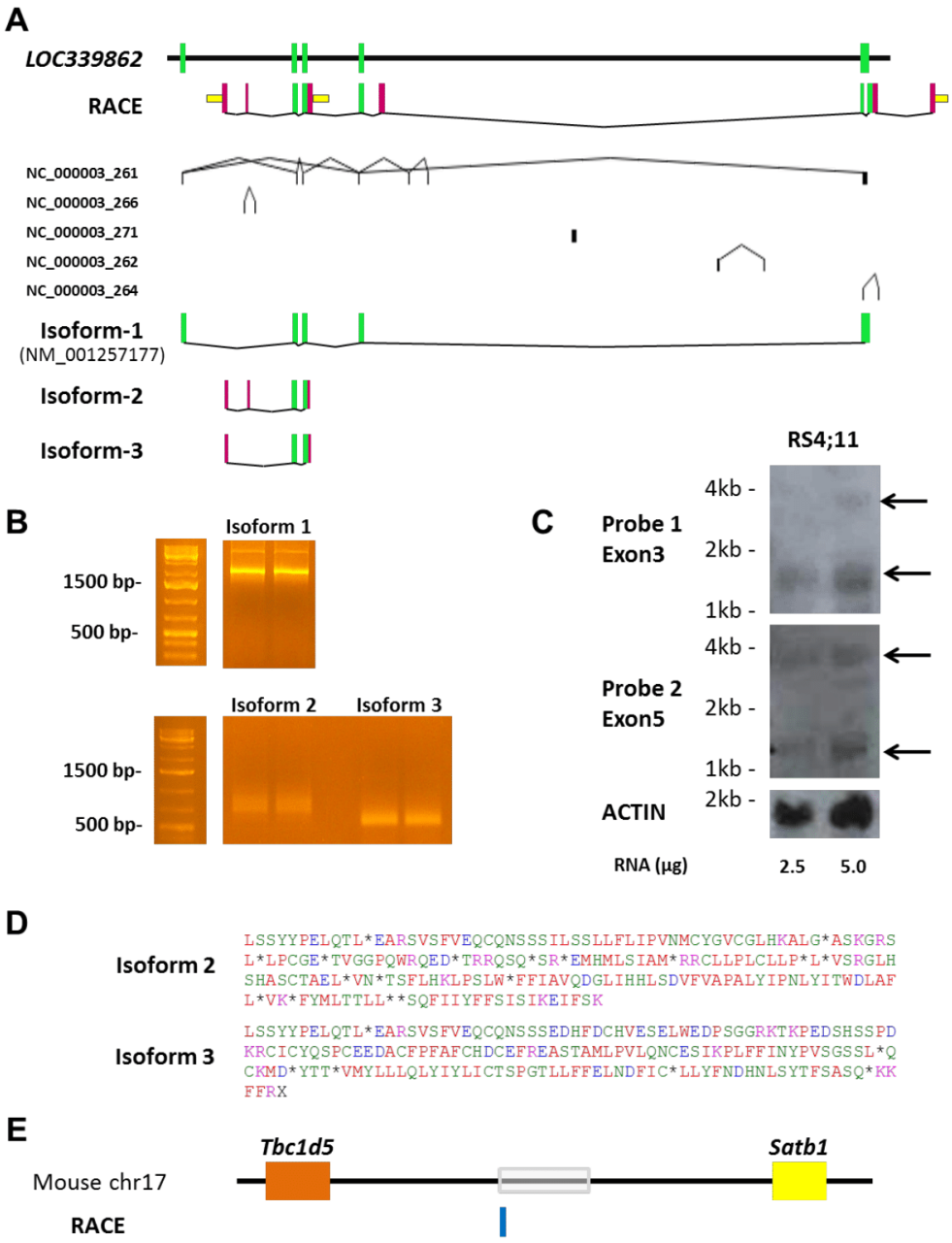

Supplemental Figure 1. BALR-6 locus encodes numerous alternative splice forms.
(**A**) Top: Diagram of RACE products obtained from *LOC339862*. 5' and 3' RACE primers are shown in yellow, with the newly discovered exons shown in magenta, as seen in Figure 1C. Known annotated exons are shown in green. Middle: Alternative splicing graph from the Swiss Institute of Bioinformatics of the predicted alternative splicing transcripts shown in the SIB Genes track. Blocks represent exons, lines indicate introns. Bottom: Schematic depiction of BALR-6 isoforms cloned from RACE sequences. Annotated exons in green, unannotated in magenta. (**B**) Gel confirmation of the isoforms cloned, including the annotated mRNA sequence (Isoform 1). (**C**) Northern blot of endogenous levels of two BALR-6 isoforms in RS4;11 cells. (**D**) EMBOSS analysis of the new isoforms confirmed lack of open reading frames, and lack of translation initiation sites. (**E**) Diagram of RACE products obtained from mouse cell lines with homology to BALR-6. chr, chromosome.

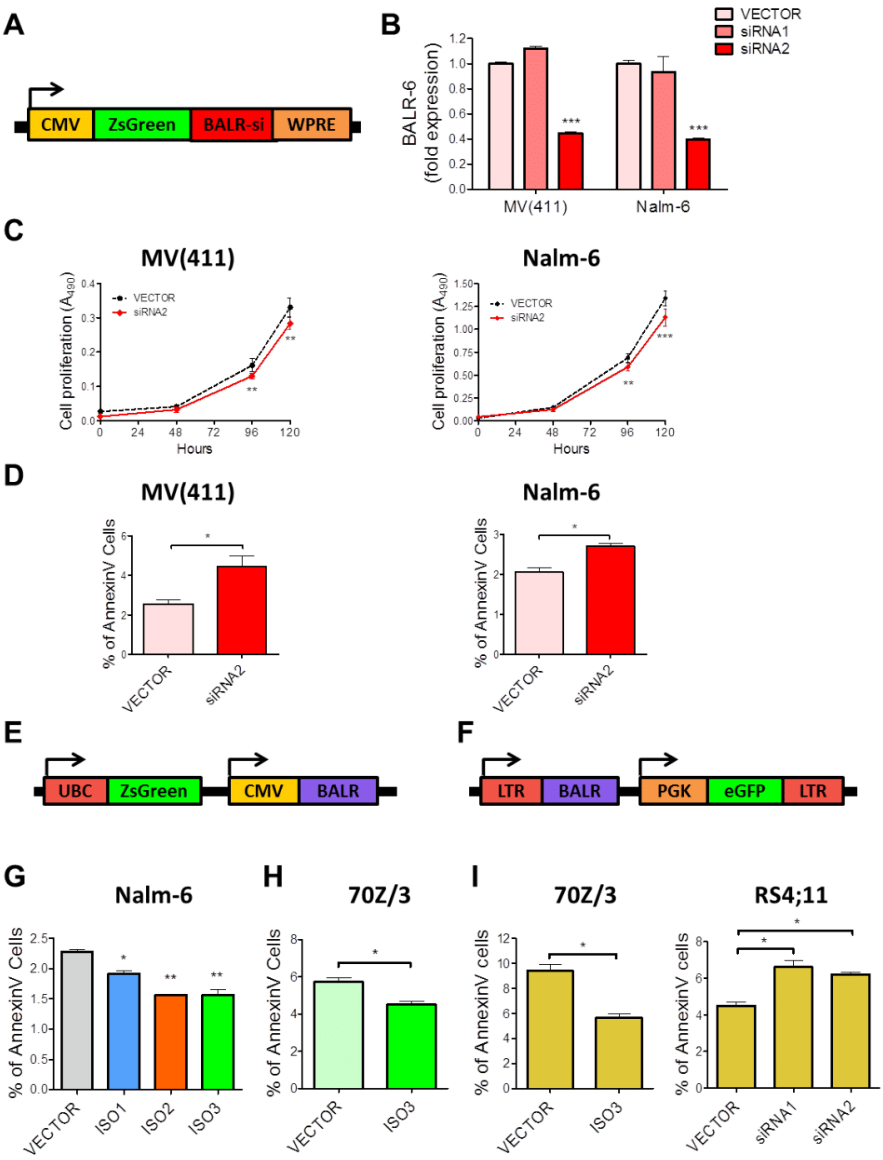

Supplemental Figure 2. Knockdown and overexpression of full length BALR-6 isoforms in mammalian cell lines.

(**A**) Schematic representation of mmu-miR-115 knockdown expression cassette. (**B**) Successful knockdown of BALR-6 using siRNA2 in MV(411), and Nalm-6 cells. (**C**) Decreased cell proliferation in transduced MV(411), and Nalm-6 lines as measured by MTS assay. (**D**) Increased apoptosis at basal levels in MV(411), and Nalm-6 stable lines as measured by AnnexinV staining. (**E-F**) Schematic representation of dual promoter phage (**E**) and MSCV (**F**) expression cassettes. (**G**) AnnexinV staining showed that Nalm-6 stably transduced with BALR-6 isoforms, had lower number of apoptotic cells at basal level. (**H**) 70Z/3 cells overexpressing BALR-6 Isoform 3 had fewer apoptotic cells at basal level, as analyzed by AnnexinV staining. (**I**) 70Z/3 cells stably transduced with BALR-6 Isoform 3, resulted in reduction of apoptosis upon treatment with 250 µg/mL prednisolone for 6 hours. The opposite effect was seen with RS4;11 cells with siRNA mediated knockdown of BALR-6 and treated with 250 µg/mL prednisolone for 24 hours. Evaluations were made using a two-tailed T-test, $p<0.05$ (*); $p<0.005$ (**); $p<0.0005$(***). UBC, ubiquitin C promoter; ZsGreen, Zoanthus green fluorescent protein; CMV, cytomegalovirus promoter; LTR, long terminal repeats; PGK, phosphoglycerate kinase promoter; eGFP, enhanced green fluorescent protein.

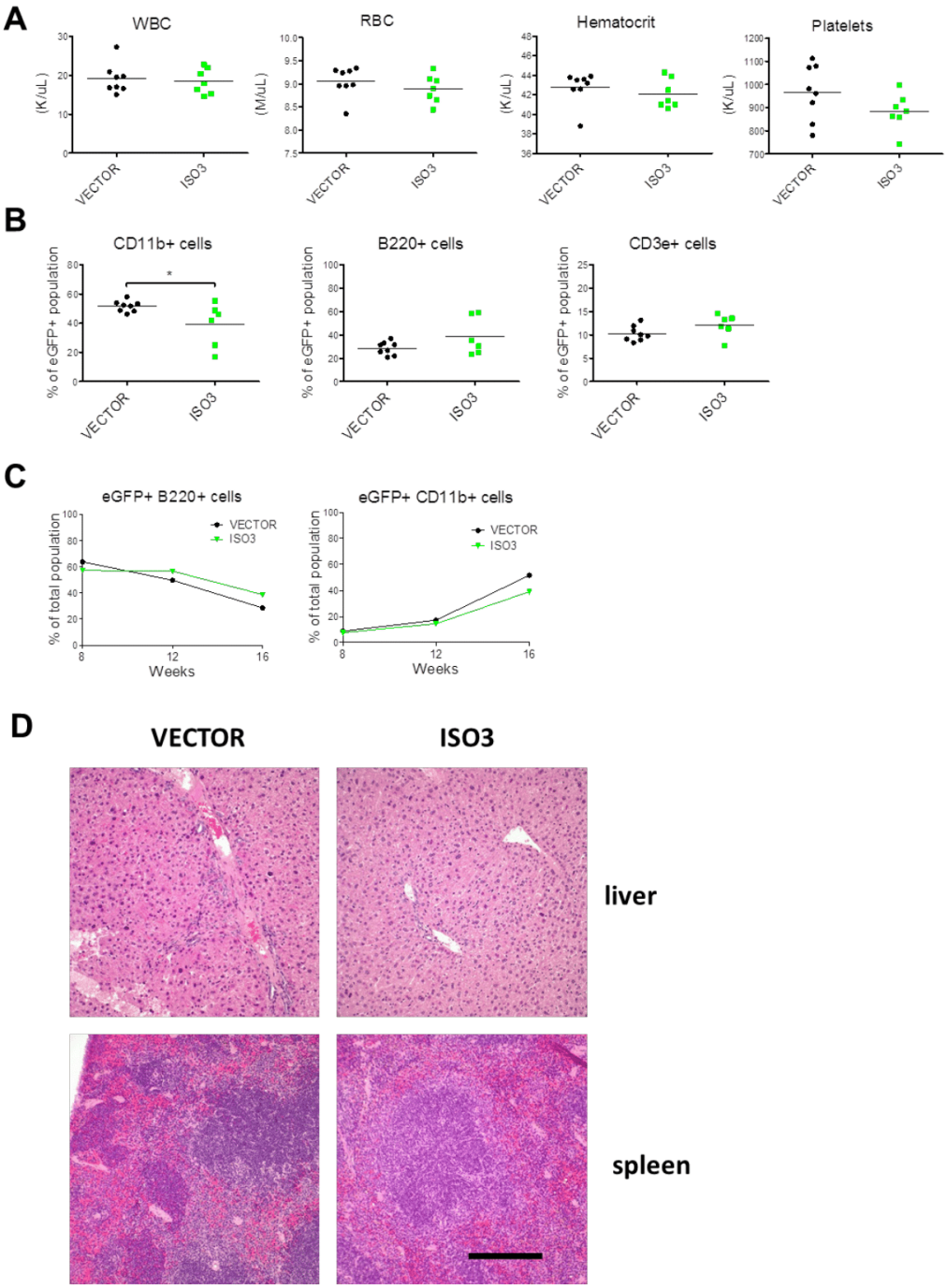

Supplemental Figure 3. Constitutive expression of BALR-6 in mice periphery.
(**A**) Peripheral white and red blood, hematocrit, and platelet cell counts. (**B**) Levels of B-cells (B220+), T-cells (CD3e+) and Myeloid cells (CD11b+) in the eGFP+ compartment of the peripheral blood at 16 weeks. (**C**) Average levels of eGFP+ B cells (B220+) and eGFP+ Myeloid (CD11b+) cells in the peripheral blood throughout the experiment. Number of mice used in this analysis: VECTOR, n=8; ISO3, n=6. (**D**) Hematoxylin and eosin stained liver and spleen samples from bone marrow transfer mice. Scale bar, 200 mm. ISO3, Isoform 3. Evaluations made using a two-tailed T-test, $p<0.05$ (*).

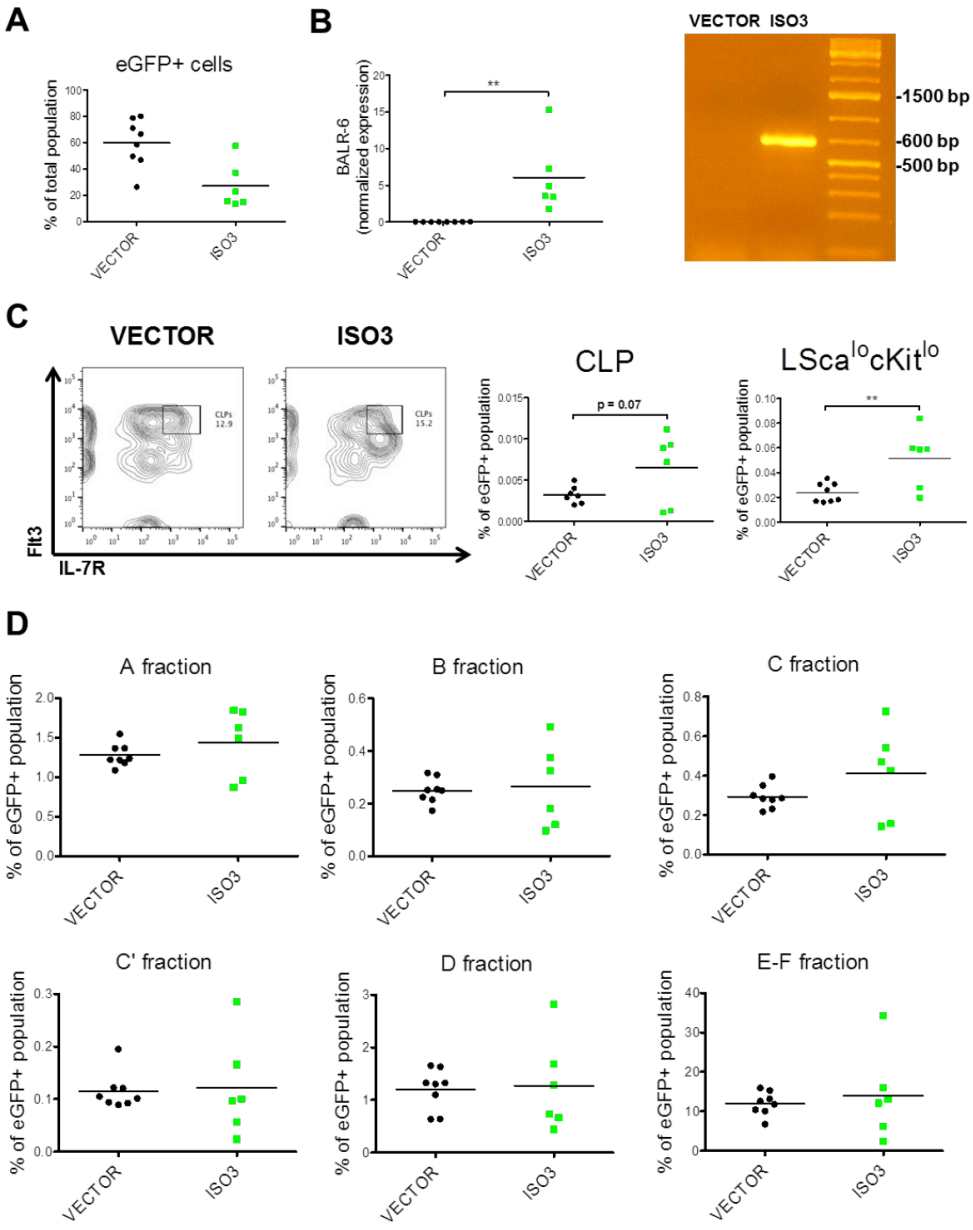

Supplemental Figure 4. Elevated levels of immature B cell populations in mice with BALR-6 overexpression.

(**A**) Levels of e+ cells in the bone marrow of experimental mice. (**B**) Expression levels of BALR-6 Isoform 3 in the experimental mice by qRT-PCR. Normalized to L32. Gel of cDNA PCR, obtained from bone marrow samples, confirming expression of full length transcript, shown to the right. (**C**) Representative FACS plots of CLP cells in the eGFP+ compartment of the experimental mice. Quantitation of the population gating and of LSca^{lo}c-Kit^{lo} cells, shown to the right. (**D**) Percentage of cells in the Hardy fractions from the eGFP+ compartment of experimental mice. Number of mice used in this analysis: VECTOR, n=8; ISO3, n=6. ISO3, Isoform 3. Evaluations made using a two-tailed T-test, $p<0.005$ (**).

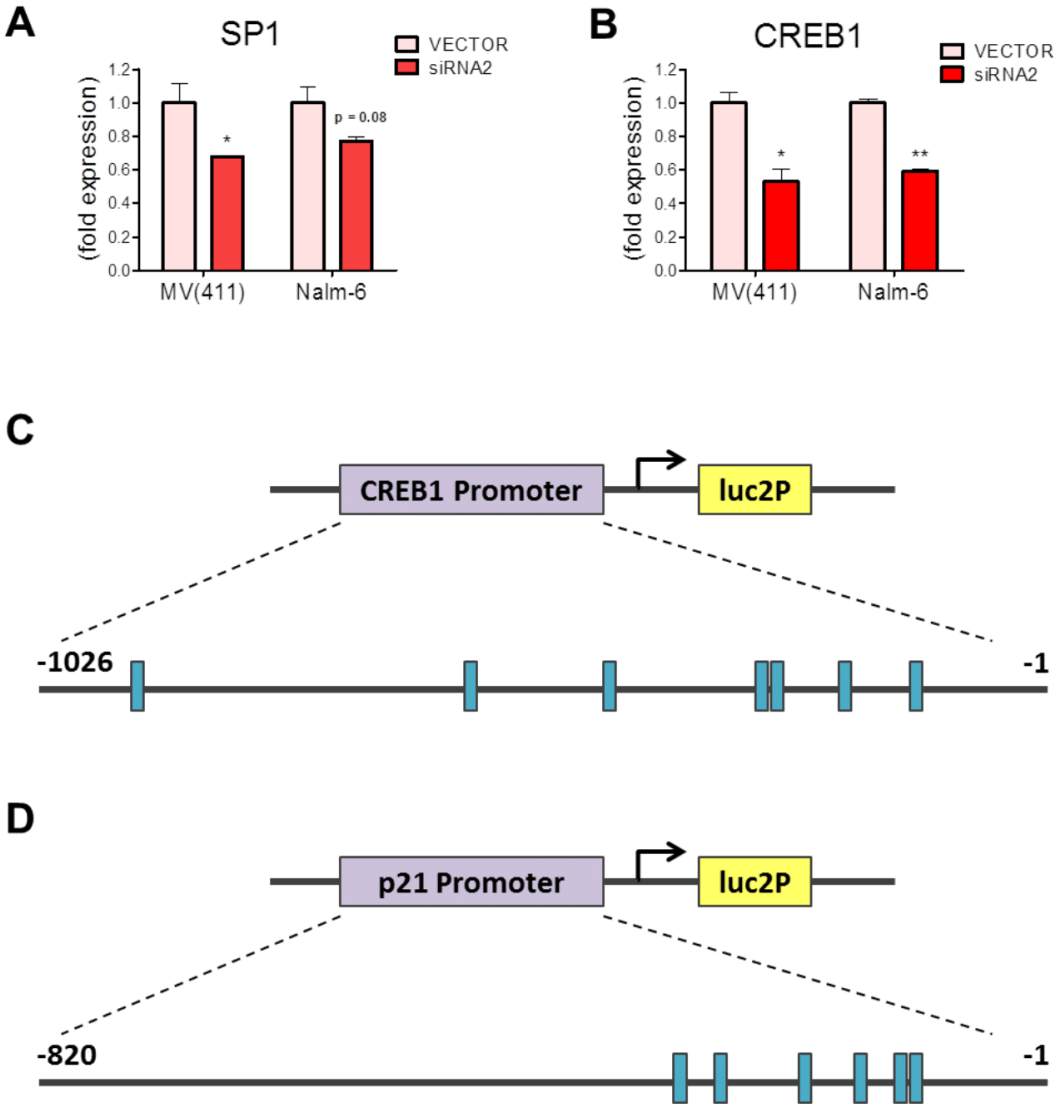

Supplemental Figure 5. SP1 targets in siRNA mediated knockdown cell lines.
(**A-B**) Transcript levels of SP1 (**A**) and CREB1 (**B**) in MV(411) and Nalm-6 knockdown cells. qRT-PCR quantitation of expression, normalized with ACTIN. Only expression levels upon siRNA2 mediated knockdown, which was successful, are shown. (**C-D**) Schematic representation of CREB1 (**C**) and p21 (**D**) promoter sequences cloned into the pGL4.11 luciferase expression vector. Promoter sequence distance shown in relation to the luc2p start codon. SP1 binding sites shown as blue boxes. luc2p, synthetic firefly luciferase.

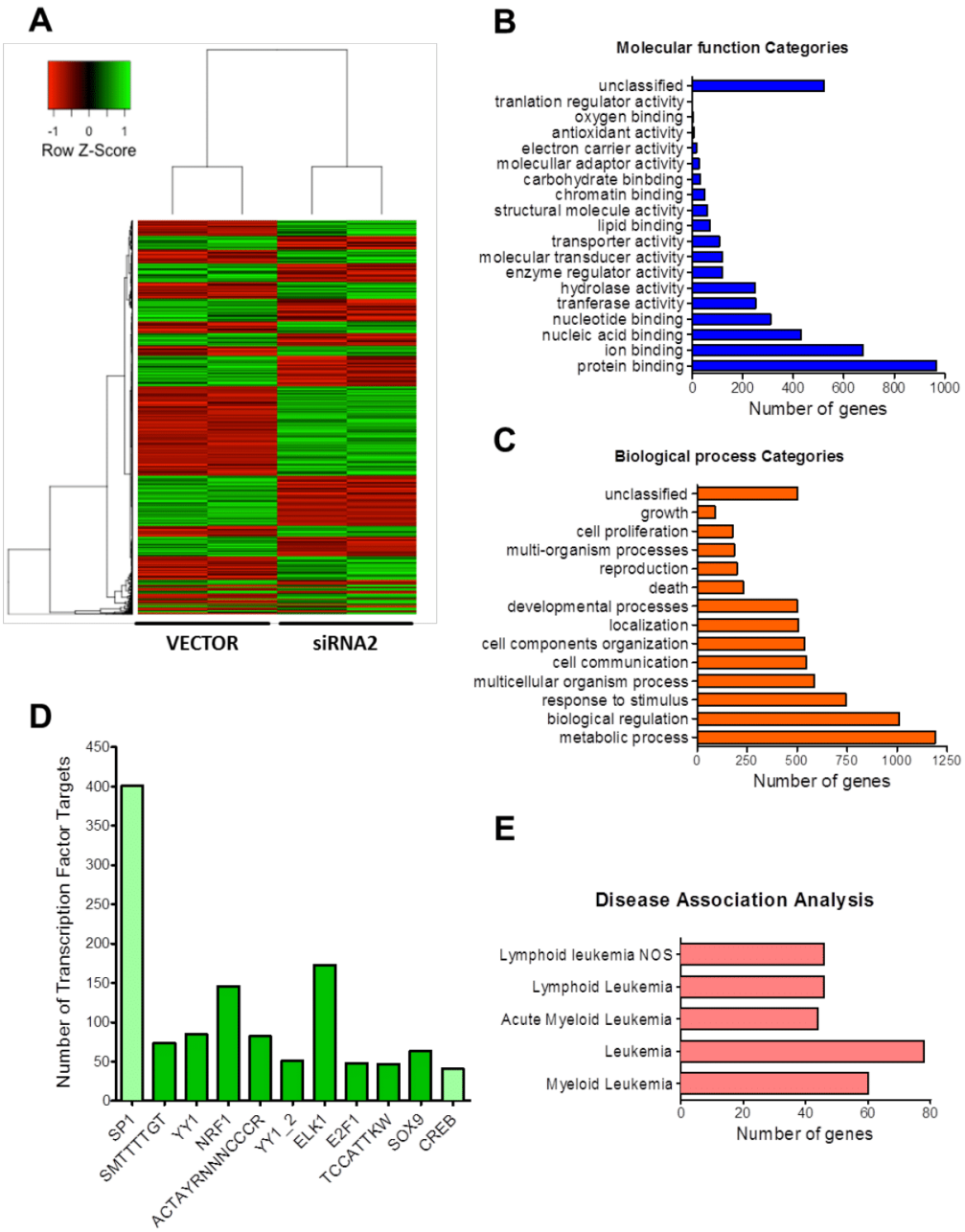

Supplemental Figure 6. Confirmation of global differential expression findings seen in initial microarray.

(**A**) Hierarchical gene clustering of differentially expressed genes in validation microarray upon siRNA2-mediated knockdown of BALR-6 in RS4;11 cells, p-value ≤ 0.05. Technical replicates of samples shown. (**B-C**) Bar graphs of GO Slim classification enrichment analysis of differentially expressed genes by molecular function (**B**) and biological processes (**C**) as analyzed by WebGESTALT. Proportions are highly similar to initial microarray. (**D**) Enrichment analysis of transcription factor targets. Top ten transcription factors with a p-value ≤ 0.02 are shown. In addition, CREB1 was shown as a significantly enriched for its targets with p-value = 0.04. For unknown transcription factors, transcription site sequence is shown. SP1 (shown in light green) had the most dysregulated targets. (**E**) Disease association analysis by GLAD4U, revealed a significant enrichment of genes solely associated to leukemic diseases, p-value ≤ 0.05.

Supplemental Table 1: Primers and RACE sequences for BALR-6

RT-qPCR primers		
BALR-6 Set 1	FOW	5' CGTGTGCTGGGGAAGGCACTG 3'
	REV	5' CCAGGCTCAGAGCAACACAGGGA 3'
BALR-6 Set 2	FOW	5' GATCACTTTGATTGCCATGTGGA 3'
	REV	5' ATCTCTTATCTGGACTACGGTGAC 3'
ACTIN	FOW	5' CATGTACGTTGCTATCCAGGC 3'
	REV	5' CTCCTTAATGTCACGCACGAT 3'
SP1	FOW	5' TGGCAGCAGTACCAATGGC 3'
	REV	5' CCAGGTAGTCCTGTCAGAACTT 3'
CREB1	FOW	5' TTAACCATGACCAATGCAGCA 3'
	REV	5' TGGTATGTTTGTACGTCTCCAGA 3'
Sp1	FOW	5' AGGGTCCGAGTCAGTCAGG 3'
	REV	5' CTCGCTGCCATTGGTACTGTT 3'
Creb1	FOW	5' TGTAGTTTGACGCGGTGTGT 3'
	REV	5' GCTGGTTGTCTGCTCCAGAT 3'
L32 (mouse)	FOW	5' AAGCGAAACTGGCGGAAAC 3'
	REV	5' TAACCGATGTTGGGCATCAG 3'
Actin	FOW	5' GCTACAGCTTCACCACCACA 3'
	REV	5' GGGGTGTTGAAGGTCTCAAA 3'
Cloning primers for P6UZCL		
NotI site-1	FOW	5'ATGGGCTTAGCTGCGGCCGCTTTCTTCATACTATCCAGAGCT CCAAA3'
BamHI site-1	REV	5'ATGGCAATTATCGGATCCTTTTTTTTTTTTCGAAAAAATTTCT TTTATTGAGATGCT3'
NotI site-2	FOW	5'ATGGCA ATTGCGGCCGCCCACGCGTCCGGGACTGAGCA 3'
BamHI site-2	REV	5'ATGGGCTGATGATCATTTTTTTTTGGTTCATAGAAAGTATTT TCTTCTAGAGTCTC3'
Cloning primers for MSCV		
HindIII_eGFP	FOW	5'ATGGGCTTAGCTAAGCTTATGGTGAGCAAGGGCGAGGAGC3'
DraIII_eGFP	REV	5'ATGGCAATTATCCACCTGGTGTTTACTTGTACAGCTCGTCCA TGCCGA3'
BclI_BglII site	FOW	5' ATGGGCTGAGGATCTCCACGCGTCCGGGACTGAGCA 3'
XhoI site-1	REV	5'ATGGCAATTCTCGAGTTTTTTTTTGGTTCATAGAAAGTATTTT CTTCTAGAGTCTC3'
BamHI_BglII site	FOW	5'ATGGGCTTAGCTGGATCCTTTCTTCATACTATCCAGAGCTCC AAA3'
XhoI site-2	REV	5'ATGGCAATTATCCTCGAGTTTTTTTTTTTTCGAAAAAATTTCT TTTATTGAGATGCT3'
Sequencing primers for MSCV		
Upstream_Puro	FOW	5' GCTGTTCTCCTCTTCCTCATCTCC 3'
Upstream_eGFP	FOW	5' CTTTATCCAGCCCTCACTCCTTCTCT 3'

RACE primers		
3-RACE_6	FOW	5' CCATGTGAAGAAGATGCTGGCTTC 3'
3-RACE_7	FOW	5' TAGGAAGCCAGAAGCGTCTCCTTT 3'
3-RACE_8	FOW	5' GGAGGCAGGAAGACTAAACCAGAA 3'
5-RACE_2	REV	5' CTCGCGAAACTCACAATCATGGCA 3'
5-RACE_4	REV	5' ATCTTCCATGTGCATGTGGCTGCA 3'
Northern probes		
BALR-6 probe 1		5'GGGCACAGAGTGTTGCATGCTCATTTCTGTTGATTTTTAATT AGCAGTAATTCATTT/3DiG_N/3'
BALR-6 probe 2		5'CTGGAAATCTAGGATCAGGACTAGCCTAAATTAGTAGATCT ATGTGATAGTATATTGGTA/3DiG_N/3'
mmu-miR-155 formatted siRNA oligos		
siRNA1		5'GAAGGCTGTATGCTGGTGAACATACCACTTACCATTGTTTTG GCCACTGACTGACAATGGTAAGGTATGTTCACCAGGACACAA GGCCTG3'
siRNA2		5'GAAGGCTGTATGCTGGACTTCTGCACACCATGCCTGGTTTTG GCCACTGACTGACCAGGCATGGTGCAGAAGTCCAGGACACAA GGCCTG3'
BALR-6 sequences		
Isoform-2		5'TTTCTTCATACTATCCAGAGCTCCAAACTTTGTAGGAAGCCA GAAGCGTCTCCTTTGTTGAACAGTGCCAAAATAGCAGCTCTAT CCTTTCCTCTCTCCTCTTTCTGATTCCAGTCAATATGTGTTATG GAGTCTGTGGTCTCCACAAGGCCTTGGGATAGGCATCCAAAG GAAGATCACTTTGATTGCCATGTGGAGAGTGAACTGTGGGAG GACCCCAGTGGAGGCAGGAAGACTAAACCAGAAGACAGTCA CAGTAGTCCAGATAAGAGATGCATATGTTATCAATCGCCATG TGAAGAAGATGCTTGCTTCCCCTTTGCCTTCTGCCATGATTGT GAGTTTCGCGAGGCCTCCACAGCCATGCTTCCTGTACTGCAGA ACTGTGAGTCAATTAAACCTCTTTTCTTCATAAATTACCCAGT CTCTGGTAGTTCTTTATAGCAGTGCAAGATGGACTAATACACC ACCTAAGTGATGTATTTGTTGCTCCAGCTCTATATATACCTAA TTTGTACATCACCTGGGACCTTGCTTTTCTTTGAGTTAAATGA TTTTATATGTTAACTACTCTACTTTAATGATCACAATTTATCAT ATACTTTTTCAGCATCTCAATAAAAGAAATTTTTTCGAAA3'
Isoform-3		5'TTTCTTCATACTATCCAGAGCTCCAAACTTTGTAGGAAGCCA GAAGCGTCTCCTTTGTTGAACAGTGCCAAAATAGCAGCTCTG AAGATCACTTTGATTGCCATGTGGAGAGTGAACTGTGGGAGG ACCCCAGTGGAGGCAGGAAGACTAAACCAGAAGACAGTCAC AGTAGTCCAGATAAGAGATGCATATGTTATCAATCGCCATGT GAAGAAGATGCTTGCTTCCCCTTTGCCTTCTGCCATGATTGTG AGTTTCGCGAGGCCTCCACAGCCATGCTTCCTGTACTGCAGAA CTGTGAGTCAATTAAACCTCTTTTCTTCATAAATTACCCAGTC TCTGGTAGTTCTTTATAGCAGTGCAAGATGGACTAATACACCA CCTAAGTGATGTATTTGTTGCTCCAGCTCTATATATACCTAAT TTGTACATCACCTGGGACCTTGCTTTTCTTTGAGTTAAATGAT TTTATATGTTAACTACTCTACTTTAATGATCACAATTTATCATA TACTTTTTCAGCATCTCAATAAAAGAAATTTTTTCGAAA3'

Supplemental Table 2: Antibodies used for bone marrow transplant flow cytometry analysis, and population gating schematics.

Marker	**Fluorochrome**
CD3e	PE
CD11b	PE-Cy7
B220	PerCP-Cy 5.5
CD117	APC-Cy7
Sca1	PerCP-Cy 5.5
CD135	APC
CD127	PE-Cy7
CD150	PE
IgM	PE
CD43	APC
CD24	PE-Cy7
Ly51	APC-Cy7
For lineage negative staining	
Biotin	CD3e, CD4, CD8, B220, NK1.1, Ter119, TCR beta, TCR gamma-delta
Streptavidin	eFluor 450 (pacific Blue)
Population	**Defined markers**
HSC	Lin- CD117 hi Sca1 hi CD150++
LMPP	Lin- CD117 hi Sca1 hi CD135+ CD127-
CLP	Lin- CD117 lo Sca1 lo CD135+ CD127+
A	B220+ IgM- CD43+ CD24- Ly51-
B	B220+ IgM- CD43+ CD24+ Ly51-
C	B220+ IgM- CD43+ CD24+ Ly51+
D	B220+ IgM- CD43-
E and F	B220+ IgM+

Antibodies were procured from eBiosciences (San Diego, CA) or Biolegend (San Diego, CA).

Supplemental Table 3: Antibodies used for CD34 enrichment of human bone marrow flow cytometry analysis, and population gating schematics.

Marker	**Fluorochrome**
CD34	APC-Cy7
CD38	APC
CD10	PE-Cy7
CD20	FITC
CD45RA	PerCP-Cy 5.5
IgM	PerCP-Cy 5.5
For lineage depletion	
FITC	CD3, CD14, CD15, CD19, CD56, and CD235a
Population	**Defined markers**
HSC	Lin- CD34+CD38-
CLP	Lin- CD34+CD10+CD45RA+
progenitor B	Lin- CD34+CD19+
precursor B	CD34-CD10+CD19+IgM-CD20-
Immature B	CD34-CD19+IgM+CD20+

Antibodies were procured from Becton Dickinson (BD, San Jose, CA) or Biolegend (San Diego, CA).